NATIONAL TECHNICAL UNIVERSITY OF ATHENS

SCHOOL OF MECHANICAL ENGINEERING

Numerical Simulation of Fire and Smoke Development in Road Tunnels

DIPLOMA THESIS

Of

PAPADIMA GEORGIA

Section: FIRE ENGINEERING

Supervisor: DIONYSIS KOLAITIS, Ph.D. MECHANICAL ENGINEER N.T.U.A.

Athens 2020

ΕΘΝΙΚΟ ΜΕΤΣΟΒΙΟ ΠΟΛΥΤΕΧΝΕΙΟ

ΣΧΟΛΗ ΜΗΧΑΝΟΛΟΓΩΝ ΜΗΧΑΝΙΚΩΝ

ΥΠΟΛΟΓΙΣΤΙΚΗ ΠΡΟΣΟΜΟΙΩΣΗ ΦΑΙΝΟΜΕΝΩΝ ΦΩΤΙΑΣ ΚΑΙ ΚΑΠΝΟΥ ΣΕ ΟΔΙΚΕΣ ΣΗΡΑΓΓΕΣ

ΔΙΠΛΩΜΑΤΙΚΗ ΕΡΓΑΣΙΑ

της

ΠΑΠΑΔΗΜΑ ΓΕΩΡΓΙΑ

Τομέας: ΘΕΡΜΟΤΗΤΑΣ

Επιβλέπων: ΔΙΟΝΥΣΗΣ ΚΟΛΑΪΤΗΣ, Δρ. ΜΗΧΑΝΟΛΟΓΟΣ ΜΗΧΑΝΙΚΟΣ Ε.Μ.Π.

Αθήνα 2020

CONTENTS

ABSTRACT

The occurrence of a fire incident in road tunnels is a particularly severe event, jeopardizing tunnel's integrity and motorist's safety while causing major financial losses and physical impairments or even fatalities to its users. Since the introduction of tunnel structures to the transportation network, numerous fire incidents have occurred, highlighting those severe hazards. To improve the understanding of such incidents, an extensive database has been established, consisting of the main existing fire incidents of the last 20 years, various sequences of full-scale and model-scale fire experiments and numerical simulations, along with several full-scale evacuation tests. As it regards fire protection strategies, a conventional approach for unidirectional road tunnels has been to employ longitudinal ventilation with jet fans to eliminate the hazards associated with smoke backlayering at the direction that the entrapped motorists are located or attempting to escape. Consequently, the primary design objective of this tactic is the determination of the critical ventilation velocity that prevents entirely the flow development of toxic smoke in the upstream direction of the fire. The evolution of fire and smoke characteristics in a tunnel is widely investigated with the utilization of CFD codes. Fire Dynamics Simulator (FDS), developed by NIST, is a computational model, specially designed to resolve fire-driven fluid flows. A numerical series of large-scale tunnel experiments has been conducted, via FDS, in an 854m long, non-inclined tunnel, with various exhaust volume flow rates delivered by the jet fans in order to create the required critical ventilation conditions for three different fire heat release rates (20, 50 & 100MW). It is found that critical ventilation velocity increases with increasing fire size but above a certain HRR value, it becomes independent of the fire size. The design of longitudinal ventilation systems, employing jet fans do meet the requirements at all fire sizes in managing the adverse spread of smoke, upstream of the fire site. The resulting critical velocity for a 20MW fire is 2.75m/s, while a corresponding velocity of approximately 3.10m/s can diminish the backlayering effect for both a fire of 50 and 100MW, for the particular tunnel structure. Existing empirical correlations for critical ventilation have been also proposed, depending on their appropriateness for the respective fire sizes. Before the numerical tests, a twofold validation study has been performed against actual experimental data of Test Case 502 and 615b, of the Memorial Tunnel Fire Ventilation Test Program, to verify the credibility and fidelity of the numerical findings, produced in the present thesis.

ΠΕΡΙΛΗΨΗ

Η πρόκληση πυρκαγιάς σε μια οδική σήραγγα είναι ένα ιδιαίτερα επιζήμιο γεγονός, καθώς θέτει σε κίνδυνο την ακεραιότητα της και την ασφάλεια των οδηγών, προκαλώντας αφενός σημαντικές οικονομικές ζημίες, αφετέρου σωματικές βλάβες ή ακόμη και ανθρώπινες απώλειες. Από καταβολής της προσάρτησης των σηράγγων στο οδικό δίκτυο, έχουν σημειωθεί πολλά ατυχήματα πυρκαγιάς που αναδεικνύουν τους προαναφερθέντες κινδύνους. Αποσκοπώντας στην κατανόηση των φαινομένων που διέπουν τέτοια περιστατικά, δημιουργήθηκε μια εκτενής βάση δεδομένων. Στην τελευταία συμπεριλαμβάνονται τα σημαντικότερα ατυχήματα των τελευταίων 20 ετών, μεγάλης και μικρής κλίμακας πειράματα και υπολογιστικές προσομοιώσεις φωτιάς σε οδικές σήραγγες, όπως επίσης και πειράματα εκκένωσης. Η επικρατέστερη πρακτική για την αντιμετώπιση πυρκαγιών σε οδικές σήραγγες μονής κατεύθυνσης, είναι η χρήση διαμήκους αερισμού με αξονικούς ανεμιστήρες ώσης, για την αποφυγή της εξάπλωσης του καπνού προς τους οδηγούς που επιχειρούν να διαφύγουν. Κατά συνέπεια, ο πρωταρχικός σχεδιαστικός στόχος αυτής της στρατηγικής είναι ο προσδιορισμός της κρίσιμης ταχύτητας αερισμού που αποτρέπει εξ ολοκλήρου την ανάντι ροή των καυσαερίων. Η εξέλιξη των χαρακτηριστικών της φωτιάς και του καπνού διερευνάται ευρέως με τη χρήση υπολογιστικών προγραμμάτων, CFD. Το λογισμικό προσομοιώσεων Fire Dynamics Simulator (FDS), που αναπτύχθηκε από το ερευνητικό ινστιτούτο NIST, είναι ένα υπολογιστικό εργαλείο προσομοίωσης της πολύπλοκης συμπεριφοράς των ρευστών σε περιπτώσεις φωτιάς. Με την χρήση αυτού, μια σειρά αριθμητικών πειραμάτων πραγματοποιείται στην παρούσα μελέτη, σε μια σήραγγα μήκους 854 μέτρων, μηδενικής κλίσεως, εξετάζοντας διάφορες παροχές όγκου αέρα στους ανεμιστήρες, προκειμένου να δημιουργηθούν οι απαιτούμενες κρίσιμες συνθήκες αερισμού, για 3 διαφορετικούς ρυθμούς έκλυσης θερμότητας (20, 50 & 100MW). Διαπιστώνεται πειραματικά ότι η κρίσιμη ταχύτητα αερισμού αυξάνεται με την αύξηση του μεγέθους της φωτιάς, αλλά πάνω από μια συγκεκριμένη τιμή της θερμικής ισχύος καθίσταται ανεξάρτητη του μεγέθους της. Η επιλογή του υπό κρίση συστήματος διαμήκους αερισμού με ανεμιστήρες ώσης ανταποκρίνεται καθολικώς στον περιορισμό της εξάπλωσης του καπνού στην ανάντι κατεύθυνση της φωτιάς, ανεξαρτήτως μεγέθους. Η προκύπτουσα κρίσιμη ταχύτητα για μια πυρκαγιά 20MW είναι 2,75m/s, ενώ η αντίστοιχη για φωτιές ισχύος 50 και 100MW, είναι περίπου 3,10m/s, για τη συγκεκριμένη σήραγγα. Από τις υπάρχουσες εμπειρικές συσχετίσεις για την κρίσιμη ταχύτητα αερισμού, έχουν προταθεί οι πλέον κατάλληλες για τα εξεταζόμενα μεγέθη πυρκαγιάς. Σημειώνεται πως πριν από τις υπολογιστικές προσομοιώσεις, διενεργήθηκε μια διμερής μελέτη επικύρωσης, με γνώμονα τα πειράματα υπ΄ αριθμόν 502 και 615b του Memorial Tunnel Fire Ventilation Test Program, με σκοπό την επαλήθευση της αξιοπιστίας και της πιστότητας των αριθμητικών ευρημάτων της παρούσας μελέτης.

ACRONYMS & ABBREVIATIONS

Acronyms & Abbreviations	
FDS	Fire Dynamics Simulator
FH	Flame Height
FLC	Flammable Liquid Cargo
FS	Fire Size
FT	Fuel Type
HRR	Heat Release Rate
MBR	Mass Burning Rate
MLR	Mass Loss Rate
MOD	Mass Optical Density
MTFVTP	Memorial Tunnel Fire Ventilation Test Program
nD	Non-Dimensional
OD	Optical Density
PS	Pool Size
PSD	Particle Size Distribution
SH	Smoke Height
SV	Smoke Velocity
T	Temperature
TP	Temperature Profiles
TPM	Total Particulate Matter
Trans	Transmissivities
u	Velocity

1. INTRODUCTION

1.1 Fire in Road Tunnels

Although major fires in tunnels seem to occur less frequently than fires on the open road, owning to the unique nature of a tunnel fire, such incidents are far more difficult to confront, suppress and extinguish. Fires that develop inside a confined space, tend to elaborate more vigorously in comparison with open fires, due to the feedback of the heat and radiation from the surrounding environment. Burning vehicles and flammable materials, for example, are the primary sources of heat and radiation in a tunnel's fire scenario. The long and confined space of a tunnel's construction reinforce the development of high temperatures, challenging people's evacuation attempt and fire-fighting procedures. Additionally, this type of fires is evidently strongly interacting with the ventilation airflow or the lack of it, with the containment usually leading to drastic changes in the smoke flow patterns and heat fluxes produced from the fire, as well. Thus, either it regards a ventilation or a fuel-controlled fire scenario, a variation in the type or size of the fire, the heat release rate, a change in ventilation velocity or ambient conditions, could drastically affect the fire growth, smoke propagation and distribution and determine fire-fighting procedures' outcome.

The frequency and the ferocity of tunnel fires depend on several extraneous factors, as well. Some of the main variables are, for instance, the geometry of the tunnel, the traffic density, and the utilization of the tunnel. The geometry of a tunnel is one of the primary examined factors in fire-safety analysis for a tunnel case scenario since the length, the cross section and the slope can significantly affect the fire spread tendency and the severity of an ongoing fire. Buoyancy forces, for instance, owning to the slope of the tunnel, may create strong ventilation conditions which could either potentiate or hinder the development of the fire and define the level of success of an evacuation performance. Additionally, long flames and high temperatures, owing to large fires, could also cause the fire to spread to other vehicles or flammable materials inside the tunnel. This phenomenon is magnified when it regards a tunnel in which intense traffic congestion is noted. Fire safety engineers should also examine if a fire incident concerns a unidirectional or bidirectional tunnel, since the forced ventilation velocity that should be applied to control the smoke distribution, in that case, cannot be derived from a premediated or an obvious ventilation strategy. Furthermore, a significant disparity is marked whether it regards a road or rail tunnel. The materials involved in the fire as well as the internal layout of each tunnel pose a notable difference to the fire development and the evacuation strategies and estimated time as well.

In general, fires mainly produce heat, which is allocated to the surroundings through convective heat transfer and radiation, while giving rise to large amounts of toxic gases and products of incomplete combustion. The temperature that hot fumes can reach, the density of the smoke and toxic gases can cause structural damage to the tunnel, human injuries and even loss of life. Heat is the main cause of damage to structure and installations, whereas it is rarely the original cause of fatalities. Low visibility and exposure to toxic gases for a long time are usually responsible for loss of life in tunnel fire accidents. More specifically, loss of visibility, owing to smoke, poses the primary threat to the tunnel's users while it prohibits the evacuation and firefighting procedures, leading concurrently to inhalation of toxic fumes. The lack of oxygen in such an event, could also cause death due suffocation when evacuation is not feasible. A subordinate risk is that a fire could pose a considerable environmental hazard to the entire vicinity of the incident, triggered by the toxicity of the smoke and the increased heat release rates and temperatures of the fire.

Another challenging issue that comes along with a fire incident inside a tunnel is the economic losses associated to the burnt vehicles and properties and the cost of the tunnel's reconstruction along with equipment's installation expenses. In particular, damage to the tunnel construction or even collapse of some expendable parts, such as false ceilings and ventilation ducts or destroyed tunnel equipment, could claim a momentous capital investment afresh. Ventilation shafts, jet fans, telecommunications, lightning and electrical short circuits are some of the existing equipment that may need replacement. Furthermore, in some cases, tunnel rehabilitation after a fire incident can take weeks or months causing traffic congestion on the roads in the district of the closed tunnel.

Figure 1.1 Structural damage of Mont Blank Catastrophic Tunnel Fire

To include all the potential imperilments of a fire event in a tunnel, one ought to consider the behaviour of the road tunnel users and its complicity in a tunnel evacuation performance. In a tunnel fire, passing drivers do not always realize the danger to which they are exposed, especially if the fire is not conspicuous in their view, and may choose to remain in their vehicles in the early stages of a fire. In such cases, despite of the toxic gases and hot smoke inside the tunnel that directly threatens the drivers lives, fire spread between vehicles is another major threat that could occur even at a great distance from the fire, under certain ventilation conditions. Thus, the deceptive feeling of safety inside the vehicle along with the misleading desire of protecting their own property, may render the self-rescue procedure for some drivers unfeasible, after a certain time period. After all, the main consequence of a fire in a road or rail tunnel is the fatalities and injuries of passing drivers, operating and rescue personnel.

Road and Rail Tunnels are a key element of transportation infrastructure. Frustratingly, disastrous fires have occurred over the last years, both in road and rail tunnels, and they have evidently shown the importance of effective and prompt evacuation. In a tunnel fire event, smoke, toxic gases, heat and radiation are produced. Hot fumes from the fire tend to form a stratified toxic flow which diffuses inside the enclosed space, rendering the evacuation, rescue and fire extinguishing activities considerably challenging, even in small incidents. Thus, it is critical for fire safety or fire protection engineers to predict the underlying behaviour and human responses when exposed to these hazardous events.

To evaluate tunnel fire safety qualitatively, especially regarding evacuation strategies, occupants' characteristics and behavioural constrains should be taken under thorough examination. Given the foregoing, it should be noted that drivers in the early stages of an ongoing fire, is unlikely to realize what is happening immediately and they tend to remain in their cars assuming that the halt is due to traffic congestion. When emergency announcements and alarming cues or even direct signals from the fire, namely smoke, heat or smell, reach their attention, they start analyzing the situation and search for additional information. At that point, they have to process the information received

and decide whether or not it is necessary to protect themselves. The time period of drivers' hesitation, trading off between the costs and benefits of evacuation, is extremely crucial for pursuing a feasible and safe self-evacuation. Technical installations and immediate action from tunnel's operator are also required to eliminate the pre-movement time and urge people to organize their course of actions more rapidly.

Social influence, such as other drivers' reaction, is a factor that may either facilitate an evacuation attempt, when people actively seek for a safe evacuation route or hinder it if they decide to stay passive and engulfed in anxiety and indecision. Evidently, affiliation effect in fire entrapment, impel people to gather in groups and evacuate towards familiar people and places. In some tunnel fires, motorists even tend to remain in their cars for a long time, eliminating their chances of safe evacuation, owning to the fact that the vehicle constitutes something familiar and provides the misinterpretation of safety, whereas the tunnel is an unfamiliar environment.

To eliminate the underlaying risks in human behaviour that threat the evacuation, way finding systems should be utilized for people's alert and guidance. Way-finding systems incite drivers engage in certain actions, during their effort to self-evacuate, e.g., illustrating the need of an immediate evacuation, providing guidance for one to protect self or others, pointing out the closest emergency exit and the distance one has to travel to get there, etc. The design of way finding systems and emergency exits, in a fire emergency should be taken under careful consideration, especially in these types of facilities when people encountering additional environmental cues in low visibility. Insufficiency in reaching or recognizing the emergency exits or even ineffective use of them may lead to prolonged evacuation times and could induce dreadful consequences due to the rapid development of untenable conditions. The fire safety engineering design and analysis for tunnels is responsible for examining in depth the choice and use of assorted fire detection and alarm systems and illustrating their efficiency given the tunnel's geometry, technical settings and fire scenario with respect to motorist cue reception, recognition, interpretation and response. By investigating their strengths and limitations, opportunities occur for their enhancement possibly through the use of some combination among them, which will support and expand the benefits provided. The following figure illustrates with chronological order, all phases of the human response, when exposed in fire incidents, for providing adequate information in fire safety strategies and life safety analysis of road and rail tunnel structures.

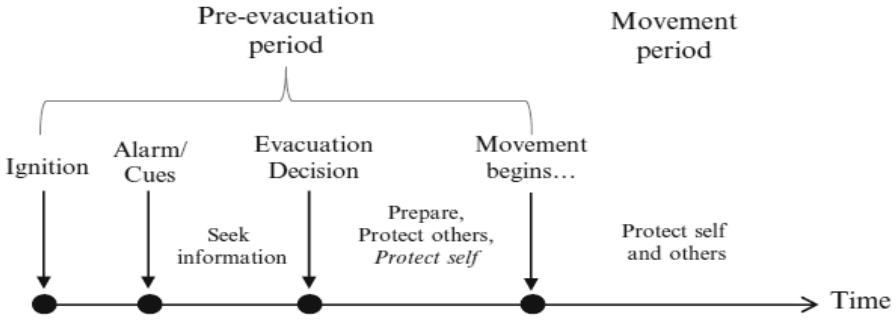

Figure 1.2. Timeline of human behaviour during a fire emergency, by SFPE Handbook of Fire Protection Engineering, 2016.

Additionally, many issues including motorists' special characteristics such as number and distribution of drivers, gender, age, psychical and sensory impairments, form evacuee's egress feasibility and level of success. For example, given a research study on world population prospects, the old age dependency ratio has almost doubled since 1960 and is expected to accommodate a

further addition until 2050 (United Nations, Department of Economic and Social Affairs, 2015). Similarly, obesity rates over the last years, tend to rise vigorously in many developed countries (OECD Obesity Update, 2017). These and several other changes, on general human characteristics, highlight the need of enhancement in an increasing variety of fire incident scenarios to adequately address these vulnerable populations.

Human behaviour and interactions in dangerous situations should be cautiously considered by people responsible for the safety of tunnel design and operation. In conclusion, in a road and rail tunnel, an engineer should comprehend how the users will respond in order to assess whether the tunnel and the fire safety features provide an adequate level of safety during a fire emergency event. Comprehending the complexity of human behaviour in this type of emergency, via the development of experimental procedures and simulation tools, could aid in safer tunnel technical installations design and evacuation strategies, such as more effective emergency procedures, emergency communication systems, and pre-event emergency training and briefing for tunnel environment. Thus, an anticipated aim is for human behaviour to be thorough investigated through its interaction with a tunnel infrastructure, technical installations and other tunnel users, in a fire emergency.

1.2 Aim of the Thesis

The purpose of this thesis is to opt the understanding of the current state of knowledge, regarding fire and smoke related phenomena in road tunnels, and to provide applicable solutions to existing challenges on ventilation strategies. For that cause, the main fire and smoke flow characteristics, provided by actual fire incidents, full and reduced scale experimental tests, numerical simulations and evacuation experiments at tunnel fire emergencies, are intended to be collected, creating a wide database, for fires in road tunnels. Additionally, the configuration of a longitudinal ventilation system is aimed to be assessed by the computational FDS code, in an unidirectional tunnel, in terms of providing the required critical ventilation velocity to prevent backlayering phenomenon at the upstream side of the fire site.

2. FIRE IN ROAD TUNNELS

2.1 Fire Incidents

Road tunnels have played a key role in transportation systems since the mid-20th century, due to their elevated utility as practical means of facilitating the smooth traffic circulation at both mountainous and crowded metropolitan areas. However, the occurrence of a tunnel fire incident is an issue of great importance in several aspects since it jeopardizes a tunnel's safety and, therefore, the implementation of specific fire protection means regarding the construction and operation of a tunnel network, is fundamental. The gravity of fire incidents lies in the severe consequences they may entail, like the considerable amount of economic losses, potential deterioration of the tunnel's integrity, physical injuries, or even casualties. Owning to the confined space, fire incidents can be more grave and difficult to be contained, in terms of fire growth rate, resulting temperature distributions and combustion product concentrations within the tunnel, compared to equivalent phenomena in open fires.

Figure 2.1. Burning HGVs in the fire incident of Gotthard Tunnel, leading to the death of 11 people, in Switzerland, 2001.

In the light of recent statistics, the accident rates in road tunnels are higher than the respective ones in motorways (Caliendo and Guglielmo, 2012). However, multiannual incident analyses indicate that the frequency of fire incidents is significantly lower than the frequency of non-fire related incidents (Ren et al., 2020; Borghettia et al., 2020). Considering the very own nature of a tunnel's structure, in general, in conjunction with the constantly growing number of operational road tunnels existing in the international road network and the ever-increasing traffic density, the possibility of fire incidents inside a tunnel demands particular attention. Indeed, severe and fatal accidental fires in tunnels have occurred, since the entry into service of tunnel structures, as depicted in Figures 2.1 to 2.4. Table 2.1 offers an extensive review of tunnel fire incidents that have taken place over the last twenty years worldwide. More details of tunnel fire accidents since 1949 are available online, in various Tunnel Fire Databases and accidents reports, as established for example in the Table 2.1 references. The relatively modest number of severe fire incidents in road tunnels occurred worldwide, presented in Table 2.1, can be attributed to the rather cautious driving behaviour of tunnel users in association with the controlled prevailing conditions inside the tunnel which allow further advantages over the open road.

Figure 2.1. A tour bus caught on fire at San Bernardino Tunnel, in Switzerland, 2017.

With respect to these and previous events, several full-scale and reduced-scale tunnel fire tests (Section 3.1), as well as numerical simulations (Section 3.3) have been performed, a posteriori, to specify the key fire characteristics and critical parameters in order to optimize fire safety guidelines for these occasions. It is apparent that this type of fire incidents do not only constitute a significant challenge at present, but they may lead to adverse prospects in the future in the view of the constantly increasing complexity and number of operational tunnels and traffic densities. In the light of both theoretical predictions and actual data, this chapter aims to present a summery that includes the main existing fire and smoke related phenomena, based on findings of actual fire incidents or experimental tests. A better understanding of the main characteristics of the fire development inside a tunnel is imperative, besides educational or research purposes, in order for the tunnel's personnel, fire fighters and motorists to be able to cope with the situation properly, when necessary.

Figure 2.4. Newhall Pass (I-5), Fire at tunnel exit on October 12, 2007, USA.

According to Table 2.1, vehicle collision is a major origin of fire incidents in road tunnels resulting in multiple injuries and even fatalities. It is widely known that human behaviour holds an integral role in every car accident, in general, contributing to the level of severeness of the incident. However, it must be noted that even if the main source of most collision cases is identified to be the drivers' behaviour and interaction, this cannot necessarily be attributed to human error or incautious driving behaviour, since insufficient lighting, road surface's wear or other factors may hinder the driving conditions. In any case, most tunnel fires have started as a consequence of a collision. It is estimated that less casualties would have occurred in many fire incidents, if the drivers and passengers had immediately evacuated their vehicles and moved hastily towards the nearest emergency exit, avoiding the toxic effluents of the fire and the rising temperatures. Mechanical or electrical vehicle failures appear to account for numerous fire incidents as well. A less frequent, but with a higher potential for hazardous consequences, cause of fire incidents is arson attacks.

Figure 5.4. Three people lost their lives and other forty-three were injured in multiple expressway pileups, at Samae Tunnel fire, 2020.

One of the primary lessons to be considered from all of the above categories of fire incidents in road tunnels is that a more enhanced and in depth understanding of tunnel emergency situations would have proven a crucial determinant in fire safety scenarios, particularly in long and complex road tunnels. Therefore, a comprehensive framework for tunnel design and operation should be established accounting for human behaviour and the level of knowledge regarding tunnel emergency situations. However, at present, very little is known about human behaviour in emergency situations in tunnels. This limited knowledge has been derived from actual fire incidents or experimental testing under controlled conditions, which due to the rising ethical considerations for those testing procedures, render these findings rather non representative. Furthermore, despite the source of the actual fire incident, the consequences of the fire may be magnified by the appliance of inappropriate ventilation strategies or delayed response time. For example, adopting a tactic of either supplying fresh air to the fire or extracting smoke through the existing mechanical ventilation system is a multivariate decision which depends on several parameters in each fire situation, including the fire size, the fire source location and the region of the higher traffic density within the tunnel. So, every fire scenario requires a specialized approach, concerning the imposed ventilation conditions. Without a doubt, the response time in such an emergency, determines the development and the magnitude of severeness, in general, of the entire situation.

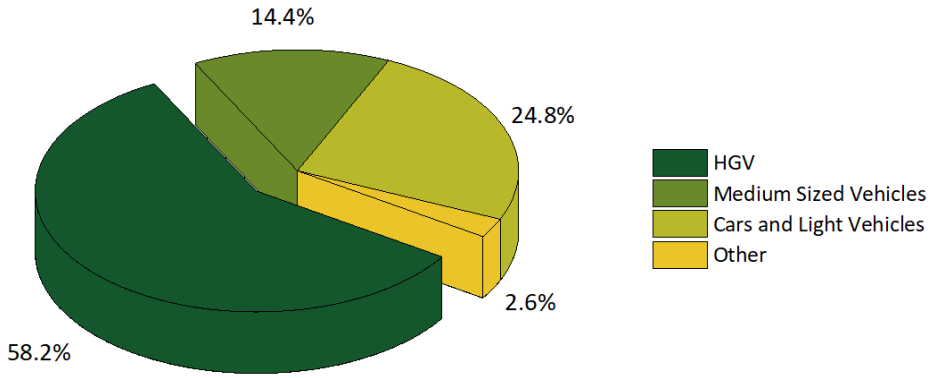

Figure 2.5. Vehicle types involved in fire accidents, as reported by a multiannual survey on the Chinese transportation network (Ren et al., 2020).

The most common vehicle type involved in fire incidents is the Heavy Good Vehicles (HGV), according to a multiannual survey on the Chinese transportation network (Ren et al., 2020). This type of vehicles can create a fire of several MWs and thereby the occurrence of a fire incident inside a tunnel that includes those vehicles is often characterized as the worst-case scenario. Other vehicles such as cars or motorcycles (Light Vehicles), lorries and buses (Medium Sized Vehicles) tend to also participate in road fire situations, as depicted in Figure 2.5. In fact, the reported fire incidents indicate that despite the type of vehicles engaged in the initial incident, a fire can still expand to several MWs via the contribution of additional multiple vehicles to the available fire load. Large fires caused by multiple vehicle collisions or involvement of vehicles with hazardous materials directly aggravate fire-fighting procedures which often last several hours while rendering evacuation operations and attempts more challenging. Additionally, the vast majority of fire incidents in either road or rail tunnels, that have resulted in multiple casualties, have been observed at particularly long tunnels or at tunnels with complex configurations, where evacuation and firefighting procedures were extremely difficult. An illustrative example is the funicular railway fire incident in the Austrian Alps in 2000, as portrayed in Figure 2.6, where more than 150 people have lost their lives trapped in an intense fire or by the buoyant toxic smoke flow while attempting to escape moving upwards to the ascending tunnel. Particular attention and thorough evaluation should be also attributed to future infrastructure projects such as the undersea road tunnel, in Western Norway, Figure 2.7, in advance regarding fire and rescue services due to the complex

tunnel configuration established underwater. As expected, the consequences of an intense fire in such structures could be catastrophic if the fire technical specifications are poorly defined. Concluding, both the size of the fire and the tunnel's configuration in general, contribute essentially to the overall fire incident and its magnitude of severity. However, in the review of fire accidents in Table 2.1, one may identify serious fire incidents in relatively short tunnels, as well. Furthermore, through the following database of fire incidents it is demonstrated that an emergency situation may arise in tunnels which are already in operation, but also during the excavation and construction phase, or repair and refurbishment procedures. During the construction or repair phase, evacuation strategies and paths are often limited or possibly not even constructed yet, while fire loads of several MWs may occur, requiring particular emergency response methods.

Figure 2.6 Picture of a funicular railway incident, in the Austrian Alps, where more than 150 people have lost their lives in an intense fire, in 2000.

As shown in Table 2.1, fires in tunnels constitute an international problem. Report findings indicate that while fires in metro rail tunnel fires have led to a larger number of fatalities per incident, fires in road tunnels tend to occur more often and on a systematic basis (Krausmann and Mushtaq, 2005). For that reason, constantly evolving fire safety designs are required for road tunnels with the aim of reducing the risk of fatalities. The lack of further serious incidents in recent years is possibly owned to the advance of safety features and more thorough and strict regulations regarding tunnel safety that are already in use. Additionally, the level of awareness amongst tunnel users regarding safety issues has been elevated as well, whereas the driving behaviour within the tunnels has been improved, since drivers have become acquainted with the tunnel's terrain. Nevertheless, considering that the number of potential victims in a tunnel fire, due to the long and confined space, significantly outnumbers the overall death toll of a respective accident in the open road it is imperative that fire safety regulations be considered and applied at the design stage of the tunnel's construction, and not later as an 'add on' after the occurrence of a fire incident as it is ill-advised to "anticipate" a disaster occurrence over pursuing to avoid such events in the first place. A common international certified database of fire incidents in tunnels should be created as part of future initiatives which will offer valuable insights to such incidents to the wide population, allowing for constant updating of data reports.

Figure 2.7. Future project of submerged floating tunnels in Western Norway (https://www.ctif.org/news/explosions-fire-and-overload-biggest-challenges-norway-builds-worlds-first-floating-tunnel).

Table 2.1. Review of fire incidents in road tunnels of the last twenty years.

Year	Location of the Tunnel	Tunnel's Length	Cause of the Fire	Casualties/ Injuries	References
2000	Seljestad Tunnel Norway	1.3km	Multiple Vehicle Collision	0 / 6	Maevski, 2011
2000	Rotsethhorn Tunnel Norway	1.2km	Collision and Fire	2 / 0	Beard and Carvel, 2005
2001	St. Gotthard Tunnel Switzerland	16.9km	HGVs Collision	11 / 0	Maevski, 2011
2001	Gleinalm Tunnel Austria	8.3km	Collision	5 / 4	Maevski, 2011
2001	Prapontin Tunnel Italy	4.4km	Spontaneous combustion	0 / 19	Maevski, 2011
2001	Madaoling Tunnel China	-	Engine Fire	12 / 6	Ren et al., 2020
2002	A86 Road Tunnel France	0.6km	Construction turnover	2 / 0	Maevski, 2011
2002	Roppener Tunnel Austria	5.1km	Motor Fire	0/ 2	https://tunnelsmanual.piarc.org/sites/tunnels/files/public/wysiwyg/import/Chapters%20PIARC%20reports/2006%2005.16.B%20Table%202.1.pdf
2002	Maoliling Tunnel China	3.7km	Engine Fire	-	Ren et al., 2020
2003	Vincenza Italy	0.6km	Bus turnover	6 / 50	Vianello et al., 2012
2003	Fløyfjell Tunnel Norway	3.1km	Collision	1 / 0	https://vegvesen.brage.unit.no/vegvesen-xmlui/handle/11250/190129
2003	Shidaoshan Tunnel China	-	Spontaneous Combustion	-	Ren et al., 2020
2003	Baregg Tunnel Switzerland	1.4km	Collision	2 / 21	Maevski, 2011
2004	Dullin Tunnel France	1.5km	Engine Failure	-	Beard and Carvel, 2005
2004	Niuguantou Tunnel China	-	Spontaneous Combustion	-	Ren et al., 2020

2004	Baregg Tunnel, Switzerland	1.1km	Multiple Vehicle Collision	1 / 1	Beard and Carvel, 2005
2005	Frejus France -Italy	12.9km	Car Accident	2 / 21	Maevski, 2011
2005	Highway tunnel on B31, Germany	0.2km	Collision	5 / 0	Beard and Carvel, 2005
2005	Channel Tunnel UK	During Construction	Explosion	2 / 0	Beard and Carvel, 2005
2005	Feiluanling Tunnel China	-	Brake Failure	0 / 8	Ren et al., 2020
2006	Viamala Switzerland	0.8km	Car & Bus Collision	9 / 6	Maevski, 2011
2006	Eidsvoll Tunnel Norway	1.2km	Car & Fuel Tanker Collision	1 / 1	Beard and Carvel, 2005
2006	Wenquan Tunnel China	-	Truck tire burst into flames	-	Ren et al., 2020
2007	Burnley Tunnel Australia	2.9km	Multiple Vehicles Collision	3 / 0	Maevski, 2011
2007	Santa Clarita I-5 US / Canada	0.2km	Collision and Fire	3 / 23	Maevski, 2011
2007	San Martino Italy	4.8km	Collision and fire	2 / 10	Maevski, 2011
2007	Ehrentalerberg Tunnel Austria	3.3km	Collision	0 / 12	Vianello et al., 2012
2007	Chongqing University city Tunnel, China	3.8km	Technical problems	0 / 6	Ren et al., 2012
2007	Newhall Pass Tunnel USA	166m	Multiple Vehicle Collision	3 / 23	Beard and Carvel, 2005
2008	Ofenauer Austria	1.4km	Collision	0 / 17	Vianello et al., 2012
2008	Dabaoshan Tunnel China	3.4km	Collision and fire	2 / 0	Ren et al., 2020
2009	Gubrist Switzerland	3.2km	Collision and fire	0 / 4	Maevski, 2011

2009	Arlberg Austria	13.9km	Collision	1 / 2	Vianello et al., 2012
2009	Qinling zhongnanshan Tunnel China	-	Truck	-	Ren et al., 2020
2009	Eiksund Tunnel Norway	7.7km Underwater Tunnel	Collision	5 / 0	Maevski, 2011
2010	Huishan Tunnel China	-	Arson	24 / 19	Bai et al., 2020
2010	Zhujiayan Tunnel China	1.3km	Collision	2 / 0	Ren et al., 2020
2010	Wuxi Lixu China	10.9km	Bus Fire	24 / 19	Maevski, 2011
2011	Xinqidaoliang China	-	Shunt	4 / 1	Ren et al., 2020
2011	New Qiaoliang Tunnel China	4km	Collision	4 / 0	Bai et al., 2020
2011	Futuyu No.5 Tunnel China	-	Collision	15 / 3	Bai et al., 2020
2012	Xueshan Tunnel China	12.9km	Collision and fire	2/ 31	Bai et al., 2020
2013	Liushiliang Tunnel China	-	Multiple Car Collision	6 / 2	Ren et al., 2020
2014	Yanhou China	-	Collision	40 / 12	Bai et al., 2020
2015	Fenghuangshan Tunnel China	0.8km	Collision and fire	-	Ren et al., 2020
2016	Mangshan Tunnel China	1km	Collision and fire	1 / 0	Ren et al., 2020
2017	Tao Jia Kuang Tunnel China	-	Arson	12 / 1	Bai et al., 2020
2017	San Bernardino Switzerland	6.6km	Bus Crash	-	https://www.dw.com/en/san-bernardino-bus-crash-causes-switzerlands-longest-traffic-jam-in-19-years/a-43857500

2018	Detroit-Windsor Tunnel Canada	1.6km	Collision	0 / Multiple	https://www.cbc.ca/news/canada/windsor/multiple-people-sent-to-hospital-accident-tunnel-1.4961987
2019	Maoliling Tunnel China	3.7km	Spontaneous Combustion	5 /36	Bai et al., 2020
2019	Rannersdorf Tunnel Austria	1.9km	Wheel Failure	-	https://dev.tunprotec.com/storage/documents/rannersdorf-tunnel-hgv-fire-may-pdf.pdf
2020	Samae 2 Tunnel Korea	-	Collision and fire	3 / 43	https://en.yna.co.kr/view/AEN20200217009953315
2020	Sydney Harbour Tunnel Australia	2.3km	Spontaneous Combustion	-	https://www.smh.com.au/national/nsw/sydney-harbour-tunnel-closed-after-car-fire-20200825-p55p15.html

2.2 General Characteristics

In general, the main fire and smoke characteristics that have been observed due to fire physics from actual tunnel fire accidents and experimental tests are governed by certain principles, while the tunnel's usage or its geometrical complexity formulate the "framework" for each scenario. In particular, factors such as the tunnel's length, the cross-sectional geometry and the longitudinal inclination are evidently important, affecting both the prevailing ventilation conditions within the tunnel and the total fire development. Tunnel fires, like compartment fires, are defined by the strong interaction of the fire with the surrounding environment, due to the enclosed nature of each space. The confined terrain generates a consistent heat feedback to the fuel surface of the fire source and to the smoke layer, augmenting the fire related phenomena which are enhanced by the temperature rise while speeding up the combustion processes. This fundamental redistribution of heat is essential for the general characteristics of the fire inside the tunnel in contrast to open fires where the concentration of the toxic effluents from the fire along with the high temperatures of the smoke layer are discharged to the ambient environment. In addition, the use of ventilation systems of certain configuration and capacity, in conjunction with the resulting available ventilation strategies, offer an important tool in the field of fire and smoke control. The number and type of vehicles involved in the fire, the intensity of traffic inside the tunnel, along with the presence of blockages near the induced fire may also have a key role in determining the magnitude of the fire incident. The number and type of burning vehicles constitute the existing fire load, while the traffic density along with the relative distance between the fire and the other vehicles contribute to the potential fire load within the tunnel and the propagation of smoke, since they act like obstacles blocking the transit flow.

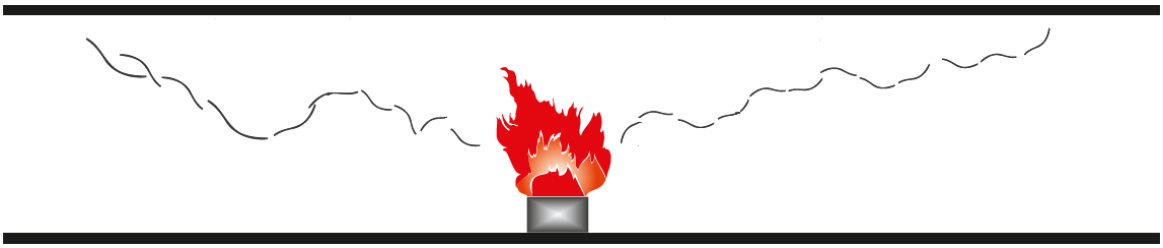

Figure 2.8. Smoke propagation, at the early stages of a tunnel fire, under low or no ventilation conditions.

A fire occurring inside a tunnel interacts vigorously with the ventilation airflow, giving rise to the development of complicated turbulent air flow patterns, especially in the vicinity of the fire source. In fact, when fresh air is supplied towards the fire source, it is practically conducive for the development of the fire. The supply of oxygen facilitates the combustion processes, preserving or even enhancing the fire growth rate. The air supply in a tunnel structure can be created naturally, owing to pressure differences between the portals or by the pressure differences between the hot fire gases and the prevailing airflow within the tunnel. A characteristic example of a tunnel structure with different pressure conditions at both ends, is a tunnel with a longitudinal inclination where the two portals are located at different altitudes. In these cases, where a longitudinal slope exists inside the tunnel, buoyancy forces are automatically formed along the tunnel, governing the movement of air and hot smoke, especially in cases when no additional ventilation is applied. The combination of the meteorological conditions at the entrance and exit of the tunnel along with the size of the fire which induce the pressure differences between the hot fire gases and the prevailing airflow within the tunnel, comprise the main factors that directly form the natural ventilation conditions within the tunnel. Additionally, the relative fire source location inside the tunnel and the geometry of the tunnel in general (length, cross-sectional layout) also contribute to the characteristics of the developing airflow. Therefore, the main challenge of natural ventilation in

tunnels, not only regards the wind and atmospheric conditions outside the tunnel's portals but also lies on the inclination and the general geometry of the tunnel which may strongly influence the entire developing airflow. Nevertheless, even when low velocities via a mechanical ventilation system are implemented, drastic changes may still occur in the airflow pattern inside the entire tunnel, due the buoyancy forces from the tunnel's slope.

The development of a fire within a tunnel under natural ventilation is accompanied by the formation of an intense smoke flow right above the fire source. Due to the high temperatures of the combustion gases, thermal buoyancy forces emerge, elevating the flow of smoke towards the tunnel's ceiling. When no ventilation conditions exist within the tunnel, the combustion products from the fire impinge on the tunnel's ceiling right above the fire source and then the smoke flow splits, creating two diverse longitudinal flows traveling towards both the tunnel's portals, Figure 2.8. Progressively, increasing the distance from the fire source, these layers become thicker but less uniform, due to the entrainment of fresh air to the smoke flow, and they eventually descend towards the tunnel's floor. The above-mentioned behaviour is established when there is no inclination in the tunnel configuration, since the existence of a slope would entail buoyancy forces which would progressively create an additional ventilation airflow.

However, the effect of natural ventilation in a fire incident and the uncertainty regarding the smoke distribution that this scenario entails, pose a severe hazard, since toxic gases from the fire are rapidly spreading away from the fire without a control mechanism to create a "safe" route for evacuation or to discharge the combustion products. Unexpected changes in the airflow may also occur due to pressure changes inside and outside the tunnel, which significantly affect the ventilation conditions when the tunnel is only naturally ventilated. In this context, combining the knowledge of the underlying ventilation conditions that prevail outside the tunnel and the tunnel's geometry with the appliance of a mechanical ventilation system inside a tunnel, may offer a great advantage in terms of fire and smoke control. The benefits from mechanical ventilation are apparent also in the combustion efficiency, since a lower concentration of toxic gases is produced from the fire, and in the distribution of heat and smoke inside the tunnel. Although the combustion efficiency enhancement results also in an increase of the fire's heat release rate, the forced longitudinal ventilation is important and necessary to prevent the smoke adverse flow in most tunnel fires.

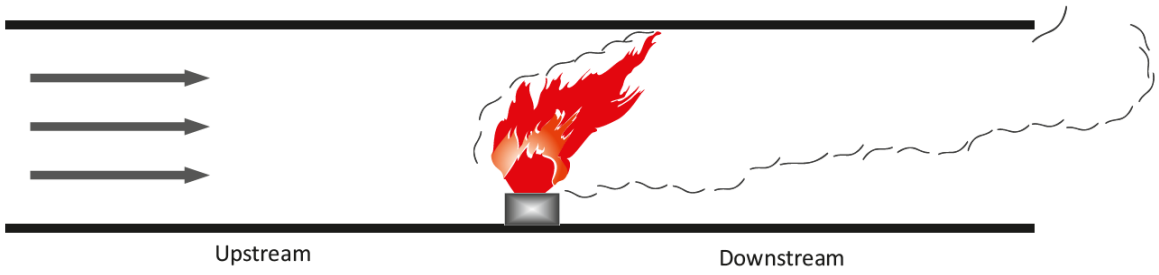

Figure 2.9. Smoke propagation in a tunnel fire under forced ventilation.

The presence of a stronger airflow, either naturally induced due to slope or forced owning to a mechanical ventilation system, directly affects the smoke stratification characteristics. In general, the main smoke flow shifts to the direction dictated by the governing airflow, Figure 2.9. The strong imposed airflow pushes the stratified layer on one side of the fire and in that manner the smoke tends to scatter more easily, covering even the whole cross-sectional area of the tunnel, under robust ventilation velocities. Therefore, downstream from the fire there may not even be present the two distinct layers of smoke and air - the "smoke" one established near the ceiling and the

“air” one located just above the floor - since these layers tend to merge and create a less uniform flow of combustion products. If the ventilation velocity is not high enough, an adverse smoke layer will continue to exist at the upstream side of the fire. This phenomenon is widely known as the “backlayering” effect.

Backlayering, also known as backflow, refers to a condition where the hot gases from the fire floe not only towards one of the tunnel portals, downstream of the fire source, but “turn back” and flow in the upstream direction as well. When the longitudinal wind speed is equal or higher than the critical wind speed, the hot combustion products will only spread in one direction, Figure 2.9. Thus, when efficient longitudinal ventilation is established and the smoke is being forced to follow a route towards only one portal of the tunnel, a smoke-free path can be created for evacuation and the fire brigade personnel. However, if the ventilation velocity is not high enough, backlayering occurs, leading to high concentrations of toxic smoke and an increase of the heat fluxes in the emergency route, as well. The key role of the applied air velocity inside the tunnel, regarding the development of smoke distribution, is therefore apparent, in a road tunnel fire incident.

In this context, a large amount of fundamental research is also devoted to the stratification mechanisms of the transit smoke flow. The smoke spread in tunnels in association with the fire development, is a challenge as there are multiple parameters that effectively affect them. In fact, smoke stratification is directly affected by the existing ventilation velocity and the buoyancy forces due to pressure differences inside the tunnel, as stated before. The latter is the reason why the hot products from the fire are occupying mostly the upper region of the tunnel’s cross-section. Experimental findings from tunnel fires show that at the early stages of fire development, the released smoke from the fire is quite uniform. Especially in the case of natural ventilation, with mild prevailing winds inside the tunnel, the smoke volume flow is expanding at both sides of the fire, forming a jet flow beneath the ceiling. In this case there are two distinct layers in the tunnel’s longitudinal layout. At the lower region fresh air exists, whereas at the upper region a resulting layer of hot fire gases predominates. However, as the distance from the fire source increases, the thermal pressure which elevates the hot gases tends to decrease. When external sources of ventilation, such as jet fans, are present, or buoyancy forces due to tunnel inclination govern the flow, the smoke layer tends to disperse in a more immediate way. This tendency is also observed in the produced smoke when the fire continues to burn over a large period of time, while growing in size. In this case, an increasing proportion of smoke occupies almost the entire cross-sectional area of the tunnel. Evaluation of data from fire incidents and experimental tests indicate that the smoke stratification in under-critical conditions result in a uniform and thick layer of smoke travelling upstream from the fire while its cohesion is diminished at the downstream side. Increasing the ventilation rates, the smoke layer, which exists only in the downstream region from the fire, is difficult to preserve a distinctive stratified form even close to the fire source. The entrainment of fresh air in the smoke layer and vice versa, aggravate the tenability condition at the downstream side of the tunnel since the is no smoke-free path, even at low heights. Based on experimental studies, the entrainment velocity is proportional to the velocity difference between the two layers. Therefore, a grave risk appears for people trapped in the downstream region of the fire, when smoke stratification disappears. This assumption takes for granted that the smoke and gases produced from the fire source consist mainly of hazardous combustion products.

Another issue becoming increasingly important in tunnel fire safety research is the levels of visibility in a tunnel fire incident. The respective analysis is focused on the estimation of the visibility levels, via optical density, since this parameter is highly associated with the smoke propagation and stratification and subsequently with the tenability conditions inside the tunnel. In particular, in a long and confined space, such as a tunnel, where a fire of several MWs may be induced, the concentration of soot particles from the fire may significantly downgrade people’s

visual acuity. In that manner, the walking speed of people will be greatly reduced, since their sense of direction will be gradually diminished. Additionally, as the smoke concentration is getting thicker and more uniform, the tenability limits can be reached, regarding the combustion products that travel within the layer of smoke. One should keep in mind that the main elements forming the tenability levels are asphyxiant and irritant fire effluents, high temperatures and intense heat fluxes as well as visual obscuration. For the above, the main desired outcome from the installation of certain mechanical ventilation installations in tunnels is the establishment of a safe route for people to evacuate without additional hindrance. Hence, adequate knowledge concerning visibility related phenomena is always required in a fire analysis and the factors that affect them shall be submitted under thorough consideration. Although there is no universal way to mathematically determine the correlation between the smoke density and visibility precisely, since the particles forming the smoke have varying sizes, depending on the fuel and the combustion processes, a common approach to estimate the resulting smoke density is to use the extinction coefficient, C_s, defined in Equation (2.1), where I_0 is the intensity of the incident light, I is the intensity of the light through the smoke layer, and L (m) is the path length of the light. The knowledge of the tunnel's geometry, fire size and the governing ventilation conditions is of great importance to obtain a holistic perspective of the visibility-related phenomena, through the distribution and propagation of the smoke flow.

$$C_S = \frac{1}{L} \ln\left(\frac{I_o}{I}\right) \quad 2.1$$

The ventilation conditions inside the tunnel may either facilitate a well-ventilated fire, where the fuel determines the fire's intensity and duration, or an under-ventilated fire scenario where the air, and most specifically oxygen supply, is not sufficient. Although most tunnel fires are well ventilated and thus fuel-controlled, there are cases where multiple vehicles are involved in the incident, consuming a large amount of the fresh air supply and after a while, due to lack of oxygen, the combustion process transits to incomplete. As a result, the concentration of the main product of incomplete combustion, Carbon Monoxide, automatically increases; therefore, the concentration of CO is one of the most reliable factors that indicate the ventilation conditions near the fire source. Indeed, oxygen, which is required for the combustion processes, is not abundantly available in many tunnel fire cases, owning to the long and confined space of a tunnel's construction and the governing ventilation conditions, in contrast to an open fire where access to oxygen supply is inexhaustible.

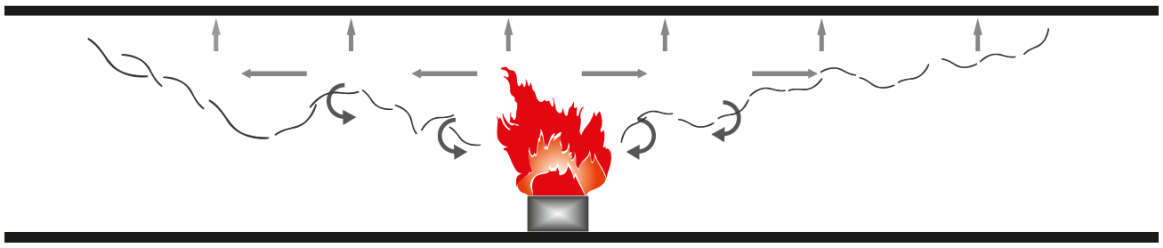

Figure 2.10. Heat distribution from the smoke flow within the tunnel, under natural ventilation conditions.

The flashover phenomenon, observed in other confined spaces like compartment fires, is not likely to occur in a tunnel structure. The lack of potential combustible materials within the tunnel in association with the long space with the openings on both ends result in a negligible possibility regarding the occurrence of a flashover, at least in the traditional form. In addition, owning to the considerable interaction of the fire with the surrounding environment, like the tunnel's lining, and the openings at the portals, considerable heat losses are arising that lead to reduced temperatures throughout the entire tunnel length and thereby, impending even more the possibility of flashover. However, even if a flashover in the conventional form seems to be unattainable, a case of an under-ventilated fire involves the risk of a similar phenomenon. In particular, in an under ventilated fire

it is imperative to be taken into account the influence of a robust ventilation airflow. By supplying a large volume flow of air to the previously incomplete combustion of the fire, the flame may be abruptly magnified and get closer to the preheated vehicles at the direction of the imposed airflow. Certainly, this phenomenon is not comparable with the typical flashover but yet, it may significantly augment the fire related conditions inside the tunnel.

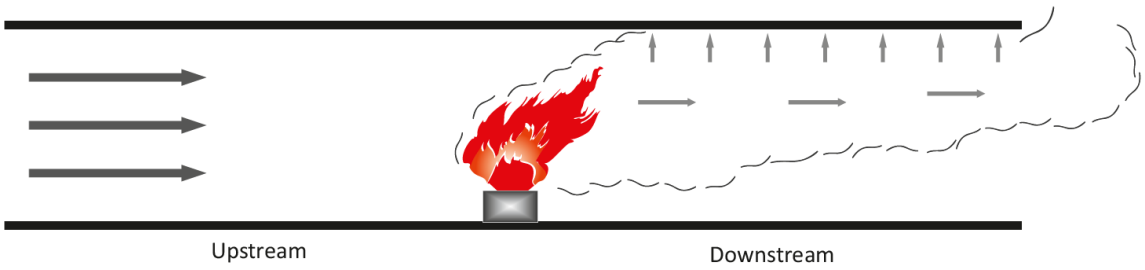

Figure 2.11. Heat distribution from the smoke flow at the downstream area from the fire, under forced ventilation conditions.

Heat transfer in tunnel fires is governed by two fundamental modes, convection and radiation. Convection holds a primal role in heat transfer in a tunnel fire scenario. In fact, the majority of the thermal energy produced in the fire source is conveyed within the tunnel by the motion of the smoke flow. Even if there is no prevailing wind inside the tunnel, e.g. due to mechanical ventilation, an air flow is induced by the fire itself, due to the developing pressure differences. Convective heat transfer requires direct contact between a moving fluid and a solid surface, at different temperatures in order to transmit the heat, Figures 2.10 and 2.11. This heat exchange takes place through the boundary layer. On the contrary, thermal radiation does not involve direct contact; it is defined as a mechanism of energy transfer that enables spatially separated objects at different temperatures to emit heat. In order to obtain a quantitative description of the resulting radiation inside a tunnel, one should consider that all bodies are able to emit energy through electromagnetic radiation. However, the magnitude of the emitted heat mostly depends on the object's temperature and the properties of the radiating surface. In a tunnel fire scenario, one should also keep in mind that the smoke layer is not only responsible for absorbing the heat from the flames and hot surfaces but also to emit and even scatter radiation towards the fuel surface or to other surfaces close to the vicinity, Figure 2.12. Concluding, one of the primal objectives of any fire study is to offer a firm understanding of the physical mechanisms that enable convective and radiative heat transfer in the investigated fire scenario. Only in that manner, the main characteristics of the fire and the developed flow patterns can be adequately described and, thus, analyzed in detail.

A great interest has been attributed to the vicinity of the fire source in the case of a tunnel fire due to the vigorous changes that take part in this area and its dynamic interaction with the entire airflow within the tunnel. The primary interest in every fire scenario is focused on the source of the fire, the relative distance of potential sources of additional fuel and the total amount of fire load "available" within the tunnel. For instance, if a fire is initiated by a car crash to one of the participating vehicles, there is a high potential of fire spreading to vehicles close to the burning one, either directly by flame impingement or progressively by excessive heat transfer through convection and radiation from the initial fire source. The governing ventilation conditions have a direct influence on the fire progression, especially at the early stage of fire development, since their contribution to fire spreading amongst vehicles can be either positive or negative, depending on the intensity and direction of the resulting airflow. As illustrated in Figure 2.9, the airflow can "bend" the fire flames towards the downstream direction. In that manner, the flames may be able to reach the vehicles that stand near the fire and trigger the ignition of another fuel source.

However, even if the flames' length is not long enough to actually reach the other vehicles, as depicted in Figure 2.12, the convectional heat transfer through the outgoing fire products along with the radiation emitted from both the fire and the incandescent particles of smoke, result in preheating the vehicle up to such levels that self-ignition may be caused. This phenomenon can take place when the surface temperature exceeds the pyrolysis temperature of the vehicle's materials, even if combustion processes do not yet exist.

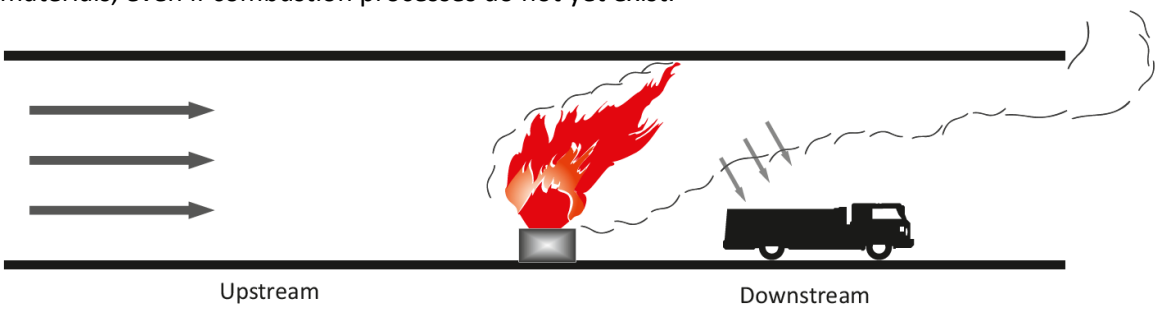

Figure 2.12. A schematic diagram of flame and smoke, preheating a vehicle at a near distance downstream from the fire source, under strong ventilation conditions.

In a naturally ventilated compartment fire scenario, where no additional amount of air is supplied to the fire source, there is a slight chance that the fire may even self-extinguish. This is a highly unlikely situation in a tunnel fire scenario since it requires certain conditions to occur. First, this scenario may regard fires that are controlled by ventilation, and not by fuel, since the depleted amount of oxygen does not favor the combustion processes. Additionally, when the fire is enveloped by air that combines fresh air and combustion products with high concentrations of inert gases, for example CO_2, it may be detained. This prospect mainly regards very long tunnels without a slope, where low natural ventilation conditions from the portals are only available. In that case, the combustion gases travelling on both sides of the fire, may create a recirculation zone at a certain distance and blend with the fresh air at the lower section of the tunnel that provides the fire with oxygen. Consequently, the combustion process may cease as inert combustion products mainly surround the fire source. Nevertheless, fire self-termination is difficult to occur by this adverse flow as it entails that the entire cross-sectional area in that vicinity is filled with smoke, resulting in the fully engulfment of the fire with inert air of a very low oxygen concentration. This, however, is not typically the case when tunnels with one portal available, such as a mine or an under-construction tunnel, are considered. The tenability conditions in these structures, with reduced levels of fresh air stored for human presence and fire development are extremely aggravated, especially if no mechanical ventilation system is applied. In Figure 2.13, the depicted fire tetrahedron reflects the four fundamental elements of a fire. The lack of even only one of them is enough to provoke the self-extinguishing of a fire.

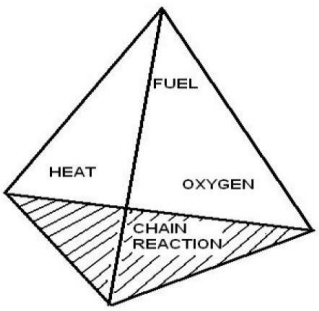

Figure 2.13. "Fire Tetrahedron" stipulating the four main parameters responsible for the initiation and maintenance of the combustion process.

One of the main objectives of fire research is the quantification of the energy released from a fire over a given time period. For this cause, the evaluation of fire development is expressed via the instantaneous Heat Release Rate (HRR) value. The HRR summarizes the energy produced from the fire indicating the level of severeness of a fire. In a tunnel fire where multiple types of vehicles, flammable solid material and liquids may be involved, it is imperative to know the order of HRR and the factors that influence its development. The ignition source, type of material or type of vehicles evidently significantly affect the fire power. The ventilation conditions as well as the tunnel's geometry are directly associated with the fire development, too. While enforcing a certain airflow towards the fire via a mechanical ventilation system, to drive the smoke away, the imposed flow of fresh air automatically supplies the fire source with oxygen, thus enhancing significantly the combustion process. Increasing the airflow velocity will inevitably increase the fire size and thus there should be a thorough tradeoff between the benefits and drawbacks of this approach. The situation may be aggravated when Heavy Good Vehicles are involved in the fire, which implies that the potential stock of fuel is plenty, guaranteeing higher fire load values. Thus, in fire incidents where the appliance of the high ventilation velocities is selected, the tunnel's operator should consider, at first, the interaction of the airflow with the existing fire and its consequences. Additionally, the tunnel's geometry is a fundamental factor, affecting the fire growth. Its influence lies on the way of heat transfer within the structure and the resulting temperature distribution, due to the confined space configuration. Outward airflow patterns, the shape and the relative position of the fire in the tunnel's length and cross section can also alter the development of an on-going fire. It must be noted that the flame length of a fire is directly correlated with the fire size, with increased HRR values resulting in higher flame lengths. Ventilation velocity may also play an important role in the formation of the flame but it is not as dominant as the HRR influence. A large fire under the influence of natural ventilation, in a tunnel with relatively low ceiling height, may cascade to flame existence both on the upstream and downstream direction from the fire source, as presented in Figure 2.14. Accordingly, in case of strong ventilation the flame tends to acquire an approximately horizontal orientation, beneath the tunnel's ceiling, as pictured in the Figure 2.15, threatening with direct impingement or indirect preheating effect the objects and vehicles close to it, at the downstream side from the fire, as displayed in Figure 2.12.

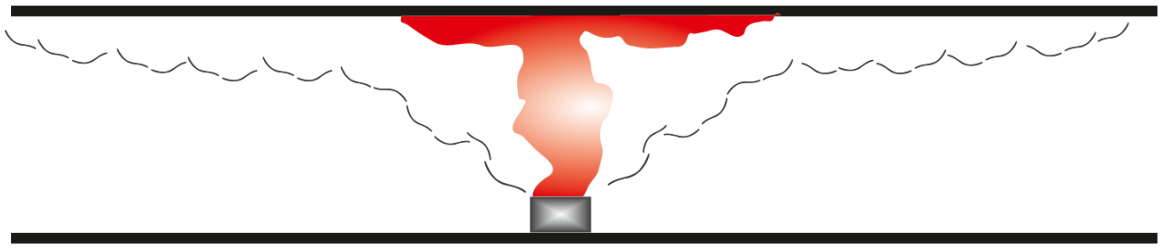

Figure 2.14. Illustration of a large tunnel fire where the flame deflects horizontally at the ceiling at both sides under low ventilation rate or natural ventilation.

The interaction of a tunnel fire with its environment is fundamental as it has a great influence on fire development. According to the governing ventilation conditions, the hot gases produced from the fire source either directly reach the tunnel's ceiling and spread on both sides of the fire, Figure 2.14 under natural ventilation, or they can drift away towards one direction, parallel to the tunnel's ceiling, under forced ventilation, Figure 2.15. Extensive research work has been dedicated, in the assessment of the former cases, to the estimation of the maximum ceiling gas temperature, as well. It is apparent that the lower the ventilation velocity, the higher the maximum temperature beneath the ceiling, provided that there is enough oxygen for complete combustion. When forced ventilation is applied the combustion products diffuse downstream from the fire and get mixed with the layer of fresh air near the floor, resulting in lower temperature values at that area.

Therefore, the hot smoke flow creates the most aggravating circumstances right above the fire source, in case of mild ventilation conditions, Figure 2.8, or near the ceiling close by, if strong ventilation is applied, Figure 2.9. However, the hot layer of combustion products and smoke, heat transfer via convection and radiation to the surrounding walls and other vehicles, in any case, significantly increase the initial temperature of the air and surfaces in that vicinity. Apart from the smoke flow, the fire source surface is gaining heat from the flames' volume radiation, too. Additionally, the portion of radiative heat transfer that does not get absorbed by the tunnel's linings or vehicle surfaces, at the first place, is reflected and impinges, once again, back to the internal tunnel's area, forming an important source of radiation to the combustion zone while reducing the heat losses of the flow. As the fire grows, the temperatures within the tunnel rise, and all the heat transfer related phenomena tend to augment, especially near the fire zone. After a certain time, if the produced layer of smoke from the fire does not get efficiently dispelled by the ventilation and continues to accumulate above the fuel source, thick and uniform, acting like an obstacle and thereby the radiation influence from the near surfaces is depleted.

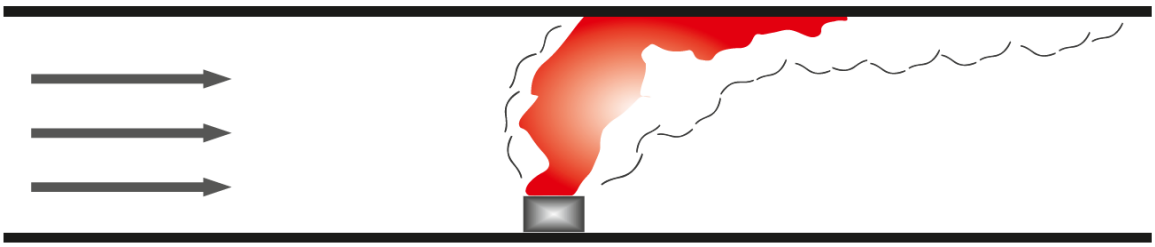

Figure 2.15. A schematic diagram of turbulent flame impinging on the ceiling in a large tunnel fire with forced longitudinal ventilation.

\ire dynamics interact strongly with the fire chemistry related to the type of the burning fuel along with the size and shape of the fire source. A fire inside a tunnel is identified by the highly uncontrollable and incomplete nature of the combustion processes. The development of the fire and its emissions depends on a large number of elementary factors. In particular, the type of fuel along with the ventilation conditions are highly associated with the combustion release energy and the fire effluents. Therefore, knowledge regarding the different products generated during a fire is key matter in estimating the risk level of a tunnel fire accident. The conditions of toxicity within the tunnel along with the level of visibility are directly dependent on the fuel type, the combustion efficiency and the ventilation conditions in the vicinity of the fire source. The main combustion products released from the fire, which comprise the resulting smoke flow, are summarized in Table 2.2.

Table 2.2. Typical combustion products emitted in a tunnel fire.

Combustion Products	
Carbon Monoxide	CO
Carbon Dioxide	CO_2
Hydrogen Chloride	HCl
Sulphur Dioxide	SO_2
Volatile Organic Compounds	VOCs
Polycyclic Aromatic Hydrocarbons	PAHs
Polychlorinated Dibenzo-p-dioxins & Dibenzofurans	PCDDs & PCDFs
Total Unburnt Hydrocarbons	THC
Hydrogen Cyanide	HCN
Soot Particles	Soot

Fire research is focused on the composition of the combustion gases owed to the fact that in many fire accidents inhalation of toxic combustion products is the most common cause for fatalities. The single most hazardous component released from the fire is Carbon Monoxide. Exposure to high concentrations of the above effluent for some time, is highly unsafe and it evidently constitutes the main cause for fatalities in actual fire incidents. Whether the conditions inside the tunnel have a negative impact on the tenability depends also to the concentration of Carbon Dioxide. The presence of this component augments the toxicity of the prevailing smoke flow, as well. In a ventilation-controlled fire scenario, where insufficient air is available for stoichiometric combustion, larger amounts of toxic products are generated as the efficiency of the combustion is reduced due to the incomplete burning processes. As a result, it is apparent that ventilation is a fundamental means to control and enhance the tenability conditions within the tunnel. Furthermore, in tunnel fires, it is imperative to acknowledge the toxic compounds from the combustion of common vehicle fabrication materials and compartments, like for example the upholstering materials, tyres, electrical wiring, dashboards and engines. The effluents derived from a vehicle fire, such as HCl, SO_2, Volatile Organic Compounds, for example, benzene, Polycyclic Aromatic Hydrocarbons (PAHs), and Polychlorinated Dibenzo-P-Dioxins and Dibenzofurans (PCDDs/PCDFs), have a negative impact on both human's physical health and environmental conditions. In the early stages of the fire's development the emitted heat may be the least of a motorist's concerns but, on the contrary, the elevated concentrations of some combustion products such as carbon monoxide and other toxic gases could easily cause deaths on a short time period. As the fire continues to grow the excessively high temperatures as well, threaten the individual's physical integrity and evacuation attempts while low levels of visibility continue to hinder even more the capacity to escape. The combination of the previous factors is responsible for multiple sublethal effects that may lead to life threatening risks. In such conditions one may confront mental and physical incapability, clouding judgment, hesitation, reduced visual acuity, decreased egress movement speed and impaired mobility. Prolonged exposure to toxic gases may progressively bear serious health problems. This issue particularly affects the firefighting personnel.

2.2.1 Backlayering and Critical Ventilation Velocity Correlations

When the ventilation conditions inside a tunnel are relatively weak due to natural ventilation, the smoke flow tends to spread towards both tunnel's portals, downstream and upstream from the fire source. As described in the previous section, the backlayering effect refers, in particular, to the condition where an adverse layer of hot gases from the fire spreads in the upstream direction of the tunnel. With the aim of preventing this phenomenon from happening, a longitudinal wind speed can be applied within the tunnel via a mechanical ventilation system. An indispensable condition, though, to completely hinder the spreading of the hot combustion products in the upstream direction is for the value of the imposed wind velocity to be equal or greater than its critical value. The estimation of that particular "critical" value is at the core of every tunnel fire study as it is directly associated with the facilitation of tenable conditions inside the tunnel for evacuation and firefighting purposes. For that cause, the critical velocity is the single most investigated parameter in tunnel fire research. To choose the appropriate correlation for the ventilation conditions within a particular tunnel, quantitative analysis of fire and fluid dynamics and specific knowledge on the particular fire scenario's details, are required. It is for this reason that the main factors which determine the essential nature of the backlayering phenomenon have been investigated in-depth through both experimental testing and theoretical analysis.

A series of noteworthy tunnel large scale (Hinkley, 1970; Bechtel/Parsons Brinckerhoff, 1995; Lee and Ryou, 2005; Hu et al., 2008; Li et al., 2010) and model scale fire experiments (Thomas, 1968; Oka and Atkinson, 1995; Wu and Bakar, 2000; Lee and Ryou, 2005; Li et al., 2010; Lee and Tsai, 2012; Tang et al., 2013; Yi et al., 2014; Weng et al., 2015; Jiang et al., 2018b; Tang et al., 2018b) and CFD studies (Wu and Bakar, 2000; Hu et al., 2008; Lee and Tsai, 2012; Weng et al., 2015; Li and Ingason, 2017), accompanied by the respective theorical analyses, have been conducted during the last 50 years to investigate the potential crucial factors that directly affect the value of the required critical velocity in a tunnel fire incident. In particular, experimental and numerical findings indicate that the effect of the fire size (Thomas, 1968; Hinkley, 1970; Bechtel/Parsons Brinckerhoff, 1995; Wu and Bakar, 2000; Kunsch, 2002; Hu et al., 2008; Li et al., 2010; Lee and Tsai, 2012; Tang et al., 2013; Yi et al., 2014; Weng et al., 2015; Jiang et al., 2018b; Tang et al., 2018b), fire shape (Oka and Atkinson, 1995) and fire location (Bechtel/Parsons Brinckerhoff, 1995; Oka and Atkinson, 1995) and the ventilation arrangements and strategies (Thomas, 1968; Hinkley, 1970; Bechtel/Parsons Brinckerhoff, 1995; Tang et al., 2013; Tang et al., 2018b) has been proven to be essential in the specification of the appropriate critical velocity. The influence of the tunnel's cross-sectional geometry (Wu and Bakar, 2000; Kunsch, 2002; Kunsch, 2002; Lee and Ryou, 2005; Li et al., 2010; Lee and Tsai, 2012; Weng et al., 2015; Li and Ingason, 2017) and more specifically the influence of its height and width, has been also studied along with the impact of the tunnel's longitudinal inclination (Yi et al., 2014; Weng et al., 2015). The derived results from these experimental and numerical studies have been enriched with the addition of the blockage existence effect near the fire (Li et al., 2010; Lee and Tsai, 2012; Tang et al., 2013). More specifically, the blockage dimensions (Lee and Tsai, 2012; Jiang et al., 2018b) along with the influence of the distance between the fire and the blockage (Lee and Tsai, 2012; Tang et al., 2013) on the critical ventilation conditions have been examined, as well. In this section, after introducing the fundamentals of smoke stratification and its interaction with ventilation conditions, will present several existing correlations for calculating the required critical velocity in a typical tunnel fire scenario, as established during the last 50 years. The investigated correlations for estimating the critical ventilation velocity, along with relevant details, are presented in Table 2.4. Additionally, a comprehensive nomenclature, Table 2.3, is provided, where all the required parameters and quantities involved in the correlations of Table 2.4 are defined.

Tunnel fires constitute a major infrastructure hazard in many aspects, but the key issue in every survey remains the safeguarding of each individual's physical integrity. For this reason, knowledge regarding the impact of the potential fire load in a fire scenario is a primary objective in most experimental testing, including the experimental estimation of the critical velocity. Large scale (Hinkley, 1970; Danziger and Kennedy, 1982) and model scale experimental testing (Thomas, 1968; Oka and Atkinson, 1995; Wu and Bakar, 2000) has been also conducted to gain insights regarding the actual relationship between the critical velocity and HRR, whereas some studies have also accounted for the influence of the fire source size, as well (Oka and Atkinson, 1995). However, it must be noted that various tests have utilized water sprays as fire-fighting systems during the experimental procedures, to protect the tunnel's integrity. This strategy is questionable due to the fact that devices such as water sprays significantly increase the heat losses through the walls, while significantly reducing the convective heat of the smoke flow through the water particles (Lee et all., 1979; Oka and Atkinson, 1995; Wu and Bakar, 2000). In that manner, the test values acquired for the critical velocity could be quite lower than in an actual fire scenario. Furthermore, regarding the relationship between the critical velocity and the induced HRR from the fire, results of almost every relevant experimental study have shown that the resulting critical velocity is analogous to the HRR to the one third power for small and medium fires (Thomas, 1968; Wu and Bakar, 2000; Lee and Ryou, 2005). In other words, by increasing the fire size, the required critical velocity increases as well (Thomas, 1968; Wu and Bakar, 2000; Lee and Ryou, 2005; Hu et al, 2008; Li et al., 2010; Weng et al., 2015). Nevertheless, when the HRR reaches a certain value, the critical velocity

becomes independent of the fire size, since any additional increase to the fire's heat release rate does not result in an alteration of the critical conditions (Oka and Atkinson, 1995; Wu and Bakar, 2000; Krunch, 2002; Li et al., 2010). This change in the interdependence of critical velocity and fire size may emanate from the fact that the flame length of a large fire has grown enough to directly impinge the tunnel's ceiling. In that way the flames are drifting away towards the direction of the implied ventilation, while tangent to the tunnel's ceiling, thus hindering an adverse smoke flow. In total, the former findings indicated that the value of the critical velocity reaches approximately a constant value with increasing HRR, contradicting the initial simple theory proposed by Thomas (1968).

Since the produced effluents and smoke from the fire pose a significant threat to people's physical health, one of the main concerns in this thematic area, is the determination of the appropriate ventilation system for each tunnel structure and, progressively, the optimization of the design of the tunnel's mechanical ventilation system in order to respond sufficiently to every fire emergency scenario. The strong interaction between fire size and longitudinal ventilation conditions is beyond doubt in a fire scenario, and thereby the quantification of this relation has been an issue of key importance in the early stages of the backlayering phenomenon examination. For this particular purpose, the critical Froude number, Fr_c, has been introduced, expressing the ratio of the buoyancy force of the induced smoke flow to the inertial force of the prevailing ventilation airflow (Thomas, 1968). This theoretical approach is utilized several times in the studies that followed (Hinkley, 1970; Danziger and Kennedy, 1982; Kennedy and Parsons, 1996; Hu et al, 2008;). Based on the initial expression, proposed by Thomas (1968), adequate ventilation conditions to completely prevent backlayering from occurring are achieved when the critical Froude number equals 1 (Thomas, 1968). However, later findings from model scale tunnel experiments have indicated that the critical Froude number varies from 4.5 to 6.7 (Lee et al., 1979a,b; Danziger and Kennedy, 1982), when the dimensionless fire size, Q^*, exceeded the value of 1.3 (Kennedy and Parsons, 1996) and thereby a critical Froude Number of 4.5 has been proposed for large fires (Lee et al., 1979; Danziger and Kennedy, 1982; Kennedy and Parsons, 1996; Li et al., 2010) and 1.15 for smaller ones (Li et al., 2010). Therefore, a specific critical Froude number may not be appropriate for the entire range of potential tunnel fire scenarios. Experimental data show that the relation between the ratio of ventilation velocity to critical velocity and the dimensionless backlayering length follows an exponential relation (Li et al., 2010).

In terms of alternative ventilation systems, with different configurations, such as ceiling centralized mechanical smoke exhaust systems, additional research has been required to determine their effect on the efficient air velocity that inhibits the reverse flow of smoke inside the tunnel (Tang et al., 2018b). As an outcome from the utilization of such systems, it has been determined that the required critical velocity tends to drop off with increasing mass flow rates of the mechanical smoke exhaust vents, while the value of the critical Froude number tends to rise for a given dimensionless fire heat release rate value (Tang et al., 2018b). The above findings have been derived with the employment of both ceiling centralized mechanical smoke exhaust vents, for the thermal smoke decay and a longitudinal ventilation system to provide the required airflow within the tunnel (Tang et al., 2018b).

One of the main research goals on this topic, is also the identification of the tunnel cross-sectional geometry influence on the ventilation conditions. Several experimental relationships have been proposed for that cause, accounting for the height, H and width, W of the tunnel. Experimental findings indicate that the tunnel's height mainly influences the vertical smoke flow, while the width of the tunnel has a greater impact on the transverse transportation of combustion products. Based on experimental findings, the tunnel's height has the most important influence among all the tunnel's cross-sectional area dimensions (Oka and Atkinson, 1995; Kunsch, 2000; Li et al., 2010; Li

and Ingason, 2017). In particular, for small fires, the required critical velocity evidently decreases with increasing tunnel height (Oka and Atkinson, 1995; Li and Ingason, 2017), in contradiction to large fire scenarios, where the critical ventilation velocity significantly increases with increasing tunnel height (Oka and Atkinson, 1995; Li and Ingason, 2017). Some researchers claim that in both cases of small and large fires, the critical velocity is independent of the tunnel's width (Oka and Atkinson, 1995) and subsequently they have utilized the tunnel's height as the "characteristic length" (Oka and Atkinson, 1995; Kunsch, 2000; Li et al., 2010), while others insist that the tunnel's width contributes equally to the formation of critical velocity but only for the case of small fires (Wu and Bakar, 2000). Based on the latter findings, increasing the width of the tunnel results in a decrease in critical velocity (Li and Ingason, 2017). In any case, although the relationship between the tunnel's width and the resulting critical velocity is not unambiguous, the fact that the critical velocity varies notably with the tunnel cross-sectional geometry is beyond doubt. Consequently, neither the tunnel height nor the tunnel width alone, is suited for the characteristic length in the assessment of the critical velocity (Wu and Bakar, 2000). Based on that, several studies have adopted as the characteristic length of the tunnel its hydraulic diameter (Wu and Bakar, 2000; Li et al., 2010; Tang et al., 2013; Weng et al., 2015; Li and Ingason, 2017; Jiang et al., 2018b; Tang et al., 2018b). In that manner, the effect of height and width is equivalent in the calculation of the relevant expressions. Additionally, when the influence of the above individual parameters is intended to be investigated , several model-scaled tests have been conducted with fixed tunnel height or width while varying the hydraulic diameter. The drawback of that approach lies on the fact that the hydraulic diameter cannot accurately account for the contribution of the actual tunnel shape. To remedy this problem, another theoretical approach has been proposed (Kunsch, 2002) which has incorporated the tunnel's aspect ratio, A_s. The aspect ratio (tunnel width over tunnel height) is an important factor which mainly affects the growth in a tunnel fire and thereby the visibility levels within the tunnel, but as it regards the critical velocity's value it has no distinct effects (Kunsch, 2002; Ingason and Lonnermark, 2015). However, some researchers claim that the critical velocity increases with increasing height and thereby increasing aspect ratio, due to the more complete fire growth conditions in the extended cross-sectional area (Lee and Ryou, 2003). Apart from the actual HRR value and the prevailing conditions prior to the start of the experiment, the dimensionless HRR, Q^*, utilized by many researchers, may account also for the characteristic geometrical features of a tunnel's structure, which is claimed to be accordingly either the tunnel's height (Oka and Atkinson, 1995; Hu et al, 2008;), the hydraulic diameter (Wu and Bakar,2000; Lee and Ryou,2005; Li et al., 2010; Tang et al., 2013; Weng et al.,2015; Li and Ingason,2017), or the aspect ratio (Lee and Ryou, 2005). However, the aspect ratio expression is strictly valid for only square and rectangular cross-sectional areas.

The requirement for stronger ventilation airflow to preclude the backlayering effect is effectively downgraded as the longitudinal inclination of the tunnel increases (Yi et al., 2014), when the resulting buoyant forces from the inclination are in favor of the implied critical velocity. Otherwise, the value of the critical velocity is increased with increasing slope (Danziger and Kennedy, 1982; Kennedy and Parsons, 1996; Lee and Tsai, 2012; Yi et al., 2014).

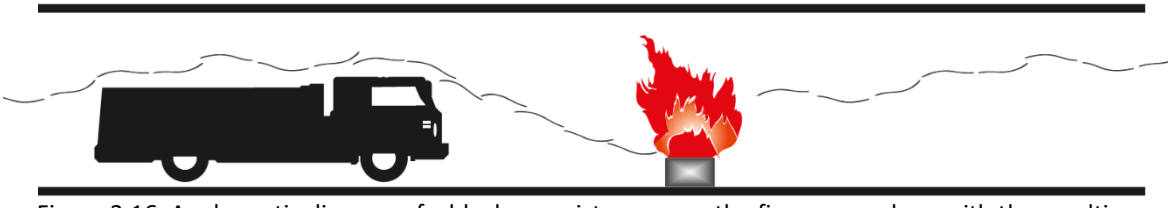

Figure 2.16. A schematic diagram of a blockage existence near the fire source along with the resulting smoke spreading upstream and downstream from the fire.

The performance data indicate that the minimum longitudinal ventilation velocity, that hinders the transportation of the combustion products upstream of the fire, is significantly affected by the existence of some blockage (e.g. vehicle) near the fire (c.f. Figure 2.16). The presence of large objects, like vehicles of various sizes and utilities, near the fire source results in a decrease in the measured critical velocity (Li et al., 2010; Tang et al., 2013), but only when the longitudinal ventilation flow reaches the fires directly. In fact, experimental results indicate that the critical velocity decreases with the increase of the blockage ratio (Li et al., 2010; Lee and Tsai, 2012; Jiang et al., 2018). The reduction rate of critical velocity due to obstruction existence is approximately equal to the aspect ratio of the cross-sectional area of vehicles to the tunnel cross- sectional area (Li et al., 2010; Lee and Tsai, 2012; Jiang et al., 2018). The height of the burning surface and the relevant position of the fire source on the vehicle's geometry along with the relative distance between the fire source and the blockage, consist the main factors that lead to discrepancies in the relationship between the reduction rate of the critical velocity and blockage ratio (Jiang et al., 2018). However, the heat feedback from the surrounding vehicles may contribute to the augmentation of the fire size, and thus the required critical velocity needs to be higher (Lee and Tsai, 2012). The relative distance between the fire source and the existing obstructions affects the critical velocity but holds a secondary role. With increasing distance between the fire source and the blockage, as the obstacle moves further from the main area of influence of the fire, the critical ventilation condition remains unchanged (Tang et al., 2013). With respect to the findings of the above survey, several experimental correlations have been produced for the determination of sufficient ventilation velocity, depending on the fire size, ventilation conditions, the tunnel's cross section and inclination, as well as the presence of obstacles near the fire source. The derived empirical correlations are presented in Table 2.4 with emphasis on the underlying conditions of the fire scenario. The respective nomenclature is presented at the Table 2.3.

Table 2.3 Nomenclature.

Parameter	Quantity	Units	Parameter	Quantity	Units
V_{cr}	Critical Velocity	m/s	W	Tunnel Width	m
V_{cr}^{*}	Dimensionless Critical Velocity	-	L_b	Back-layering Length	m
V_{cr_ob}	Critical Velocity with Blockage	m/s	α	Tangent of The Slope Angle	%
$V_{cr\_ob}^{*}$	Dimensionless Critical Velocity with Blockage	-	A_s	Aspect Ratio	-
V_{cr_slope}	Critical Velocity at a Sloped Tunnel	m/s	Ψ	Blockage Ratio	%
V_e	Ceiling Extraction Velocity	m/s	$\overline{H}$	Hydraulic Diameter of the Tunnel	m
Fr_c	Critical Froude Number	-	S_e	Extraction Opening Area	m^2
Q	Heat Release Rate, HRR	kW	g	Gravitational Acceleration	m/s^2
Q_c	Convective Heat Release Rate	kW	ρ_a	Ambient Air Density	kg/m^3
Q^{*}	Dimensionless Heat Release Rate	-	ρ_f	Smoke Density	kg/m^3
Q^{**}	Dimensionless Heat Release Rate with Ceiling Smoke Extraction	-	C_p	Thermal Capacity of air	$KJ/(kgK)$
A	Cross-Sectional Areal of the Tunnel	m^2	$\Delta\rho$	Density Difference	kg/m^3
A_{ob}	Cross-Sectional Area of the Blockage	m^2	T_a	Ambient Air Temperature	K
H	Tunnel Height	m	T_f	Smoke Temperature	K
H_d	Height from The Fire Surface To The Tunnel Ceiling	m			

Table 2.4 Review of the main Critical Velocity's Correlations.

Correlations for Critical Velocity	Complementary Correlations and Details	HRR	Parametric Study	Comments	References
$V_{cr} = k\left(\frac{gQH}{\rho_\alpha C_p T_f A}\right)^{1/3}$	k is constant derived from experimental testing, which varies with the position and the size of the fire ($k \sim 1$, non-inclined ducts). $Fr_c = \frac{\Delta\rho g H}{\rho_a V_{cr}^2}$	-	HRR, Ventilation Velocity, Duct's Geometry	Derived from: **Model Scaled Experiments** Based on the theory of Froude Number.	Thomas, 1958; 1968
$V_{cr} = K\left(\frac{gQ_c T_f}{\rho_\alpha C_p T_a^2 W}\right)^{1/3}$	$\mathrm{K} = 0.8$ is determined from experimental data of hot smoke layers.	23 to 200kW	Ventilation Velocity, HRR	Derived from: **Large Scale Experiments** With one end of the corridor Closed. Based on the theory of Froude Number.	Hinkley, 1970
$V_{cr} = K_1 K_g\left(\frac{gHQ}{\rho_a C_p A T_f}\right)^{1/3}$	$K_1 = (Fr_c)^{-1/3} = 0.606, Fr_c = 4.5$, $K_g = 1 + 0.0374(grade)^{0.8}$ $T_f = \frac{Q}{\rho_a C_p A V_{cr}} + T_a$	10 to 100MW	Ventilation Velocity, Ventilation Strategies & Systems Configuration, HRR, Slope	Derived from: **Large & Model Scale Experiments** A constant value is assigned to the Froude Number, regardless the fire size.	Danziger and Kennedy, 1982; Lee et all., 1979; Bechtel/Parsons Brinckerhoff, 1995; NFPA 502, 2011
$V_{cr}^* = \begin{cases} V_{cr-\max}^* \left[\frac{Q^*}{0.12}\right]^{\frac{1}{3}}, & Q^* \le 0.12 \\ V_{cr-\max}^*, & Q^* > 0.12 \end{cases}$	$V_{cr-\max}^*$ depends on type of fuel, burner size and position ($0.22 < V_{cr-\max}^* < 0.38$). $Q^* = \frac{Q}{\rho_\alpha C_p T_a g^{\frac{1}{2}} H^{\frac{5}{2}}}$, $V_{cr}^* = \frac{V_{cr}}{\sqrt{gH}}$	2 to 150MW (Scaling of HRR)	Fire Shape, Size & Location, Blockage	Derived from: **Scale-Model Tunnel (1:10)** Employment of Water Sprays	Oka and Atkinson, 1995

$V_{cr} = K_1 K_g \left(\frac{gHQ_c}{\rho_a C_p A T_f} \right)^{1/3}$	$K_1 = (Fr_c)^{-1/3} = 0.606, Fr_c = 4.5$ $K_g = 1 + 0.0374(grade)^{0.8}$ $T_f = \frac{Q_c}{\rho_a C_p A V_{cr}} + T_a$	-	Slope	Derived from: **Scale-Model Experiments**	Kennedy and Parsons, 1996
$V_{cr}^* = \begin{cases} 0.4\left[\frac{Q^*}{0.2}\right]^{\frac{1}{3}}, & Q^* \le 0.2 \\ 0.4, & Q^* > 0.2 \end{cases}$	$Q^* = \frac{Q}{\rho_\alpha C_p T_a g^{\frac{1}{2}} \overline{H}^{\frac{5}{2}}}$, $V_{cr}^* = \frac{V_{cr}}{\sqrt{g\overline{H}}}$, $\overline{H} = 4\frac{A}{X} = 2\frac{WH}{(W+H)}$	1.4 to 28kW- 2.5 to 50MW (Scaling of HRR)	HRR, Cross-Section	Derived from: **Scale-Model Experiments & CFD**, Employment of Water Sprays	Wu and Bakar, 2000
$V_{cr}^* = C_3\sqrt{C_1 \Delta T_o^*}\left(Q^*\right)^{1/3} \frac{\sqrt{1+\left(1-C_2/C_1\right)\Delta T_o^* Q^{*2/3}}}{1+\Delta T_o^* Q^{*2/3}}$	$C_1 = \frac{1-0.1A_s}{1+0.1A_s}\left[1+0.1A_s-0.015A_s^{\,2}\right]$ $C_2 = 0.574\left[\frac{1-0.1A_s}{1+0.1A_s}\right]\left[1-0.2A_s\right]$, $C_3 = 0.613$, $A_s = H/W$, $V_{cr}^* = \frac{V_{cr}}{\sqrt{gH}}$	-	HRR, Cross-Section	Derived from: **Theoretical Analysis & Large-Scale Experiments** Strictly valid for square cross-sections only.	Kunsch,2002
$V_{cr}^* = 0.73(Q^*)^{1/3}, Q^* \le 0.2$	$Q^* = \frac{Q}{\rho_\alpha C_p T_a (A_s g)^{\frac{1}{2}} \overline{H}^{\frac{5}{2}}}$, $V_{cr}^* = \frac{V_{cr}}{A_s^{0.2}\sqrt{g\overline{H}}}$, $A_s = H/W$	2.5 to 12.3kW- 4.4 to 22MW (Scaling of HRR)	Cross-Section	Derived from: **Large Experiments & Scaled-Model Tunnel (1:20)** Strictly valid for rectangular cross-sections only.	Lee and Ryou, 2005
$V_c = \left[C_K g H \gamma Q^{*\frac{2\varepsilon}{3}} \left(gH_d\right)^{\frac{\varepsilon}{3}} \right]^{1/(2+2\varepsilon)}$	$Fr = \frac{V^2}{gH_d}$, $Q^* = \frac{Q}{\rho_\alpha C_p T_a g^{\frac{1}{2}} H_d^{\frac{5}{2}}}$	1.8 & 3.2MW	Mesh Resolution, HRR	Derived from: **Large Scale Experiments & CFD** Valid for relatively small fires.	Hu et al, 2008

$\begin{cases} Q^{*\frac{2}{3}} / Fr^{\frac{1}{3}} < 1.35, \gamma = 1.77, \varepsilon = 6/5 \\ Q^{*\frac{2}{3}} / Fr^{\frac{1}{3}} \geq 1.35, \gamma = 2.54, \varepsilon = 0 \end{cases}$ C_K is an empirical constant $[0.19, 0.39]$ $V_{cr}^{*} = \begin{cases} 0.81 Q^{*1/3} & , Q^{*} \leq 0.15 \\ 0.43 & , Q^{*} > 0.15 \end{cases}$ $V_{cr-ob}^{*} = \begin{cases} 0.63 Q^{*1/3} & , Q^{*} \leq 0.15 \\ 0.33 & , Q^{*} > 0.15 \end{cases}$ $V_{cr\_slope} = V_{cr}(1 + 0.014 \tan^{-1}(a/100))$	$Q^{*} = \dfrac{Q}{\rho_\alpha C_p T_a g^{\frac{1}{2}} H^{\frac{5}{2}}}$, $V_{cr}^{*} = \dfrac{V_{cr}}{\sqrt{gH}}$	0.7 to 23.2kW	Cross Section, Blockage, Slope	Derived from: **Large Scale & Scale-Model Tunnel** Froude Scaling	Li et al., 2010
$V_{cr\_ob} = \dfrac{A(1-\Psi)}{A_{ob}} V_{cr}$		4 to 16kW	Blockage Ratio, Blockage- Fire Distance, Fire Position, Cross Section	Derived from: **Scale-Model Tunnel & CFD**	Lee and Tsai, 2012
$V_{cr-ob}^{*} = \begin{cases} \dfrac{0.4}{\left[\dfrac{A - A_{ob}}{A} + \dfrac{A_{ob}}{A}(0.3L/\overline{H})\right]} \left(\dfrac{Q^{*}}{0.2}\right)^{1/3} & , Q^{*} \leq 0.2, L \leq 3.3\overline{H} \\ 0.4 \left(\dfrac{Q^{*}}{0.2}\right)^{1/3} & , Q^{*} \leq 0.2, L > 3\overline{H} \\ \dfrac{0.4}{\left[\dfrac{A - A_{ob}}{A} + \dfrac{A_{ob}}{A}(0.3L/\overline{H})\right]} & , Q^{*} > 0.2, L \leq 3.3\overline{H} \\ 0.4 & , Q^{*} > 0.2, L > 3\overline{H} \end{cases}$	$Q^{*} = \dfrac{Q}{\rho_\alpha C_p T_a g^{\frac{1}{2}} \overline{H}^{\frac{5}{2}}}$	50 to 100kW 2.8 to 5.6MW (Scaling of HRR)	Blockage- Fire Distance, Ventilation Velocity, HRR	Derived from: **Scale-Model Tunnel (1:10)**	Tang et al., 2013

$V_{cr\_slope} = (1-0.0374a^{0.8})V_{cr}$		92 & 156kW	Slope (-3% to 3%), HRR	Derived from: **Scale-Model Tunnel (1:10)** Froude Scaling	Yi et al., 2014
$V_{cr}^{*} = 0.82Q^{*1/3}$	$Q^{*} = \frac{Q}{\rho_\alpha C_p T_a g^{\frac{1}{2}} \bar{H}^{\frac{5}{2}}}$, $V_{cr}^{*} = \frac{V_{cr}}{\sqrt{g\bar{H}}}$	1.6 to 12.4kW 0.5 to 3.9MW (Scaling of HRR)	Cross-Section Slope HRR	Derived from: **CFD & Scale-Model Tunnel (1:10)** Froude Scaling. Valid for relatively small fires.	Weng et al., 2015
$V_{cr}^{*} = \begin{cases} 0.81A_s^{1/12}Q^{*1/3}, Q^{*} \le 0.15A_s^{1/4} \\ 0.43, Q^{*} > 0.15A_s^{1/4} \end{cases}$	$Q^{*} = \frac{Q}{\rho_\alpha C_p T_a g^{\frac{1}{2}} H^{\frac{5}{2}}}$, $V_{cr}^{*} = \frac{V_{cr}}{\sqrt{gH}}$ $A_s = \frac{H}{W}$	1.6 to 30kW 2.9 to 53.7MW (Scaling of HRR)	Cross-Section	Derived from: **CFD**	Li and Ingason, 2017
$V_{cr-ob} = (1-0.545\Psi)V_{cr}$, $V_{cr\_ob}^{*} = \frac{V_{c-ob}}{(1-0.545\beta)\sqrt{g\bar{H}}}$		2.8 to 5.88kW 5 to 10.5MW (Scaling of HRR)	Blockage Ratio (9.4% to 59.5%), HRR	Derived from: **Scale-Model Tunnel (1:20) Experiments**	Jiang et al., 2018b
$V_{cr}^{**} = \begin{cases} 0.81Q^{*1/3}, Q^{*} \le 0.13 \\ 0.42, Q^{*} > 0.13 \end{cases}$	$Q^{**} = \frac{Q - c_p \dot{m} \Delta T_{\max}}{\rho_a C_p T_a g^{1/2} \bar{H}^{5/2}}$ $\dot{m} = \rho_f V_e S_e$	1.5 to 18kW 2.6 to 36MW (Scaling of HRR)	Fire Size, Ventilation Velocity	Derived from: **Scale-Model Tunnel (1:20) Experiments** Centralized Mechanical Smoke Exhaust & Longitudinal Ventilation	Tang et al., 2018b

3. EXPERIMENTAL TESTS AND NUMERICAL SIMULATIONS

3.1 Tunnel Fire Experimental Tests

A significant number of experimental large-scale fire tests has been carried out in different types of tunnels, since the early 1960s. The observations and the experimental data produced from these tests, have established a broad database of fundamental knowledge regarding fire dynamics in general, as well as specific phenomena related to tunnel fires. The information obtained fosters the level of knowledge on specific issues such as the fire development in different type of vehicles and ignitable materials, the temperature and smoke distribution along the tunnel, the influence of different ventilation systems and the impact of heat exposure on the integrity and mechanical properties of the tunnel construction.

More specifically, a large number of experimental studies have been performed on tunnel fires to investigate thoroughly a range of parameters, such as the temperature distribution along the tunnel (Heselden and Hinkley, 1970; Heselden 1978; Public Works Research Institute, 1993; Pucher K., 1994; Haerter, 1994; Bechtel/ Parsons Brinckerhoff, 1995; Haack, 1998; Ingason and Lönnermark, 2005; Lönnermark and Ingason, 2005; Hu et al., 2005; 2007; Lemaire and Kenyon, 2006; Yan et al., 2006; Lönnermark et al., 2008; Roh et al., 2008; Kashef et al., 2009; Wang et al., 2009; Ingason et al., 2011; 2012; 2015; 2015; Borghetti et al., 2017; Li et al., 2011; Zhong et al., 2011; 2016; Ji et al., 2012; Cheong et al., 2014; Zhang et al., 2015; Liu et al., 2017; Tian et al., 2017; Yan et al.,2017), the Heat Release Rate of the fire (Pucher K., 1994; Bechtel/ Parsons Brinckerhoff, 1995; Haack, 1998; Hu et al., 2005; 2007; Ingason and Lönnermark, 2005; Lönnermark and Ingason, 2005; Lemaire and Kenyon, 2006; Roh et al., 2008; Ingason et al., 2011; 2012; 2015; 2015; Li et al., 2011; Cheong et al., 2014; Borghetti et al., 2017; Liu et al., 2017; Yan et al.,2017), the smoke stratification and propagation (Heselden and Hinkley, 1970; Heselden 1978; Public Works Research Institute, 1993; Pucher K., 1994; Bechtel/ Parsons Brinckerhoff, 1995; Oka and Atkinson, 1995; Ingason and Lönnermark, 2005; Lönnermark and Ingason, 2005; Hu et al., 2005; 2007; 2018; Yan et al., 2006; Wang et al., 2009; Zhong et al., 2011; 2016; Zhang et al., 2015), the radiation (Public Works Research Institute, 1993; Lemaire and Kenyon, 2006; Ingason and Lönnermark, 2005; Lönnermark and Ingason, 2005; Ingason et al., 2011; 2012; 2015; 2015; Yan et al.,2017) and the toxic gases production and distribution (Heselden and Hinkley, 1970; Heselden 1978; Public Works Research Institute, 1993; Pucher K., 1994; Haerter, 1994; Bechtel/ Parsons Brinckerhoff, 1995; Haack, 1998; Ingason and Lönnermark, 2005; Lönnermark and Ingason, 2005; Ingason et al., 2011; 2012; 2015; 2015; Cheong et al., 2014; Borghetti et al., 2017; Xu et al., 2018). Additionally, the fire growth rate (Ingason and Lönnermark, 2005; Lönnermark and Ingason, 2005; Ingason et al., 2011; 2012; 2015; 2015), the Mass Loss Rate (Haack, 1998; Lemaire and Kenyon, 2006; Roh et al., 2008; Yan et al.,2017), heat fluxes (Ingason and Lönnermark, 2005; Lönnermark and Ingason, 2005; Ingason et al., 2011; 2012; 2015; 2015; Cheong et al., 2014), visibility levels (Heselden and Hinkley, 1970; Heselden 1978; Public Works Research Institute, 1993; Pucher K., 1994; Haerter, 1994; Haack, 1998; Ingason and Lönnermark, 2005; Lönnermark and Ingason, 2005; Lemaire and Kenyon, 2006; Kashef et al., 2009; Ingason et al., 2011; 2012; 2015; 2015; Borghetti et al., 2017), the smoke backlayering length (Bechtel/ Parsons Brinckerhoff, 1995; Oka and Atkinson, 1995; Roh et al., 2008), the critical velocity (Bechtel/ Parsons Brinckerhoff, 1995; Oka and Atkinson, 1995; Roh et al., 2008) and several ventilation strategies (Pucher K., 1994; Haerter, 1994; Bechtel/ Parsons Brinckerhoff, 1995; Ingason et al., 2015; Borghetti et al., 2017), as well as the flame length (Pucher K., 1994; Ingason and Lönnermark, 2005; Lönnermark and Ingason, 2005; Ingason et al., 2011; 2012; 2015; 2015; Tian et al., 2017), and fire spread among vehicles (Public Works Research Institute,

1993; Bechtel/ Parsons Brinckerhoff, 1995; Ingason and Lönnermark, 2005; Lönnermark and Ingason, 2005; Ingason et al., 2011; 2012; 2015; 2015), have also been studied.

Figure 3.1. A vehicle fire test in an Immersed Model Tunnel, China (Xu et al. 2018).

The effects of several parameters on the above-mentioned phenomena have also been investigated. Multiple pool fires (Heselden and Hinkley, 1970; Heselden 1978; Public Works Research Institute, 1993; Pucher K., 1994; Haerter, 1994; Bechtel/ Parsons Brinckerhoff, 1995; Haack, 1998; Hu et al., 2005; 2007; 2018; Lemaire and Kenyon, 2006; Yan et al., 2006; Roh et al., 2008; Kashef et al., 2009; Ingason et al., 2015; Zhang et al., 2015; Borghetti et al., 2017; Tian et al., 2017) and simulated vehicle fires tests (Public Works Research Institute, 1993; Pucher K., 1994; Haack, 1998; Ingason and Lönnermark, 2005; Lönnermark and Ingason, 2005; Lemaire and Kenyon, 2006; Lönnermark et al., 2008; Ingason et al., 2011; 2012; 2015; 2015; Cheong et al., 2014; Xu et al., 2018), as depicted in Figure 3.1, have been carried out in experimental tunnels. The location of the fire source (Heselden and Hinkley, 1970; Heselden 1978; Bechtel/ Parsons Brinckerhoff, 1995; Oka and Atkinson, 1995; Yan et al., 2006; Wang et al., 2009; Kashef et al., 2009; Ji et al., 2012; Liu et al., 2017), the fire size (Heselden and Hinkley, 1970; Heselden 1978; Public Works Research Institute, 1993; Pucher K., 1994; Haerter, 1994; Oka and Atkinson, 1995; Haack, 1998; Ingason and Lönnermark, 2005; Lönnermark and Ingason, 2005; Hu et al., 2005; 2007; 2018; Lemaire and Kenyon, 2006; Yan et al., 2006; Roh et al., 2008; Kashef et al., 2009; Ingason et al., 2011; 2012; 2015; 2015; Li et al., 2011; Zhong et al., 2011; 2016; Ji et al., 2012; Cheong et al., 2014; Zhang et al., 2015; Liu et al., 2017; Yan et al.,2017) and shape (Bechtel/ Parsons Brinckerhoff, 1995; Oka and Atkinson, 1995; Ingason and Lönnermark, 2005; Lönnermark and Ingason, 2005; Hu et al., 2007; Ingason et al., 2011; 2012; 2015; 2015) have been also modified in the tests to simulate the heat release rate and the smoke flow patterns in an actual tunnel fire scenario. The impact of ventilation velocity (Public Works Research Institute, 1993; Pucher K., 1994; Haerter, 1994; Bechtel/ Parsons Brinckerhoff, 1995; Oka and Atkinson, 1995; Haack, 1998; Ingason and Lönnermark, 2005; Lönnermark and Ingason, 2005; Hu et al., 2005; 2007; 2018; Lemaire and Kenyon, 2006; Yan et al., 2006; Roh et al., 2008; Ingason et al., 2011; 2012; 2015; 2015; Kashef et al., 2009; Li et al., 2011; Cheong et al., 2014; Zhang et al., 2015; Tian et al., 2017; Yan et al.,2017) and different ventilation strategies (Pucher K., 1994; Haerter, 1994; Bechtel/ Parsons Brinckerhoff, 1995; Yan et al., 2006; Ingason et al., 2015; Borghetti et al., 2017;) on the temperature distribution and smoke spread along the tunnel has also been assessed. Various tunnel geometries have been utilized in these experimental tests (Bechtel/ Parsons Brinckerhoff, 1995; Hu et al., 2005; 2007; Li et al., 2011), providing a large and thorough database of the effects of a long and confined space geometries on fire dynamic phenomena. Table 3.1 and Table 3.2 provide a concise overview of the findings of large- and model-scale tunnel fire tests, respectively.

Compared with reduced-scale models and numerical simulation studies, a full-scale tunnel fire test is, naturally, a more realistic representation of an actual tunnel fire, since it captures the vast majority of fire related phenomena developed in this type of structural geometries (Heselden and Hinkley, 1970; Heselden 1978; Public Works Research Institute, 1993; Pucher K., 1994; Haerter, 1994; Bechtel/ Parsons Brinckerhoff, 1995; Hu et al., 2005; 2007; 2018; Ingason and Lönnermark, 2005; Lönnermark and Ingason, 2005; Ingason et al., 2011; 2012; 2015; 2015; Wang et al., 2009; Kashef et al., 2009; Zhong et al., 2011; 2016; Cheong et al., 2014; Zhang et al., 2015; Liu et al., 2017; Tian et al., 2017; Yan et al.,2017). Additionally, errors due to scaling effects, which may occur in reduced scale model tests, do not emerge in full-scale experiments. However, large-scale testing is expensive, as well as time consuming and logistically complicated to design and execute. More specifically, technical and financial difficulties occur in organizing and performing fire testing of several MWs, as well as in applying and shielding sufficiently the instrumentation through the entire length of the tunnel in such tests. The latter procedure is clearly depicted in Figure 3.2. Consequently, there is a narrow number of real-life, large-scale tunnel fire tests and the probability of adequate repeatability studies is limited. Furthermore, in some cases, the knowledge retrieved from the experimental tests may be even incomplete and the instrumentation installed may be inadequate. Therefore, researchers soon realized the necessity of another source of information, in order to perform comprehensive studies on tunnel fires. A sufficiently reliable and more affordable alternative to large scale fire tests, aiming to gain insights to the fire dynamics phenomena inside tunnels, is small- or model- scale testing. Several model scale tunnel fire tests have also been conducted through the past years, to investigate the characteristics of tunnel fires (Oka and Atkinson, 1995; Yan et al., 2006; Lönnermark et al., 2008; Roh et al., 2008; Kashef et al., 2009; Li et al., 2011; Ji et al., 2012). Although the focus of this chapter is large-scale testing, it must be noted that essential knowledge can be obtained also from intermediate size as well as laboratory testing.

Figure 3.2. Applying fire protection in Runehamar Tunnel Fire Test, during fire tests of several MWs, (Ingason et al., 2011).

3.1.1 Heat Release Rate

The Heat Release Rate (HRR), as well as the fire growth rate and Mass Loss Rate (MLS), depend on various factors, such as the ignition source, the fire size (Heselden and Hinkley, 1970; Heselden 1978; Haerter, 1994; Bechtel/ Parsons Brinckerhoff, 1995; Oka and Atkinson, 1995; Haack, 1998; Ingason and Lönnermark, 2005; Lönnermark and Ingason, 2005; Hu et al., 2005; 2007; 2018; Lemaire and Kenyon, 2006; Yan et al., 2006; Roh et al., 2008; Kashef et al., 2009; Ingason et al., 2011; 2012; 2015; 2015; Li et al., 2011; Zhong et al., 2011; 2016; Ji et al., 2012; Cheong et al., 2014; Zhang et al., 2015; Liu et al., 2017; Yan et al.,2017), the type of the burning

material (Heselden and Hinkley, 1970; Heselden 1978; Haerter, 1994; Bechtel/ Parsons Brinckerhoff, 1995; Haack, 1998; Hu et al., 2005; 2007; 2018; Ingason and Lönnermark, 2005; Lönnermark and Ingason, 2005; Lemaire and Kenyon, 2006; Yan et al., 2006; Lönnermark et al., 2008; Roh et al., 2008; Kashef et al., 2009; Ingason et al., 2011; 2012; 2015; 2015; Cheong et al., 2014; Zhang et al., 2015; Tian et al., 2017; Xu et al., 2018), the length and cross section of the tunnel (Bechtel/ Parsons Brinckerhoff, 1995; Hu et al., 2005; 2007; Li et al., 2011) and the ventilation conditions (Haerter, 1994; Bechtel/ Parsons Brinckerhoff, 1995; Oka and Atkinson, 1995; Haack, 1998; Ingason and Lönnermark, 2005; Lönnermark and Ingason, 2005; Hu et al., 2005; 2007; 2018; Lemaire and Kenyon, 2006; Yan et al., 2006; Roh et al., 2008; Ingason et al., 2011; 2012; 2015; 2015; Kashef et al., 2009; Li et al., 2011; Cheong et al., 2014; Zhang et al., 2015; Tian et al., 2017; Yan et al.,2017).

As a first step of studying different fire scenarios, one ought to define the size, shape and location of the fire source, as well as the heat release rate it produces. The size of the fire has a large impact on the gas temperatures, the smoke stratification, flame length, the emitted radiation and the possibility of fire spread among the vehicles. Specifically, it has been established through experimental research in a pool fire, that the heat release growth rate per unit area increases significantly with the fuel area (Ingason et al.,2015; Yan et al., 2017), whereas the average Mass Loss Rate (MLR) is independent of the pool area (Yan et al., 2017). However, the mass loss rate at high altitude tests, is lower than anticipated (Yan et al., 2017) since the high-altitude environment, exhibiting reduced atmospheric pressure, low air and oxygen density, as well as low temperatures, significantly affects the growth rate and the smoke spread characteristics of a tunnel fire.

The vast majority of real fires inside road tunnels are usually caused by engine failure or vehicles collisions. The main characteristics of these fire depend on the different types of vehicles involved in the incident and the presence or absence of congestion inside the tunnel. The circulation inside a road tunnel may include motorcycles, passenger cars, utility vehicles, buses and heavy goods vehicles (HGVs). It is common for HGVs to have larger dimensions and carry goods which may cause more severe fires compared to normal passenger cars, as it is illustrated in Figure 3.3. Therefore, HGV fires may present a greater threat to life safety and property protection than fires caused by other types of vehicles and thus, this type of vehicles is typically studied as the worst-case scenario in the majority of relevant experimental tests (Haack, 1998; Lönnermark and Ingason, 2005; Ingason and Lönnermark, 2005; Ingason et al., 2011; 2015; Cheong et al., 2014). Even the radiation from the flames produced from such fires can be lethal within the distance of a few meters (Lemaire and Kenyon, 2006).

Figure 3.3. A simulated HGV, consisting of wooden & plastic pallets, utilized in San Pedro Tunnel Fire Experiment, Spain (Cheong et al., 2014).

However, by evaluating up-to-date tunnel fire accident reports, it has been determined that in many cases, a fire can develop up to several MWs, without hazardous materials or HGVs being involved in the incident. Nevertheless, limited experimental research has been conducted in tunnel fires using fire sizes up to 100MW, due to the fact that this type of tests demands increasingly complex logistical procedures to ensure the safe conduction of the experiment, while posing a significant risk to the integrity of the tunnel's construction. In such fire tests, when well ventilated conditions are applied, the maximum heat release rate has been proven to be directly proportional to the burning rate per unit fuel area, the heat of combustion and the total fuel area, provided the fuel is fully involved in the fire (Ingason and Lönnermark, 2005; Lönnermark and Ingason, 2005; Ingason et al., 2011; 2012; 2015; Yan et al. 2017). Additionally, factors such as the thermal inertia, heat of combustion, fuel's pool diameter and mass burning rate per unit area have a large influence on the fire growth rate. Also it has been observed that the heat release rate as well as the fire growth rate increase rapidly from the early stage of an ongoing fire (Lönnermark and Ingason, 2005; Ingason and Lönnermark, 2005; Ingason et al., 2011; 2015). Long flames and high temperatures, owing to large heat release rates, may also result in the fire spreading to other vehicles (Public Works Research Institute, 1993; Ingason and Lönnermark, 2005; Lönnermark and Ingason, 2005).

By comparing the key parameters in pool fires and vehicle fires, it is a reasonable assumption for experimental research to replace burning vehicles with pool fires (Hu et al, 2018). In experimental tests, the real-time MLR of a fuel pool is usually measured by a weighing system with load cells (Bechtel/ Parsons Brinckerhoff, 1995; Roh et al.,2008; Lönnermark et al., 2008; Borghetti et al., 2017) or strain gauges (Yan et al. 2017), as illustrated in Figure 3.4.

Figure 3.4. Weighing system of a fuel pool, in Baimang Snow Mountain No.1 Tunnel Experiment, China (Yan et al. 2017).

Fire detection systems are essential fire protection elements for road tunnels to detect fires, activate safety systems and direct evacuation and firefighting. In general, roadway tunnels are challenging environments for effective operation of fire detection systems, both in terms of technical difficulties in fire detection as well as the environmental conditions under which these systems need to operate. The performance of several fire detection systems, such as air sampling detection systems, linear and spot heat detection systems, field-of-view as well as optical flame and visual-based Video Image Detectors, (VID) detectors, has been investigated under different longitudinal ventilation velocity conditions for various tunnel fire scenarios. In general, the performance of fire detection systems is strongly dependent on the fuel type, the fire size, location and growth rate, as well as the detection method (Kashef et al., 2009). Results of these tests, suggest that it is quite difficult for most detection systems to respond to small fires, located for example underneath an obstruction, such as a fire inside a vehicle (Kashef et al., 2009). In cases like these, the flame and heat produced by the fire are confined by the vehicle body making it difficult for the detectors to promptly detect the fire (Haack,

1998; Kashef et al., 2009). Thus, the response time of detection systems to stationary vehicle fires have been found to be alarmingly slow due to the slow fire growth rate. However, with an increase in fire size, more detectors manage to respond to the fire and the detection times are significantly diminished as well (Kashef et al., 2009). It must be noted that the response time is further delayed under intense ventilation velocity conditions (Kashef et al., 2009).

Tunnel fire tets can be used to evaluate various technical installations, such as ventilation systems. A series of fire tests has been performed to establish realistic fire scenarios, using both pool and vehicles fires, utilizing several ventilation strategies and conditions. It has been found that an increase in ventilation velocity results in increasing heat release rate values and burning rate (Public Works Research Institute, 1993; Haerter, 1994; Ingason and Lönnermark, 2005; Roh et al., 2008; Ingason et al.,2011; 2015; 2015), since the oxygen supply effect prevails rather than the cooling effect as the ventilation velocity increases. In fact, the non-dimensional heat release rate has been proven to be proportional to the non-dimensional critical velocity, in a tunnel fire (Roh et al., 2008). Additionally, the fire growth rate, up to a fire power of 100MW appears to develop approximately linearly, according to research findings and is directly proportional to the ventilation velocity (Ingason and Lönnermark, 2005; Ingason et al.,2011; 2015).

Experimental research has also been conducted to test and evaluate other technical installations, such as the fire suppression systems. Specifically, a series of large-scale road tunnel fire tests has been performed in order to investigate the effects of fire suppression strategies and technical installations, like for example, low-pressure deluge systems, Figure 3.5. Such experimental data provide realistic and in-depth information about the actual effect of low-pressure deluge systems on the heat release rate. Experimental findings indicate that a significant reduction of fire heat release rate can be achieved using a low-pressure deluge fire suppression system, compared to the heat release rate of unhindered burning fires, as long as timely activation of the water is provided (Public Works Research Institute, 1993; Haerter, 1994; Cheong et al., 2014; Ingason et al., 2015). The prompt activation of a deluge fire suppression system is critical, since it helps to reduce the severity of the fire during the fire growth phase (Cheong et al., 2014), especially in cases where HGVs, carrying material with high energy content, are involved.

Figure 3.5. Deluge fire suppression system with standard spray and directional 180° nozzle, used in San Pedro Tunnel Experiment, Spain (Cheong et al., 2014).

3.1.2 Smoke Stratification and Visibility

The size of the fire has a large impact on the stratification of the smoke and visibility inside the tunnel. The larger the fire the deeper and denser the layer of smoke (Heselden and

Hinkley,1970; Haerter, 1994; Yan et al., 2006; Hu et al, 2018). In a real-life tunnel fire incident, a distinct interface appears between the high-temperature smoke and the underlying cold air, since the early stage of fire growth, a phenomenon known smoke stratification (Figure 3.6) (Heselden and Hinkley, 1970; Heselden 1978; Haerter, 1994; Pucher K., 1994; Bechtel/ Parsons Brinckerhoff, 1995; Lönnermark and Ingason, 2005; Ingason and Lönnermark, 2005; Ingason et al., 2011; 2015; 2015 Cheong et al., 2014; Hu et al, 2018). It is well established that increasing the fire size results in intense smoke stratification as well as increasing gas temperatures (Heselden and Hinkley,1970; Heselden 1978; Haerter, 1994; Bechtel/ Parsons Brinckerhoff, 1995; Lönnermark and Ingason, 2005; Yan et al., 2006; Zhong 2011; 2016; Hu et al, 2018). A thinner smoke layer may also appear below the dense layer of stratified smoke, where the smoke diffuses and ends up reaching, in some cases, the tunnel's floor (Heselden and Hinkley,1970; Heselden 1978; Hu et al. 2005; Lemaire and Kenyon, 2006; Cheong et al., 2014; Ingason et al., 2015). This effect is further enhanced when forced ventilation (Hu et al. 2005; Lemaire and Kenyon, 2006;) or fire suppression systems (Cheong et al., 2014) are applied or in the case of closed tunnel portals (Heselden and Hinkley, 1970; Heselden, 1978; Ingason et al., 2015). The smoke travelling speed has also been proven to increase, proportionally with the size of the fire (Heselden and Hinkley, 1970; Heselden, 1978; Ingason et al., 2015).

Apart from creating a high toxic and high temperature environment, the produced smoke greatly affects also the visibility level inside the tunnel, thus threatening the feasibility of an evacuation attempt. Even a relatively small fire can produce a large volume of hot gases and smoke (Heselden and Hinkley,1970; Heselden 1978; Haerter, 1994; Bechtel/ Parsons Brinckerhoff, 1995; Lönnermark and Ingason, 2005; Ingason and Lönnermark, 2005; Lemaire and Kenyon, 2006; Ingason et al., 2011; 2015; Hu et al, 2018). Therefore, there is a great need for further research efforts on the smoke spread dynamics inside tunnels.

A thorough study of the experimental tests performed through the years, suggests that in a fire incident of more than 100MW, smoke volumetric flows are higher than theoretically expected from an early stage of the fire growth (Heselden and Hinkley,1970; Heselden 1978; Haerter, 1994; Bechtel/ Parsons Brinckerhoff, 1995; Lönnermark and Ingason, 2005; Ingason and Lönnermark, 2005; Ingason et al., 2011; 2015; Cheong et al., 2014; Hu et al, 2018). Pulsations of the main airflow may even occur during tests with fires that exceed 130MW (Ingason and Lönnermark, 2005; Ingason et al.,2011; 2015). Additionally, the mass optical density in a tunnel fire, is mainly dependent on the fuel type (Haerter, 1994; Ingason et al., 2011; 2015; 2015). In fact, the mass optical density (MOD) is much higher and approximately constant where a liquid fuel (e.g. Diesel) is used since it produces a large amount of soot (Heselden and Hinkley,1970; Lönnermark and Ingason, 2005; Ingason and Lönnermark, 2005; Ingason et al.,2011; 2015; Hu et al, 2018). In cases using commercial commodities as fuels the mass optical density is far lower. However, in such a case, the MOD is higher at the early stage of the ongoing fire and then decreases to a lower level when the fire becomes fully developed (Ingason et al., 2015). Moreover, according to experimental research, higher smoke transmissivities result in higher visibility and lower smoke concentration (Tian et.al, 2017). In a large tunnel fire, the incident heat flux at the ceiling is often found to be a blackbody with approximately unit emissivity (Ingason et al., 2011; 2015).

When a fire occurs in a high-altitude tunnel the smoke concentration of the area near the fire source increases rapidly, and the visibility within this area reduces faster compared to a fire at the lower altitude (Zhang 2015).If there is no external wind or forced longitudinal ventilation in the tunnel, the buoyancy forces dominate the smoke spread patterns, especially in the vicinity of the fire (Bechtel/ Parsons Brinckerhoff, 1995; Oka and Atkinson, 1995; Zhong

2011; 2016; Yan et al. 2017; Hu et al, 2018). However, at a larger distance from the fire the ventilation velocity is mostly responsible for smoke distribution (Bechtel/ Parsons Brinckerhoff, 1995; Oka and Atkinson, 1995; Zhong 2011; 2016; Tian et.al, 2017; Yan et al. 2017; Hu et al, 2018). In any case, when a fire is located in a sloped tunnel, a natural draught is created due to buoyancy forces, establishing a natural ventilation flow (Bechtel/ Parsons Brinckerhoff, 1995; Zhong 2011; 2016; Yan et al. 2017).

Smoke spread and stratification are not only affected by the fire size; they are influenced by the ventilation conditions as well (Heselden and Hinkley,1970; Heselden 1978; Public Works Research Institute, 1993; Pucher K., 1994; Haerter, 1994; Bechtel/ Parsons Brinckerhoff, 1995; Lönnermark and Ingason, 2005; Hu et al., 2005; Ingason and Lönnermark, 2005; Ingason et al.,2011; 2015; Hu et al, 2018). In fact, smoke layer height and spread have been found to be more affected by the longitudinal air velocity than the fuel type or the HRR of the fire (Heselden and Hinkley,1970; Heselden 1978; Bechtel/ Parsons Brinckerhoff, 1995; Hu et al, 2018), even when the air ventilation velocity is relatively low (Oka and Atkinson, 1995; Hu et al., 2005; Yan et al., 2006; Zhong 2011; 2016; Tian et.al, 2017; Yan et al. 2017; Hu et al, 2018). When the longitudinal wind velocity is lower than a critical value, hot combustion products spread both downstream and upstream of the fire source. The presence of backlayering in tunnel fires is clearly apparent in cases with no forced ventilation (Bechtel/ Parsons Brinckerhoff, 1995; Oka and Atkinson, 1995; Hu et al., 2005; Zhong 2011; 2016).

Figure 3.6. Smoke stratification and propagation, during a vehicle fire, (Xu et al. 2018).

The fire geometry has a relatively minor effect on the critical velocity and the backlayering length. However, if the fire occupies a large proportion of the width of the tunnel, the critical velocities are slightly reduced (Oka and Atkinson, 1995). Solid blockages near the fire result in minor decreases in the critical velocity as well. (Oka and Atkinson, 1995). In addition, the backlayering length is nearly independent of the heat release rate; it is mainly affected by the ventilation velocity (Bechtel/ Parsons Brinckerhoff, 1995; Hu et al., 2005; Ingason et al., 2011; Hu et al, 2018). Experimental results suggest that intense smoke stratification appears in the absence of ventilation (Bechtel/ Parsons Brinckerhoff, 1995; Hu et al., 2005; Lemaire and Kenyon, 2006; Zhong 2011; 2016; Borghetti et al., 2017; Hu et al, 2018), since high air velocities results in increased turbulence and air recirculation, thus promoting smoke destratification (Lemaire and Kenyon, 2006; Borghetti et al., 2017). However, increased turbulence may influence the smoke dynamics, but it does not affect the smoke composition or mean soot particles size (Borghetti et al., 2017). The longitudinal air flow velocity holds a

vital role in the safe walking speed in an evacuation during a tunnel fire. Owing to this, fire-fighting personnel have to keep considerably longer distances from the fire source in still conditions, compared to windy ones, for a safer firefighting performance (Hu et al, 2018). One must take into account that a reduction in the longitudinal airflow velocity may even occur in a large tunnel fire due to flow resistance owned to the fire and hot gases resistances (Ingason et al., 2011 ;2012).

However, forced ventilation conditions may have both positive and negative effects on fire spread (Yan et al., 2006) and thus it should be activated based on the fire position, fire load and evacuation procedures (Public Works Research Institute, 1993; Yan et al., 2006). When a fire occurs, the primary objective of forced ventilation in the stage of evacuation is to control the smoke propagation and to prevent the backlayering of smoke, since the longitudinal wind velocity has evidently a great impact on the development of fire flame, fire plume and the spread of fire (Public Works Research Institute, 1993; Pucher K., 1994; Hu et al, 2005; Lemaire and Kenyon, 2006). In general, proper ventilation can prevent the backlayering of smoke and maintain a clear atmosphere over one side of the tunnel for evacuation. In the stage of firefighting, forced ventilation serves to cause the fire to burn out faster, to allow relatively safe access for fire fighters and to minimize the damage to the structure (Hu et al., 2005).

In a tunnel structure with passive roof openings the majority of the produced smoke is discharged directly off the tunnel through them, so roof openings are favorable for exhausting smoke and reducing the temperature of the combustion products (Wang et al., 2009). However, along with the decrease of smoke temperature, some smoke may backflow and mix with the smoke-free layer below, which may lead in decreasing visibility, thus being unfavorable for personnel evacuation. Therefore, it is suggested to utilize another technical installation for preventing backflow and enhancing the smoke exhausting efficiency of the roof openings (Wang et al., 2009). This phenomenon has also been observed with deluge sprinkler nozzles, which tend to spread smoke, through the water suppression particles, even in smoke-free parts along tunnel (Public Works Research Institute, 1993; Haerter, 1994; Ingason et al., 2015).

3.1.3 Temperature Profiles

Extensive research has been conducted on gas temperatures in tunnel fires (Heselden and Hinkley, 1970; Haerter, 1994; Bechtel/ Parsons Brinckerhoff, 1995; Haack, 1998; Ingason and Lönnermark, 2005; Lönnermark and Ingason, 2005; Hu et al., 2005; 2007; Yan et al., 2006; Lönnermark et al., 2008; Roh et al., 2008; Kashef et al., 2009; Wang et al., 2009; Ingason et al., 2011; 2012; 2015; 2015; Li et al., 2011; Zhong et al., 2011; 2016; Ji et al., 2012; Cheong et al., 2014; Zhang et al., 2015; Liu et al., 2017; Tian et al., 2017; Yan et al.,2017), since the temperature distribution along the tunnel can affect both the physical health of motorists and the integrity of the structure, thus jeopardizing the feasibility of an evacuation attempt (Lönnermark and Ingason, 2005).

The size of the fire has a large impact on the gas temperatures. The increase in the gas temperature is a main aftereffect of the increasing fire size (Heselden and Hinkley,1970; Public Works Research Institute, 1993; Haerter, 1994; Bechtel/ Parsons Brinckerhoff, 1995; Lönnermark and Ingason, 2005; Yan et al., 2006; Zhong 2011; 2016; Hu et al, 2018). Even though, in the vicinity of the fire, the upstream smoke temperatures may be higher than the ones of the downstream flow (Hu et al., 2007) in general, the temperatures in the downstream area, at a certain distance from the fire, are evidently higher compared to the ones upstream

(Bechtel/ Parsons Brinckerhoff, 1995; Hu et al., 2007; Zhang et al., 2015). Moreover, in the upstream side temperature profiles tend to decrease much faster with distance (Bechtel/ Parsons Brinckerhoff, 1995; Hu et al., 2007; Yan et al. 2017). In high-altitude tunnel fires, temperatures near the fire source increase rapidly (Zhang et al., 2015) but decay slower, compared with the corresponding temperatures in lower altitude tunnel fires, leading to a longer burning time period (Yan et al., 2017).

In all experimental studies, the fire source was always located at the longitudinal centerline of the tunnel. In real life incidents, a fire can occur at any location inside the tunnel, exhibiting non-symmetric distances to the sidewalls. However, the transverse fire location seems to have limited impact on the developing temperature profiles, due to the tendency of combustion products to spread "one dimensionally" in the long-confined space (Liu et al., 2017). The maximum smoke temperature rise directly above the fire remains almost unchanged when the fire moves closer to the sidewall until the distance between the fire and the sidewall decreases to a certain value, then the maximum temperature increases significantly, owing to the radiative heat transfer from the wall (Ji et al., 2012).

Experimental findings reveal that even non-hazardous, solid commodities can cause uniformly high temperatures in a shorter than expected time period. In fact, in some cases, the gas temperatures measured by burning solid materials may by comparable to the ones developing in liquid fuel fires (Ingason and Lönnermark, 2005). One of the many hazards that a large HRR fire can pose, is that due to the development of high temperatures, the integrity and mechanical properties of the tunnel construction may be severely affected (Yan et al., 2006; Lönnermark and Ingason, 2005).

The longitudinal wind velocity has a significant influence on the temperature distribution inside the tunnel (Public Works Research Institute, 1993; Yan et al., 2006; Zhang et al., 2015) since it affects the smoke temperature decay velocity, downstream of the fire source (Hu et al., 2007). When the longitudinal ventilation velocity inside a tunnel slightly increases, a significant decrease of the smoke temperature, is observed (Public Works Research Institute, 1993; Hu et al., 2007). In fact, the smoke temperature distribution at the upstream backlayering region appears to be considerably more sensitive to the longitudinal ventilation velocity's variation than that of the downstream flow (Bechtel/ Parsons Brinckerhoff, 1995; Hu et al., 2007).

Temperature is most often measured by utilizing thermocouples or thermocouple trees (Heselden and Hinkley,1970; Bechtel/Parsons Brinckerhoff, 1995; Oka and Atkinson, 1995; Ingason and Lönnermark, 2005; Lönnermark and Ingason, 2005; Hu et al., 2005; 2007; Yan et al., 2006; Roh et al., 2008; Kashef et al., 2009; Wang et al., 2009; Ingason et al., 2011; 2012; 2015; Li et al., 2011, Ji et al., 2012; Cheong et al., 2014; Zhang et al., 2015; Borghetti et al., 2017; Liu et al., 2017; Tian et al., 2017). However, gas temperature measurements using thermocouples can be severely affected by radiation, when the thermocouple read diameter is increased. This effect indicates that the temperature measured by a thermocouple can largely differ from the actual gas temperature, especially inside a confined space, where the tunnel's linings may re-radiate incident heat. Experience gained from tests reveals that the readings of Fiber Bragg Grating (FBG) sensors are more accurate in measuring the actual gas temperatures compared to the measurements using thermocouples of different diameters (Lönnermark et al., 2008). Thus, the longitudinal gas temperatures along a tunnel are often measured by a Fiber Bragg Grating temperature measurement system (Lönnermark et al., 2008; Yan et al. 2017).

3.1.4 Ceiling Temperatures

The excess ceiling temperature profile is one of the main subjects of analysis in many research studies. Maximum ceiling gas temperatures in experimental tests show a very rapid increase after ignition and a tendency to exceed 1000℃ at the full fire growth stage (Public Works Research Institute, 1993; Haerter, 1994; Ingason and Lönnermark, 2005; Ingason et al.,2011; 2015; Cheong et al., 2014). The HRR and the wind velocity inside the tunnel, have a large impact on the location of the maximum ceiling temperature (Haerter, 1994; Haack, 1998; Ingason et al.,2011; 2015; Tian et al., 2017). When the fire size is larger, the smoke temperature below the ceiling is found to be higher, but it decays fast moving downstream the tunnel (Hu et al., 2007). Higher wind velocities tend to move the position of the maximum excess ceiling temperature farther from the fire source (Tian et al., 2017). However, for the same ventilation conditions, larger heat release rates result in the maximum excess ceiling temperature location moving closer to the fire source (Tian et al., 2017). Measurement of ceiling gas temperatures above the stationary vehicles show the existence of a critical ceiling gas temperature where an autoignition hazard may appear (Ingason, et al., 2015). The critical ceiling gas temperature could be much lower if the vehicles or flammable materials are placed at a higher level. The high temperatures produced from a fire with an HRR of more than 100MW can considerably damage not only the entire tunnel ceiling and neighbouring walls downstream of the fire, but also the tunnel's structure upstream of the fire, if backlayering occurs (Lönnermark and Ingason, 2005; Wang et al., 2009; Cheong et al., 2014). However, the ceiling temperature does not always coincide with the maximum temperature of the hot combustion products (Zhong 2011; 2016; Yan et al. 2017) due to heat losses to the tunnel's lining. (Zhong 2011; 2016; Yan et al. 2017; Liu et al., 2017). Additionally, the smoke concentration significantly influences the ceiling temperature decay; higher smoke concentrations resulting in a faster decay of the ceiling temperature (Tian et al., 2017).

In a tunnel fire, when the ventilation velocity is hired than a certain value, the maximum excess gas temperature beneath the ceiling increases linearly with the heat release rate and decreases in the same way with the longitudinal ventilation velocity (Li et al., 2011). If the ventilation velocity cannot reach that value, the maximum gas temperature under the tunnel's ceiling has been proven to be independent of the longitudinal ventilation conditions (Li et al., 2011). According to experimental findings, the fire growth rate is proportional to the ventilation velocity, and thus has an apparent effect on the flame's length (Hu et al., 2005; Ingason et al., 2011; 2015). When the fire flames reach up to the tunnel ceiling, the maximum gas temperature has been found to be constant, since it is independent of both the heat release rate and the ventilation velocity (Oka and Atkinson, 1995; Li et al., 2011). The excess smoke temperature distribution along the tunnel ceiling appears to follow an exponential decay as the longitudinal distance from the fire increases (Hu et al., 2007; Ji et al., 2012). However, the temperature decay rate along the tunnel seems to be much larger in the large-scale tunnel experiments than that in full-scale tunnels (Hu et al., 2007), highlighting the need for cautious scale modeling procedures.

In the presence of roof openings in a tunnel, the maximum smoke temperatures under the ceiling may be lower than 100℃, thus not endangering the tunnel structure. Smoke temperatures at "safety height", which is equal to the height of an average human, also decrease quickly, reaching the ambient temperature, thus enhancing people's evacuation attempts and fire-fighting procedures (Wang et al., 2009). Additionally, Fixed Fire Fighting Systems (FFFS), which comprise mostly water -based systems, have proven to be very effective in lowering the temperatures along the tunnel and prevent fire spread to neighbouring vehicles (Public Works Research Institute, 1993; Lemaire and Kenyon, 2006).

3.1.5 Toxic Gases

The main toxic products generated by an ongoing fire are Carbon Monoxide, (CO), Carbone Dioxide, (CO_2), and soot. In fact, one of the main reasons for fatalities in in road tunnel fires, is very frequently the inhalation of toxic fire gases. Among the fire products, carbon monoxide has proven to be the most hazardous component, since it is responsible for causing physical impairments and even fatalities. Carbon dioxide production is found to be directly proportional to the heat release rate while carbon monoxide production is dependent of the heat release rate, the fuel type, as well as the combustion stoichiometric conditions (Ingason et al., 2011; 2015). The majority of CO is produced during the fire development phase (Ingason et al., 2011; 2015). However, CO concentration decreases sharply with increasing distance from the fire source (Hu et al, 2018).

It is interesting to notice that increasing the ventilation velocity it would be expected to result in stronger dilution of the toxic gases and, consequently, lower concentrations of the combustion products, such as CO. However, in full scale fire tests, it has been observed that the corresponding maximum CO concentration at the downstream side of the fire is considerably higher with increasing ventilation velocity. Therefore, it can be concluded that the underlining presence of a strong turbulence, as well as significant smoke and air recirculation, when the ventilation velocity is increased, result in increasing CO concentrations, at any tunnel section, downstream from the fire (Public Works Research Institute, 1993; Borghetti et al., 2017). Fire suppression systems have been proven to be significantly effective on heat release rate and temperature distribution reduction along the tunnel. However, the influence of low-pressure deluge fire suppression systems on CO production is found to be negative since high CO concentrations have been observed in fire-suppressed experimental tests, indicating incomplete combustion due to the water suppression (Public Works Research Institute, 1993; Haerter, 1994; Cheong et al., 2014; Ingason et al., 2015).

Table 3.1. Main characteristics of full -scale tunnel fire tests.

Test Tunnel Details	Length (m)	Width (m)	Height (m)	Slope (m)	Fuel Type	Peak HRR (MW)	Ventilation (m/s)	Parametric Study	Measured Quantities	References
Railway Tunnel Bridgeton Cross Station to Dalmarnock Station, Scotland	600	7.6	5.2	0.1%	Kerosene	2 - 8	Forced 0.78 - 1.5	Fire Size & Location, Open/Closed Tunnel Ends	T, Optical Density, CO_2, Smoke Spread & Layer Depths	Heselden and Hinkley, 1970; Heselden 1978; Ingason et al., 2015
P.W.R.I Test Tunnel Facility, Japan	700	8.4	6.8	-	Gasoline, Vehicles	-	Forced 0.65 – 5.0	Fuel Type, Fire Size, Fire Fighting Systems, Traffic, Ventilation Velocity	T, CO_2, CO, Visibility, OD, Radiation	Public Works Research Institute, 1993
Kakeitou Tunnel, Japan	3277	8.6	6.7	-	Gasoline, Vehicles	-	Forced 0– 5.0	Fuel Type, Fire Size, Fire Fighting Systems, Traffic, Ventilation Velocity	T, O_2, CO, CO_2, Visibility, OD, Radiation	Public Works Research Institute, 1993
Ofenegg Tunnel, Switzerland	190	3.8	6	-	Gasoline	11 - 80	Natural & Forced 0- 1.7	Fire Size, Ventilation Strategies, Fire Fighting Systems	T, u, O_2, CO, Visibility	Haerter, 1994; Ingason et al., 2015

Zwenberg Tunnel, Austria	390	4.4	3.9	2.5%	Gasoline, Wood, Rubber	8 - 21	Forced	Ventilation Strategies & Systems, Fuel Type, Fire Size	T, O_2, CO_2, CO, CH, NOx, Visibility, OD, Flame Length	Pucher K., 1994; Ingason et al., 2015
Memorial Tunnel, United States	853.7	8.8	7.9	3.2%	Fuel Oil	10 - 100	Natural & Forced	Ventilation Strategies & Systems, Smoke Management Strategies, Fire Size	T, u, CO, Smoke Spread, Bulk Airflow	Bechtel/ Parsons Brinckerhoff, 1995; Ingason et al., 2015
Repparfjord Tunnel, Norway	2300	7	5.5	< 1.0%	Road & Rail Vehicles, Heptane, Wood Cribs	2 - 120	Forced 0.3 – 8.0	Fuel Type, Fire Size, Ventilation Velocity	HRR, T, MLR, O_2, CO_2, CO, SO_2 CxHy, NO, Visibility, Soot	Haack, 1998; Ingason et al., 2015
Yangzong Road Tunnel, China	2758	14.8	8.9	1.1 & 1.15	Gasoline	1.6 – 2.8	Natural & Forced 0.2 – 5.1	Fire Size, Ventilation Velocity, Fuel Type, Tunnel's Geometry	HRR, T, Smoke Spread Time	Hu et al., 2005; 2007
Runehamar Tunnel, Norway	1600	9	6	0.5% & 1.0%	Wood & polyurethane pallets, mattresses, furniture, truck rubber tyres, paper cartons, polystyrene cups	66 – 202	Forced 2.40 - 3.40	Fuel Type, Fire Size, Fire Source Geometry	HRR, T, u, O_2, CO_2, CO, Radiation, Visibility, Heat Fluxes, Flame Length, Fire Growth Rate, Fire Spread, Pulsation	Ingason and Lönnermark, 2005; Lönnermark and Ingason, 2005; Ingason et al., 2011; 2012; 2015

2nd Benelux Tunnel, Netherlands	872	9.8	5.1	4.4%	Heptane/ Toluene, Vehicles	3 - 26	Forced 0.0 - 6.0	Fuel Type, Fire Size, Fire Fighting Systems, Ventilation Strategies	HRR, T, MLR, Radiation, OD, Visibility	Lemaire and Kenyon, 2006
Model Tunnel, China	96	8	2.7	-	Diesel	0.75 & 1.6	Natural 0	Fire Size, Fuel Type, Tunnel's Geometry	T	Hu et al., 2007
DaFengYaKou Tunnel, China	3270	10.8	7.2	1.3%	Gasoline	1.8 & 3.2	Natural & Forced 0.5 – 1.9	Fire Size & Source Geometry, Fuel Type, Ventilation Velocity, Tunnel's Geometry	T	Hu et al., 2007
Yuanjiang Tunnel, China	1032	10.8	7.2	2.1%	Gasoline	1.8 & 3.2	Natural & Forced 0.5 – 1.0	Fire Size & Source Geometry, Fuel Type, Ventilation Velocity, Tunnel's Geometry	T	Hu et al., 2007
Experimental Tunnel, China	1410	12.4	5.8	0.8-5.0%	Diesel	7.5	Natural 0.90 - 0.95	Fire Location	T, u, Smoke propagation & sedimentation	Wang et al., 2009

Operating Road Tunnel	600	16.8	5	-	Gasoline	0.125 – 3.4	Forced 0– 2.4	Detection Methods & Locations, Ventilation Velocity, Fire Size & Location	Fire Detection Time	Kashef et al., 2009
Under Construction Tunnel	941	8	7	0.0-6.8%	Methanol	1.5- 4	Natural 0.58 – 0.70	Fire Size	T, Smoke Flow Characteristics	Zhong et al., 2011; 2016
San Pedro Tunnel, Spain	600	7.3	5.2	1.0%	Plastic & Wooden Pallets	27 -150	Forced 2.8 -3.0	Fire Size, Ventilation Velocity, Presence of Suppression System	HHR, T, u, O_2, CO_2, CO, Heat Flux	Cheong et al., 2014
Tunnel in Limestone Quarry, Finland	140	6	5	-	Wood Cribs	1.8 - 8	Forced 0.2 to 0.4	Fuel Type	HRR, T, MLR, O_2, CO_2, CO, Visibility, OD	Ingason et al., 2015
Shimizu tunnel, Japan	1119	16.5	8.5	2%	Gasoline, Vehicles	2 – 30	Natural & Forced 0- 5.0	Fuel Type, Fire Size, Fire Fighting Systems, Ventilation Velocity	T, OD, Radiation	Ingason et al., 2015
Brunsberg tunnel, Sweden	276	6.4	6.9	-	Rail Vehicles	77	Forced 2 -2.5	Fuel Type, Ventilation Velocity	HRR, T, O_2, CO_2, CO, OD, Radiation	Ingason et al., 2015

Guanjiao Tunnel, China	32,645	5.2	6.6	8.5%	Fuel Oil	0.22	Natural 0– 2.0	Fire Size, Ventilation Velocity	T, Smoke Distribution	Zhang et al., 2015
Morgex North Tunnel, Italy	2294	10.5	7.2	3.2%	Diesel	15	Forced 2.5 -7.0	Ventilation Strategies	HRR, T, u, OD, O_2, CO_2, CO, TPM, MBR	Borghetti et al., 2017
Beijing Key Laboratory, China Academy of Safety Science and Technology, China	1200	5.2	3.4	-	Methanol	0.07 – 0.5	Natural	HRR, Fire Size & Transverse Location	T	Liu et al., 2017
Fire Experimental Area, China Academy of Safety Science and Technology, China	52	3.2	3.2	-	Methanol-Gasoline Blends	-	Natural & Forced 0- 2.88	Fuel Type, Ventilation Velocity	MCGT, T Profiles, Transmittivities, Flame Height	Tian et al., 2017
Baimang Snow Mountain No.1 Tunnel, China	5180	10	6.85	0.6%	Diesel	1.55	Natural 0.45 - 0.65	Fire Size, Ventilation Velocity	MLR, HRR, T Distribution, Smoke Spread	Yan et al.,2017
Immersed Model Tunnel Simulation of Hong Kong-Zhuhai-Macao Bridge Tunnel Complex, China	150	14.5	7.1	-	Gasoline, Diesel, Vehicles	50	Forced 0- 3.0	Fuel Type, Pool Size, HRR, Ventilation Velocity	Smoke Height, u, CO	Xu et al., 2018

Table 3.2. Main characteristics of model -scale tunnel fire tests.

Test Tunnel Details	Length (m)	Width (m)	Height (m)	Slope (m)	Fuel Type	Peak HRR (MW)	Ventilation (m/s)	Parametric Study	Measured Quantities	References
Model Scale Tunnel	15	0.27	0.25	-	Propane	0.4-12kW	Natural & Forced 0.1 – 0.5	Fire Shape, Size & Location, Ventilation Velocity	U, Smoke Volumetric Flow, Backlayering	Oka and Atkinson, 1995
Model Tunnel Simulation of Qinling Tunnel, China	100	1.8	1.8	-	Diesel	-	Natural & Forced 2.0 – 6.0	Fire Load & Location, Ventilation Velocity & Measures	T, V, Pressure, Smoke Flow,	Yan et al., 2006
Model Scale Tunnel SP Technical Research Institute, Sweden	10	0.6	0.4	-	Wood Cribs & Polyethene Sticks	-	Forced 0.5	Measurements Sensors, Fuel Type	T, u	Lönnermark et al., 2008;
Model Scale Tunnel, Scaling Ratio: 1:20	10	0.4	0.4	-	Heptane	2.2-15.6kW	Forced 0– 1.68	Fire Size, Ventilation Velocity	HRR, MLR, T, Backlayering Length, Burning Rate, Critical Ventilation Velocity	Roh et al., 2008
Carleton University Laboratory Research Tunnel	37.5	10	5.5	-	Gasoline	0.125-3.4MW	Forced 0- 3.0	Fire Detection Systems, Fire Size & Location	Fire Detection Time, T, u, OD	Kashef et al., 2009
Model Scale Tunnels	12	0.25 & 0.45	0.25 & 0.40	-	Propane	2 – 15kW	Forced 0.2 - 0.8	HRR, Ventilation Velocity, Tunnel's Geometry	T	Li et al., 2011

Urban Road Tunnel Model, China Scaling Ratio: 1:6	6	2	0.9	-	Methanol	3.4–29.6kW	Natural	Fire Size & Transverse Location	T	Ji et al., 2012

3.2 Tunnel Evacuation Tests

This chapter presents a current overview of tunnel evacuation experimental tests, related to fire incidents. Parameters such as the way these tests are currently conducted, their impact on safety levels, and the insights gained on evacuee performance, are employed. Although reports of actual tunnel fire events could offer valuable and genuine remarks about human behaviour, they usually do not provide thorough data about the evacuation processes. Therefore, for more in depth studies, dedicated experimental tests are required, which can provide systematic observations of the participants' behaviour under realistic conditions.

Human behaviour in fire emergencies is at the core of all fire safety engineering studies. A better understanding of how people perceive and respond to a tunnel emergency due to the large variety of human behavioural characteristics in such situations, is required, and can be obtained by means of dedicated experimental. One important feature of any experimental research study for analyzing human behaviour is the need of multiple sources of evidence, e.g. video cameras, thermal imaging cameras, questionnaires, interviews and focus group sessions, which are required in order to access participants characteristics and actions in a holistic fashion.

More specifically, many experimental studies have been performed, simulating realistic tunnel fire scenarios, to investigate thoroughly human's behaviour (Norén end Winér, 2003; Boer and Veldhuijzen van Zanten, 2005; Fridolf et al., 2013; 2014; 2019; Porzycki et al., 2018), and emotional state during an evacuation performance (Nilsson et al., 2009; ISO/TC 92/SC 4, 2020), perception of the technical installations and wayfinding systems (Nilsson et al., 2009; Fridolf et al., 2013; 2014; 2019; Fridolf and Frantzich 2015; Nilsson et al., 2018; Ronchi et al., 2018; ISO/TC 92/SC 4, 2020), as well as, the choice of exit (Frantzich,2000; Frantzich and Nilsson, 2003; Norén end Winér, 2003; Fridolf et al., 2014; 2016; 2019 Fridolf and Frantzich 2015; Nilsson et al., 2018; Ronchi et al., 2018;), in such emergency incidents. Additionally pre-movement time before the attempt of self-evacuation (Porzycki et al., 2018), movement speed (Frantzich,2000; Norén end Winér, 2003; Fridolf et al., 2013; 2014; 2016; 2019; Seike et al., 2016; 2016; Porzycki et al., 2018), evacuation time (Nilsson et al., 2009; Porzycki et al., 2018; ISO/TC 92/SC 4, 2020; Chung et al., 2020) and level of success for the whole procedure (Boer and Wijngaarden, 2004), have also been studied and evaluated.

As a first step of studying human behaviour in fire emergencies, one ought to comprehend the level of people's arousal or awareness in such cases. Compered to actual report data from real life fire incidents in tunnels, the user's response during experimental tests tunnel is, in general, unexpectedly homogenous and immediate to the situation. This result is due to the partial awareness of the test participants that "something" may happen, owing to the ethical requirements for such tests (Nilsson et al., 2009; Hsu et al., 2017; ISO/TC 92/SC 4, 2020; Chung et al., 2020). The participants' interpretation of the experiment as a drill may lead to increased alertness compared to tunnel users in general (Kinateder et al. 2013; Hsu et al., 2017; Porzycki et al., 2018; Chung et al., 2020).

Evidently, studies of emotional state in tunnel fires reveal that people's arousal level has a large impact on the amount of information that is perceived by them. This implies that technical installations should be tested under "stressful" conditions, before they can be relied upon in an actual tunnel fire incident. In general, motorists drive through tunnels at high speeds and, consequently, they do not have the time required to observe the tunnel's structure, emergency exits or technical installations and evacuation provisions. Thus, even if a tunnel is a familiar environment, research questionnaires reveal that drivers do not interpret

the tunnel background as pedestrians would do (Boer and Veldhuijzen van Zanten, 2005). In accordance with affiliation theory (Sime, 1984), motorists tend to evacuate towards places or people of familiarity (Porzycki et al., 2018; Ding and Sun, 2020). In the case of tunnels, there are higher odds of people trying to evacuate via a familiar place, e.g., the tunnel entrance or exit portal, even if they are in the middle of the tunnel or near an emergency exit. However, evacuation drill data are generally affected by behavioural uncertainty and ethical constrains and further investigation is needed to gain insights on the actual evacuation behaviour of motorists. It must be also noted that evacuees begin to feel emotional instability and anxiety in presence of smoke, however the threshold of the smoke density that irritates each participant varies by subjects (Jin, 1997; Porzycki et al., 2018).

Figure 3.7. People collectively leaving their cars, in Benelux tunnel Evacuation Experiment, January 2002.

Reports indicate that prerecorded evacuation messages may be difficult to hung upon in a road tunnel emergency, but an acoustic signal is confidently suggested since it alerts motorists and actuate them to search for additional information and wayfinding systems (Nilsson et al., 2009; Nilsson et al., 2018; Ronchi et al., 2018; Porzycki et al., 2018; ISO/TC 92/SC 4, 2020). In fact, a direct and prompt vocal announcement has been proven to encourage the tunnel's users to overcome their hesitation regarding the need of immediate evacuation, leading to shorter evacuation times (Proulx and Sime 1991; Norén and Winér, 2003; Boer and Wijngaarden, 2004; Boer and Veldhuijzen van Zanten, 2005; Nilsson, 2009; Porzycki et al., 2018). Additionally, information signs constitute an effective way to deliver brief but precise information regarding a fire emergency (Nilsson et al., 2009; Fridolf and Frantzich 2015; Nilsson et al.,2018; Ronchi et al., 2018; ISO/TC 92/SC 4, 2020). The evacuation behaviour of others is also an important cue that influences people to respond, when exposed to hazard (Boer and Veldhuijzen van Zanten, 2005). Based on research, social influence decreases when the information becomes more distinct (Nilsson and Johansson, 2009). In conclusion, it is established that arousal level influences the amount of information noticed by motorists, which implies that technical installations, e.g., wayfinding systems, should be tested under stressful conditions before they can be relied upon in a real tunnel fire.

Experimental research has also been conducted in order to obtain insight into factors affecting the decision to leave the vehicle and evacuate. At an early stage of the emergency incident, the majority of drivers and passengers may have difficulty in estimating the severity of the hazard they are exposed to, based on their initial perception of the situation. Thus, they do not decide immediately, or in some cases at all, to leave their vehicle and urgently evacuate the tunnel (Boer 2002, 2003; Norén and Winér, 2003; Boer and Wijngaarden, 2004; Boer and Veldhuijzen van Zanten, 2005; Hsu et al., 2017; Chung et al., 2020). In some cases, it has been observed that they return to their vehicles to retrieve some of their belongings (Boer and

Veldhuijzen van Zanten, 2005). Based on research evidence, it is clear that the evacuation behaviour of others is an important factor that influences people to evacuate (Boer and Veldhuijzen van Zanten, 2005); it has been established that social influence plays an important role on the initial decision of the motorists to leave their vehicle (Norén and Winér, 2003; Boer and Veldhuijzen van Zanten, 2005; Nilsson et al., 2009; Porzycki et al., 2018; ISO/TC 92/SC 4, 2020). Unfortunately, a poor decision that some drivers may make, when exposed to a fire emergency, is that they choose to evacuate using their vehicles, through the tunnel's portals. Although traffic information sings display short messages that urge people to evacuate the tunnel, some motorists ignore or misinterpret the message. Instead of leaving the vehicle and approach the nearest emergency exit on foot, they choose to drive through the tunnel, amid dense smoke (Oberg et al, 2008). This behaviour may pose a significant risk of harming or even killing the people who have chosen to run to the exit. Additionally, in the case of a unidirectional tunnel, this type of behaviour may lead to a collision and consequently to another potential source of fire.

Pre-movement time, namely the time between a fire alarm signal and initialization of evacuation is another key matter in a real-life tunnel fire. To accelerate the evacuation time period, particularly the time until people leave their vehicles, specific fire alarming systems should be installed, based on how people perceive those systems, as well as their behaviour and cognitive respond to them. Although various types of alarm and informative systems have already been installed in many new as well as older tunnels to hasten evacuation times, research is still ongoing regarding the tunnel's users underlying behaviour in a fire incident and their perception of technical installations and information conveyed in realistic fire scenarios. In addition of accelerating the pre-movement time, the presence of a "leader" is also important, since they are usually the ones who trigger the evacuation procedures of a particular group. The rest of evacuees usually follow their lead, due to a "herd" instinct (Norén and Winér, 2003; Boer and Veldhuijzen van Zanten, 2005; Porzycki et al., 2018; Chung et al., 2020).Research findings show that interacting with others may lead evacuees to respond faster but may limit their escape alternatives since they evacuate in herds (Cuesta al., 2020). Being familiar with the specific tunnel environment, as well as having experience in evacuation procedures, reduces the time required for participants to evacuate (Kinateder et al. 2013; Porzycki et al., 2018).

Social influence has been found to be essential with regards to the choice of evacuation exit, too (Frantzich, 2000; Nilsson et al., 2009; Fridolf et al., 2016; Porzycki et al., 2018; Ding and Sun, 2020; Cuesta et al., 2020). Individuals with stronger relationships in social networks tend to cooperate and evacuate in groups (Ding and Sun, 2020). Actually, in stressful conditions, such as reduced visibility in a smoke-filled tunnel, the tendency of the participants to congregate or to follow the person in front of them appears more frequently, but based on recent research results, the role of a leader is not so vital (Ding and Sun, 2020).

However, large increase in smoke density, prohibits collective action, due to insufficient visibility and reduced interaction between people (Porzycki et al., 2018). Assisting behaviour among participants also occurs during some evacuation drill (Fridolf et al., 2016). A key aspect during evacuation in tunnels is the impact of the smoke on human behaviour and egress performance. People may need to change their initial choice of exit or decide to perform a different course of action, in low visibility, by reducing their speed or crawling (Fridolf et al., 2013).

Experimental fire tests have been additionally conducted in order to study the effectiveness of different emergency exit door designs. Lack of information and knowledge about the topic,

may lead to costly installations of evacuation equipment, which only provide very limited benefit. Emergency signs can, for example, be used to influence exit choice (Jin, 1997; Filippidis et al., 2008; Nilsson, 2009; Xie et al., 2009; Xie,2011) The impact of signage on exit choice is affected by several factors, such as visibility conditions, sign design or the cognitive state of the tunnel users. Tests of wayfinding systems, such as signs showing distances to the closest emergency exit, in a smoked filled road tunnel have shown that their installation is vital in order to guide people finding the nearest emergency exit (Fridolf et al., 2013; Fridolf and Frantzich 2015; Fridolf et al., 2016; Nilsson et al., 2018; Ronchi et al., 2018). Moreover, it has been demonstrated that emergency exit way-finding installations are most beneficial for evacuees moving on the opposite side of the emergency exit (Fridolf et al., 2013; Nilsson et al., 2018; Ronchi et al., 2018). The merits of technical installations, such as telephones, are usually limited, since they delay prompt evacuation of the motorists, who try to make phone calls and raise awareness for the danger (Boer and Veldhuijzen van Zanten, 2005). Green flashing lights may be an important factor in pointing the emergency exit (Jin 1997), but some research results indicate that motorist do not always effectively notice lights at emergency exits (Nilsson, 2009; Nilsson et al., 2009). Furthermore, although flashing lights towards the emergency exit can provide the tunnel users with intense and continuous escape guidance even in relatively thick smoke conditions (Jin, 1997) they could also contribute to increasing "visual noise" when a tunnel is filled with cars with flashing alarm lights (Boer and Veldhuijzen van Zanten, 2005).

Figure 3.8. Flashing Alarm Lights In Traffic Congestion In Benelux Tunnel Evacuation Experiment, 2005.

Smoke produced by a fire in a tunnel environment may obscure way-finding light installations. To further increase the probability that people will find and evacuate through the nearest emergency exit it is suggested that evacuation exits should also be equipped with active speakers (Fridolf et al., 2013; Fridolf et al., 2016; Nilsson et al., 2018; Ronchi et al., 2018). Evacuation guidance aided by directional sound produced by a sound beacon appears to be an effective solution, as long as it is combined with vocal instructions (Boer 2002, 2003; Boer and Wijngaarden, 2004). Evacuation experiments also demonstrate that certain emergency exit door designs are preferable than others in terms of attracting participants (Boer and Veldhuijzen van Zanten, 2005; Fridolf et al., 2013; Nilsson et al., 2018; Ronchi et al., 2018). In case of rail tunnels, a combination of green and white continuous lights on both sides of the emergency exit at a low height, is frequently misleading to the participants, many of whom interpret it as a train (Fridolf et al., 2013). In general, fire evacuation experiments, reveal that participants frequently choose the nearest emergency exit (Norén and Winér, 2003; Boer and Wijngaarden, 2004; Nilsson et al., 2009; Fridolf et al., 2016), except when they need to walk past the fire source in order to reach it (Norén and Winér, 2003; Boer and Veldhuijzen van Zanten, 2005).

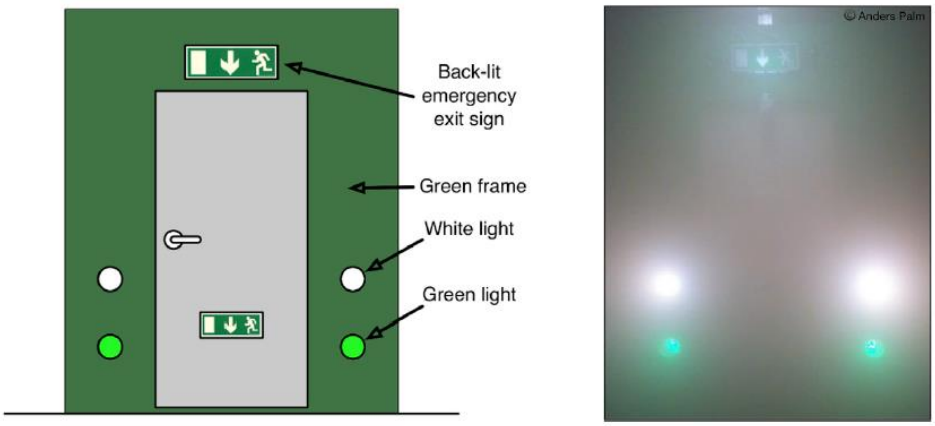

Figure 3.9. Design of emergency exit portal, in smoke filled environment, Stockholm Bypass Project.

By investigating real fire incidents, it has been proven that the presence of smoke is essential in achieving more realistic conditions in a tunnel fire evacuation test. The presence of artificial smoke is aimed at reducing the visibility levels and inflict a sentiment of discomfort and stress to the participants. Artificial cold non-toxic smoke is a mixture of polyglycole and distilled water and it usually produced and directed into the tunnel, via multiple smoke machines to preserve its density. The cold smoke is comparable to what is used, for instance, at entertainment shows and night clubs, and has no adverse consequences on people's health. To establish a more realistic scenario acetic acid, in low concentration levels, can be introduced into the smoke. Exposure to this substance, even for a very short time period, can cause a burning sensation in the evacuees' nose and throat, eye-irritation, and even coughing. These adverse physical effects are sharp but temporal. Acetic acid is boiled in pots in order to disperse. Both the smoke and the acetic acid can be evenly distributed inside the tunnel by utilizing a fan. In reality, the movement and cognitive abilities of evacuees in an actual fire incident might be impeded not only by the reduced visibility conditions and the irritant effects of the smoke, but also by the increased temperatures, radiation and fire products, such as carbon monoxide. These adverse effects should be taken in great consideration while analyzing the findings of human behaviour during evacuation experiments.

Figure 3.10. Visibility Levels during an evacuation Experiment in "Emilia" Tunnel, Poland, 2016.

Experiments have been performed to develop a relation between the brightness of the emergency sign, the motorists' visual distance and the extinction coefficient. The results provide some empirical correlations. The extinction coefficient in the instant of obscuration threshold is logarithmically proportional to the brightness of the sign for a given smoke, intensity of external light and visual distance (Jin, 1976; 1978). Presence of smoke, in a tunnel evacuation drill, has a noteworthy impact on the participants, compelling them to adjust their speed. The results illustrate that the movement speed decreases with increasing light extinction coefficient as well as the presence of irritant and dense smoke (Jin, 1976; 1978; Fridolf et al., 2013; Fridolf et al., 2104; Seike et al., 2016; Sieke et al.,2016). In addition, lucidity and the ability of processing and making judicious decisions decreases with increasing smoke density and increasing temperatures, owing to psychological and physiological reasons (Jin, 1997). Based on research, social influence, which is a key factor in evacuation performance, seems to decay when the vision has been compromised, owing to thick smoke (Boer and Wijngaarden, 2004). The presence of a side wall, on the other hand, is found to be of great importance to the participants, who use it as an aid during the evacuation (Boer 2002, 2003; Boer and Wijngaarden, 2004; Fridolf et al., 2013; Fridolf et al., 2014). However, evacuees who do not move at the "correct" side of the tunnel where the emergency exit is located, may stay attached to the wall. This strong fear of leaving or changing the orientation in dense smoke, owing to the misinterpreted feeling of reassurance that a wall provides, prevents them from abandon it even if there are direct and clear way finding sound systems to the emergency exit (Boer 2001, 2002).

Experimental data have made it possible to estimate the average movement speed of a tunnel's user when exposed to a fire emergency, attempting to evacuate. The average movement speed is defined by diving the total distance a motorist walked inside the tunnel by the time utilized. In view of this aspect, complex movement behaviours are excluded, namely the duration of the stops to decide which route to follow or zig zag walking. Therefore, the need of an additional speed is needed. The modelling speed is determined by the ratio of the distance between two points inside the tunnel, divided by the time employed. When participants of an egress drill are well informed of the experiment details and purpose, which evidently affects the external validity of the results, trivial differences between the two speeds are noted (Fridolf et al., 2013). The modelling speed provides a suitable tool to understand individual responses in an evacuation situation in a tunnel environment since it offers a holistic perspective on users processing and correspondence behaviour. Results have shown that neither an inclination nor an uneven floor appear to greatly affect the movement speed (Norén and Winér, 2003; Fridolf et al., 2013; Fridolf et al., 2014; Fridolf et al., 2016; Porzycki et al., 2018). However, visibility as well as presence of smoke have a great impact on movement speed. The vast majority of evacuees move slower in a smoke-filled tunnel than in a smoke-free (Fridolf et al., 2104; Seike et al., 2016; Ronchi et al., 2018). Except of the level of visibility, people's attitude along with the effect of social influence, have a great impact on evacuee movement speed (Porzycki et al., 2018;). Additionally, the more familiar is someone with the environment of the experiment and the evacuation procedures, the more quick tends to evacuate (Fridolf et al., 2014; Porzycki et al., 2018). On a general level, obstructions inside the tunnel, during an evacuation drill, tend to enforce people reduce their speed and be more cautious (Boer and Wijngaarden, 2004; Fridolf et al., 2014; Ronchi et al., 2018).

Table 3.3. Main characteristics of full -scale tunnel evacuation experiments.

Tunnel's Details	Length (m)	Participants	Knowledge of the situation	Emergency Exits	Alert Strategies & Technical Installations	Smoke / Acetic Acid / Obstructions	Recorded Parameters	References
Stockholm metro, Sweden	400	135, General Public, 69 Men / 64 Women / 2 Others, 19 - 76 years old, Average Age: 38 Years	YES	1	1.Emergency Signs 2.Accoustic Alarm & Pre-Recorded Message 3. Way-Finding Systems	YES / NO / YES	1.People Flow Rate 2. Walking Speed 3. Exit Choice	Frantzich,2000; Norén end Winér, 2003; Fridolf et al., 2016
Training Road Tunnel, Sweden	37	46, General Public, 30 Men / 16 Women, 18 - 29 years old, Average Age: 22 Years	NO (Partially Informed that it was a drill)	2	1.Backlit Emergency Exit Signs 2.Way-Finding Systems	YES / YES / YES	Walking Speed	Frantzich and Nilsson, 2003; Fridolf et al., 2014; Fridolf et al., 2019
Benelux tunnel, Tube D, Netherlands	1000	328, General Public	NO (Partially Informed that it was a drill)	12	1.Information Systems 2. Loudspeakers 3.Emergency Phones	YES / YES / YES	Motorists' Behaviour	Norén end Winér, 2003; Boer and Veldhuijzen van Zanten, 2005;
Benelux tunnel, Tube C, Netherlands	713	75, General Public, 18 - 75 years old, Average Age: 36.4 Years	YES	9	1.Sound Beacons	YES / NO / NO	Evacuation	Boer and Wijngaarden, 2004
Göta Tunnel, Sweden	1600	29, General Public, 27 Men / 2 Women, 25 - 65 years old, Average Age: 44 Years	NO (Partially Informed that it was a drill)	15	1. Pre-recorded Fire Alarm 2. Information Signs 3. Green Flashing Lights	YES / NO / YES	1. Evacuation Time 2. Emotional State 3. Perception of technical installations 4. Perception of the evacuation	Nilsson et al., 2009; ISO/TC 92/SC 4, 2020

Engelbert Tunnel, Germany	539	43, General Public, 21 Men / 22 Women, Average Age: 28.1 Years	YES	1	1.Emergency Phones	YES / NO / YES	1.Information & Training Effects on Evacuation Performance	Kinateder et al. 2013
Southern Link road tunnel, Sweden	200	100, General Public, 56 Men / 44 Women, 18 - 66 years old, Average Age: 29.4 Years	YES	1	1.Emergency Sings 2.Accoustic Alarm & Pre-Recorded Message 3.Way-Finding Systems	YES / YES / NO	1.Evaluation of Way-Finding Installations, Emergency Exit's Design & Loudspeaker 2.Movement Speed 3. Human Behaviour	Fridolf et al., 2013; Fridolf et al., 2014; Fridolf et al., 2019
Northern Link road tunnel, Sweden	120	66, General Public, 46 Men / 20 Women, 25 - 65 years old, Average Age: 44 Years	YES	1	1. Traffic Information Signs 2. Acoustic warning signals 3. Flashing lights at Emergency exit	YES / NO / YES	1. Design Evaluation: Information signs, Emergency doors, Acoustic Warning Signals 2.Tests of wayfinding systems: Emergency exit portals in VR & In a smoked filled road tunnel 3.Exit Choice	Fridolf and Frantzich 2015; Nilsson et al., 2018; Ronchi et al., 2018; Fridolf et al., 2019
Test tunnel, *National Institute for Land and Infrastructure Management,* Japan	400	294, General Public, 293 Men / 1 Women, 23 - 62 years old, Average Age: 33.9 Years	YES	-	1.Emergency Announcement	YES / NO / YES	Walking & Evacuation Speed	Seike et al., 2016; Seike et al., 2016; Fridolf et al., 2019
Emilia Tunnel, Poland	678	28, Tunnel Technology Professionals 50, Students	YES	4	1.Emergency lights 2.Fire Alarm & Voice Message 3. Information Signs	YES / NO / NO	1.Evacuation's Time 2.Pedestrians' Behaviour 3.Pre-Movement Time 4.Movement Speed 5.Influence Of smoke	Porzycki et al., 2018

Sightseeing Buses, Taiwan & Japan	-	180, Students & Fire Bureau Staff, 2 - 70 years old	YES	-	1.Emergency Announcement	NO / NO / NO	Evacuation Time Gaps	Chung et al., 2020

3.3 Tunnel Fire CFD Simulation Studies

Fire incidents are amongst the most hazardous events that could occur in the modern transportation system, originating a major amount of economic losses while threatening people's lives. In particular, considerable expenses emerge from the tunnel's structure damage induced from the fire and the individual losses of the drivers' property, in general. At the same time, serious environmental threats and more importantly, the risk of compromising human's health and integrity, due to possible fire spreading, high temperatures or toxic gases inhalation, constitute some of the main factors, researchers should consider while examining and analyzing the momentousness of this type of situations. Except of actual experimental fire tests, Computational Fluid Dynamics (CFD) provides a holistic and comprehensive numerical technique to study the behaviour of these fire phenomena inside tunnels. For that cause, a variety of simulation programs using CFD models, have been developed to compute and present the dynamic characteristics of thermally driven turbulent flows. Therefore, CFD modeling is established as a valuable tool that could be used to enhance the knowledge of the evolution of different fire scenarios and augment the value of the results obtained from large or model scale experimental testing.

As with any other type of computational models, CFD simulations do have limitations in predicting the dynamics of fluids, as defined by assumptions and convections associated with each model's code. When an algorithm's design aim to "capture" more accurately real-life fire phenomena, it is declared that the complexity of the code will significantly increase along with its capability and thus, the detection of the limitations of the model becomes harder. Hence, evaluating the model under known conditions and comparing the simulated results to data from actual fire tests, is vital, before applying the model to predict the results of a similar, untested scenario. This methodology demonstrates, in practice, the computational limitations of the CFD models, while it validates user's competence and acquaintance regarding the model's utilization.

Many numerical studies have been conducted, focusing on the main characteristic of a fire's development inside a tunnel as well as the distribution of smoke flow. The numerical results have produced a great deal of information, regarding the temperature profiles inside the tunnel when a fire occurs (McGrattan and Hamins, 2001; Hu et al., 2006; 2007; 2008; 2010; Mawhinney and Trelles, 2007; 2008; 2012; Kashef and Bénichou, 2008; Kim et al., 2008; Migoya et al., 2008; 2011; Vega et al., 2008; Hui et al., 2009; Nilsen and Log, 2009; Vigne and Jönsson, 2009; Wang, 2009; Binbin, 2011; Colella et al., 2011; Trelles and Mawhinney, 2011; Blanchard et al., 2012; Li et al., 2012; Ko and Hadjisophocleous, 2013; Lin et al., 2014; Wang and Wang, 2016; Wang et al., 2016; Vermesi et al., 2017; Glasa et al., 2018; Ji et al., 2019; Tomar and Khurana, 2019; Zhang et al., 2021), the Heat Release Rate (Hwang and Edwards, 2005; Hu et al., 2007; 2008; Mawhinney and Trelles, 2007; 2008; 2012; Cheong et el., 2009; Hui et al., 2009; Nilsen and Log, 2009; Wang, 2009; Migoya et al., 2011; Trelles and Mawhinney, 2011; Blanchard et al., 2012; Ko and Hadjisophocleous, 2013; Wang et al., 2016; Glasa et al., 2018; Ji et al., 2019; Tomar and Khurana, 2019), the fire development (Cheong et el., 2009; Tomar and Khurana, 2019), as well as the heat fluxes produced from it (Mawhinney and Trelles, 2007; 2008; 2012; Vigne and Jönsson, 2009; Wang, 2009; Trelles and Mawhinney, 2011; Blanchard et al., 2012; Tomar and Khurana, 2019). Smoke distribution and propagation (Hu et al., 2007; 2008; Kashef and Bénichou, 2008; Hui et al., 2009; Binbin, 2011; Wang and Wang, 2016; Glasa et al., 2018; Ji et al., 2019), CO production (Hu et al., 2007; 2010; Vega et al., 2008; Wang, 2009; Wang et al., 2016), optical density (Kashef and Bénichou, 2008; Glasa

et al., 2018;), visibility (Kashef and Bénichou, 2008; Lin et al., 2014), and radiation (Wang, 2009;) via CFD modelling, have also provided in depth knowledge regarding the severity of a fire scenario while declaring the feasibility of an evacuation attempt at any location inside the tunnel depending on the smoke characteristics at this area. Furthermore, the ventilation velocity which can sufficiently prevent backlayering -critical velocity- is a key parameter to the vast majority of previous studies since its prediction through both experimental and numerical data is required to fashion the appropriate evacuation strategies (Hwang and Edwards, 2005; 2005; Hu et al., 2007; 2008; Kashef and Bénichou, 2008; Hui et al., 2009; Wang, 2009; Colella et al., 2011; Wang and Wang, 2016; Glasa et al., 2018; Zhang et al., 2021).

From the above review it is established that a wide numerical survey and analysis of large-scale tunnel fires tests have been conducted and validated using CFD modeling. The effects of several parameters of the above-mentioned fire phenomena have been also investigated. More specifically, fires of different shape (Hwang and Edwards, 2005; 2005; Hu et al., 2007; Cheong et el., 2009; Hui et al., 2009; Nilsen and Log, 2009; Wang et al., 2016; Ji et al., 2019) and size (McGrattan and Hamins, 2001; Hu et al., 2006; 2007; 2007; 2010; Mawhinney and Trelles, 2007; 2008; 2012; Kashef and Bénichou, 2008; Migoya et al., 2008; 2011; Vega et al., 2008; Nilsen and Log, 2009; Wang, 2009; Colella et al., 2011; Trelles and Mawhinney, 2011; Li et al., 2012; Ko and Hadjisophocleous, 2013; Zhang et al., 2021) have been simulated in order to be explored their influence on the fire development and smoke distribution and the required ventilation velocity prohibiting backlayering from occurring, to be declare. The longitudinal or transverse location of the fire have been proven to affect the previous phenomena, as well (Hu et al., 2008; Kashef and Bénichou, 2008; Wang and Wang, 2016). The influence of ventilation velocity (Hwang and Edwards, 2005; 2005; Hu et al., 2007; 2008; 2010; Mawhinney and Trelles, 2007; 2008; 2012; Kim et al., 2008; Migoya et al., 2008; 2011; Cheong et el., 2009; Hui et al., 2009; Nilsen and Log, 2009; Wang, 2009; Colella et al., 2011; Trelles and Mawhinney, 2011; Blanchard et al., 2012; Li et al., 2012; Ko and Hadjisophocleous, 2013) along with the implementation of different ventilation strategies and conditions (Kashef and Bénichou, 2008; Vega et al., 2008) on the formation of the backlayering and the development of the fire have been also studied. Additionally, tunnel's geometry has been proven to be an important factor regarding the development of the fire and smoke propagation. Owning to that, multiple parametric studies have been conducted, simulating different geometrical characteristics of a tunnel structure, such as different length, height, width or slope to scrutinize the magnitude of their impact (Hwang and Edwards, 2005; 2005; Hu et al., 2006; Cheong et el., 2009; Nilsen and Log, 2009; Wang, 2009; Migoya et al., 2011; Lin et al., 2014; Glasa et al., 2018; Zhang et al., 2021). Furthermore, CFD modeling have been utilized to improve the knowledge of the performance of various suppression systems (Mawhinney and Trelles, 2007; 2008; 2012; Trelles and Mawhinney, 2011; Ko and Hadjisophocleous, 2013). In some cases, when simulating a fire scenario, various CFD models and programs are selected to be utilized in order for their efficiency to be evaluated comparatively (Migoya et al., 2008; Nilsen and Log, 2009; Binbin, 2011; Lin et al., 2014).

However, as a primary objective of most of the previous studies, various numerical simulation details have been examined first, such as the grid's resolution (Hwang and Edwards, 2005; 2005; Kim et al., 2008; Vigne and Jönsson, 2009; Wang, 2009; Colella et al., 2011; Blanchard et al., 2012; Vermesi et al., 2017; Zhang et al., 2021), number of utilized meshes (Vigne and Jönsson, 2009), several turbulent parameters (Kim et al., 2008) as well as CFD Software Uncertainty (Vigne and Jönsson, 2009), to ensure that these numerical parameters do not alter the fundamental characteristics of each fire scenario. It must be also noted that the numerical findings have been validated against actual experimental data for assessing this sensitivity study. In the Table 2.1, specific details, such as the simulated tunnel's

characteristics (Name and length), the fundamental factors of each fire scenario (Fuel Type, Peak HRR, Ventilation Conditions), as well as the parametric study conducted, and the measured quantities, are comprehensively mentioned. Only validated studies, compared with actual experimental data, have been included in this research review.

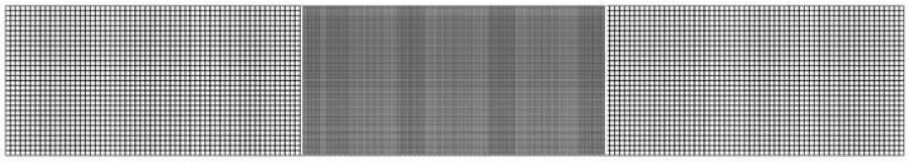

Figure 3.11. A representation of a refined grid resolution at the fire region, at YingZuiYan Road Tunnel simulation (Hu et al., 2010)

The CFD models are evidently a critical key parameter when studying and analyzing tunnel structures with premium complexity and fire related phenomena and details. More specifically, CFD techniques can be utilized to clarify and augment the value of experimental results, when analyzing different fire or ventilation scenarios, with different tunnel geometries, since they have been validated with actual experimental data to demonstrate their legitimacy. Hence, they constitute a valuable tool, especially for the situations where the actual fire test data are found to be inadequate or infeasible to be retrieved. Many CFD programs have been used for examining several fire scenarios. Based on that, the following conclusions and comments can be established on several eminent CFD programs. Fire Dynamics Simulator (FDS) (McGrattan et al. 2020), which is a three-dimensional large eddy simulation CFD program, developed by the National Institute of Standards and Technology (NIST), is a widely known, valid program, used extensively in tunnel's fire simulations (McGrattan and Hamins, 2001; Hwang and Edwards, 2005; 2005; Hu et al., 2006; 2007; 2007; 2008; 2010;\ Mawhinney and Trelles, 2007; 2008; 2012, Kashef and Bénichou, 2008; Kim et al., 2008; Cheong et el., 2009; Vigne and Jönsson, 2009; Wang, 2009; Binbin, 2011; Trelles and Mawhinney, 2011; Blanchard et al., 2012; Li et al., 2012; Ko and Hadjisophocleous, 2013; Wang et al., 2016; Vermesi et al., 2017; Glasa et al., 2018; Ji et al., 2019; Tomar and Khurana, 2019; Zhang et al., 2021). The numerical data derived from this program evidently prove that the code has a decent performance in predicting the temperature's distribution magnitude inside a tunnel (McGrattan and Hamins, 2001; Mawhinney and Trelles, 2007; 2008; 2012; Kashef and Bénichou, 2008; Vigne and Jönsson, 2009; Wang, 2009; Hu et al., 2006; 2007; 2007; 2010; Trelles and Mawhinney, 2011; Blanchard et al., 2012; Li et al., 2012), fire growth characteristics (Cheong et al., 2009) and backlayering related phenomena at different ventilation conditions (Mawhinney and Trelles, 2007; 2008; 2012; Hu et al., 2007; Kashef and Bénichou, 2008; Wang, 2009; Trelles and Mawhinney, 2011; Blanchard et al., 2012; Li et al., 2012), even at a presence of suppression systems (Mawhinney and Trelles, 2007; 2008; 2012; Trelles and Mawhinney, 2011; Ko and Hadjisophocleous, 2013). However, the general tendency of the FDS models is to slightly overpredict the temperature profiles (Mawhinney and Trelles, 2007; 2008; 2012; Vigne and Jönsson, 2009; Trelles and Mawhinney, 2011). In fact, the mean error which emerging, against experimental data, range from 5% to 40% (Mawhinney and Trelles, 2007; Kashef, and Bénichou, 2008; Vigne and Jönsson, 2009; Blanchard et al., 2012; Ko and Hadjisophocleous, 2013). As it regards the HRR, the mean numerical error is found to be between 3% and 18% (Blanchard et al., 2012), while for the CO production, the numerical error is lower than 11% (Hu et al., 2007). However, smoke optical density profiles have been resulting in an error higher than 30% (Kashef, and Bénichou, 2008).

An overall good agreement regarding temperature distributions, has been achieved among the results of the FLUENT CFD code and actual full-scale experimental measurements, as well (Migoya et al., 2008; Vega et al., 2008; 2011; Lin et al., 2014; Wang and Wang, 2016). FLUENT

is a simulation software utilized to predict fluid flow, heat and mass transfer, chemical reactions and other related phenomena and thus several simulations of fires inside tunnels have been conducted via this program (Migoya et al., 2008; 2011; Vega et al., 2008; Binbin, 2011; Colella et al., 2011; Lin et al., 2014; Wang and Wang, 2016). More specifically, the comparison of experimental and numerical temperature results has revealed a good agreement in general, verifying the FLUENT modelling effectiveness and accuracy (Vega et al., 2008). However, slight discrepancies have been distinguished in the temperatures profiles, especially around the fire location, with a mean error from 30 to 35% (Vega et al., 2008) while the estimation of the heat release rate leads to a mean error less than 15 % (Migoya et al., 2011). The velocity profiles, computed by FLUENT also exhibit a good agreement, with a numerical error lower than 15% (Vega et al., 2008; Wang and Wang 2016) except for the area near the floor, where the velocity from CFD is greater than experimental results (Wang and Wang 2016).

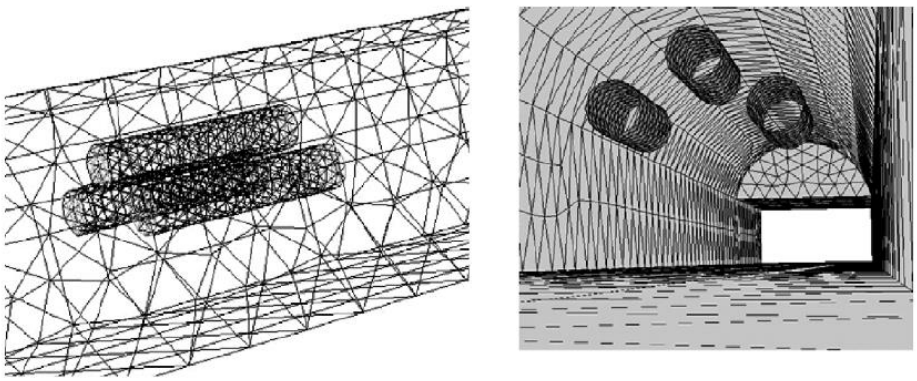

Figure 3.12. Simulation of a Ventilation System, via FLUENT (Vega et al., 2008)

Additionally, comparative research has been conducted among several simulation software, assessing the mathematical models utilized by them (Binbin, 2011). More specifically, many fire tests have been reconstructed both by FLUENT and FDS (Binbin, 2011; Lin et al., 2014). As far as the simulation area is concerned, FLUENT's program code provide the user with more extensive options, than FDS, promoting the construction of a more accurate mesh. In FLUENT simulations, depending on the geometrical requirements of each tunnel fire scenario, the user has a large variety of shapes for cells available to select, such as cylinders, rectangular or pentagonal prism and other, as illustrated in *Figure 2.2* (Vega et al., 2008; Binbin, 2011). In the contrary, FDS provides only the choice of rectangular mesh and therefore when the representation of a complex tunnel's geometry is required to be more detailed and precise, FLUENT code is suggested instead of the FDS. In alliance with the simulation dominance of FLUENT, regarding the design of the mesh, it should be noted that, FLUENT offers several different turbulence models to be applied in the representation of any fire scenario. However, the software of FDS in the field of reproducing fires simulation is more targeted. When the fire occurs, the simulation data extracted from the FDS modelling are closer to the experimental results, in comparison with those of FLUENT, as regarding for example, the temperature distribution and the smoke layer thickness (Binbin, 2011).

As far as simulations of experiments with relatively small fires are concerned, the computed temperature profiles comply sufficiently well with the experimental data from the tests, using models such as Kamelon FireEx CFD (kfx) model and SOLVENT model. Nevertheless, when assessing simulations of larger fires, notable deviation has been observed (Nilsen and Log, 2009). The calculated data give, however, comparable results with respect to ''order of severity'', against the actual test fires, and consequently they succeed in predicting adequately

the hazards of such types of incidents (Nilsen and Log, 2009). Another CFD code utilized for modelling tunnel fires is CFX (Hui et al., 2009). CFX is a general purpose CFD code used for several purposes including simulation of fire and smoke movement for steady state and time-dependent applications, in three-dimensions. Furthermore, in contradiction to the general belief, it has been proven that even more simple models may provide, equally as good results as the CFD codes, estimating well the level of severity documented in the test fires regarding to the HRR of the fires and plume's temperatures (Nilsen and Log, 2009). Simple models, like "hand" models, may therefore be a valuable tool in risk analysis for simple tunnel structures and fire scenarios, eliminated the computational time and complexity, required (Nilsen and Log, 2009).

In cases of large fires, when the HRR reaches to an excess value, the high temperatures that govern the smoke layer and the strong heat fluxes produced from the fire, especially at the downstream region of the tunnel, can pose a significant threat to the tunnel's structure and its combustible materials integrity as well as the people's health, potentially causing parts of tunnel's structure to collapse or physical impairments and even fatalities amongst the entrapped drivers (Wang, 2009). Thus, it is critical to firmly evaluate the numerical prediction with respect to the measurement data from the tests. But, while assessing the agreement between the numerical and experimental data of temperature profiles and heat fluxes, one may consider that an important difference between them may appear due to the location of the measurement sensors and their distance from the fire source (Blanchard et al., 2012). This phenomenon is well- justified provided that the vigorous changes from the combustion processes and radiation from the fire interact intensly with the flow, especially near the fire source. In alliance with that, the computational results indicate that the discrepancies of the numerical data against experimental measurements abate, increasing the distance from the fire (Blanchard et al., 2012). Furthermore, the results from CFD modelling reveal that the ventilation velocity inside the tunnel influence significantly the heat release rate of a certain fire, with a higher airflow resulting in greater heat release rates (Cheong et al., 2009). It should be also noted that the tunnel's ventilation conditions along with the ignition location of the fire source, especially in solid fuels, can either delay or accelerate the propagation of the fire during the initial stages of fire development and therefore have a great impact on the fire's peak HRR (Cheong et al., 2009). Thus, promptly, in the early stages of tunnel fires, while the fire growth rate drastically changes the environmental conditions in the near region due to the confined space, the ventilation system have to confront and attenuate the development of the incident. Consequently, the reaction time of the ventilation strategies constitutes a key factor in fire safety analysis, especially when the heat release rate of a fire is high enough to compromise the integrity and efficacy of the ventilation system. (Vega et al., 2008). Numerical findings confirm that the smoke mass flow rate also increases with HRR, as expected from experimental tests, due to the augmentation of fire products production which simultaneously weakens gradually the fresh air entrainment to the smoke flow (Ji et al., 2019). Additionally, both experimental and numerical results indicate that the backlayering length significantly increases with the increase of fire size (Hu et al., 2007).

As expected, several different geometrical shapes are often utilized, to simulate in the most accurate way, the flammable materials involved in a tunnel fire. The shapes of fire source may affect the characteristics of smoke movement in tunnels. Owing to the previous technique, the influence of different fire source shapes on temperature profiles and smoke movement can be investigated. Evidently, the utilization of the geometrical shapes of fires provokes considerable variations in flame extension lengths of a fully developed fire (Wang et al., 2016). The longitudinal temperature distribution increases, for a certain HRR, with the decreasing value of length–width ratio of the fire source, especially near the combustion zone, due to the

fact that the flames could even directly reach the ceiling when a fire source has a small surface area (Ji et al., 2019). In alliance with that, results also indicate that with decreasing length–width ratio of the fire source and augmentation of the fire size, the hot smoke flow near the tunnel ceiling becomes more difficult to be uniform along the longitudinal direction (Ji et al., 2019). Due to the change of smoke distribution tendency in that case, for the same HRR, the smoke mass flow rate decreases when the length and the width of the fire source become more even, as it is proportional to the perimeter of the fire source (Ji et al., 2019). Additionally, using different fuel shapes establish significant differences in the temperature profiles predictions (Hui et al., 2009; Wang et al., 2016). However, in cases where a large target has been placed behind the fire, for example a bus or a HGV, the fire shape has a weak effect on the temperature distribution (Wang et al., 2016). An omitting obstacle does not coincide with that observation, especially during the fully developed phase of a fire (Wang et al., 2016).

In literature there is a limited number of numerical simulations involving solid commodities, which are often the main cargo of HGVs (Cheong et al., 2009; Tomar and Khurana, 2019). Lack of solid fuels simulations, using CFD modelling, is a consequence of CFD model's limitation. In conjunction with experimental data, recent studies reveal that when a solid fuel fire is induced, only limited to some portion of fuel involves in the fire and consequently an amount of fuel remain unburnt (Tomar and Khurana, 2019). More specifically, when the combustion of such fuels is modeled, a pyrolysis model is needed in order to establish the required heat inside the tunnel. The kinetic properties of all the materials involved, are also mandatory, for calculating properly the pyrolysis rates of the fuel. The phenomenon of undeveloped fire is observed in this type of simulations because the pyrolysis process is usually slow, given the material is solid with a dense molecular structure and therefore all its molecules are not thermally decomposed. In case of solid commodities with gaps, e.g. pallets, in simulations they cannot be sharply reconstructed (Tomar and Khurana, 2019). Thus, there is a need of significantly increased fuel weight, compared with the actual fuel weight utilized in full scale experiments, for representing the combustion surface area (Tomar and Khurana, 2019). This accretion in the fuel weight leads to heavy fuel load and dense structure and hence the pyrolysis of fuel and fire spread become vastly slower, resulting in most cases, in underdeveloped fire. On the contrary, when attempting to preserve the same weight among the numerical and experimental data, less effective surface area is modelled, and still an undergrowth fire may emerge (Tomar and Khurana, 2019). In addition, although, the fire growth rate and peak heat release rates from the simulations are approaching the order of magnitude of the experimental data, most CFD models are unable to reproduce phenomena such as collapse of the fuel package (Cheong et al., 2009). Similarly, it is observed a lower growth on the incident heat fluxes and temperatures released from the fire (Tomar and Khurana, 2019).

The vast majority of the foregoing studies have been conducted with the key assumption that the fire source originates at the centerline of the tunnel. However, in many real cases, in road tunnels, the fire is located near the tunnel's sidewalls. Simulation studies reveal that the critical velocity required for a near-wall fire source varies compared to a fire at the center line, owning to their different smoke propagation performance (Hu et al., 2008). In fact, in that case, higher critical velocity is needed to avert the upstream dispersion of the hot fire products (Hu et al., 2008; Wang and Wang, 2016). However, the differences amongst the critical ventilation conditions required for the different transverse fire locations, decreases with the augment of the fire size (Hu et al., 2008). It is also established that the backlayering length for a fire in the middle of the tunnel, is approximately two times longer than that of a fire occurring at the left or right lane, although they are under the same ventilation velocity. However, the backlayering length is noted to be remarkably short for a fire right next to the

side walls under the same ventilation velocity (Wang and Wang 2016). Evidently, the maximum smoke temperature is obtained for a fire next to the wall, while it decreases gradually for a fire at the lanes and a centerline one (Wang and Wang, 2016).

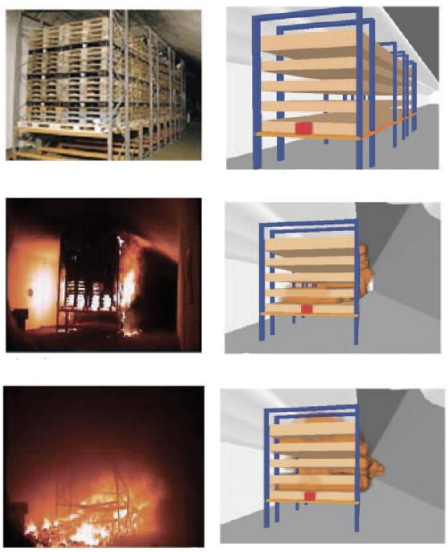

Figure 3.13. Fire growth characteristics on Runehamar tunnel through experimental documents and FDS modelling (Cheong et al., 2009).

In tunnel fires with natural ventilation conditions, CFD modelling declares that high-temperature smoke of combustion products, e.g. CO and Soot, form a dense layer near the ceiling and flow in both directions inside the tunnel (Hwang and Edwards, 2005; Mawhinney and Trelles, 2007; 2008; 2012; Hu et al., 2008; Kashef and Bénichou, 2008; Hui et al., 2009; Wang, 2009; Trelles and Mawhinney, 2011; Blanchard et al., 2012; Lin et al., 2014). Even when forced ventilation velocity is applied, the hot smoke may still spread at the direction opposite to the ventilation stream. As the longitudinal ventilation velocity increases, the backlayering length abbreviates (Hu et al., 2007). The formation of this reverse stratified flow can only be entirely prevented when the utilized ventilation velocity reaches the critical ventilation conditions (Hwang and Edwards, 2005; Hu et al., 2008; 2010; Kashef and Bénichou, 2008; Hui et al., 2009; Wang, 2009; Blanchard et al., 2012). Thus, it is clearly illustrated, by both experimental data and numerical calculations, that the backlayering length is significantly sensitive to the longitudinal ventilation velocity. In addition, although the critical ventilation velocity, which is just sufficient to prevent backlayering, augment with the fire size, simulation results indicate that it tends to remain constant as the heat release rate exceeds a certain value (Hwang and Edwards, 2005; Hui et al., 2009; Wang, 2009). This observation is highly associated with the fact that temperature stratification, when critical ventilation conditions are applied, only exists downstream from the fire and the ceiling temperature above the fire region reaches a maximum value, when the upstream flow of the smoke is entirely prohibited (Hwang and Edwards, 2005).

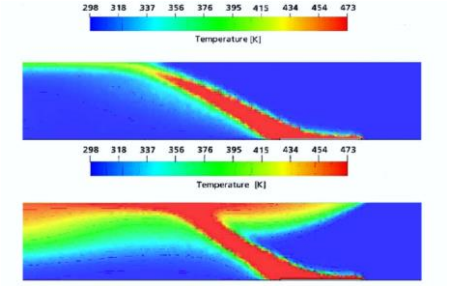

Figure 3.14. Temperature distributions near the fire source region for descending critical ventilation velocity conditions. (Hui et al., 2009)

The critical ventilation velocity which is just sufficient to prevent the formation of a reverse stratified layer is evidently different for tunnels of different configuration, but it is roughly proportional to the 1/5 power of the heat release rate, according to the utilized theoretical correlations (Hui et al., 2009; Hwang and Edwards, 2005; Wang, 2009). However, according to computational results, critical velocity of approximately 3m/s is capable of extinguishing the upstream reverse flow regardless the tunnel size (Wang, 2009). As expected, in tunnel with an inclination, when ascensional ventilation is utilized a smaller ventilation velocity is required to prevent back layering compared with a horizontal one (Hwang and Edwards, 2005). CFD results reveal as well, that the fuel type and the ambient temperature have negligible impact on the required critical velocity (Hwang and Edwards, 2005).

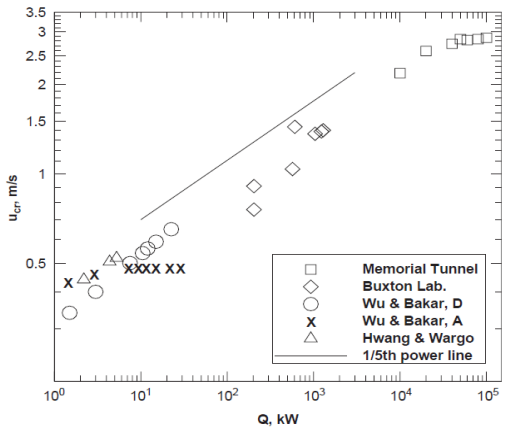

Figure 3.15. Comparison between the theoretically predicted and experimentally measured critical ventilation velocity, as a function of the theoretical Heat Release Rate (Hwang and Edwards, 2005)

Energy released by the fire is diffused inside the tunnel. According to CFD modelling, walls tend to capture the main part of the heat release, highlighting the intense heat exchanges of the walls with the hot combustion products due to the confined nature of the tunnel configuration (Hu et al., 2010; Blanchard et al., 2012). But the energy distribution inside the tunnel is estimated to be utterly different whether the ventilation velocity is above or below the critical ventilation conditions. Concerning a fully developed fire, it is found that a greater amount of heat interacts with the tunnel surfaces when sub-critical ventilation conditions are applied (Blanchard et al., 2012). In order of significance, the variation in the energy distribution has been attributed to the reverse smoke layering existence which expands the surface area in contact with hot smoke while facilitating the heat transfers between tunnel surfaces and the hot products flow. Additionally, the ventilation velocity tends to even the temperature profiles of fresh air and hot smoke while decreasing heat losses to surfaces, as the blending of these layers is significantly accelerated, increasing the ventilation velocity. (Hu et al., 2010; Blanchard et al., 2012)

CFD modelling can be also utilized for predicting the smoke spread and CO concentration distribution along the tunnel, for fire safety requirements. Numerical results imply that the vertical and longitudinal distributions of the CO concentration are linearly increased with the height above the ground and tend to exponentially decay with the distance from the fire source, respectively (Hu et al., 2007). To augment this observation, it should be noted that longitudinal distributions of CO concentration along the tunnel, have been proven to fall into good agreement with experimental data, under different longitudinal ventilation conditions. Furthermore, it is established that the smoke temperature profiles decrease much faster than the CO concentration along the tunnel, under a certain longitudinal ventilation velocity (Hu et al., 2010). This experimental and numerical observation has been expected, given that the dilution of CO concentration along the tunnel is mainly affected by the fresh air entrainment

into the smoke layer. But the decay in the smoke temperature along the tunnel is both facilitated by the smoke blending with cold air as well as the heat loss from the hot smoke to the tunnel's surfaces and therefore the discrepancies observed between its quantity's abatement, increase gradually along with the distance downstream from the fire (Hu et al., 2006; 2010). However, a rise in the longitudinal ventilation velocity results in acceleration of fresh air and smoke mixing (Hu et al., 2006; 2010). As anticipated, this leads to a decrease of the longitudinal differences between the decay of CO concentration and temperature profiles although numerical findings reveal that CO concentration decays relatively slower than temperature along the tunnel under an increasing longitudinal ventilation velocity (Hu et al., 2010). Nevertheless, as the fire size increases, the CO concentration is found to be less influenced by the longitudinal ventilation conditions (Hu et al., 2010).

.

CFD modeling have been also used to enhance the knowledge of the performance of various suppression systems while enhancing the importance of their utilization, in a tunnel structure. In particular, several computational simulations of Water based Fixed Fire Fighting Systems (WFFFS), such as water spray or water mist systems, have been conducted in order to investigate specifically their effectiveness and interaction with longitudinal forced ventilation conditions inside a tunnel. Simulation results validate that, in spite of ventilation velocity, water based suppression systems have a vital role in eliminating the backlayering phenomenon, and therefore the critical ventilation velocity required when both of these measures are utilized, is remarkably lower, for the same fire size (Ko and Hadjisophocleous, 2013). Longitudinal ventilation system succeeds in preventing the backlayering of hot combustion products at a lower velocity than the anticipated critical velocity, as a consequence of lower smoke temperatures due to the suppression system operation (Ko and Hadjisophocleous, 2013). In fact, an accurate estimation of how a water mist system might perform under different conditions and its impact on the ongoing fire can be obtained via FDS modelling (Mawhinney and Trelles, 2007; 2008; 2012; Trelles and Mawhinney, 2011). The merits of the activation of water mist suppression system against large fires are striking illustrated in both experimental testing and modeling results and therefore a careful selection of performance criteria for these systems is essential in order for them to deliver adequately to different fire scenarios Mawhinney and Trelles, 2007; 2008; 2012; Trelles and Mawhinney, 2011).

Various full-scale tunnel fire tests have been selected and simulated using CFD modelling, in order to determine the effect of tunnel configuration (Hwang and Edwards, 2005; 2005; Cheong et el., 2009; Nilsen and Log, 2009; Migoya et al., 2011; Zhang et al., 2021) and slope (Hwang and Edwards, 2005; Hu et al., 2006; Wang, 2009; Lin et al., 2014; Vermesi et al., 2017; Glasa et al., 2018; Zhang et al., 2021) on the development of the fire and smoke's distribution. Simulation results also highlight the requirements of ventilation and suppression strategies, at different tunnel's geometries and inclination for upcoming simulation studies. More specifically, the pivotal impact of the tunnel's slope on smoke propagation, including the development of backlayering, is clearly illustrated in several simulation studies, *Figure 2.6* (Hwang and Edwards, 2005; Wang, 2009; Glasa et al., 2018; Zhang et al., 2021) and thus tunnel slope is one of the main parametric factors that have been studied over the years, via the CFD modeling. In addition, the simulation of fires of various heat release rates indicates that the smoke spread inside a tunnel can be significantly influenced by its slope especially when it regards more intensive fires (Glasa et al., 2018). Modelling findings demonstrate that an increase in the tunnel slope or a reduction of the tunnel width, results in reduced maximum temperature under the ceiling (Zhang et al., 2021). On the contrary, the increasing of heat release rate of the fire or the decreasing the height between the fire source and the ceiling has as a consequence an advance in the maximum ceiling temperature (Zhang et al., 2021). As it regards the smoke backlayering length, the fire source heat release rate and the tunnel

width had negligible influence on it (Zhang et al., 2021). However, it has been proven, through numerical survey, that the length of backlayering smoke decays as the slope of the tunnel increases or with the decreasing of the distance between the fire source and the ceiling of the tunnel (Zhang et al., 2021). As far as the simulation of tunnel's length is concerned, a challenging dilemma is arousing. More specifically, the representation of the whole length implies a tremendous increase in the computational time required, while on the other hand when only a part of a tunnel's length is modelled, several fire related phenomena do not develop adequately and hence the simulated fire scenario may not even correspond to a similar real one. Consequently, a multiscale modelling of tunnel fires, which utilize a combination of three-dimensional (combustion and near the fire area) and one dimensional (far from the fire area) model has been proposed as the alternative for large CFD domains associated with long tunnels (Colella et al., 2011; Vermesi et al., 2017). It has been also stated that the combination of both, multiple meshes and multiscale modelling, is a verified technique. As a consequence, the requested accuracy to the results is maintained, by adding only a negligible numerical error to the results (less than 3.5%), while the computational time is reduced significantly (Colella et al., 2011; Vermesi et al., 2017).

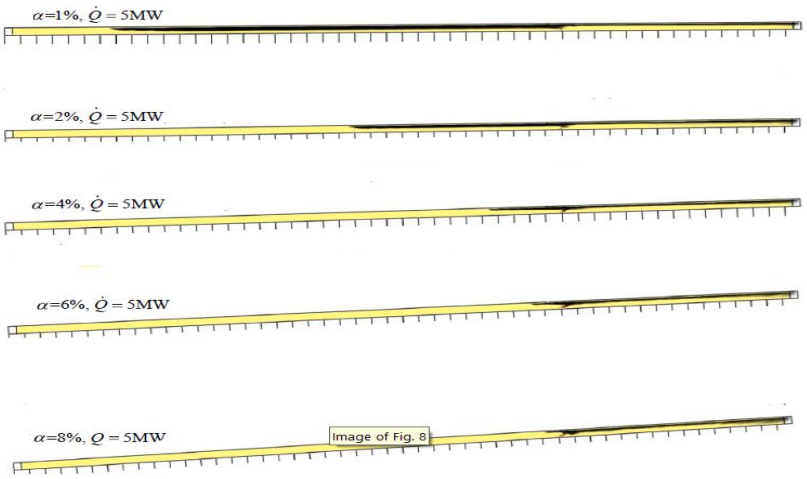

Figure 3.16. The impact of tunnel's inclination on the backlayering smoke length (Zhang et al., 2021).

Finding an adequate grid size is one of the main challenges while using CFD modelling. A relatively fine mesh resolution may generate more thorough and credible simulation findings but, it will excessively augment the computational time, requiring, at the same time, advanced hardware specifications. In some cases, the computation cost as an aftereffect of a fine mesh, may be unaffordable or even unbefitting for practical applications. Hence, it is critical to choose a suitable mesh resolution with a grid size that can compromise the simulation time with reliable and accurate results. According to an extent evaluation of several fire numerical simulations, it is suggested as a guideline the use of the characteristic fire diameter, *D**, as defined in equation 5.1, which is a function of heat release rate and ambient conditions. In particular, the more cells spanning the fire, the better the resolution of the calculation and thus the characteristic diameter is recommended to extend over at least, ten grid cells (McGrattan et al., 2020). In this manner, the mesh resolution near the fire region can be defined, producing dependable results, in a reasonable simulation time. Based on that, simulation surveys, have been conducted with the non-dimensional expression $D^*/\delta x$ -where δx is the nominal size of a mesh cell- ranging from roughly 3 to 57 , in large scale simulations (McGrattan and Hamins, 2001; Hwang and Edwards, 2005; Hu et al., 2007; 2007; 2008; 2010; Mawhinney and Trelles, 2007; 2008; 2012, Kashef and Bénichou, 2008; Kim et al., 2008; Cheong et el., 2009; Vigne and Jönsson, 2009; Wang, 2009; Trelles and Mawhinney, 2011; Lin

et al., 2014; Wang and Wang, 2016; Wang et al., 2016; Vermesi et al., 2017; Glasa et al., 2018; Ji et al., 2019; Tomar and Khurana, 2019; Zhang et al., 2021) and from approximately 5 to 120 (Hwang and Edwards, 2005; Blanchard et al., 2012; Li et al., 2012; Ko and Hadjisopho-cleous, 2013), in model scale simulations. It is clearly illustrated that several different mesh sizes on the cross-section of each tunnel case have been applied to assess the mesh through accuracy and time requirements. The simulation results have been then validated against experimental data from fire test incidents, and the significance of applying an adequate grid resolution in each simulation computational domain to obtain reliable results, have been highlighted and tested via grid sensitivity analysis (Hwang and Edwards, 2005; 2005; Kim et al., 2008; Cheong et al., 2009; Vigne and Jönsson, 2009; Wang, 2009; Colella et al., 2011; Blanchard et al., 2012; Wang and Wang, 2016; Vermesi et al., 2017; Zhang et al., 2021).

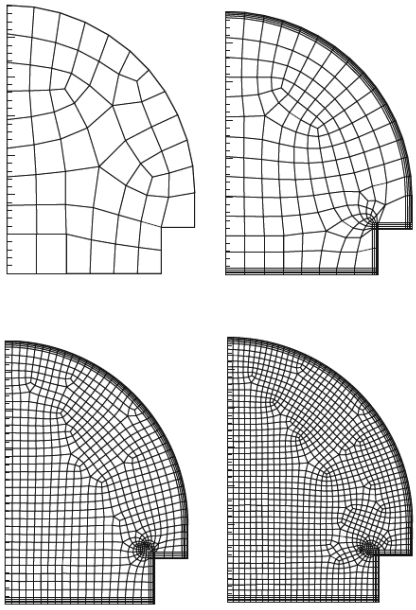

Figure 2.17. Illustration of different meshes -from a denser mesh to a finer one-, via FLUENT Modeling (Colella et al., 2011).

Various tunnel fire tests were selected and simulated via CFD modelling in a model scale environment (Hwang and Edwards, 2005; Blanchard et al., 2012; Li et al., 2012; Ko and Hadjisopho-cleous, 2013). The numerical results of model scale simulations have been then compared as well with experimental data in order for the use of CFD modelling to be verified in reduced scale applications and the value of its findings to be enhanced. However, there are a few challenges regarding this approach. Research studies have pointed out that the Froude modeling utilized in the most cases involves necessarily geometric similarity. When such similarity is not sustained, no accurate performance of Froude's modeling could be anticipated (Hwang and Edwards, 2005; Wang 2009). Nonetheless, the preservation of geometrical similarity, according to simulation findings does not entail the maintenance of kinematical similarity, as well. This observation clearly evince that the Froude-scaling law is an approximation for tunnel fires applications (Hwang and Edwards, 2005; Wang 2009). Thus, it is advisable to perform large-scale numerical simulation, too, in order to attain adequate verification for real scale fire incidents.

Table 3.4. Main characteristics of full-scale numerical simulations of fire tests.

Simulated Tunnel Details	CFD Code	Length (m)	Fuel Type	Peak HRR (MW)	$D^*/\delta x$	Ventilation (m/s)	Parametric Study	Measured Quantities	References
Memorial Tunnel, United States	FDS	130	Fuel Oil No.2	20 & 50	10.7 – 15.5	Natural Ventilation	Fire Size	T	McGrattan and Hamins, 2001
Memorial Tunnel, United States	FDS	190	Heptane & Propane	0,0266 - 144	8.8 – 11.2	Forced 3.2	Tunnel's Geometry, HRR, Fire Source Shape, Grid's Resolution, Ventilation Velocity, Ambient T	Critical Velocity, Backlayering	Hwang and Edwards, 2005
Mojiang & YuanJiang &Yu Tunnel,	FDS	50	Crude Oil	1.6 & 3.0	-	Forced 0.3 – 1.9	Fire Size, Slope	T	Hu et al., 2006
YuanJiang Road Tunnel, China	FDS	420	Crude Oil	1.8 & 3.2	9.4 – 11.8	Forced 0.6 – 1.1	Fire Size & Shape, Ventilation Velocity	T, Backlayering	Hu et al., 2007
Underground Channel	FDS	88	Crude Oil	0.75 – 1.6	8.6 – 11.7	Natural	Fire Size	HRR, T, CO, Smoke distribution	Hu et al., 2007
San Pedro Tunnel, Spain	FDS	140	Wood ''Euro-pallets''	40 - 100	18.4 – 26.5	Forced 1.9 – 3.5	Fire Size, Ventilation Velocity, Suppressed/ Unsuppressed Fire Scenario	HRR, T, Heat Flux	Mawhinney and Trelles, 2007; 2008; 2012,

									Trelles and Mawhinney, 2011
Model Tunnel, China	FDS	50	-	0.5 - 16	8.9 – 35.6	Forced 1.1 – 3.8	HRR, Ventilation Velocity, Fire Location	T, Critical Velocity, Dispersion of Smoke Particles	Hu et al., 2008
Louis-Hippolyte-La Fontaine Road Tunnel, Canada	FDS	1400	Propane Gasoline	2 & 20	14.2 - 35.7	Forced 0 - 14	Fire Size, Ventilation Scenarios, Fire Location	T, Backlayering, Volumetric Airflow, OD, Visibility	Kashef and Bénichou, 2008
Memorial Tunnel, United States	FDS	345	Fuel Oil No.2	100	10.3 – 20.5	Forced 2.5 – 3.0	Ventilation Velocity, Grid Resolution, Smagorinsky Constant, Prandtl & Schmidt Number	T, u	Kim et al., 2008
Madrid–Barajas Airport	FLUENT PHOENICS	-	Heptane	5 & 10	-	Forced 2.4 -6.0	CFD Code, Fire Size, Ventilation Velocity	T	Migoya et al., 2008
Memorial Tunnel, United States	FLUENT	854	Volumetric Heat Source	10 & 50	-	Forced 34.2 (Jet Fans)	Fire Size, Ventilation Conditions	T, u, CO, Turbulent Variables	Vega et al., 2008
Runehamar Tunnel, Norway	FDS	36 - 102	Solid Fuels (Wood & Plastic)	190	26.3 – 52.7	Forced 1.0 – 3.0	Tunnel's Geometry, Ventilation Velocity, Fire Shape & Ignition Location	HRR, Fire Development	Cheong et el., 2009

Beijing Subway Line 4, China	CFX	300	Heat Source, Methane	2 - 100	-	Forced 0.004 – 0.185	HRR, Ventilation Velocity, Fire Source Model, Fire Source Shape	T, u, Critical Velocity, Heat & Smoke Distribution	Hui et al., 2009
Repparfjord Tunnel, Norway	KFX & SOLVENT Model	2000	Heptane (Gasoline)	3.5 - 128	-	Natural & Forced 0.4 – 3.0	HRR, Fire Source Size Shape, Ventilation Velocity, Tunnel's Geometry	HRR, T	Nilsen and Log, 2009
Bømlafjord Tunnel, Norway	KFX & SOLVENT Model	7800	Heptane	5 - 11	-	Forced 3.0	HRR, Fire Source Size Shape, Ventilation Velocity, Tunnel's Geometry	HRR, T	Nilsen and Log, 2009
Byfjord Tunnel, Norway	KFX & SOLVENT Model	5800	Heptane	5 - 12	-	Forced 3.0	HRR, Fire Source Size Shape, Ventilation - Velocity, Tunnel's Geometry	HRR, T	Nilsen and Log, 2009
Baneheit Tunnel, Norway	KFX & SOLVENT Model	785	Heptane	7 - 11	-	Forced 3.0	HRR, Fire Source Size Shape, Ventilation Velocity, Tunnel's Geometry	HRR, T	Nilsen and Log, 2009
Hanekleiv tunnel, Norway	KFX & SOLVENT Model	1765	Heptane	6 - 12	-	Forced 1.5 - 2.5	HRR, Fire Source Size Shape, Ventilation Velocity, Tunnel's Geometry	HRR, T	Nilsen and Log, 2009
Memorial Tunnel, United States	KFX & SOLVENT Model	853	Heptane	120	-	Forced 2.5 – 3.0	Fire Source Size Shape, Ventilation Velocity, Tunnel's Geometry	HRR, T	Nilsen and Log, 2009

Runehamar Tunnel, Norway	KFX & SOLVENT Model	1600	Heptane	60 & 180	-	Forced 3.0	HRR, Fire Source Size Shape, Tunnel's Geometry	HRR, T	Nilsen and Log, 2009
Tunnel at La Ribera del Folgoso, Spain	FDS	100	Heptane	5.3	9.4 – 37.8	Natural < 0.5	Grid's Resolution, Number of Meshes, CFD Software Uncertainty	T, Heat Flux	Vigne and Jönsson, 2009
Mine Roadway, Australia	FDS	90	Octane	2 - 66	14.3 – 57.9	Forced 0.5 – 3.5	HRR, Fire Size, Ventilation Velocity, Slope, Mesh Resolution	T, u, Critical Velocity, CO, Soot, Heat Fluxes, Radiation, Turbulence Intensity	Wang, 2009
YingZuiYan Road Tunnel, China	FDS	600	Crude Oil	4 - 20	13.4 – 25.7	Forced 0.0 – 4.0	Fire Size, Ventilation Velocity	T, CO	Hu et al., 2010
Tianjin Xiawafang Subway Station, China	FDS FLUENT	120	Volumetric Heat Source	5		Forced	CFD Code	T, CO_2, Smoke Layer Thickness	Binbin, 2011
"Modern Tunnel"	FLUENT	400	-	10 - 100	-	Forced 3.0 – 7.0	Mesh Resolutions, Fire Size, Ventilation Velocity	T, Backlayering, Critical Velocity	Colella et al., 2011

San Pedro Test Tunnel, Spain	Fluent	600	Heptane Gasoil	1 - 25		Forced 2.0 – 2.6	Fire Size, Ventilation Velocity, Tunnel's Geometry	HRR, T, u	Migoya et al., 2011
Memorial tunnel, United states	FDS FLUENT	500	Methane	20 & 50	12.9 – 18.7	Forced	Slope, CFD Code	T, Visibility, Mass Flow Rate	Lin et al., 2014
Memorial Tunnel, United States	FLUENT	300	Volumetric Heat Source	10	12.2 - 24.3	Forced 2.3 – 2.8	Fire Location	T, Critical Velocity, Smoke Propagation	Wang and Wang, 2016
San Pedro Tunnel Test, Spain	FDS	240	$CH_2O_{0.62}$	70- 150	17.8 – 24.1	Forced 3.0	HRR, Fire Source Shape	T, O_2, CO_2, CO, Flame Length	Wang et al., 2016
Dartford West Tunnel, United Kingdom	FDS	400	-	30	4.7 – 18.9	Forced 3.8 – 6.6	Mesh Resolution	T, u	Vermesi et al., 2017
Polana Highway Tunnel, Slovakia	FDS	900	-	1 - 5	3.3 – 6.2	Natural 2.0	HRR, Slope	T, u, OD, Smoke Spread & Backlayering	Glasa et al., 2018
Test Corridor Delichatsios' Data	FDS	150	-	5 - 15	9.2 – 14.3	Natural	HRR, Fire Source Shape	T, u, Smoke Distribution & Mass Flow Rate, *1D* Smoke Spread	Ji et al., 2019

Runehamar Tunnel, Norway	FDS	150	Solid Fuels (Wood & Plastic)	12 - 21	10.5 -13.1	Forced 3.0	-	HRR, T, Heat Flux, Fire Development	Tomar and Khurana, 2019
Underground Model Tunnel	FDS	96	-	5 & 7.5	14.7 -17.2	Natural	Fire Size, Mesh Resolution, Tunnel's Geometry, Slope,	T, Backlayering	Zhang et al., 2021

Table 3.5. Main characteristics of model-scale numerical simulations of fire tests.

Simulated Tunnel Details	**CFD Code**	**Length (m)**	**Fuel Type**	**Peak HRR (MW)**	**$D^*/\delta x$**	**Ventilation (m/s)**	**Parametric Study**	**Measured Quantities**	**References**
Test Tunnel	FDS	4.9	Methane & Propane	0.003 – 44.8	5.4 – 8.9	Forced	HRR, Tunnel's Geometry, Slope, Fire Source Shape, Grid's Resolution, Ventilation Velocity, Ambient T	Critical Velocity, Backlayering	Hwang and Edwards, 2005
Scale Tunnel	FDS	43	Heptane	3.4	15.9 – 31.8	Forced 1.0 & 2.2	Ventilation Velocity, Mesh Resolution	HRR, T, Heat Flux, Volumetric Flow Rate, Rate of Enthalpy Change	Blanchard et al., 2012
Reduced Scale Tunnel	FDS	10.4	Heptane Gasoline	2.5 - 10	69.5 – 121.4	Forced 0.4 – 0.7	Fire Size & Type, Ventilation Velocity	T,u	Li et al., 2012
Laboratory Tunnel, Carleton University, Canada	FDS	53	Propane	5 - 40	7.4 – 16.9	Forced 0.5 – 1.6	Fire Size, Ventilation Velocity, Presence of Sprinkler Suppression System, Water Spray Densities	HRR, T, Dimensionless Richardson Number *Ri**	Ko and Hadjisopho-cleous, 2013

4. COMPUTATIONAL FLUID DYNAMICS CODE, FDS

The advancement of the knowledge of computational fluid dynamics (CFD) over the years accompanied by the vigorous development of the computing power has led to the establishment of CFD based "field" models, intended to resolve fire-related engineering problems. The utilization of CFD models has enabled the numerical computation of fire-fields even at complex geometries with the additional incorporation of a variety of other physical phenomena (McGrattan et al., 2020a; 2020b). A thermally driven fire-flow is exhibiting a significantly turbulent nature. The approach to modeling turbulence in many commercial and fire specific CFD models is to solve a statistically time-averaged form of the conservation equations of mass, momentum and energy, often referred as the Reynolds-averaged Navier-Stokes (RANS). In this type of simulations, a two-equation eddy viscosity model is generally applied. This model, in effect, allows the turbulence to be characterized by a velocity and a length scale that varies at each grid cell, in the computational domain. The most paramount two-equation model that is employed in the majority of RANS applications in fire engineering is the model k-ε. However, the averaging procedure which governs the resolution of this model equations renders fundamental limitations for fire applications. As stated, RANS models have been developed as a time-averaged approximation to the conservation equations of fluid dynamics. This technique is inaccurate as the averaging time in a fire simulation, although it is not specified, is long enough to necessitate the involvement of large eddy transport coefficients for describing the unresolved fluxes of mass, momentum and energy (Hurley, 2016).

To remedy this problem the appliance of the "Large Eddy Simulation" (LES) technique has been proposed. The implementation of LES to a numerically described fire scenario evidently results in greater temporal and spatial fidelity in the numerical results, given that the fire event is performed on a fine enough mesh grid. The LES approach regards the description of turbulent mixing of a gaseous fuel and combustion products with the neighboring atmosphere near the fire source. This process, which establishes the burning rate in most fires and manages the propagation of smoke and hot gases, is particularly challenging to be calculated (McGrattan et al., 2020a; 2020b). The basic idea behind the LES technique is that the eddy viscosity must be small enough to avoid flattening out the small but resolvable eddies but large enough to ensure numerical stability and account for the dissipation of energy at sub grid scales (Hurley, 2016).

Fire Dynamics Simulator (FDS) constitutes a computational fluid dynamic (CFD), model designed to resolve fire-driven fluid flows. In particular, the model solves numerically a form of the Navier-Stokes equations suitable for low-speed (Ma < 0.3), thermally- driven flow with particular regard on smoke and heat propagation from fires. FDS utilizes a three-dimensional rectilinear mesh. The partial derivatives of the conservation equation of mass, momentum and energy are estimated as finite differences, and the solution is updated in time, complying with the underlying mesh. The transportation of thermal radiation is also computed by employing the finite volume technique on the same grid as the flow solver. In order to simulate smoke movement, sprinkler discharge or fuel sprays, Lagrangian particles are used (McGrattan et al., 2020a; 2020b).

In general, the complete form of conservation equations of mass, momentum and energy may describe a large variety of physical processes in the field of fluid dynamics, but many of existing source terms in these equations are irrelevant to fire events. Therefore, these equations can be simplified for fire simulations, rendering the numerical calculations more affordable,

without distorting though, the original governing principles of the equations. Otherwise, preserving the universal character of those equations, would entail an enormous computational cost as the complexity of the numerical calculations would be more than challenging, without practically contributing to gaining further insights on fire dynamics. The resulting simplified equations are referred as the "low Mach number" combustion equations. They efficiently describe the low-speed movement of a gas driven by chemical heat release and buoyancy forces. The phrase low speed refers to gas velocities less than a Mach number of 0.3 (100 m/s) (McGrattan et al., 2020a; 2020b).

FDS offers valuable insights regarding fundamental phenomena of fire dynamics and combustion processes, augmenting the current level of understanding on that field while enhancing fire research studies. Throughout the model's evolution, FDS have been an important tool for fire protection engineering applications, resolving practical fire problems of, namely, fires in residential or industrial constructions, while including the provision for various ventilation and smoke management systems, sprinklers, multiple sensors and detectors. With the aim of reviewing the main FDS features, the following list outlines the fundamental models that rule the FDS performance (McGrattan et al., 2020a; 2020b).

- ***Hydrodynamic Model*** As stated FDS computes a form of the Navier-Stokes equations suitable for low speed, thermally driven flows with particular regard on smoke and heat transport from fires. The fundamental algorithm of the flow solver is an explicit predictor-corrector scheme, second order accurate in space and time. The thermally driven fluid flow is mainly identified by its strongly turbulent character. FDS employs the technique of Large Eddy Simulation (LES) to describe the turbulence of the flow. There are four main simulation approaches of operation in FDS, which are presented in Table 4.1.

Table 4.1 Overview of the simulation approaches of operation, in FDS.

Simulation Mode	
DNS	Direction Numerical Simulation
LES	Large Eddy Simulation
VLES	Very Large Eddy Simulation
SVLES	Simple Very Large Eddy Simulation

Simple Very Large Eddy Simulation correspond to VLES mode with more simplified physics. The above-mentioned modes include several physical and numerical parameters that stipulate the degree of physics involved in numerical model, defining the accuracy of the simulation results. The LES equations are obtained by using a low-pass filter, parameterized by a width Δ, to the DNS equations for mass, momentum and energy. In FDS, the filter width Δ is equivalent to the local cell size *dx* and it is a crucial parameter in the sub-models for the turbulent viscosity. The practice of taking *Δ = dx* is advocated as implicit filtering. Nevertheless, it must be noted, that implicit filtering does not imply dissipative numerics. FDS employs kinetic-energy-conserving central difference schemes for momentum with physically based closures for the turbulent stress. It is possible by interchanging the turbulent simulation mode, namely from LES to VLES, the accuracy of the numerical findings to alter. Such outcome is anticipated as the physics involved in each of the utilized models, may correspond differently to the physical model. Although LES is the default mode of operation, the program offers the capability of performing a Direct Numerical Simulation (DNS) when

the optimal level of fidelity in the findings is imperative, but this approach would necessitate the underlying numerical mesh to be fine enough.

- ***Combustion Model*** For applications where there is no particular interest in the combustion process themselves, FDS employs a single step, mixing-controlled chemical reaction which includes three lumped species. The latter term is a reacting scalar quantity that refers to a generalized species which actually represents a group of species. For instance, air, in FDS is a mixture of nitrogen, oxygen, water vapor and carbon dioxide. Particularly, the employed lumped species in the combustion model are the air, fuel, and fire products. By default, the last two lumped species are explicitly computed. For an infinitely fast reaction, reactant species in a given grid cell are converted to product species at a rate determined by a characteristic mixing time. Based on that, a flame surface is generated by requiring that fuel and oxidizer simultaneously vanish in the given grid cell. The single-step, mixing-controlled combustion model is described by means of mixture fractions for every component that once was originated as fuel. In particular, this approach to combustion, referred to as the "simple chemistry" combustion model, considers a single fuel species that is composed primarily of C, H, O, and N that reacts with oxygen in one mixing-controlled step to form H_2O, CO_2, soot, and CO, as depicted in the Equation 4.1.

$$\mathrm{C_xH_yO_zN_v} + \mathrm{v_{O_2}O_2} = \mathrm{v_{CO_2}CO_2} + \mathrm{v_{H_2O}H_2O} + \mathrm{v_{CO}CO} + +\mathrm{v_S Soot} + \mathrm{v_{N_2}N_2} \qquad 4.1$$

  The heat release rate per unit volume, is defined by summing the lumped species mass production rates times with their respective heats of formation. However, further options are offered by FDS, for simulating a combustion process including multiple reactions and reactions that are not necessarily mixing-controlled. The latter approaches usually require very fine grid resolution that is neither practical nor computationally affordable for largescale fire applications.

- ***Radiation Transport*** Radiative heat transfer is entailed in the model through the solution of the Radiation Transport Equation (RTE) for a gray gas, and in some limited cases using a wide band model. Employing the wide band model for radiation transport, even with a reasonably small number of bands, namely six (six-band model), adds a significant computational cost to the simulation and for that cause, it is recommended only for fuels with relatively low soot yield. This is due to the fact that in most large-scale fire simulations, soot is the most important combustion product, governing the thermal radiation from both the fire and the hot smoke. Regarding the "gray gas" model, it is reported that since the radiation spectrum of soot is continuous, it is reasonable to adopt the assumption that the gas behaves as a gray medium. The spectral dependence then results in one absorption coefficient (N = 1) and the source term for radiation is described by the blackbody radiation intensity. The Radiation Transport Equation (RTE) for a gray gas is solved employing an approach similar to finite volume methods for convective transport, and therefore it is called Finite Volume Method (FVM). Employing approximately 100 discrete angles, the finite volume solver necessitates about 20% of the total CPU time of a computation. However, this is a modest computational cost given the complexity of radiation heat transfer. Liquid droplets can also absorb and scatter thermal radiation. This is particularly essential in cases where mist sprinklers, are involved, but in general it is a key parameter in all the sprinkler cases. The absorption and scattering coefficients are based on Mie theory.

- ***Geometry*** FDS approximates the governing equations on a rectilinear mesh. In particular, the low Mach number equations are solved numerically by dividing the physical space where the fire is to be simulated into a large number of rectangular cells. Within each cell the gas velocity, temperature, etc., are assumed to be uniform, changing only with time. The accuracy on which the fire dynamics can be simulated is dependent on the number of cells that can be incorporated into the simulation. This number is ultimately limited by the computing power available. In total, this type of mesh is the simplest approach for simulating thermally driven flows within confined spaces. The user shall only specify the three dimensions which characterize the computational grid. However, in order to meet the numerical grids requirements all, the utilized obstructions, should be rectangular, since they ought to conform with the underlying mesh. This automatically implies that the level of geometrical resolution attributed to the fire scenario is directly determined by the grid size. As it regards the appropriate grid size for a numerical simulation study, it is advocated by a sensitivity analysis. In general, a sensitivity analysis accounts for the extent to which uncertainty in model inputs influences model output. In a mesh sensitivity study, the numerical parameter investigated is the grid size. In fact, the grid size is the most important numerical parameter in the FDS code, in general, as it dictates the spatial and temporal accuracy of the discretized partial differential equations. The recommended value for the mesh resolution, derived by the sensitivity study, is the traced at the point where additional reduction on the grid size does not result in more precise numerical findings. In general, the finer the numerical grid, the better the numerical solution of the equations. However, increasing the numerical accuracy by means of mesh resolution, it automatically increases significantly the computational cost.

- ***Multiple Meshes*** In a numerical calculation more than one rectangular meshes can be employed. This option, offered by the FDS code, is a handy technique at simulation cases where different mesh resolutions are needed. For example, a large computational domain does not necessarily require fine mesh resolution through its whole length. However, at the region where the fire is located, the grid size shall comply with the requirements of the vigorous character of combustion processes. Without the appliance of multiple meshes at such cases, one rectangular mesh would result either in unaffordable computational cost or in significantly degraded accuracy in the predicted results.

- ***Parallel Processing*** FDS utilizes OpenMP, a programming interface that exploits multiple processing units on a single computer. In that manner, the total computational time required for a single simulation can be significantly reduced. In accordance with that, the MPI (Message-Passing Interface) enables to multiple computers, or multiple cores on one computer, to run a multi-mesh FDS simulation. The feasibility of that technique is promoted by the option of multiple meshes. The main idea lies on breaking up the computation domain into multiple meshes, and then the flow field of each mesh, to be computed as a separate MPI process. In that manner, each processor claims the resolution of the thermally driven flow located in the assigned computational domain while MPI handles the transfer of information between the meshes, i.e., MPI processes.

- ***Boundary Conditions*** Thermal boundary conditions are assigned to all the solid surfaces. In addition, certain information is provided about the burning properties of a material, which is used as fuel. Heat and mass transfer to and from solid surfaces is

usually ascribed by empirical correlations, although FDS allows the direct computation of heat and mass transfer by performing a Direct Numerical Simulation (DNS).

Concluding, FDS is designated as a “fire model” because it includes source terms and boundary conditions that describe the turbulent combustion of gaseous fuel and oxygen, the transport of thermal radiation through hot, soot-laden gases and the thermal decomposition of real materials. Additionally, the model enables the activation of sprinklers and smoke detectors, the transport of water and liquid fuel droplets, and a variety of other features that describe fires inside and outside of confined spaces. The provided capabilities render the model practical for thermally driven flow simulations. Further information about the FDS -*Sixth Edition*- can be found in the *Fire Dynamics Simulator Technical Reference Guide Volume 1: Mathematical Model* and *Fire Dynamics Simulator User’s Guide* (McGrattan et al., 2020a; 2020b).

5. FDS VALIDATION STUDY

A validation study is a challenging area for tunnel fire modelling, since the experimental data are far from complete, considering the complexity of the actual testing process. This chapter presents a numerical simulation of the Memorial Tunnel Fire Ventilation Test Program, outlines the degree to which a quantitative agreement with available experimental data is achieved and identifies potential sources of discrepancies.

The Memorial Tunnel Fire Ventilation Test Program (MTFVTP) comprised 98 full-scale fire tests, conducted in an abandoned road tunnel, near Charleston, West Virginia (U.S.A.). Various tunnel ventilation systems and ventilation configurations have been applied attempting to evaluate their respective smoke and temperature management capabilities, when exposed to fires of several MW's. These tests have generated a comprehensive database relevant to the design and operation of road tunnel ventilation systems under fire emergency conditions.

Figure 5.1. View of the north portal area of the Memorial Tunnel located near Charleston, West Virginia. (https://transportation.wv.gov/Turnpike/about*/turnpike_history/Pages/default.aspx)*

5.1 Description of validation Test Cases (502, 615)

The Memorial Tunnel (c.f. *Figure 5.1*,) was built in 1953 and was operating for 30 years. After its decommission, a large number of fire experiments have been performed in the Memorial Tunnel's facilities, from September 1993 to March 1995. The experiments included tests with fire sizes of 10, 20, 50 and 100MW along with a series of alternative ventilation systems and arrangements, such as full and partial ventilation, partial transverse ventilation with a single point extraction and with oversized exhaust points, point supply and point exhaust operation, natural and longitudinal ventilation with jet fans. As far as the tunnel structure is concerned, the Memorial Tunnel is a two-lane, 853.8m long mountain tunnel which has a 3.2% ascending grade from the south to the north portal. The main tunnel section is rectangular, attached with a semi-circular ceiling. However, for each test conducted, specific modifications have been made regarding the tunnel's configuration to enhance the proper implementation and operation of each ventilation concept. For that reason, in some cases, a false ceiling was placed throughout the entire length of the tunnel, creating a rectangular tunnel configuration. The width of the tunnel is 8.8m and the center-line height 7.9m. At each portal there is a horizontal ceiling, 19.2m long at the south side and 18.5m at the north side, and a sidewalk is also located on one side through the entire length of the tunnel. *Figure 5.2*

depicts the internal view of the Memorial Tunnel, as it was originally designed, with the arched ceiling.

Figure 5.2. Internal view of the Memorial Tunnel, illustrating the cross-sectional geometry of the tunnel's configuration.
(https://www.clui.org/ludb/site/center-national-responsememorial-tunnel)

As stated, during the Memorial Tunnel Test Program, fires of various sizes have been tested with the intention of evaluating the efficiency of several ventilation systems and configurations, under different fire conditions. In particular, four steel pans of different sizes provided the capability of producing fires with a nominal heat release rate ranging from 10MW to 100MW, *Figure 5.3*. With the aim of preserving the integrity of the tunnel's linings from the fire, the walls near the fire region had been protected with a fireproofing covering before the experimental testing, which was mainly composed of cement and vermiculite. The fire pans were set approximately 0.76m above the tunnel's floor and were filled with 0.15m of water. Above the layer of the water, Fuel Oil No.2 was poured in the pan as fuel. The inflow of the Fuel Oil No.2 was remotely regulated, given the readings of the weighting cells under the fire pans, from automatic controllers at the control room, *Figure 5.4.* In that way, the requested fire load was maintained approximately constant during the test, since the fuel oil consumption was continuously measured.

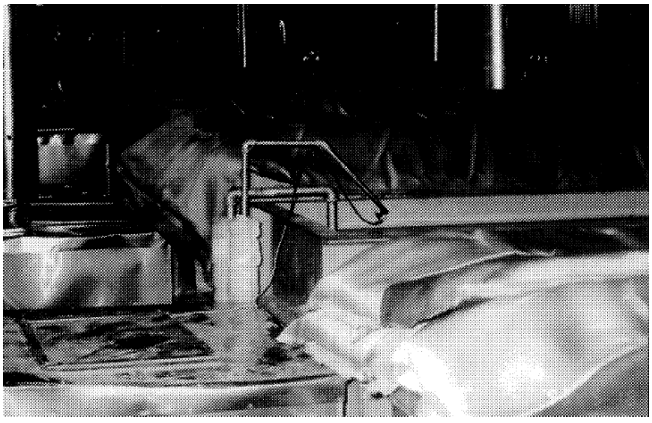

Figure 5.3. View of the Memorial Tunnel's fuel pans. The pans that are not in use for the current experiment are covered with alumina silica fiber blankets, (Bechtel/Parsons Brinckerhoff, 1995).

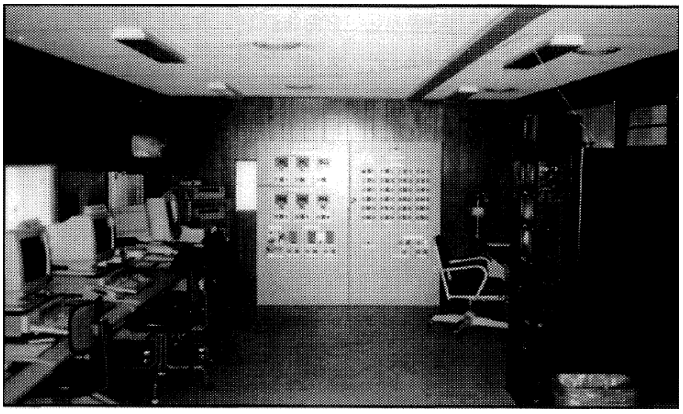

Figure 5.4. Image of the control room-trailer located outside the south portal of the tunnel, (Bechtel/Parsons Brinckerhoff, 1995).

Various technical instruments were installed with the aim of collecting data of the main fire and ventilation related variables throughout the fire tests. The air and smoke temperature and velocity profiles along with the concentrations of the fire products have been monitored and recorded at several cross-sections throughout the tunnel. More specifically, the air-smoke temperature was recorded using groups of thermocouples at different cross sections inside the tunnel while the measurement of the airflow was accomplished by the utilization of Bi-directional Pitot tubes. The exploitation of differential pressure instrumentation, designed to measure very low-pressure ranges, combined with the readings of the air temperature, at the bi-direction pitot tubes region, and the ambient barometric pressure conditions, have contributed to the calculation of the air velocity. Gas analyzers were utilized for obtaining the concentrations of carbon monoxide (CO), carbon dioxide (CO_2) and the total hydrocarbon content (THC), existing in the smoke airflow. All of the above-mentioned sensors were arranged in instrumentation trees, denoted as "loops" in the project's technical report. The allocation of these sensor groups throughout the tunnel's length is presented in *Table 5.1*. The data series recorded from the Memorial's Tunnel Tests, form a significantly thorough and dependable database for validation of any CFD code, including FDS which specializes in fire driven fluid flows.

Table 5.1. Memorial Tunnel's Instrumentation Locations

Loop	**Instrumentations Location (Distance from the North Portal)**	**Sensors Employed**
214	20m	T, u, CO, CO_2, THC
213	106m	T
211	211m	T
209	321m	T, u, CO, CO_2
208	426m	T, u
207	508m	T, u, CO, CO_2
307	554m	T, u, CO, CO_2
306	584m	T
305	603m	T, u
205	615m	T
304	629m	T, u
303	650m	T
302	681m	T, u, CO, CO_2
301	723m	T, u, CO, CO_2
202	834m	T, u, CO, CO_2, THC

5.1.1 Test Case 502 - Natural Ventilation

Out of 98 tests, Test 502 was selected to be the main validation case. In the selected test case, a fire of approximately 50MW was employed during the experiment while no mechanical ventilation was imposed. In fact, except from Test 502, only one other experiment, Test 501, was performed at the Memorial Tunnel's Test Program, with natural ventilation conditions. However, considering the similarity in terms of fire size to a potential normal fire load scenario in a tunnel incident, Test 502 was selected instead of Test 501, as the later referred to a mild fire of 20MW. The fire source was located at the position of "loop 205", 615.4m from the north portal of the tunnel. The fire load curve for Test Case 502, is illustrated in Figure 5.5.

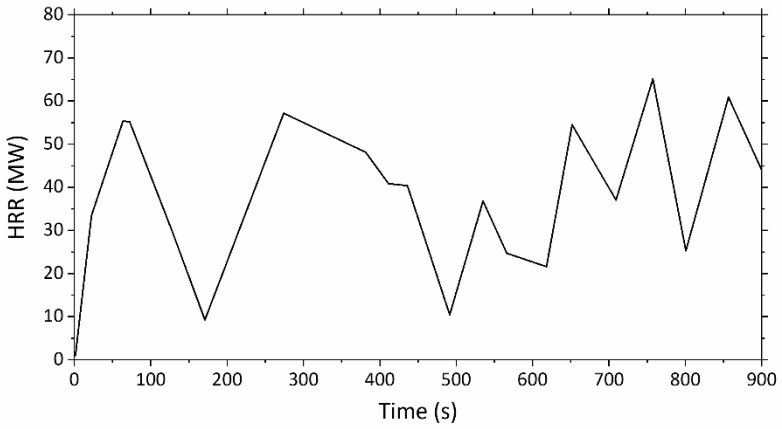

Figure 5.5. Time variation of Heat Release Rate, for Test Case 502 (Chalasani et al., 2010).

Regarding the tunnel ceiling characteristics utilized in this test, no false ceiling was employed to form an entirely rectangular configuration. The ambient temperature was measured to be 10℃. The time variation of the external wind conditions prevailing near the south portal, at loop 202, are presented in Figure 5.6; the depicted volume flow, is entering the domain of the tunnel through the south portal, heading north. In total, the main characteristics of Test Case 502 are summarized in Table 5.2.

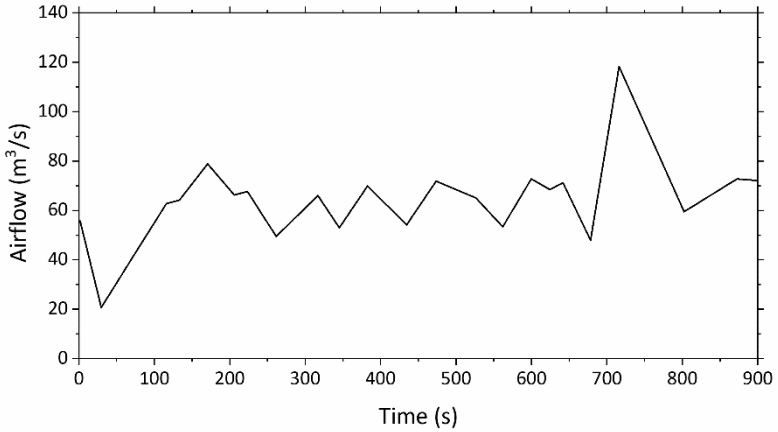

Figure 5.6. Time variation of the bulk airflow at the south end of the tunnel for Test Case 502 (Chalasani et al., 2010).

Table 5.2 Brief overview of the experimental details of Test Case 502.

Test Case	Fuel Type	Fire Source Location	Nominal HRR	Ventilation System	Ventilation Conditions
502	Fuel Oil No.2	238.4m from the South Portal	50MW	Natural	Figure 5.6

5.1.2 Test Case 615b- Longitudinal Ventilation with Jet Fans

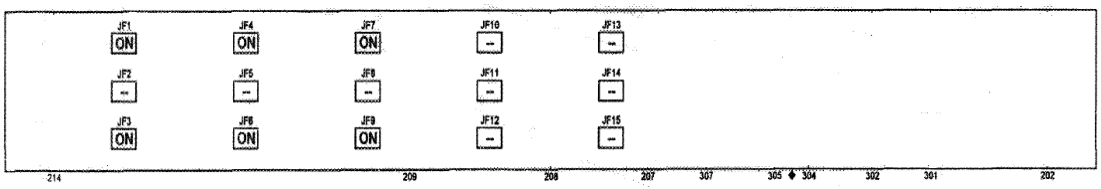

Figure 5.7 Jet Fans arrangement and approximate location throughout the tunnel's length (Bechtel/Parsons Brinckerhoff, 1995).

Test Case 615b belongs in a sequence of tests investigating longitudinal ventilation by the use of jet fans. It was conducted with an approximate fire size of 100MW, whereas the fire source was located 238.4m from the south portal. The actual time evolution of the Heat Release Rate is depicted in Figure 5.8. The surface of the fuel pans was located approximately 1m above the floor and the utilized fuel was Fuel Oil No.2, for this case as well. The ambient air temperature is taken to be 8℃ and the tunnel wall temperature 12℃. Prior to the ignition of the fuel oil, measurements of air temperature and velocity were undertaken to establish the initial flow conditions within the tunnel. No external wind data were available and hence it is not clear whether the initial velocity is due to external wind or buoyancy forces of the sloping tunnel.

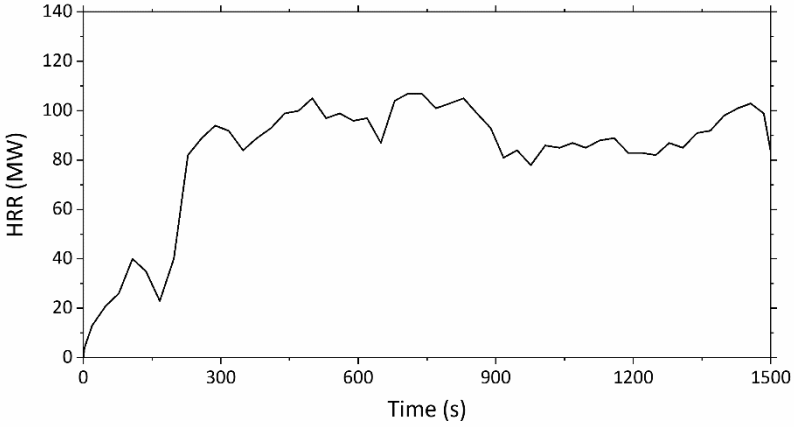

Figure 5.8. Time evolution of Heat Release Rate for Test Case 615b (https://www.kbwiki.ercoftac.org/w/index.php/Test_Data_AC4-04).

The jet fan tests were performed after the natural ventilation tests. Before the start of the longitudinal ventilation tests, 15 axial flow fans were installed north of the fire, in groups of three, as shown in *Figure 5.9*. The groups of jet fans were nearly equally spaced to the selected part of the tunnel. For the sake of clarity, in Figure 5.7 a number has been assigned to every jet fan installed for Test Case615B; this does not necessarily mean that all of these jet fans were actually in operation during the test. Each jet fan has a length of 6.7m and an inside diameter of 1.35m. Each fan is equipped with a 56kW motor, designed to deliver43 m^3/s at an exit velocity of 34.2 m/s.

The maximum temperature associated with the strength of materials of the jet fans reaches 300℃. The longitudinal central positions of the jet fans, measured from the north portal, as well as the operational period of each fan during the test, are given, in Table 5.3 and Table 5.4, respectively.

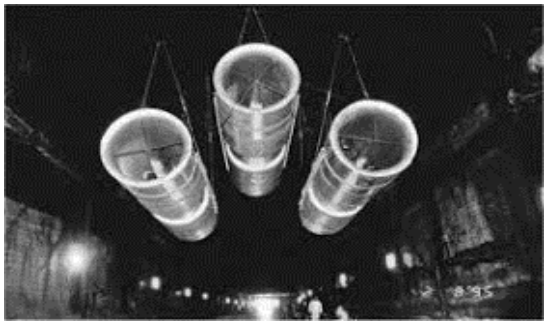

Figure 5.9. Relative arrangement of the three axial flow fans, composing a jet fan group (Bechtel/Parsons Brinckerhoff, 1995).

Table 5.3. Overview of the longitudinal central positions of the jet fans.

Jet Fan Group	Distance from North Portal (m)
Group 1 – [JF1 to JF3]	95
Group 2 – [JF4 to JF6]	190
Group 3 – [JF7 to JF9]	285
Group 4 – [JF10 to JF12]	379
Group 5 – [JF13 to JF15]	474

The interval between the onset of the fire and the activation of the ventilation system was set at 2min. The purpose of the delayed response time was to investigate the ability of the jet fans to reverse the buoyancy driven airflow using a minimum number of jet fans. In Test Case 615B, the maximum number of jet fans in operation is 6, at each time period, creating initially a steady airflow with a direction to the south portal. 26 minutes after the beginning of the test, the last group of fans, which are closer to the fire source reverse their functioning mode to draw smoke back towards the north portal, while the rest continued to push the airflow to the south end, like before. However, since the examination of the capacity of the jet fan system handling the airflow through different ventilations strategies, is not the aim of the current work, the time period after 25 minutes, is entirely excluded in the validation study.

Table 5.4. Overview of the activation period of each jet fan, during Test Case 615B.

Jet Fan	Operation Period (min:s)
None	0:00-2:00
JF1, JF3, JF4, JF6, JF7, JF9	2:00-14:00
JF1, JF3 , JF4 , JF6 , JF9	14:00-22:00
JF1, JF3, JF4, JF6, JF7, JF9	22:00-25:53
None	25:53-26:03
JF5, JF8, JF11 (R)	26:03-34:19
JF5, JF8, JF11, JF14 (R)	34:19-35:11
JF5, JF8, JF11, JF13, JF14, JF15 (R)	35:11-43:22 (End of the test)

Similar to Test Case 502, the volume airflow has been measured in Test Case 615b, as well. The only difference is that the boundary condition in Test Case 615b, corresponds to the north end of the tunnel. As demonstrated in Figure 5.10, the initial direction of the airflow was from the south to the north portal. Following the activation of the jet fan system, the airflow's direction was reversed, heading to the south end of the tunnel, until the end of the investigated 25-min period.

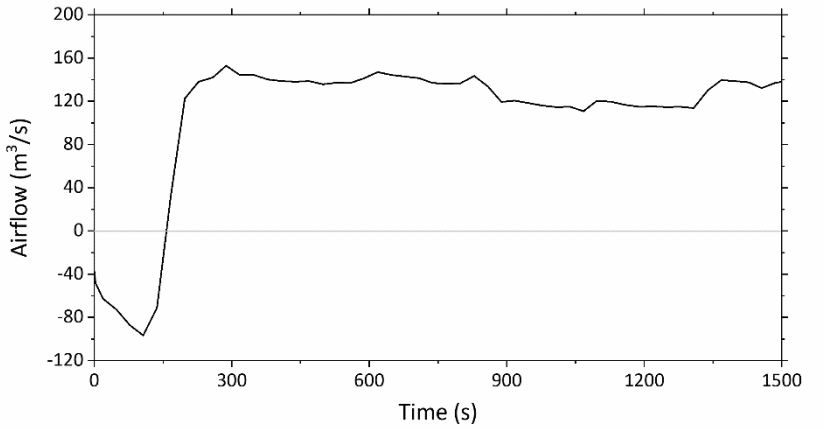

Figure 5.10. Time evolution of the bulk airflow at the north end of the tunnel, for Test Case 615b (https://www.kbwiki.ercoftac.org/w/index.php/Test_Data_AC4-04).

In total, the sequence of the tests, at which Test 615B is included, investigates the ability of a longitudinal ventilation system using jet fans, to manage smoke and heat. This survey was conducted under the influence of a number of varying parameters including the number of jet fans in operation and their airflow direction, the ventilation's system response time as well as the imposed fire size. Table 5.5 provides a concise summary of the main experimental parameters for Test Case 615b.

Table 5.5 Brief overview of the experimental details of Test Case 615b.

Test Case	Fuel Type	Fire Source Location	Nominal HRR	Ventilation System	Ventilation Conditions	Jet Fans in Operation	Ventilation System Response Time
615b	Fuel Oil No.2	238.4m from the South Portal	100MW	Forced, Jet Fans	Figure 5.10	6	2 min

It should be noted that Test Case 615b does not constitute the main validation case in the current work. As far as it may be relevant, the provided information has been included for the sake of a forthcoming validation study in the next chapter, regarding to road tunnel fire simulations under forced longitudinal ventilation conditions. So, further information about this test trial will be presented in the next chapter.

5.2 Numerical simulation details

In order for any simulation study to provide reliable results, various modelling parameters should be specified first, after thorough consideration. In particular, when a large computational domain is required, as in the case of Memorial Tunnel Fire Test Experiments, the complexity of the simulation model increases significantly, along with the required computational time. As a consequence, further numerical adjustments and simplifications should be considered regarding the ascription of the physical model. Although an extensive effort is made in rendering the simulation as simple as possible, reducing accordingly the computational time and resources it entails, the preservation of an adequate level of accuracy against experimental results, remains the primary objective of any numerical study. In the case of the Memorial Tunnel, the entire length of the tunnel is selected to be represented in the simulation. Figure 5.11 visualizes the Memorial Tunnel's simulation domain, created by the post-processing software Smokeview.

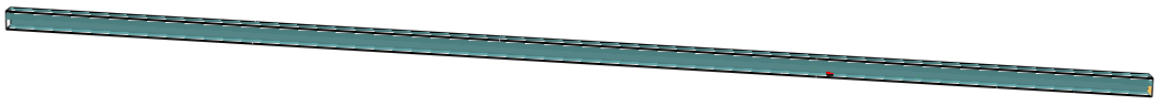

Figure 5.11. View of the Memorial Tunnel's simulation domain.

As stated, the preliminary stage of any computational study involves the determination of various modelling parameters along with the sensible reduction of the computational cost. In particular, finding a suitable grid size is one of the main challenges when simulating a large physical domain. In general, a fine resolution grid generates more accurate and reliable simulation results but, at the same time, it is associated with increased simulation times. The demands on the computer resources as well, for certain CFD applications, may act as an additional constrain in conducting a thorough sensitivity analysis of the grid size. Therefore, since the increase of the total computational cost can be sometimes prohibitive for research purposes, selection of an appropriate grid size is important in order to balance constrains such as simulation time and computer resources with the required results accuracy. For physical domain areas ranging from several meters to even kilometers, such as a road tunnel structure, the affordable grid resolution for most LES fire simulations, ranges from centimeters to meters. In fact, an FDS input file is suggested to be built using a relatively coarse mesh at first, and then gradually be refined until there are no considerable differences spotted in the simulation results; this process is also referred as a mesh sensitivity study. For simulations concerning buoyant smoke flows, the level of accuracy regarding the flow field numerical resolution is given, as a guideline, by the non-dimensional expression $D^*/\delta x$, where D^* is the characteristic fire diameter and δx is the nominal size of a mesh cell.

$$D^* = \left(\frac{\dot{Q}}{\rho_\infty C_P T_\infty \sqrt{g}}\right)^{\frac{2}{5}} \qquad 5.1$$

In Equation 5.1, the quantity $\dot{Q}$ (kW), is the total heat release rate of the fire, whereas ρ_∞, C_P, T_∞, is the air density, thermal conductivity and temperature, respectively, far away from the fire source. The quantity $D^*/\delta x$ actually corresponds to the number of grid cells covering the characteristic diameter of the fire. In particular, the more cells are applied in the fire source, the better and more accurate the resolution of the numerical calculation is, regarding the combustion-related processes; as a result the characteristic diameter is recommended to extend over at least, ten grid cells (McGrattan et al., 2020). In this manner, the mesh resolution near the fire region can be initially defined, with the expectation of producing dependable results, in a reasonable simulation time. It must be noted that the value of D^* does not necessarily coincide with the physical fire

diameter, in fact, it is reasonable to assume that the determination of the mesh resolution is better assessed in terms of this non-dimensional parameter, rather than an absolute mesh cell size, so that the expression of $D^*/\delta x$ prescribes qualitatively the precision of the calculation.

In terms of reducing the required computational time, multiple meshes can be used, as an option, in the FDS code. The application of multiple meshes uses a Message-Passing Interface, MPI, to allow multiple Central Processing Units (CPUs) to run a single FDS simulation at the same time (McGrattan et al., 2020). More specifically, according to this procedure, it is required for the CFD domain to be divided into several smaller areas with the same or different mesh resolutions, and then each sub-domain to be assigned to its own processor. In that manner, all of the allocated computational subdomains can be resolved simultaneously, equipped with the capability of exchanging information and data where necessary. This approach is suggested, especially in large CFD domains where fine resolution is also required, like tunnel fire simulations, since it produces satisfactory numerical results in reduced simulation times (Weisenbacher et al., 2011). Previous numerical studies have also been conducted to certify that the mesh division process does not add substantial errors to the results of the simulation and confirm the validity of this technique (Vermesi et al., 2017). Based on that, in the current study, the tunnel has been divided into eleven meshes, as illustrated in Figure 5.12.; for the sake of better clarity, a different colour has been designated to each mesh. To 6 out of 11 meshes, which are far from the fire field, a "coarse" grid has been used, whereas at the remaining 5 meshes, located near the fire source, a "finer" one grid has been used, depending on the chosen combination of mesh resolution for each case. To resolve the divided computational domain with 8 processors available, a combination of 2 different subdomains have been distributed to 3 processors. In that way, the number of grid cells each processor had to resolve, has been equally allocated.

Figure 5.12 Overview of the multiple rectilinear meshes of the Memorial Tunnel Simulation.

For the multiple meshes of varying grid resolution, applied in this case, the Fast Fourier Transforms (FFT) cannot be employed for the general solution of the Poisson equation. As an alternative, the fast solver is utilized for each mesh while the preservation of the pressure field on the interfaces of the meshes is achieved by repeated solves on each individual mesh. Especially in numerical applications of long tunnels, like this one, false or misleading fluctuations in the pressure field may occur leading possibly, to numerical instabilities. The induced error from these deceptive fluctuations, is traced in the main component of the velocity, at a mesh boundary and it can be downgraded via an increase in the number of calls to the pressure solver at each time step. The default maximum pressure iterations for the VLES simulation mode by the FDS code, are 10. As advocated by the FDS User Guide, the maximum pressure iterations in the current study, are increased up to 50 (McGrattan et al., 2020). Another suggestion for this type of problem, is the reduction of the acceptable pressure tolerance between old and new pressure field data in repeated solves, to the 1/10 of its default value. The default value of the latter quantity is defined as the ½ of the cell's length for the acquired mesh resolution. Both of these remedies to numerical instabilities have been applied, realizing that they will probably increase the computational time.

The characteristic diameter, D^*, of the Test Case 502 fire, is calculated to be 4.67m, since the nominal heat release rate was approximately 50,000 kW and the ambient temperature was measured to be 10^{o}C. In terms of the grid sensitivity analysis, several values of the non-dimensional

expression $D^*/\delta x$ have been evaluated, where the δx value corresponding to the nominal cell size near the fire region. The values of the $D^*/\delta x$ expression range from approximately 8 to 23, corresponding to cell sizes from 0.60m to 0.20m, respectively. As stated, in LES simulations, a finer gird size provides more detailed information on the turbulent flow but requires increased computation resources and longer computational times. In a tunnel fire simulation, vigorous changes in the airflow mainly take place in the flow field near the fire source and, consequently the numerical predictions in this area are of central importance. Therefore, a finer mesh could be applied only to a particular sub-domain that involves the fire, where computational demands are higher than the rest of the tunnel. For the Test Case 502 simulation, this region has been selected to extend for approximately 65m downstream and upstream of the fire source. A coarser grid, twice the cell size value of the fine one, is utilized for the remaining length of the tunnel to preserve relatively accurate numerical results, without inflicting increased computational costs. While FDS allows the computational domain to consist of many connected meshes, it is mandatory that mesh alignment exists. In other words, an integer number of fine cells must be exactly abutting each coarse cell, as depicted in Figure 5.13. For the primary construction of the base case scenario, a grid resolution of 0.3m has been assigned to the region of the fire source and of 0.6m to the remaining tunnel's length, constituting a reasonable initial assumption, since the corresponding value of $D^*/\delta x$, for the mesh resolution of 0.3m, is 15.5, a value which is significantly higher than the proposed minimum value of 10.

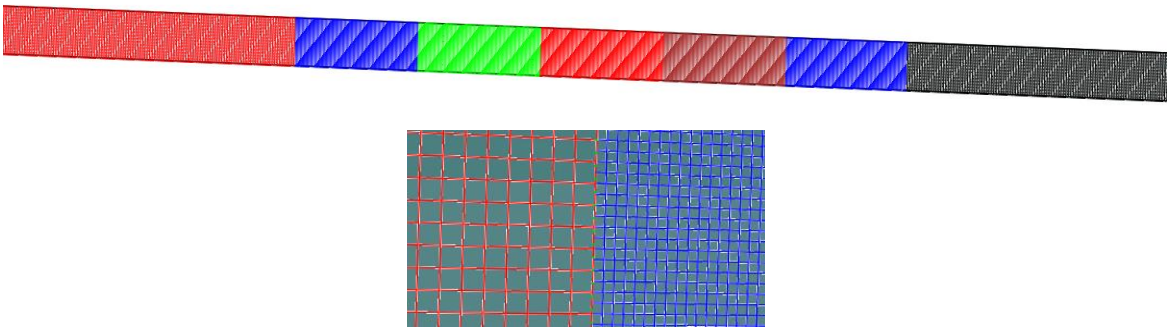

Figure 5.13. In the feature above, the five connected meshes of the fire source region are depicted, along with two coarser meshes applied on each side of this region. In the feature below, a magnified version of the mesh alignment between a coarse and a fine mesh is presented.

Because of the nominal resolution in the computational domain, the full detail of the tunnel's ceiling could not be represented via FDS modelling. FDS resolves the governing equations on a rectilinear mesh and therefore, any solid obstruction, including the tunnel's geometry or a ventilation system configuration, is necessary to conform to the underlying mesh. Consequently, the semi-circular part of the tunnel's ceiling (Figure 5.14) as well as the circular axial jet fans (Figure 5.15) have been constructed using rectangular obstructions, in the most appropriate way to resemble the original tunnel's geometry. Furthermore, regarding the modelling of the jet fans in Test Case 615b, each fan has been represented as a rectangular solid blockage with a specified fan velocity across its outlet area. At the inlet, a similar sized sink of air is prescribed, compared to the exhaust outlet area, to accord with mass continuity of the flow. In practice, the boundary conditions for a fan are more complex than the ones applied at the tunnel's portals, which are the boundaries of the CFD domain, taking into account the need for conservation of density, temperature and smoke concentration from the inlet to the outlet steam, in the jet fan's case. The above-mentioned boundary conditions have been assigned only to the fans that would be activated during the numerical simulation (shown in yellow in Figure 5.15). The rest of the fans have been ascribed as solid obstacles. In general, an obstruction that is relatively thin compared to the gas phase numerical grid spacing, like a jet fan's external envelop, can be specified as a thin

obstruction. However, using this kind of obstructions it is not possible to specify a normal velocity component on their surface. This particular constraint opposes the fundamental function of a jet fan and thus the structural thickness of the jet fan is approximated to be one mesh cell thick, for the underlying mesh. The 3.2% longitudinal gradient of the Memorial Tunnel has also been allocated through the gravitational vector, GVEC, function of the FDS code.

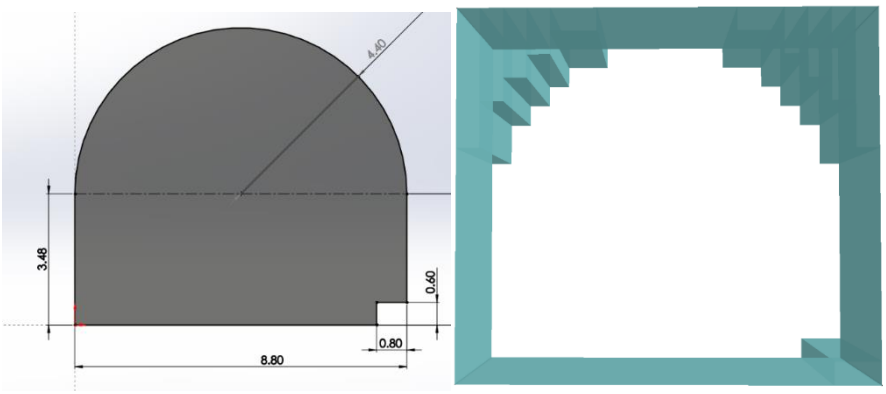

Figure 5.14. Overview of the key cross-sectional geometry, in meters, of the Memorial Tunnel configuration (left) and the respective numerical ascription via FDS modelling (right).

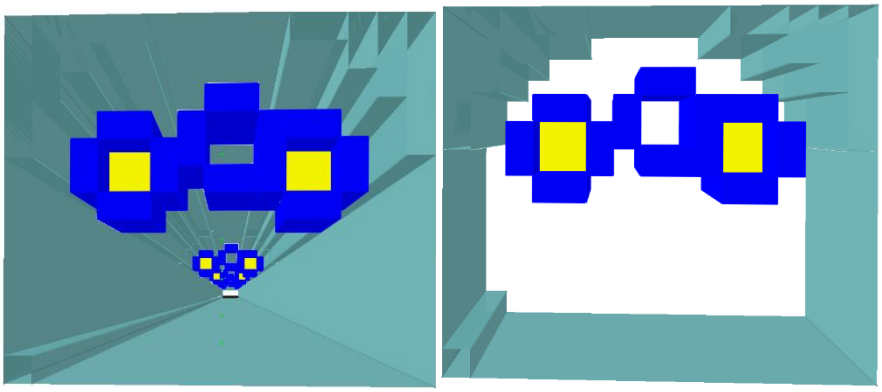

Figure 5.15. Overview of the spatial distribution of the jet fans groups throughout the tunnel's length (left) along with a magnified view of a jet fan's group cross-sectional mounting (right).

In general, there are a number of alternative approaches for representing a fire source in a CFD model. The most precise technique is the description of the actual combustion process, with all the necessary information provided to the simulation program. Nevertheless, in practice, modeling the entire combustion process would require an extremely fine grid resolution in the fire region, and only a very simple fuel with a well-known combustion chemistry, to be feasible. In the frame of the present validation study, the complete length of the tunnel is modelled. Additionally, a Fuel Oil No.2 fire was originally induced in the actual experiments (502 & 615B). Apparently, the above factors render the "detailed" approach computationally unaffordable, highlighting the need for a simpler alternative. Towards this end, the experimentally determined heat release rates can be employed in a simulation study as an input. In that way, there is no need for further specification of the fuel's properties since the fire is basically modeled as a burner, with a specified Heat Release Rate Per Unit Area, HRRPUA (kW/m^2) on its upper surface, c.f. Figure 5.16. It must be noted that by stipulating the parameter of HRRPUA, a burning rate is specified for the fire instead of the actual burning process of the fuel. The mass flow rate of the combustion products is also attributed to the domain at the upper surface of the burner, yet no velocity should be prescribed for the ejection of these combustible gases since it is computed by the FDS. To replicate the exact experimental

conditions of the fire source in the Memorial Tunnel, steel plates have been selected for the sides and bottom of the burner arrangement. Similar to the experimental procedure, the fire source is set to begin at the start of the simulation.

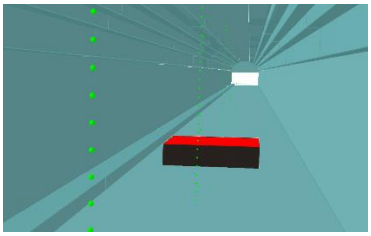

Figure 5.16. Overview of simulated fire source, via the FDS code.

The heat release rate of the pool fire has been set in the FDS input file according to the experimentally measured values, shown in Figure 5.5, for the entire test period. The RAMP_Q function, have been employed to specify the time evolution of the heat release rate. More specifically, for a fire of 50MW, in the Base Case fire scenario with a mesh resolution of 0.3m at the fire region, the pan size was selected to be 5.4m(L) x 4.2m(W) x 0.9m(H), corresponding to a fuel surface area of 22.5m^2, while the respective experimental pool surface had an area of 22.68m^2. As expected, different fuel surface areas, need to be created as a consequence of different mesh resolutions, and thus the value of heat release rate per unit area (HRRPUA) has been modified in order to match to the experimental HRR curve, in each case. Taking into account the actual experimental specifications and the selected grid resolution, the fire location of the Base Case is placed at 615.3m, from the north portal.

A common way of comparing the emissions from different burning fuels, is the yield parameter, y_i (kg/kg). y_i (kg/kg) yields, Equation 5.2, express the ratio between the mass *mi* (kg) or the mass loss rate $\dot{m}_i$ (kg/s) of a component *i* generated by the combustion of a certain mass or the total fuel mass loss of a fuel, during the studied test period, respectively.

$$y_i = \frac{m_i}{\Delta m_f} = \frac{\dot{m}_i}{\dot{m}_f} \quad 5.2$$

Based on that parameter, some fundamental parameters of the fuel combustion process can be specified in the code. In particular, when the simple chemistry model is employed, the soot and carbon monoxide yield produced from the fire ought to be defined along with the radiative heat transfer fraction. To begin with, soot is the dominant source and sink of thermal radiation. The soot yield, (y_{SOOT}), Equation 5.3, represents the mass of soot produced per mass of fuel reacted and is highly associated to the estimation of the radiation and visibility levels inside the tunnel.

$$y_{SOOT} = \frac{mass\ Soot\ in\ Products}{mass\ of\ Fuel\ Reacted} \quad 5.3$$

The CO yield (y_{CO}), *Equation 5.4*, is the mass of CO produced per mass of fuel reacted and similar to the soot yield, the CO yield is essential for assessing the tenability conditions during a tunnel fire.

$$y_{CO} = \frac{mass\ CO\ in\ Products}{mass\ of\ Fuel\ Reacted} \quad 5.4$$

The yields of soot and CO for a heptane fire, SOOT_YIELD and CO_YIELD respectively, as derived from the SFPE Handbook of Fire Protection Engineering (Hurley, 2016), are presented in Table 5.6;

heptane, is commonly used as a surrogate fuel for fuel oil. An increase in the thermal power of a fire, increases the quantity of combustion products, which confirms the experimental observation that these yields in large-scale tests are generally higher than in small-scale tests. Consequently, for the specification of these model values, the data from the experiment should be assessed in terms of scaling effects, geometrical differences, ventilation and combustion conditions and all the remaining experimental conditions, in general.

Table 5.6. Combustion properties of n-Heptane.

Fuel	SOOT_YIELD	CO_YIELD
n-Heptane	0.042	0.012

In general, approximately 30% to 40% of the total heat released from a fire can be transferred to the neighbouring walls and obstacles through radiation (McGrattan et al., 2020). Heat can be redistributed, via radiation, within the smoke-filled region, as well. Regarding the RADIATIVE_FRACTION parameter specified in an LES calculation, there are some suggested default values for several common pure fuels (Morgan, 2016). Thus, for a heptane fire of approximately 50MW, in the case of Memorial Tunnel, a radiative fraction of 40% is applied to the input file, as a reasonable approximation.

A fire in a sloped tunnel generally produces a natural draught (natural ventilation) due to the buoyancy forces regardless of the wind conditions outside the tunnel or additional forced longitudinal ventilation systems. In fact, in Test Case 502, which constitutes a natural ventilation test, a high magnitude of air flow rate has been monitored at the south portal of the tunnel during the entire experimental time period, as illustrated in Figure 5.6. Accordingly, in the simulation, a forced flow boundary condition, varying with time, has been assigned to the tunnel's south end, forcing the air to enter the computational domain. In particular, utilizing the command VOLUME_FLOW, along with the function RAMP_V, the time evolution of the bulk airflow has been sufficiently represented. At the north end of the tunnel, an OPEN boundary condition has been invoked, which denotes a passive opening to the outside of the computational domain while alleviating, to some extent, wild oscillations in pressure. In that manner, the overall natural ventilation conditions, for Test Case 502, are recreated in the numerical model.

Hot gases lose heat to the structure's walls at a rate determined by both the thermal properties of the bounding solids and the time evolution of conditions within the gas phase. As a result, in a tunnel fire, the surrounding walls' temperature rises due to radiative and convective heat transfer from the fire and the hot smoke flow. In fire simulations, any wall material can be defined and utilized if its main thermal properties, such as the thermal conductivity, density and specific heat capacity, along with the material's thickness, are specified. In the current simulation study, the selected material for tunnel's walls is assumed to be "CONCRETE". However, for the sake of model simplification, the tunnel's walls have been specified as adiabatic, since in the current study there is no particular interest in investigating the effects of heat on the tunnel's mechanical structure. Hence, no thermal properties ought to be attributed to the wall's surface. Other heat transfer boundary conditions could certainly have been employed regarding the material of the walls, yet the adiabatic condition also corresponds to a "worst-case scenario", in terms of temperature rise and buoyancy forces. The universal heat's confinement, due to adiabatic boundary condition, poses a more immediate threat to the ventilation system integrity while creating at the same time dangerous conditions for people's health and evacuation attempts. However, for the sake of completeness, the properties of the utilized materials for the current study, are reported in Table 5.7 (Morgan, 2016; McGrattan, 2020).

Table 5.7. Thermal properties of materials used in the Memorial Tunnel simulations.

Surface	Density (kg/m^3)	Thermal Conductivity ($W/m\ ^oC$)	Specific Heat ($kJ/kg\ K$)
Concrete	1,900- 2,300	1.37	0.88
Steel	7,850	45.8	0.46

A “log law” wall model is employed by default by the FDS code for the computation of the tangential velocity of air or smoke at any surface, requiring every solid surface to have a specific roughness (McGrattan, 2020). Therefore, no further wall function is needed to supplement the slip boundary condition at the walls, since it is mandatory for every surface induced in the model to have a specific roughness height. The default value for ROUGHNESS is 0.0. The wall material of the Memorial Tunnel is specified to be concrete. While the value for the roughness of concrete surfaces in the literature ranges from 0.3 to 3.0mm, in an actual tunnel configuration there are various geometric features along the walls, such as fire extinguishers, emergency phones, lightning and electrical equipment and systems that cannot usually be reconstructed in a coarse grid resolution and may be assumed as roughness elements. Apparently, these unresolved features can be counted for when specifying the ROUGHNESS parameter in FDS. As illustrated in Figure 5.17, the Memorial tunnel internal geometry has indeed a distinctive large variety of uneven geometrical structures, which are creating a particularly “rough” wall surface. However, for the preliminary development of the Base Case scenario for the Test 502, the value of ROUGHNESS has been set equal to zero. A more realistic value will be investigated later, as part of a parametric study, in order to obtain the order of magnitude of the Memorial Tunnel wall’s ROUGHNESS.

Figure 5.17. Overview of the multiple *geometric features along the walls of the Memorial Tunnel, which constitute roughness elements.*

Occasionally, when a numerical simulation refers to a significantly large physical domain but, at the same time, a fine grid resolution is required to adequately simulate the specific characteristics of the fire, the computational time demands are practically prohibitive. As a preliminary approach in these applications, the user may impose approximately steady-state conditions at the model, in a time-averaged sense, to accelerate the computational process. In this context, FDS allows to substantially reduce the time necessary to heat the walls of the tunnel until steady-state conditions are achieved, by the specification of the parameter TIME_SHRINK_FACTOR. In this case, the specific heat capacities of the various materials are reduced by a factor equal to the TIME_SHRINK_FACTOR value, thus speeding up the heating phase of these materials. An example of an application where this parameter is desired is a validation experiment where time-averaged flow quantities are examined. In the current work, a TIME_SHRINK_FACTOR of the order of 10, has been applied in all the investigated cases of the parametric study that follows. The computational time required for each case, using the TIME_SHRINK_FACTOR modification, is presented in Table 5.9. It must be

noted that the optimum case scenario, presented in Section 5.3, does not make use of the TIME_SHRINK_FACTOR parameter, to ensure the highest conceivable fidelity of the numerical results. However, this adjustment could not be applied to each case of the parametric study, since it would require significantly higher computational times, rendering the entire parametric study practically unattainable. In conclusion, Table 5.8 entails a summary of the main numerical details regarding the general configuration of the FDS input file for the Base Case Scenario.

Table 5.8 Review of the main numerical details regarding the general configuration of the Base Case Scenario.

General Configuration - Numerical Details			
Category	***Command***	***Value***	***Units***
HEAD	CHID / TITLE	Base Case	
TIME	T_END	900.0	s
	TIME_SHRINK_FACTOR	10	
MISC	SIMULATION_MODE	VLES	
	GVEC	0.314, 0.0, -9.805	m/s^2
	TMPA	10	^oC
PRES	PRESSURE_TOLERANCE	22.22	s^{-2}
	MAX_PRESSURE_ITERATIONS	50	

5.2.1. Parametric Studies- Test Case 502

FDS modelling can offer valuable insights into the development of a fire driven fluid flow. However, numerical predictions depend on a large number of both numerical and physical related details of the fire incident. The numerical model, in fact, is extremely sensitive to the input parameters and thus their proper definition is an issue of great importance in every simulation study. More specifically, numerical results depend on a variety of input values such as tunnel's geometry, material and fuel properties, ventilation conditions as well as the way of heat transfer. Since absolute knowledge of every experimental detail, like fuel load or the exact chronology of the events, can never be achieved, estimations and assumptions need to be included into the model. Aiming to investigate the impact of the numerical and physical parameters, a broad parametric study has been carried out. More specifically, the influence of the mesh resolution, the turbulent simulation mode, the radiative heat transfer from the fire and hot smoke, the CO and soot production from the fire and the effect of the roughness of the tunnel's linings on the CFD results have been studied. Overall, 28 different simulations have been performed; their specific details are reported in Table 5.9.

Figure 5.18. Display of the measurement sensors' longitudinal distribution, near the fire field.

Table 5.9. Review of the main numerical details of the parametric study.

Parametric Study - Details							
Case Name	Turbulence Model	Grid Size (m)	CO YIELD (kg/kg)	SOOT YIELD (kg/kg)	RADIATIVE FRACTION	WALL ROUGHNESS (m)	Computational Time (h:min:s)
Base Case	VLES	0.30 - 0.60	0.012	0.042	0.40	0.00	6:31:32
Case 1	LES	0.30 - 0.60	0.012	0.042	0.40	0.00	11:30:16
Case 2	SVLES	0.30 - 0.60	0.012	0.042	0.40	0.00	7:32:22
Case 3	LES	0.20 - 0.40	0.012	0.042	0.40	0.00	70:45:52
Case 4	VLES	0.20 - 0.40	0.012	0.042	0.40	0.00	49:56:37
Case 5	**LES**	**0.25 - 0.50**	0.012	0.042	0.40	0.00	24:29:02
Case 6	VLES	0.25 - 0.50	0.012	0.042	0.40	0.00	14:52:35
Case 7	VLES	0.60 - 0.60	0.012	0.042	0.40	0.00	1:16:13
Case 8	VLES	0.30 - 0.60	0.002	0.042	0.40	0.00	6:44:08
Case 9	VLES	0.30 - 0.60	0.022	0.042	0.40	0.00	6:54:37
Case 10	VLES	0.30 - 0.60	**0.032**	0.042	0.40	0.00	6:47:47
Case 11	VLES	0.30 - 0.60	0.042	0.042	0.40	0.00	6:40:53
Case 12	VLES	0.30 - 0.60	0.012	0.032	0.40	0.00	6:34:23
Case 13	VLES	0.30 - 0.60	0.012	0.052	0.40	0.00	6:28:23
Case 14	VLES	0.30 - 0.60	0.012	**0.062**	0.40	0.00	7:18:37
Case 15	VLES	0.30 - 0.60	0.012	0.072	0.40	0.00	6:57:49
Case 16	VLES	0.30 - 0.60	0.012	0.042	0.20	0.00	7:40:39
Case 17	VLES	0.30 - 0.60	0.012	0.042	0.25	0.00	7:30:25
Case 18	VLES	0.30 - 0.60	0.012	0.042	0.30	0.00	7:13:54
Case 19	VLES	0.30 - 0.60	0.012	0.042	**0.35**	0.00	6:45:33
Case 20	VLES	0.30 - 0.60	0.012	0.042	0.37	0.00	7:01:23
Case 21	VLES	0.30 - 0.60	0.012	0.042	0.43	0.00	6:21:07
Case 22	VLES	0.30 - 0.60	0.012	0.042	0.50	0.00	6:45:09
Case 23	VLES	0.30 - 0.60	0.012	0.042	0.40	0.05	6:50:13
Case 24	VLES	0.30 - 0.60	0.012	0.042	0.40	0.10	7:12:47
Case 25	VLES	0.30 - 0.60	0.012	0.042	0.40	**0.25**	6:15:59
Case 26	VLES	0.30 - 0.60	0.012	0.042	0.40	0.45	6:36:06
Case 27	VLES	0.30 - 0.60	0.012	0.042	0.40	0.90	6:27:07

It should be noted that in the simulations, the measurement sensors have been set up at the same locations throughout the tunnel's length as the ones in the actual experiment of the Memorial Tunnel (c.f. Figure 5.18). In that manner, the comparison between numerical results and experimental findings has become feasible, enhancing at the same time the value of the underlying parametric study.

5.3 Numerical Results

This parametric study focuses on the influence of several parameters on the smoke propagation originated from a fire source of approximately 50 MW, within a naturally ventilated tunnel. With respect to both theoretical and experimental remarks, the propagation and distribution of smoke is highly associated with the underlying natural smoke flow, due to the tunnel's inclination and the governing wind conditions outside the tunnel, during the day of the experiment. In the actual experiment, when the fully developed fire was established, a well-stratified smoke layer existed solely on the downstream route of the fire, heading to the north end of the tunnel. In contradiction with the experimental findings, numerical results indicate that a thick layer of smoke has also been developed on the upstream side of the fire source, towards the south portal of the tunnel. Thus, even under the influence of buoyancy forces and considerable forces due to external natural ventilation, the flow patterns occurring upstream and downstream of the fire source are distinctive in all of the parametric cases, suggesting the presence of "backlayering" upstream of the fire source, Figure 5.19.

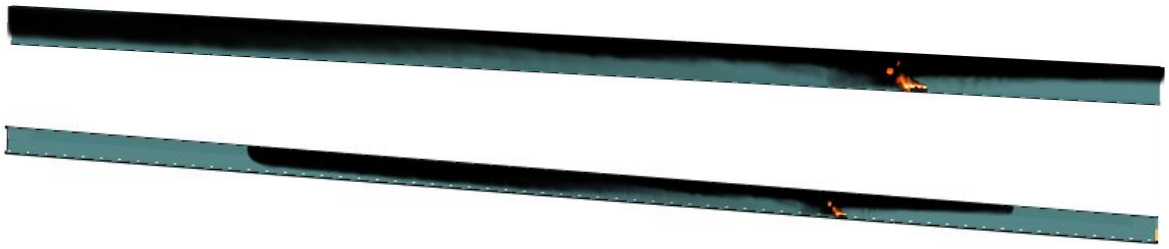

Figure 5.19. Visual representations of the soot distribution and flame envelope, inside the tunnel for the Base Case scenario, at 14 minutes. Total tunnel length (below) and detail, close to the fire source (from 300m to 700m) (above).

Throughout the tunnel, the ventilation velocity is mainly determined by its longitudinal component. Only in the vicinity of the fire source, the contribution of the vertical component becomes significant. However, aiming to compare the numerical findings with the actual experimental data, reported in the Memorial Tunnel's textbook, only the longitudinal component of the velocity was taken into account. In this context, the mean longitudinal velocity profiles at the symmetry plane of the tunnel, were recorded at 20m, 321m, 426m, 508m, 554m, 603m, 629m, 681m, 723m and 834m, downstream the tunnel's southern portal. In order for the evaluation of the numerical results to be as accurate as possible, the time of the comparison was set at 14 minutes of elapsed experimental time, when the fire is fully developed, and steady state conditions of the fire and flow have been established. Figures 5.24, 5.26, 5.28, 5.30, 5.32 and 5.34, present from left to right, the velocity distribution for the entire tunnel's length, for the selected time. For brevity, the legends are only shown in the end of each group of figures, for each parametric study. In general, in almost every parametric study, the shapes of the predicted upstream longitudinal velocity profiles are roughly following the same tendency for a particular location. The smoke flow in the upstream region of the fire source, towards the south end of the tunnel, can be generally divided into two layers according to the numerical findings, as illustrated by the velocity profiles. The upper layer is close to 6 m above the tunnel's floor whereas the lower layer is below it. The interface of these two layers of hot smoke and fresh air can be easily identified through the velocity profiles at the height where the velocity is zero. In the upper layer, the velocity direction is against the natural ventilation airflow signifying a smoke flow tendency to spread from the fire source towards the south tunnel portal. With respect to experimental data, it must be noted that at 14 minutes experimental time, no backlayering effect existed at that part of the tunnel. In the lower layer, fresh air enters the tunnel due to natural ventilation. Numerical data result in velocities around 2 m/s regarding the entrainment of fresh air in the tunnel at the south portal. When the

fresh air gets closer to the fire source, it longitudinally accelerates, as illustrated in Figure 5.20. Accordingly, the backlayering smoke begins to spread with velocities of approximately 3 m/s, at 629m, and gradually as the hot smoke flows further upstream away from the fire source, it decelerates and is finally reduced to a zero value, before reaching the end of the tunnel. Regarding the downstream route from the fire source, towards the north end of the tunnel, the exact opposite tendency is observed in the computational results. The presence of a two-layer flow structure cannot be identified owning to the fact that smoke and air are mixed and travel in the same direction. Thus, especially at the velocity profiles near the fire source, at 603 m and 553 m, only one layer is observed. There, a hot layer of the combustion products, covering the entire cross section of the tunnel start to travel with velocities of around 4 m/s towards the north end. Progressively, the magnitude of the smoke velocity increases further up to almost 12 m/s, due to the vigorous production of heat and other combustion products from the fire source, while a thin layer of fresh air begins to entrain at a lower height, whose velocities do no exceed 2m/s. Consequently, near the interface between the upper and lower layer, the magnitude of the longitudinal velocity component reduces considerably. It is clearly shown that the thickness of the smoke layer downstream from the fire is way thicker and more uniform than that of the upstream, leading to the establishment of a steady longitudinal velocity component regardless the distance from the fire source. Nevertheless, the magnitude of the longitudinal velocity component in the upper layer is far larger than the one in the layer below. Within a certain numerical range, the velocity profiles are very similar for most of the parametric studies, but the FDS code's accuracy in predicting the magnitude of the actual experimental events still depends on many numerical details.

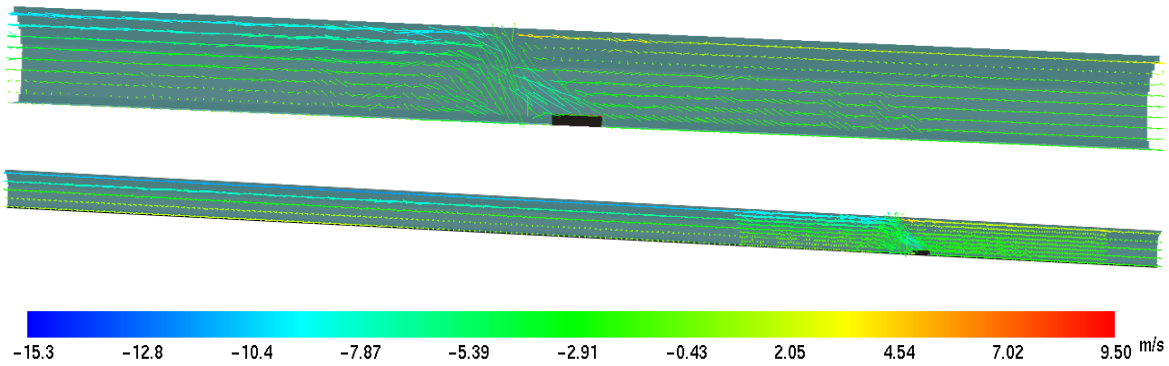

Figure 5.20. Magnified visual representations of the velocity distribution, with vectors, inside the tunnel for the Base Case scenario, at 14 minutes. Tunnel length from 300 to 700m, (below) and detail, close to the fire source, from 550m to 680m (above).

This numerical estimation of the backlayering effect, is also illustrated in the temperature distribution versus time, during the entire experimental test period, at regions close to the fire source. Evidently, the intensity of fire related phenomena is, in general, greater close to the fire source, and it tends to increase even more closer to the ceiling. In this context, in Figures 5.22, 5.25, 5.27, 5.29, 5.31 and 5.34, the time-varying temperature, estimated at the symmetry plane of the tunnel, is presented at two different positions (Loops 305 and 304), which are located in either side of the fire source. In view of any investigated parameter, the numerical results regarding the temperature are collated against experimental data at different vertical positions. More specifically, in Figures 5.22, 5.25, 5.27, 5.29, 5.31 and 5.34, the temperatures of the left column correspond to the downstream location of the fire at 603m, at heights of 7.3m, 5.7m, 2.4m and 0.3m, while those on the right are associated to the upstream location of 629m, correspondingly. For brevity, the legends are only shown once, at the end of each group of figures. Regarding the predicted temperatures in the upstream region of the fire source, several discrepancies have been

identified, against the experimental data. As demonstrated in the temperature figures, at the upper region of the tunnel's height, where the hot layer of backlayering smoke is located, the predicted temperatures are highly overestimated. The computed temperatures approximately range close to 500°C at a height of 7.3m from the tunnel's floor and around 400°C at a height of 5.7m, whereas the respective experimental values are close to 350°C and 250°C, respectively. This numerical inaccuracy of the order of 150°C is introduced to the results since the fire reaches the stage of full development, when the backlayering effect begins to form. This tendency is in contradiction with the actual experimental data, and it is maintained until the end of the test period. At heights of 2.4m and 0.3m, where smoke from the backlayering effect does not exist, the fidelity of the numerical results is remarkable. On the other hand, the backlayering phenomenon has a noteworthy impact on the downstream route from the fire source, too. As a matter of fact, since a portion of smoke is directed to the upstream end of the tunnel, the layer of the remaining smoke at the downstream side is not so thick and uniform, as suggested by the experimental data. This phenomenon results in lower predicted temperatures of the smoke layer, while allowing the entrainment of fresh air to the smoke flow. Within the upper layer of smoke at a height of 7.3m, the mean computed temperature, is around 650°C, when the fire has fully grown as illustrated in Figure 5.21, while the respective experimental value has been measured close to 850°C. Accordingly, at a height of 5.7m the mean predicted temperature is around 470°C, whereas the experimental one is close to 730°C. This numerical divergence of the order of 200-250°C, is justified due to the deficiency in the predicted flow characteristics. In agreement with the above, the predicted temperatures of the smoke flow, even at low heights, are also underestimated by the FDS code, with a discrepancy of the same magnitude. In all series of the parametric study, although an external airflow boundary condition at the south end of the tunnel is set, it is evidently not enough to prevent the development of backlayering smoke in the simulations. It is widely known that the time marching values in FDS simulation are tracing back to the prescribed initial field conditions, where in that case they may be not completely specified due to lack of experimental information. Hence, through these findings, it is evident that the insufficiency of the FDS in predicting accurately the flow characteristics, induced from the fire source, does not rest on the code's capability but on the incomplete specification of the experimental conditions via the reported boundary conditions.

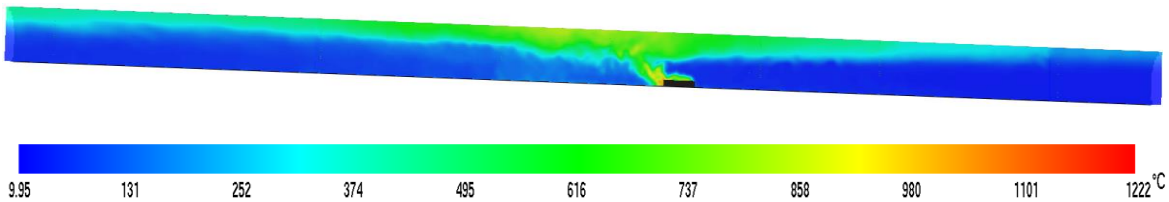

Figure 5.21. A magnified (from 500m to 700m) visual representation of the temperature distribution inside the tunnel for the Base Case scenario, at 14 minutes.

The predicted temperature and velocity profiles are recorded at the same measurement locations as the ones used in the full-scale experiments. It must be noted that the computational domain in the FDS simulation is constructed by rectilinear grid cells and thus scalar quantities, such as the temperature, are computed at the center of each grid cell, whereas vector quantities, such as velocity, are appointed at their appropriate cell faces. The individual regions on which the parametric study has been based on, are further elaborated in the following section.

5.3.1 Simulation Mode

In a sensitivity analysis, selection of the appropriate simulation mode is a key numerical variable, especially for simulations of fire driven smoke flows in tunnels. So, the main object of this sub-chapter is the selection of the proper turbulent model for the Memorial Tunnel Test 502. The four basic models of operation in FDS are the Direction Numerical Simulation, *DNS*, Large Eddy Simulation, *LES,* Very Large Eddy Simulation, *VLES*, and Simple Very Large Eddy Simulation, *SVLES*. As far as the DNS model is concerned, it is practically unfeasible to be employed in a series of simulation tests regarding an 854 m long tunnel CFD area, due to the immense computational time and the respective cost in hardware resources it entails. Therefore, this approach is excluded from the current parametric study. For the remaining three models, a parametric survey has been conducted using the Base Case Scenario, by specifying a different SIMULATION_MODE on the MISC line. The evaluation of each simulation model has been performed taking into account the possibilities and limitations of each model while trading off between the acceptable accuracy in the numerical results and the required computational cost.

Figure 5.23 shows the temperature at a distance of approximately 13m upstream (Loop 305) and downstream (Loop 304) from the fire. There is a general tendency of over-predicting the temperature upstream of the fire, at 629m, at the upper area of the cross section throughout the entire test period. On the contrary, FDS tends to seriously under-predict the temperature at all heights downstream from the fire. Based on that, it is clear that the phenomenon of backlayering is more intense on the numerical prediction than in the actual experiment. This observation may be owed to the fact that the actual meteorological conditions outside the tunnel are not provided for Test 502 and therefore the actual ventilation conditions have not been precisely specified. However, the rapid rise in temperature, at the upper cross-sectional area of the tunnel at both measurement locations, is well predicted. In terms of the simulation models, it is demonstrated that the LES model results in a more accurate prediction of the smoke temperature both downstream and upstream of the fire, compared to the VLES and SVLES models.

Figure 5.24 presents the numerical predictions of the velocity profiles throughout the tunnel length, computed by each turbulence model, against experimental data. The calculated velocity profiles demonstrate well the advantage of the VLES model compared to the LES and SVLES. However, it should be noted that in this approach additional uncertainties might have been introduced regarding the ability of the LES model to precisely predict important small-scale physical processes, such as small eddies, swirls, vortices, that occur at a large-scale CFD domain, like a tunnel, which cannot be adequately resolved on the given computational mesh. More specifically, with LES, one attempts to resolve the flow field as accurately as possible on a given mesh resolution, and thus, flow structures, such as swirling eddies, can cover only a few grid cells. To attain this result, the eddy viscosity must be small enough to prevent smoothing out these small, but resolvable, eddies, but large enough to guarantee numerical stability and account for the diffusion of energy at sub-grid scales. It would be inadvisable, therefore, to use such an approach without some previous study of the capabilities of such models, regarding the CFD domain's numerical resolution. In total, this parametric study highlights the dominance of the LES and VLES models over the SVLES, as expected. In view of these results and with consideration to the pursued numerical accuracy, the computational time and the actual tunnel dimensions, an additional approach is followed in the next group of parametric cases, regarding the mesh resolution. More specifically, every mesh resolution is tested using both the LES and VLES simulation modes, except from the case of the most coarse grid of 0.60m. In that way, the most appropriate simulation mode for the respective underling mesh resolution, can be better identified.

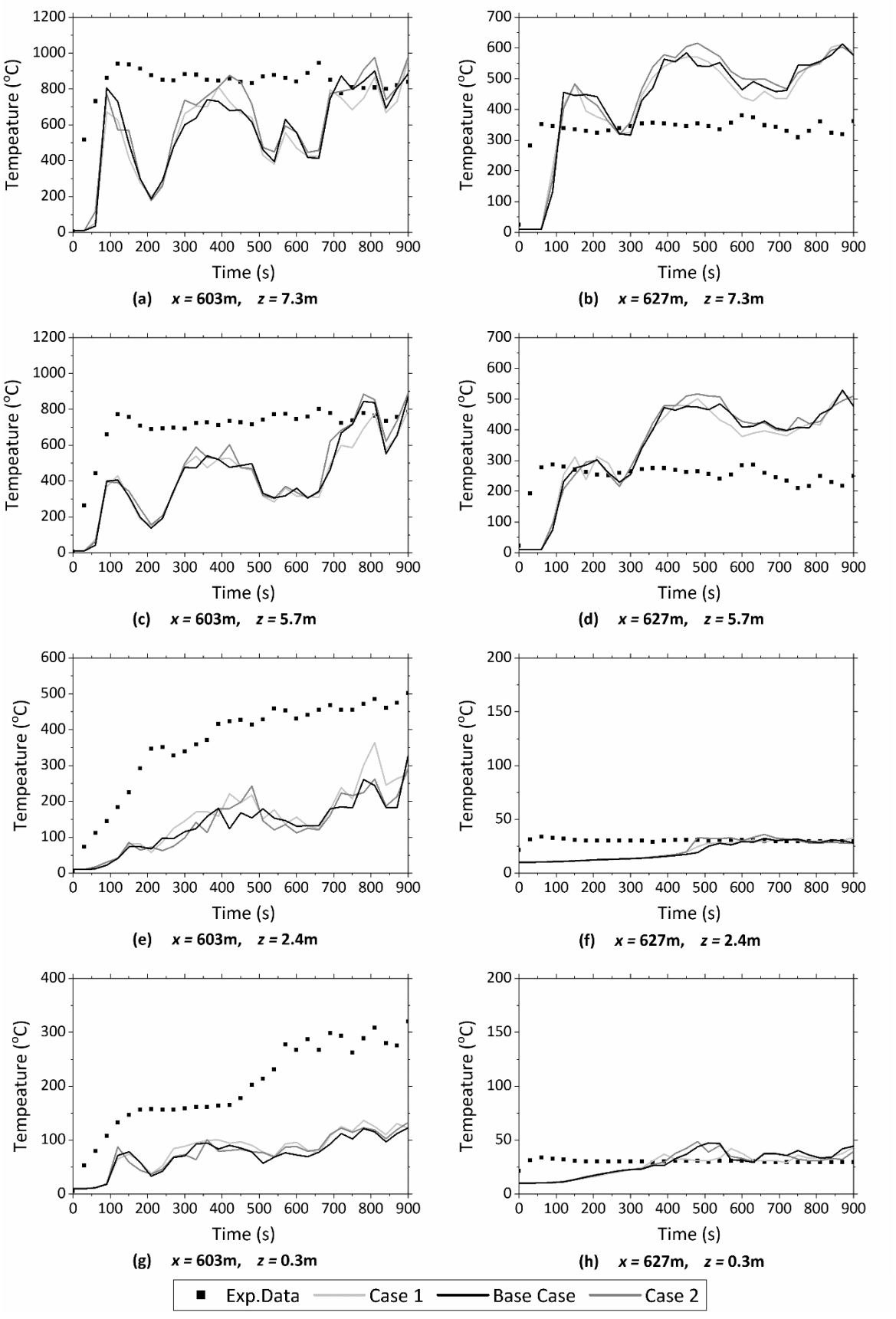

Figure 5.22 The effect of the Simulation Mode on the temperature distribution at different cross-sectional heights of the tunnel, at Loop 305 (left) & 304 (right), during the entire test period.

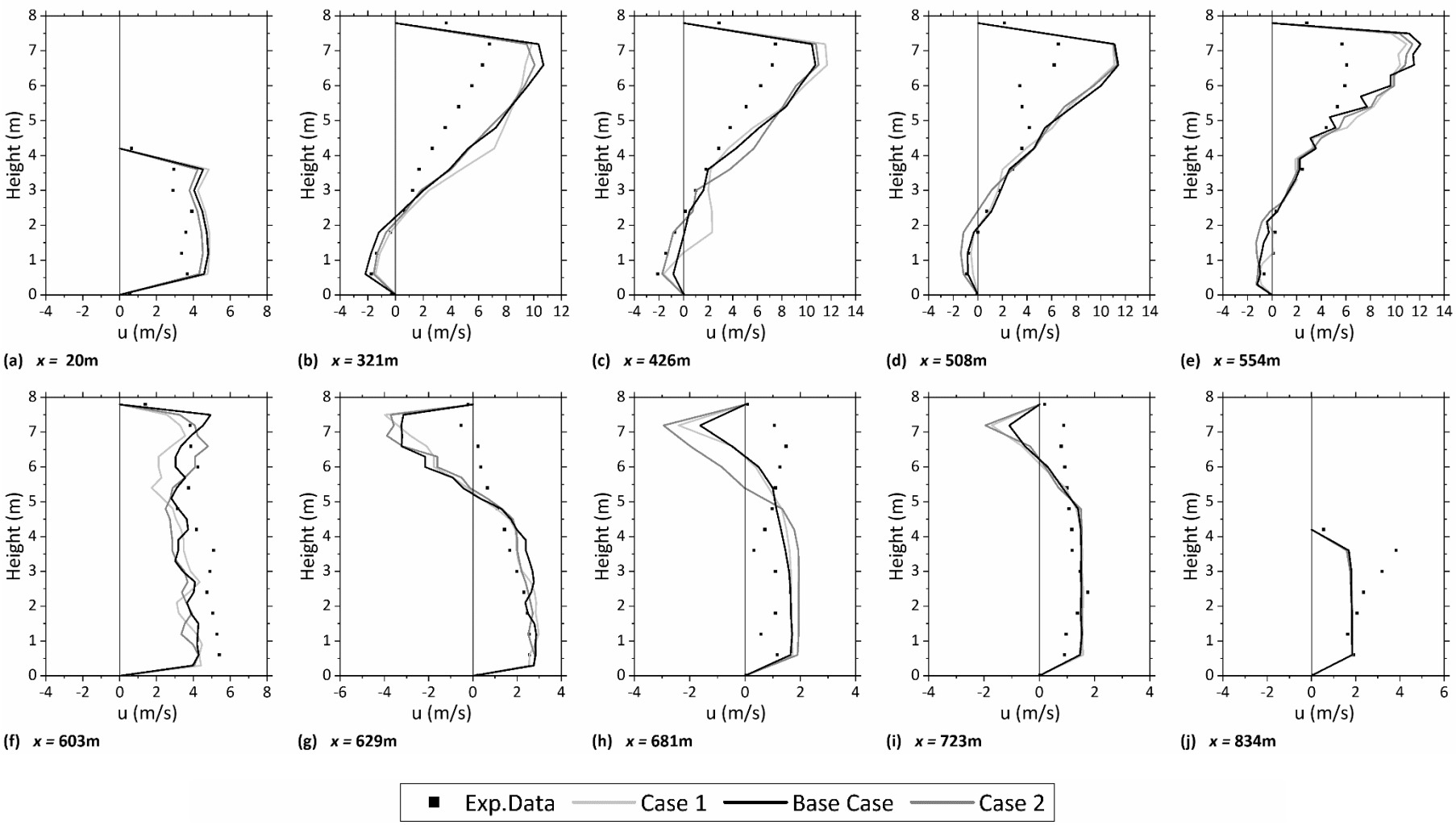

Figure 5.24. The effect of the Simulation mode on the velocity profiles throughout the entire tunnel's length, after 14 minutes since the start of the experiment.

5.3.2 Grid independence

A comprehensive sensitivity study has been undertaken to ensure that the selection of the nominal cell size will not lead to unreliable numerical results. Figure 5.25 shows the effect of different mesh resolutions on the temperature near the fire source region, while in Figure 5.26 the simulation results for the velocity are presented, for each mesh. The general tendency in all the applied mesh resolutions, is to slightly over-predict the temperature downstream of the fire, especially near the ceiling and under-predict the temperature at the upstream region of the fire, due to the presence of backlayering. This phenomenon is clearly illustrated in the velocity profiles throughout the tunnel, as well. The selected meshes for the numerical simulation are demonstrated in Table 5.9. As a reminder, in most mesh resolutions, the simulation modes of both LES and VLES have been employed.

Table 5.9. Review of the main numerical details of the grid independence parametric study.

Mesh Resolution	Simulation Mode	Grid Size Near the Fire Region	$D^*/\delta x$	Computational Time
0.20 – 0.40m	LES	0.20m	23.3	70.8h (4,246min)
0.20 – 0.40m	VLES	0.20m	23.3	49.9h (2,997min)
0.25 – 0.50m	LES	0.25m	18.7	24.5h (1,469min)
0.25 – 0.50m	VLES	0.25m	18.7	14.9h (892.6min)
0.30 – 0.60m	LES	0.30m	15.6	11.5h (690.3min)
0.30 – 0.60m	VLES	0.30m	15.6	6.5h (391.5min)
0.60 – 0.60m	VLES	0.60m	7.8	1.0h (58min)

The grid sensitivity analysis shows that a cell size of 0.25m, corresponding to value of 18.7 of the non-dimensional expression $D^*/\delta x$, demonstrates an effective advantage over the other grid resolutions, both on temperature predictions near the fire and velocity profiles throughout the entire tunnel. Cell sizes of 0.20, 0.30 and 0.60m, corresponding to $D^*/\delta x$ values of 23.3, 15.6 and 7.8, respectively, provide quite similar results for the temperature and the velocity profiles within the tunnel. This observation is well-justified, given that values of the non-dimensional expression of $D^*/\delta x$, which is directly related to the numerical resolution chosen for these parametric cases, are larger than the suggested value of 10 (McGrattan et al., 2020). Even in the case of the coarsest mesh, of nominal grid size of 0.60m and $D^*/\delta x$ slightly lower than the recommended value, the simulation results did not significantly deviate from the rest of the simulation cases. However, some noticeable discrepancies in the computed temperature and velocity profiles near the fire area have been detected in the case of the cell size of 0.20, when the VLES simulation mode was used. These results are probably owed to the sub-grid scale modelling of the LES mode, regarding turbulence phenomena, for the selected computational mesh. A mesh with a grid size of 0.20m is probably adequate enough to avoid eliminating the small, but resolvable, eddies, but not large enough to ensure the required numerical stability. However, if a finer mesh than 0.20m is employed near the fire region, for example of 0.10m, it would probably result in reduced numerical discrepancies against experimental data, providing perhaps the most accurate findings over all the other meshes. This assumption is acceptable since the FDS code computes second order accurate approximations of both the temporal and spatial derivatives of the Navier-Stokes which mean that whenever the grid cell is reduced by a factor of 2, the discretization error is reduced by a factor of 4, theoretically. The challenge in this case is the trading off between the computational power and time required, and the accuracy of the numerical results. A cell size of 0.10m near the fire would be practically inapplicable for a long tunnel application. Even a grid of 0.20m, using the LES simulation mode, is not recommended, since it requires a long computational time, see Table 5.9, without even eliminating the difference encountered between this mesh and the rest of the cases. Thus, a cell size of 0.25m or 0.30m is deemed to be adequate for the current study, since they display advanced solution fidelity, in reduced computing time.

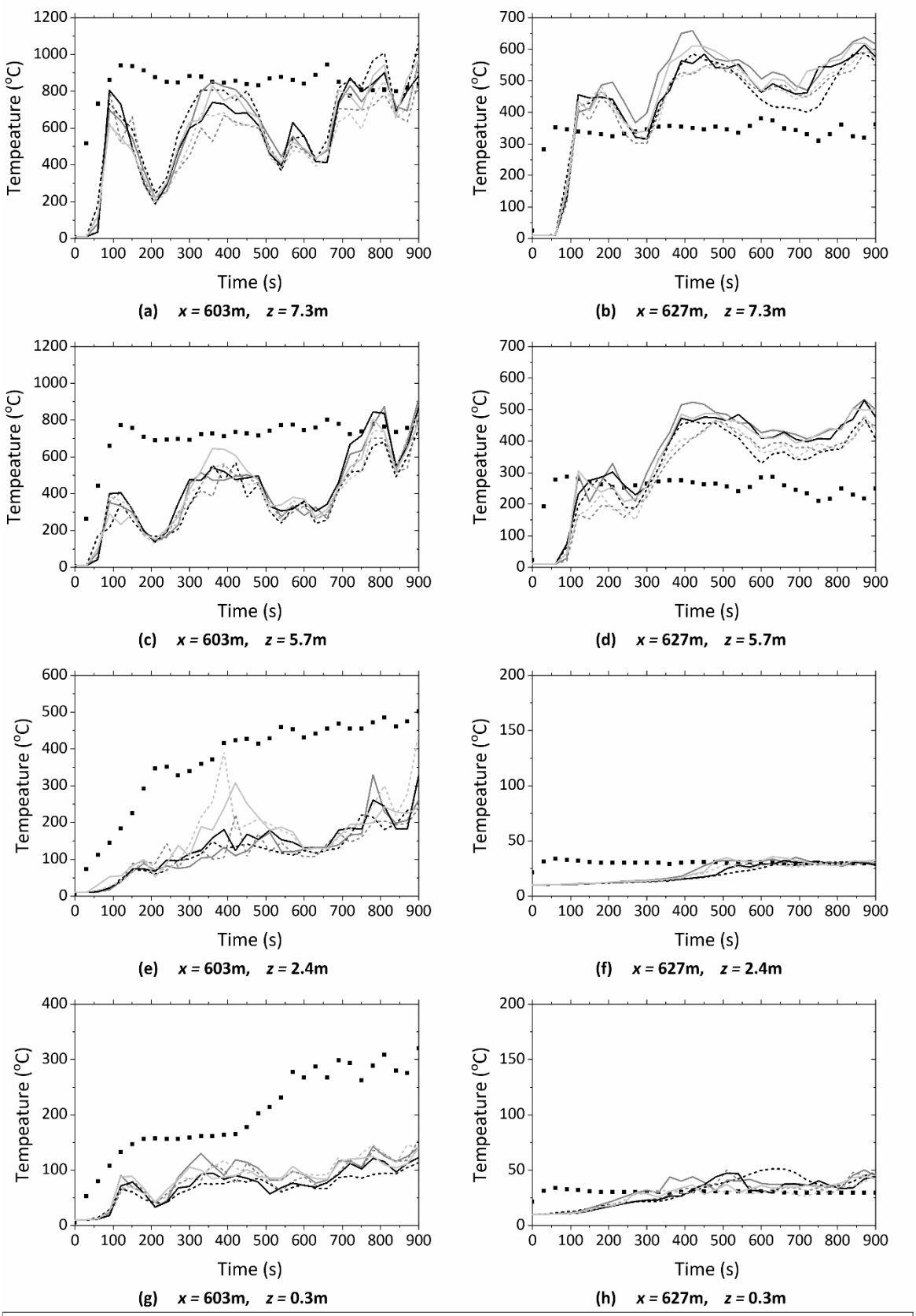

Figure 5.25. The effect of grid size, along with the simulation mode, on the temperature distributions at different cross-sectional heights of the tunnel, at Loop 305 (left) and 304 (right), during the entire test period.

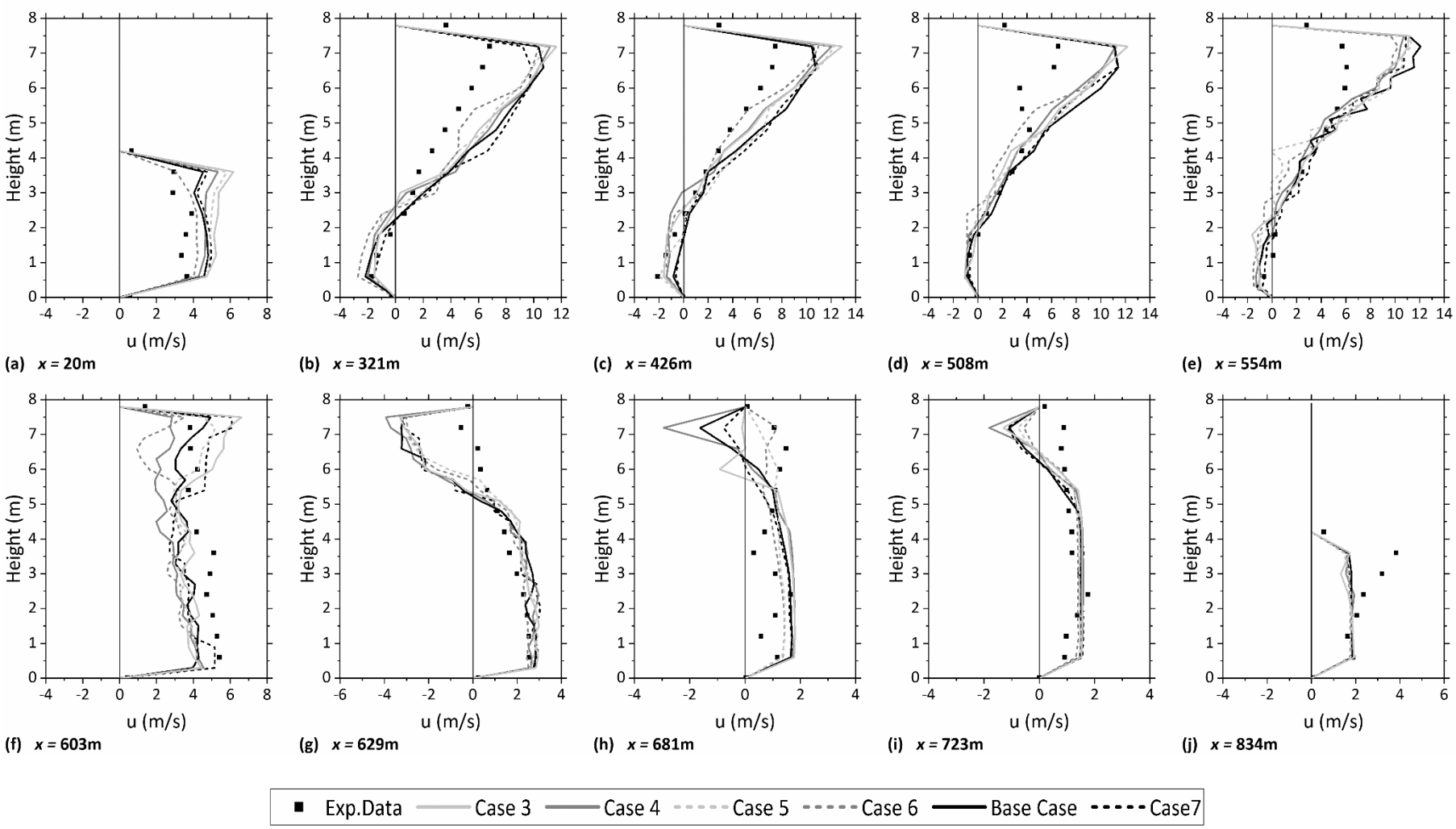

Figure 5.26. The effect of grid size, along with the simulation mode, on the velocity profiles throughout the entire tunnel length, after 14 minutes since the start of the experiment.

5.3.3 CO production

The composition of combustion products mainly depends on the type of the burning fuel and the ventilation conditions. Thus, the effect of fuel properties on the temperature and velocity profiles inside the tunnel is one of the main parameters that certainly need to be evaluated in a validation study. In the actual experiment, Fuel Oil No.2 was employed as a fuel, while in the numerical simulations *n*-heptane was used as a surrogate fuel, due to the fact that the heptane's combustion properties are constant and extensive information is available, in contrast to the diesel fuel, which has a more complex and occasionally varying composition. The combustion properties of *n*-heptane have been already presented in Table 5.6 and the suggested values for the CO yield and soot yield have been already employed for the Base Case Scenario. Previous experimental and theoretical evaluation of the CO and soot volumetric fraction among these fuels has established that n-Heptane produces lower CO and soot quantities compared to diesel fuel. Therefore, it is anticipated through the numerical results of the CO parametric study, that a higher value of CO yield would probably be more appropriate for the investigated Test Cases. It must be noted that the combustion processes of Heptane fuel have not been modeled in detail, since a simpler approach was required to reduce the computational demands of the entire tunnel simulated domain.

The time-variation of the gas temperatures, modeled by FDS, near the fire source, at Loops 305 and 304, is shown at Figure 5.27. It is clearly illustrated that no significant differences are observed in the vertical temperature distributions amongst the numerical results for each of the CO values, neither downstream nor upstream of the fire. CO production yield values of 0.012 kg_{CO}/kg_{fuel} (Base Case) and 0.022 kg_{CO}/kg_{fuel} (Case 9), demonstrate a slight advantage over the rest of the cases, but yet these values do not considerably improve the numerical results. On the contrary, the variation of the CO production yield value evidently affects the accuracy of the velocity predictions. The vertical distribution of air/smoke velocity at different cross sections inside the tunnel is presented in Figure 5.28. It can be clearly seen that approximately throughout the entire tunnel's length, at the 19m, 321m, 426m, 554m, 629m, 723m and 834m cross sections, the cases of 0.032 and 0.042 kg_{CO}/kg_{fuel} (Case 10 & 11) yield the most accurate velocity predictions. The velocity results for the other scenarios, especially at the upper locations of the tunnel, are all slightly under-predicted. However, at the upstream side of the fire, numerical results of both temperature and velocity strongly indicate that there is an adverse layer of smoke heading towards to the south end of the tunnel. This numerical observation does not agree with the experimental data, as previously stated, and through the numerical results no obvious connection has been established between the variation of CO yield value and the backlayering phenomenon.

In summary, examining the numerical results for the fire of n-Heptane, a higher value of CO production has been proven to be more appropriate, compared to the Base Case value of CO yield. The improvement of the results with this modification, regarding the velocity distribution, is clearly demonstrated. The challenge in this case, however, remains, since the correct prediction of the CO yield and all of the combustion products in general, is rather uncertain. This uncertainty is owed to the fact that there is no further experimental information available regarding the CO and soot production and distribution inside the tunnel. Nevertheless, considering the properties of the fuel employed in the actual experiment, which evidently produces a higher quantity of CO for the same fuel amount than Heptane and the numerical results of n-Heptane, the initial assumption is verified. Therefore, a greater value of the one used in the base case, in the order of 0.032 to 0.042 kg_{CO}/kg_{fuel} (Cases 10 and 11), is considered to formulate the "optimum" case for Test 502.

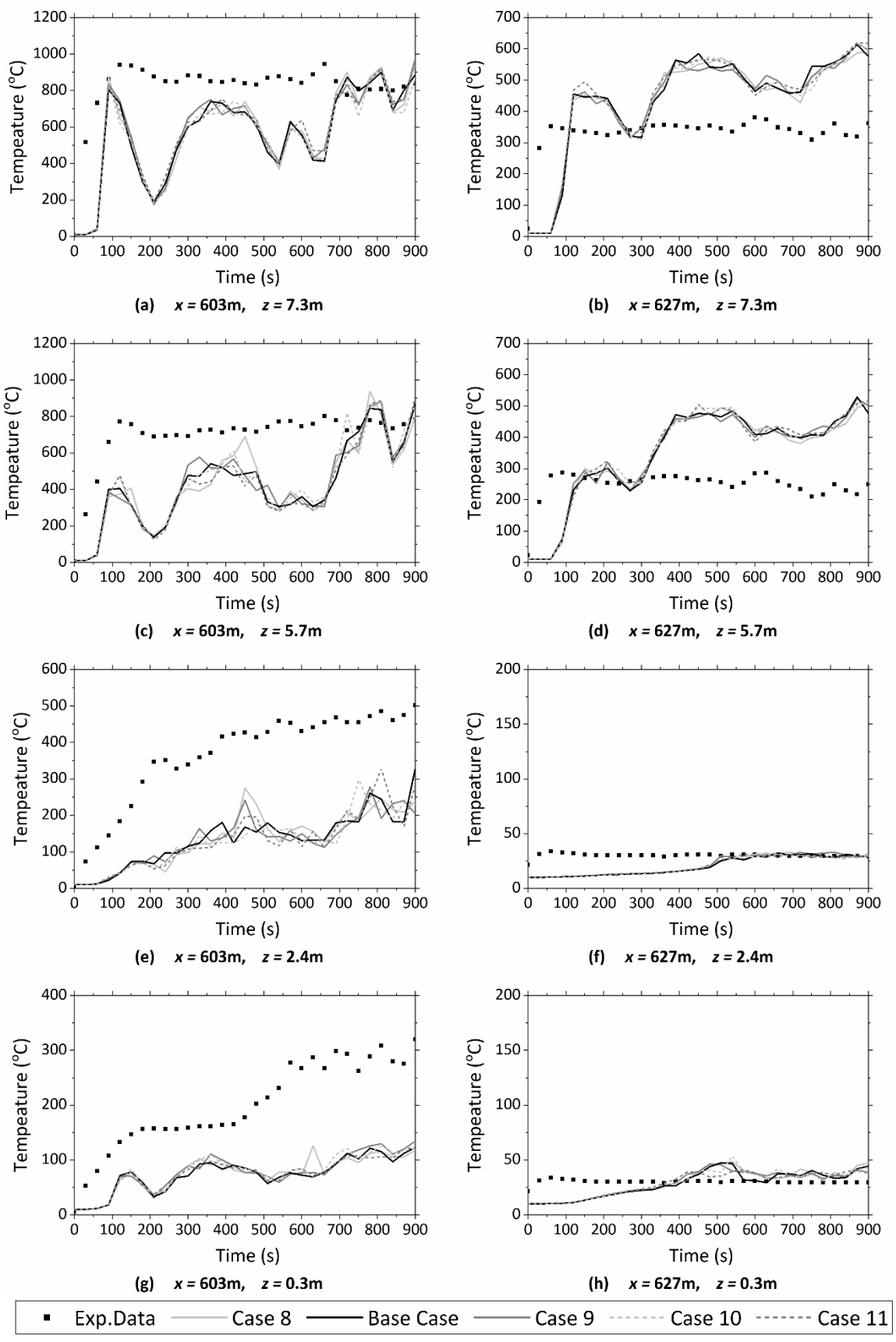

Figure 5.27. The effect of the CO_YIELD parameter on the temperature at different cross-sectional heights of the tunnel, at Loop 305 (left) & 304 (right), during the entire test period.

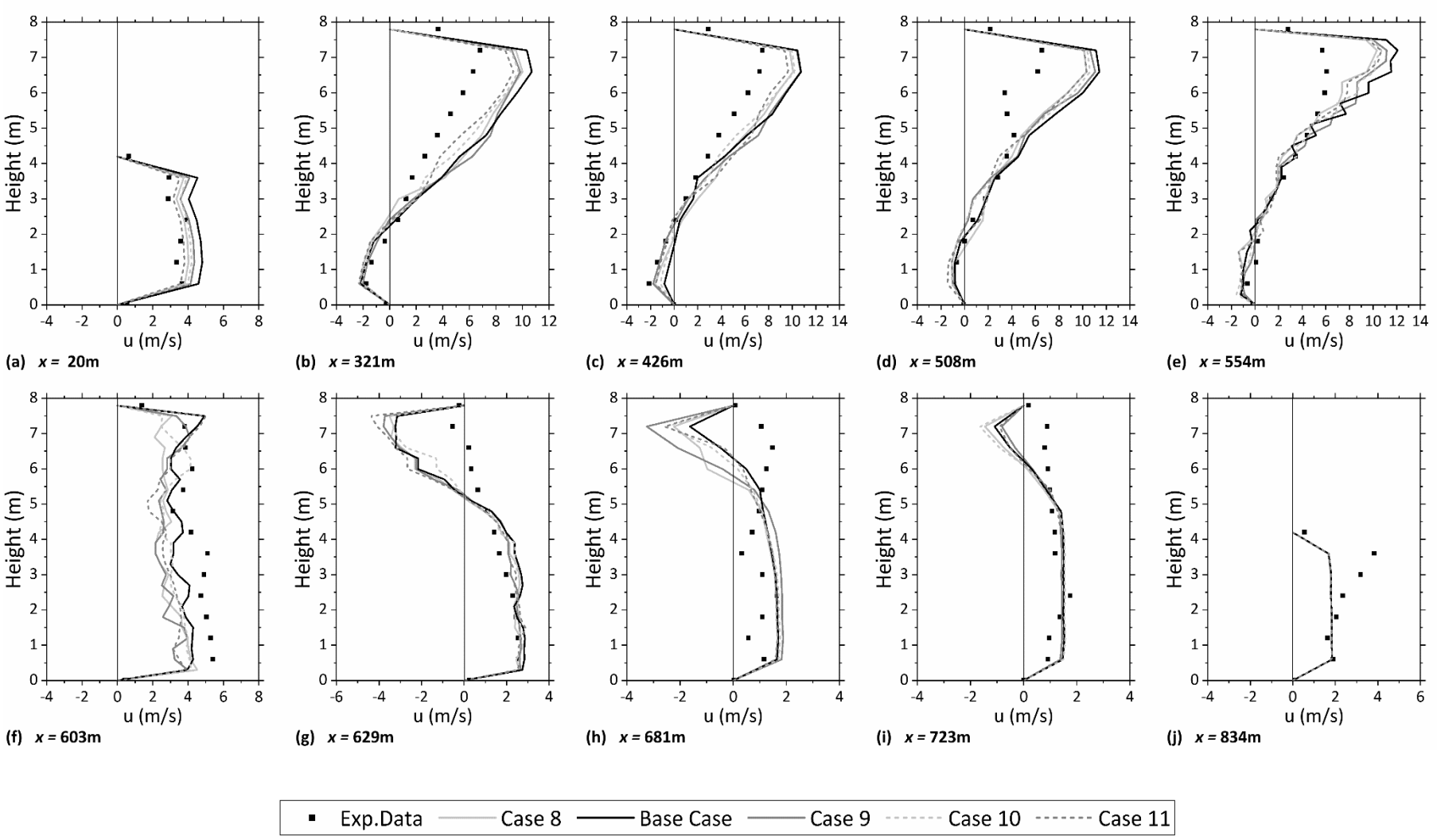

Figure 5.28. The effect of the CO_YIELD parameter on the velocity profiles throughout the entire tunnel length, after 14 minutes since the start of the experiment.

5.3.4 Soot production

In a fire, soot particles are formed as a consequence of fuel-rich combustion, following a series of complex physical and chemical steps. As stated, Fuel Oil No.2 is not characterized by a specific chemical formula due to the fuel's complex and varying composition. Thus, both specifying the fuel's properties and simulating the gas phase reaction processes, to predict with higher accuracy the smoke production, is expected to considerably increase the complexity and numerical requirements of the FDS code. By using a paraffinic fuel instead of diesel, such as n-Heptane for the simulation, the above-mentioned issues can be partially resolved but yet, particular attention is still needed for reasons of the specific nature of each fuel. Regarding the soot production of these fuels, previous experimental and theoretical work has established that diesel fuel constitutes a rather strongly "sooting" fuel, while n-Heptane is characterized by an extremely reduced soot production, with integral values of about one third lower (Mancaruso and Vaglieco, 2013). Consequently, a higher soot yield value than the one used for n-Heptane fuel, in the Base Case Scenario, is anticipated to describe more adequately the fire related phenomena in the experiments.

At this point, it must be noted that the radiative heat transfer from a fire is directly affected by the soot production, which plays an important role in the temperature distribution near the fire field and thus, the significance of a soot production-parametric study is highlighted. In general, the radiative heat transfer from the smoke is estimated by the FDS code via the solution of the radiation transport equation for a non-scattering gray gas. One should keep in mind that the absorption coefficient for a smoke-laden gas layer is a complex function of its composition, wavelength and temperature and thus the estimation of the absorption and consecutive emission of radiation is quite challenging. Owed to the simplified radiation model used in the current simulation, the chemical composition of the smoke gases of the fuel, especially the soot content, can strongly influence both the absorption and emission of thermal radiation by the smoke inside the tunnel. Through a numerical evaluation of the FDS radiation solver sensitivity, it has been established that changes in the assumed soot production indeed affect the radiative heat fluxes and thus the temperature distribution, near the field of the localized source of radiation. More specifically, a slight increase in the soot yield can cause a significant increase in the radiative flux from a simulated burner (FDS Verification guide; Hostikka, 2008). Accordingly, in this validation study, as well, numerical results indicate that an increase of the soot production yield value above the Base Case assumption, improves the predicted temperature accuracy, especially at the downstream side of the fire, where higher soot yields result in higher computed temperatures. However, Figure 5.29 also shows that for a range of different soot yields (0.032 to 0.072 kg_{Soot}/kg_{fuel}) estimation of the smoke layer temperature on both sides of the fire does not result in significant variations of the numerical results, with the exception of the temperature results established for the lowest soot value applied in the simulation (Case 12).

For all the soot production yield values, Figure 5.30 presents the velocity profiles along the tunnel length. The impact of higher soot production from the Heptane burner is evidently illustrated in these velocity profiles, where a significant improvement in the predicted velocities is achieved when the soot yield exceeds the suggested Heptane's soot production value. In conclusion, the fact that n-Heptane produces a lower amount of soot than diesel has been numerically proven in the current simulation study. By evaluating the numerical findings against the actual experimental data, it has been established that both predictions of temperature and velocity are strongly improved when a higher soot yield value is used.

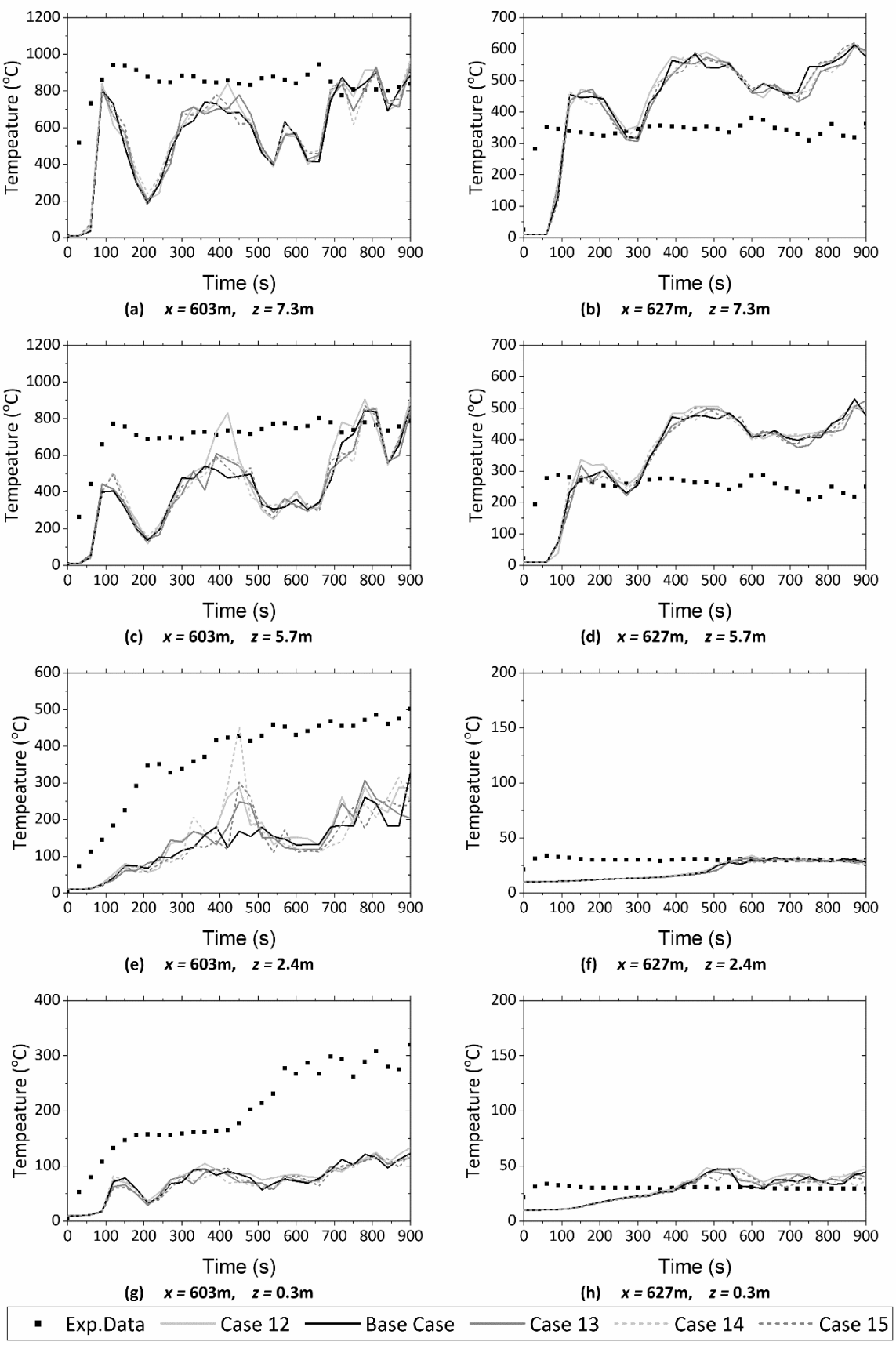

Figure 5.29. The effect of SOOT_YIELD on the temperature at different cross-sectional heights of the tunnel, at Loop 305 (left Column) & 304 (right), during the entire test period.

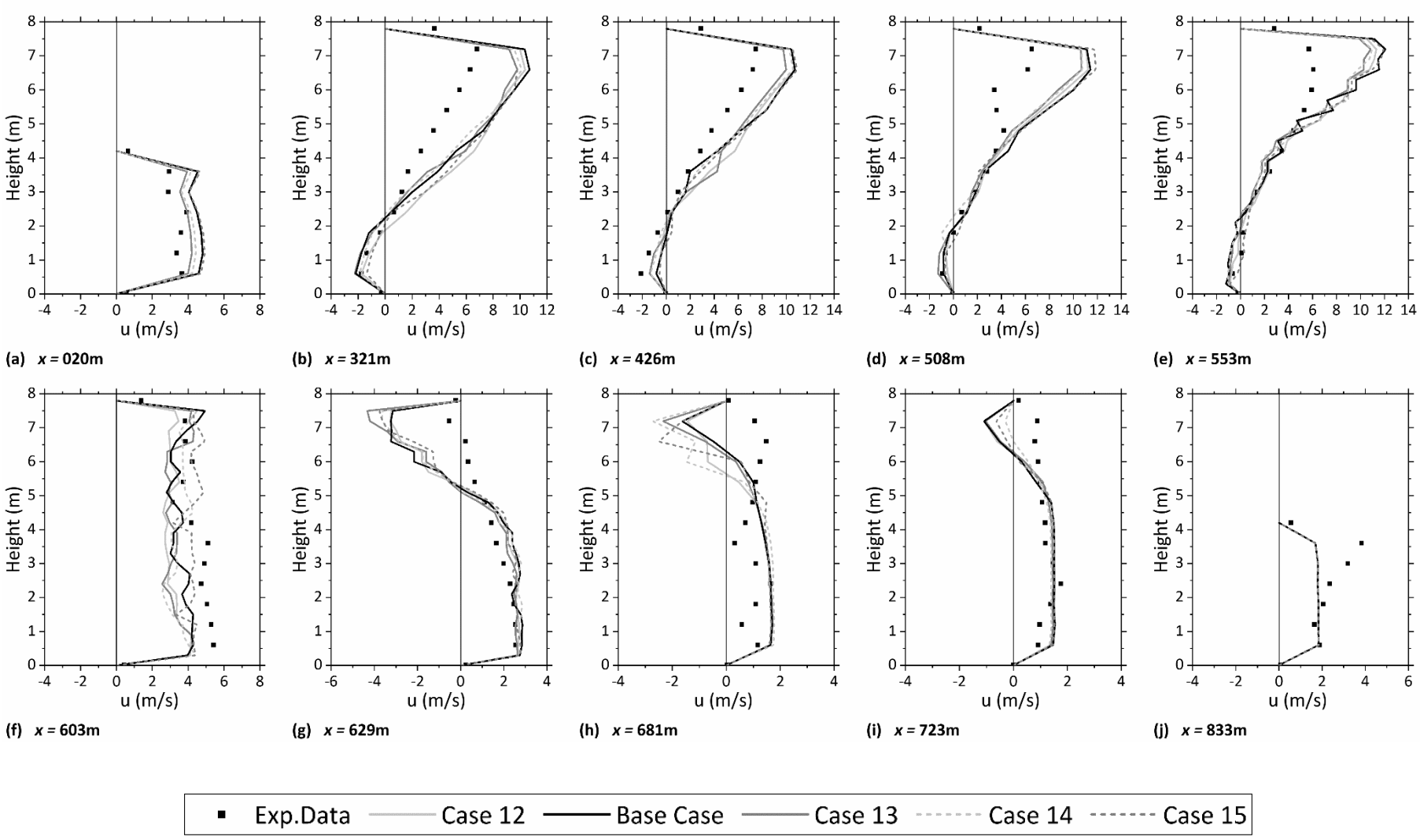

Figure 5.30. The effect of SOOT_YIELD on the velocity profiles throughout the entire tunnel length, after 14 minutes since the start of the experiment.

5.3.5 Radiation

Thermal radiation plays a very important role in the development of fires, in confined spaces, such as tunnels, by allowing the gaseous combustion products to lower their temperature due to the emitted radiation or by heating up combustible materials, such as tunnel's surrounding walls and other vehicles, owning to the absorbed radiation. It should be noted that the soot content of smoke is usually the most important source and absorber of radiation. Radiative preheating increases the rate of flame spread, while at some cases it even causes ignition of surfaces without direct flame impingement. In the current case, no stationary vehicles are employed and thus this phenomenon cannot be examined. However, due to the fact that, in enclosure fires, radiation may be a substantial source of heat transfer, a parametric study is conducted to establish the most suitable radiative fraction, for describing the thermal field developed in Memorial Tunnel's Test 502. For fires burning in an open atmosphere, the radiative fraction of the overall heat transfer ranges from less than 0.1 up to 0.4, depending on the fire size, flame temperature, and the chemical composition of the fuel and the combustion products. Due to the important role that the radiation holds in confined spaces, the radiative fraction should be specified with a higher value compared to radiation from an open fire. There is no single value of radiative fraction for a given fuel, but there might be suggested values of the radiative fraction for some common pure fuels based on measurements performed on either small or large fires. For n-Heptane the start value for the radiative fraction was chosen to be 0.40, corresponding to 40% heat transfer via radiation.

Specifying values for the radiative fraction from 0.20 to 0.50, the impact of radiation has been investigated both on the temperature distribution, Figure 5.31, and the air-smoke velocity, along the tunnel Figure 5.32. The radiative fraction has an apparent influence on the numerical predictions. To begin with, regarding the temperature distribution versus time, at 603m, applying a relatively small radiative fraction results in predicting quite well the temperature at the upper half of the tunnel. On the contrary, for the lower cross-sectional area, the higher the value of the radiative fraction the better. Since FDS seems to under-predict the temperature downstream of the fire, in the current case a relatively low radiative fraction at the upper level of the tunnel cross section, where the thick layer of smoke is located, assists in maintaining a higher temperature while, on the contrary, high radiative emission from the upper layer of smoke results in increasing the temperature of the colder layer of air and smoke at a lower height. Accordingly, at 629m, where the temperature during the entire time period of the numerical simulation is over-predicted, a higher radiative fraction contributes in "cooling off" the upper smoke layer, thus diminishing the backlayering effect, and hence, improving the numerical results. At the lower level, the temperature is well predicted for the whole range of radiation fraction values.

As far as the velocity profiles are concerned, near the fire region, a radiative factor of 35% seems to be more accurate, as depicted in Figure 5.32. Away from the fire field, downstream from the fire, at each measurement position different values of the radiative fraction give an optimal velocity profile that simulates more precisely the experimental data, without apparent connection, and thus no specific value of the radiative fraction outclasses any of the others. Thus, in general, a radiative fraction of 35% is presented to be the optimum estimation, based on the velocity profiles with the second-best estimation to be a radiative fraction of the order of 20%. The latter one does not constitute a typical value for an n-Heptane-induced fire and hence the 35% value seems to be the most reasonable choice for the current test case, based on the velocity numerical findings and the suggested radiative fractions for some common fuels.

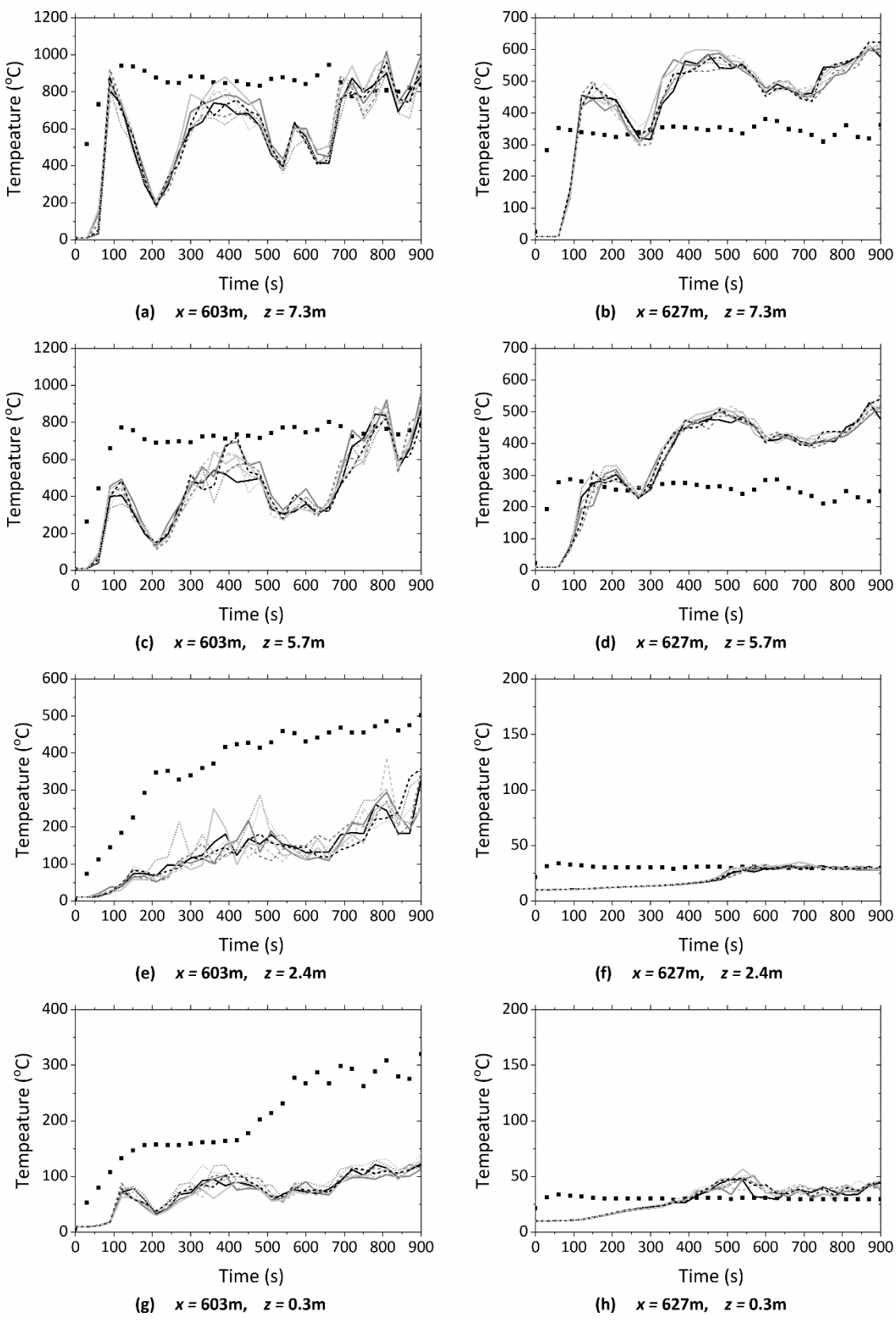

Figure 5.31. The effect of RADIATIVE_FRACTION on the temperature at different cross-sectional heights of the tunnel, at Loop 305 (left) and 304 (right), during the entire test period.

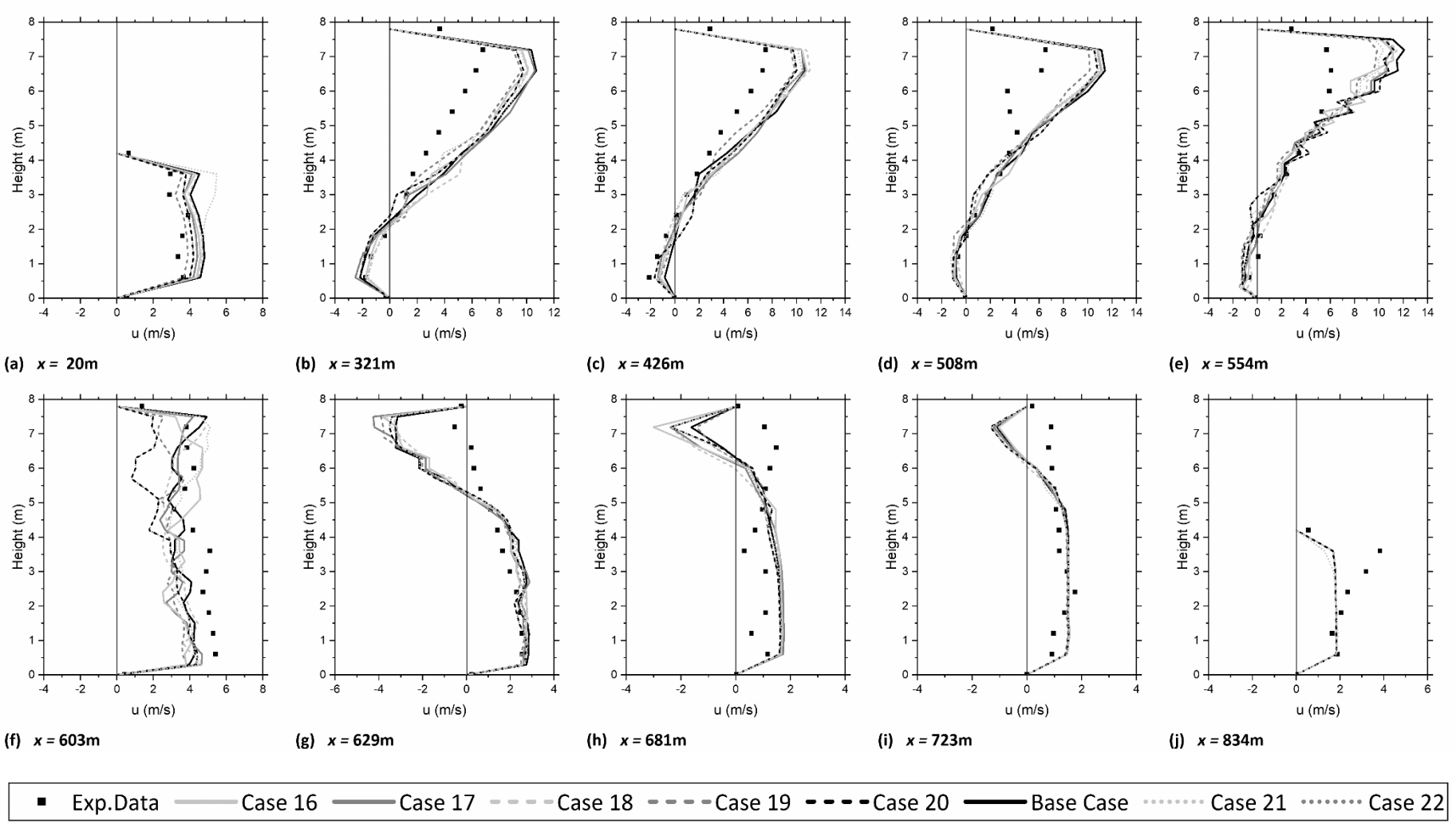

Figure 5.32. The effect of RADIATIVE_FRACTION on the velocity profiles throughout the entire tunnel length, after 14 minutes since the start of the experiment.

5.3.6 Roughness

In every simulation study, there is the primary interest of assigning the correct geometrical shapes and features to the modeled computational area. In this manner, for a tunnel fire scenario, the flow structures, originated from the fire source, will not only be affected by the turbulent combustion processes and the ventilation conditions but by the existing geometrical features inside the tunnel and the characteristics of the surface areas of the surrounding environment, as well. More specifically, in an operational tunnel, various practical installations and devices are set up to the tunnel's walls, facilitating the tunnel's functionality (lightning, information signs, etc.) while ensuring safety standards, as well (Emergency doors, fire extinguishers, emergency phones, cabins of electrical equipment, etc.). The current parametric study aims to simulate the Memorial road tunnel's internal geometry as precisely as possible. However, due to the relatively coarse mesh, with a grid size from 0.4m to 0.6m, at the far field regions, it is not feasible to precisely describe all the existent features of the Memorial tunnel's installations. The use of a finer mesh along with the exact representation of the internal geometry of the tunnel would heavily increase the computational time and complexity of the fire scenario without contributing meaningfully to the fidelity of the numerical findings. Hence, to simulate the real tunnel geometry and the pressure loss of the flow due to friction, the FDS code parameter ROUGHNESS is utilized.

As illustrated in Figure 5.33, the Memorial tunnel internal geometry is characterized by a large variety of uneven geometrical structures, which are creating a particularly "rough" wall surface. However, the Base Case scenario has been built assuming a zero wall roughness for the sake of simplicity. Thus, to further specify the order of magnitude of surrounding wall's roughness which contributes to the turbulent flow, a wide parametric study has been performed. It must be noted that the actual wall roughness, which is in order of mm, is quantitatively negligible as opposed to the rest of technical installations and features inside the tunnel. Based on the numerical findings, shown in Figure 5.35, it is demonstrated that the air velocity is better predicted for a roughness height of the order of 0.10m, downstream from the fire source and of 0.45m, at the upstream region. An overall good prediction throughout the entire tunnel's length is achieved for a roughness height of 0.25m. For lower or higher roughness values, beyond the range of 0.10m to 0.45m, the accuracy of the predicted velocity profiles is evidently reduced. Accordingly, the temperature prediction via the FDS code, downstream of the fire source is more accurate for relatively small roughness heights, as illustrated in Figure 5.34. On the contrary, towards the south portal of the tunnel, a higher roughness of the surrounding walls seems to be more appropriate. In general, the best prediction for the temperature during the entire test period, on both sides of the fire, is achieved for a wall roughness of 0.05m. Yet, values of 0.10m and 0.25 are also precise enough. In conclusion, given the numerical results, the "smooth wall" assumption is inadequate for the current case, in view of both the velocity profiles and the temperature distribution. Depending on the criterion of optimization the roughness of the "surrounding walls" should be specified by a higher value, which does not exceed the value of 0.25m.

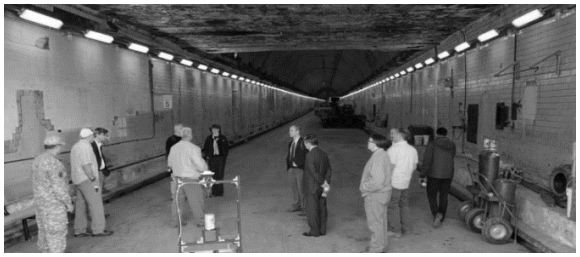

Figure 5.33. The current view of the Memorial Tunnel's internal geometry.
(https://www.statler.wvu.edu/news/2017/12/01/wvu-research-team-to-test-effectiveness-of-drones-robots-in-underground-tunnels)

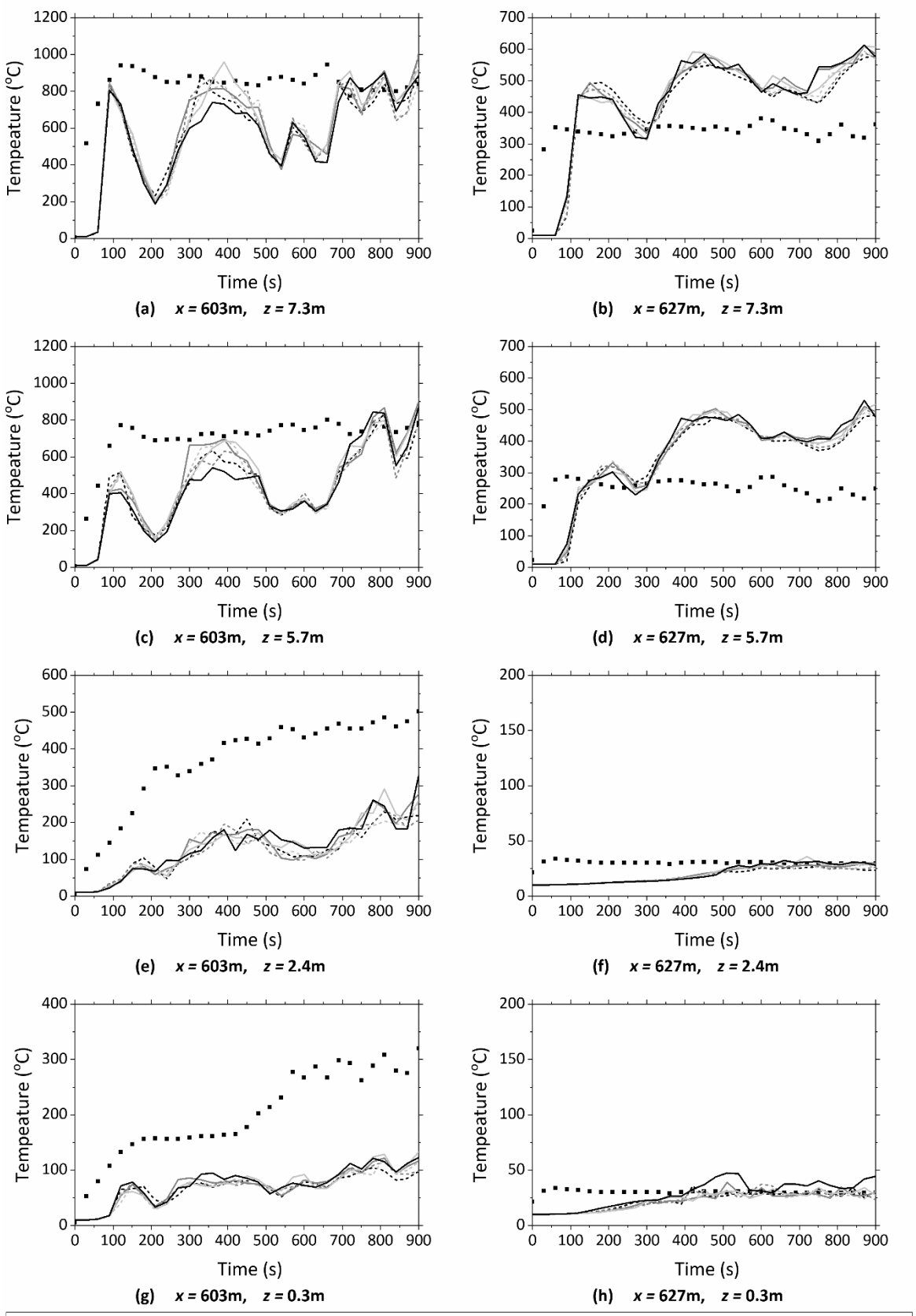

Figure 5.34. The effect of the WALL ROUGHNESS on the temperature at different cross-sectional heights of the tunnel, at Loop 305 (left) & 304 (right), during the entire test period.

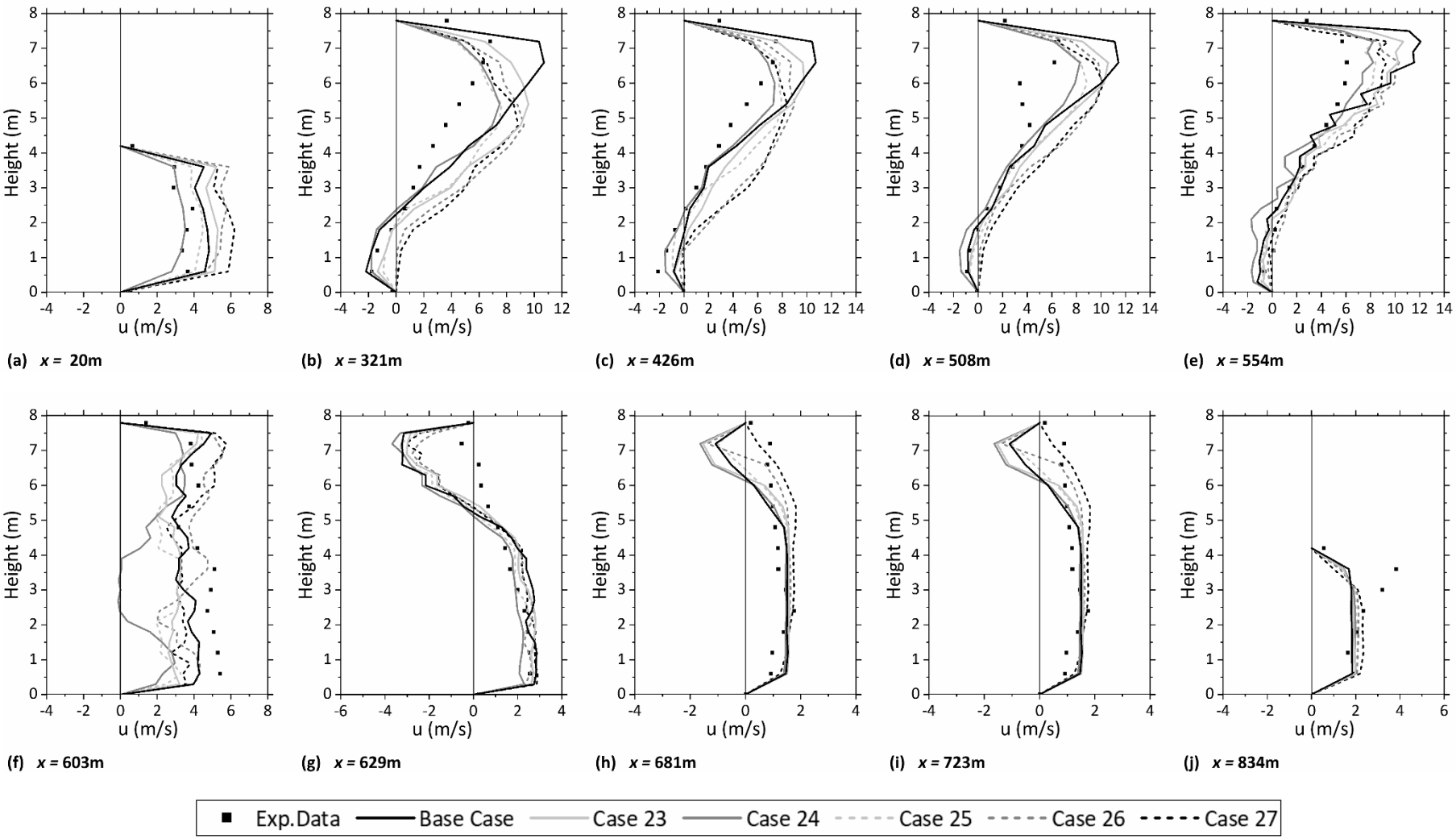

Figure 5.35. The effect of the WALL ROUGHNESS on the velocity profiles throughout the entire tunnel's length, after 14 minutes since the start of the experiment.

5.4 Comparison of Experimental and Numerical Results

Numerical errors in every Computational Fluid Dynamics code's predictions, are mainly owed to four factors. First, numerical errors can occur due to the nature of each CFD code and its capabilities. Regarding large computational domains, such as long tunnels, inconsistency between the actual flow and CFD predictions is usually induced owning to the inadequate representation of the tunnel's geometry, material properties, physical combustion processes or other simplifying assumptions in the modeling process. For example, the computational mesh used in the FDS code, is one of the main model's limitations. Every solid feature, regardless of its shape and size, is required to conform to the underlying rectilinear mesh. Additionally, the user competence in using the code holds a primary role, as well. Large numerical errors can be generated by the user's ability to interpret the physical problem and recreate it in a numerical simulation or even by his/hers lack of knowledge in CFD, in general. Another reason that considerably contributes to the existence of numerical discrepancies against experimental data, is the simplifying assumptions used in the simulation process in order to reduce the complexity of the modelled scenario. The last but certainly not least reason for numerical deviations is uncertainties in the input data. In large scale applications, such as tunnel fires, inaccuracies due to limited information of the experimental set up or approximate representation of geometry, boundary conditions, material properties, etc., may result in misleading numerical findings. In every numerical study, the primary aim is to diminish as far as possible, the effect of the above sources of error, but, in practice, it is impossible for the numerical error to be completely eliminated.

The application of CFD modeling as a tool for the study of tunnel fires can only be justified on the basis of its accuracy and the level of confidence in its results. For that reason, there are several metrics used to quantify the numerical error of CFD predictions. The most commonly used is the percent error, Equation 5.5. According to that, the absolute value of the difference between the measured value and the actual value is divided by the absolute actual value and then multiplied by 100, giving the "Percentage Error", δ.

$$\delta = \left|\frac{u_A - u_E}{u_A}\right| * 100\% \quad 5.5$$

In Equation 5.5, u_A is the actual value measured in the experiment and u_E the numerically predicted value. Numerical errors play a key role in determining the validity of any simulation study. It is clear that Equation 5.5 does not only apply only for CFD results, but also for other types of calculations. Regardless of the source of the actual error, the formula of its calculation may lead to misleading estimations, as well. For example, the quality of match between vector profiles, like velocity profiles, when quantified using the percentage error metric can be overly sensitive to the alignment of regions of low velocity, such as the region where the longitudinal velocity component changes direction. In the current study, where the magnitude of the local velocity is quite small in certain regions, their presence in the denominator of the metric may amplify tiny absolute differences in velocity, resulting in the misinterpretation of the actual numerical error. William et al. (2020) proposed a complementary weighted equation, the Weighted Magnitude Index (WMI), for the vigorous quantification of the alignment and magnitude differences between vector fields (Equation 5.6).

$$WMI\ (x,y) = \left|\frac{Q_A(x,y) - Q_B(x,y)}{median(Q_A,Q_B)}\right| * 100\% \quad 5.6$$

In Equation 5.6, $\mathrm{median}(Q_A, Q_B)$ corresponds to the median of all elements (involving duplicate values as well) of the magnitude velocity fields Q_A and Q_B. The difference in velocity magnitudes at each spatial location is normalized to generate a dimensionless metric, which is impartial to the alignment of the velocity vectors. Vectors with the same magnitude produce a WMI value of zero, while vectors with large magnitude differences produce values of WMI larger than 100. Concluding, in this work, the numerical errors of temperature are estimated using Equation 5.5, whereas the velocity fields errors are provided by Equation 5.6.

5.4.1 Numerical Errors of Temperature and Velocity Profiles

The numerical errors of temperature estimated are depicted in Figure 5.38, depending on the location of measurement. Accordingly, the velocity fields errors observed at 14minutes of experimental time, are provided by the weighted magnitude index and presented in Figure 5.39, for the entire tunnel length. The effect of every factor, in total, is briefly summarized in the respective Pareto Fronts, as illustrated in Figure 5.40. The Pareto Front is a graphical overview of a specific problem, ascribed in a non-dimensional objective space approximated by well-distributed optimal points. These points constitute, in the current case, different solutions of the CFD test cases, obtained in the parametric study. In general, the Pareto Front prioritises multiple problem solutions, in the requested fields, assisting the researcher to decide which option is the most beneficial one, in the view of all the investigated parameters. In that case, the fields of optimization may be conflicting, and consequently there might exist a large number of Pareto optimal solutions. Each solution is depicted as a vector quantity in the ranked axes. For a multi-objective optimization problem, no single solution exists that necessarily optimizes each objective, simultaneously. Thus, any solution may be appropriate depending on the objectives of the case and without additional subjective preference information, concerning the physical problem, all Pareto optimal solutions are considered equally good. As a consequence, it is common that the user may even select a solution that does not offer an optimum value for neither one of the requested solutions, with the aim of trading off the benefits of each solution and pick the one that correspond better to the overall problem needs. This process lies in the field of “decision making”. Therefore, the most distinctive particularity of this feature is that it does not provide an absolute dominant solution for the problem but forms a graphic technique that offers a “front” of optimal points, allowing the user to decide which one is the most appropriate, in the scope of each solution benefits. In this work, in Figure 5.40, one can trace both dominant and non-dominant solutions of optimization for the parametric study of the Test Case 502. The factors of optimization, corresponding to the two axes, are the mean numerical error of the temperature, calculated with the contribution of all temperature distributions on both sides of the fire, and the numerical error of all the velocity profiles throughout the tunnel, expressed by the weighted magnitude index, WMI.

Grid refinement is a key parameter in a CFD study for the improvement of the accuracy of a modeled case. Initially, the simulation of the Memorial Tunnel Tet Case 502 has been performed on a relatively coarse mesh, since it regards a fire event in a long tunnel structure, in order to get a quick overview of the overall features of the developing flow-field. Subsequently, the grid has been refined in order to investigate the impact of the underlying mesh to the numerical results. According to the comparison of the numerical results with the experimental data, regarding the temperature distribution, a computational mesh of 0.25m near the fire area and 0.50m at the far field is adequate enough to describe the requested physical model with accuracy without adding unaffordable computational cost to the calculations, Figure 5.40. Additional refinement of the mesh, with a grid size below 0.20m would render the calculations practically infeasible, since the

current work requires multiple runs of the FDS code in the frame of the parametric study. The discrepancies in the simulated temperature profiles near the fire area compared to the test data are illustrated in Figure 5.38. The mean numerical error, downstream from the fire source is in the range of 52% (Case 4) to 54% (Case 7) and upstream from the fire it ranges from 41% (Case 6) to 47% (Case 4) for the VLES turbulent model. Accordingly, for the LES simulation mode the mean numerical error, downstream from the fire source is in the range of 49% (Case 5) to 51% (Case 1) and upstream from the fire it extends from roughly 39% (Case 5) to 43% (Case 3). Regarding the velocity weighted magnitude index, it ranges from 44.8% (Case 5) to 53.5% (Case 4) for the entire tunnel length, Figure 5.39. Considering both the simulation time and the quality of the calculated results, a grid size of 0.25m (Case 5 or 6) that corresponds to a D^*/δ_x value of 18.7 is recommended for this tunnel fire scenario, since it significantly enhances the numerical accuracy in terms of both the temperature and velocity predicted results.

Turbulence modelling and time accuracy are strongly associated. In LES, the role of the turbulence model is to describe the sub-grid scale phenomena that cannot be resolved with the underlying chosen computational grid. In regions where vigorous changes of the flow take place, namely near the fire source, the sub-grid scale model has a stronger impact on the numerical predictions and cautious examination is required for each study to gain trustworthy solutions on the entire flow, in a reasonable computational time. The parametric evaluation of the "simulation mode" has demonstrated that the VLES simulation mode tends to reduce the error in the velocity profiles while the LES mode leads to enhancement of the temperature predictions (Base Case & Cases 1, 2). This parametric study has been conducted, utilizing a single mesh but this observation is also confirmed for almost every other selected mesh resolution, as illustrated in Figures 5.38, 5.39 and 5.40 for the Cases 3 to 7. Considering that the temperature error is of paramount importance for fire events, since it directly affects the survivability conditions inside the tunnel and the integrity of the entire tunnel structure and its installations, its accurate estimation is a primal objective. As a result, the LES simulation mode is suggested for the current study.

Given that n-heptane is the fuel used in the current simulation case as a surrogate for Fuel Oil No.2, the combustion properties were selected accordingly. The CO production yield used in the FDS code is the measured CO yield value for heptane, Table 5.6. A comparative investigation, using different assumptions for the CO production, has been conducted and the discrepancies of the numerical results against experimental data are presented in Figures 5.38, regarding the temperature distributions and in Figure 5.39, in view of the velocity profiles. In total, comparison of the predicted temperature distribution and the measured data, for all cases, resulted in comparable numerical errors. In contrast, the computational errors produced from the profiles of the longitudinal component of the velocity differ significantly from case to case. More specifically, CO production yield values in the order of 0.032 to 0.042 kg_{CO}/kg_{fuel} (Case 10 & 11), succeeded fairly well in modeling the development of velocity conditions inside the tunnel, with the WMI value be less than 49%. The computational error for predicted temperatures was slightly lower in the case of 0.032 kg_{CO}/kg_{fuel} (Case 10), and thus the latter value is selected for the optimum case. The graphical overview in Figure 5.40, provides a concise visual summary of the comparison of experimental measurements and numerical results, for the above parametric study.

Additionally, Fuel Oil No.2, is described as a fuel with higher soot emissions than n-heptane. For this matter, it is estimated that a larger portion of soot yield, than the selected one for the Base Case, should probably be attributed to the fire source. However, for the sake of completeness, both higher and lower values of soot production were investigated in this work. Numerical results indicate that the longitudinal velocity profiles are more similar to the respective experimental ones in the case of 0.052 kg_{Soot}/kg_{fuel} (Case 13), resulting undoubtedly in the lowest WMI value, amongst the investigated soot yields. Nevertheless, a bit higher value of soot production, in the order of

0.062 kg_{Soot}/kg_{fuel} (Case 14), improves also the index of the velocity error, giving the second most precise prediction for the velocity distribution throughout the tunnel, while it generates the most appropriate temperature predictions over all the examined soot yields. Although the temperature numerical error does not improve so distinctly, as the velocity index, the assumption of 0.062 kg_{Soot}/kg_{fuel}, allies well with the anticipated combustion properties of Fuel Oil No. 2, while enhancing the main characteristics of the developing flow field. Therefore, the latter option constitutes a solid choice, as it corresponds well to both the numerical and physical model.

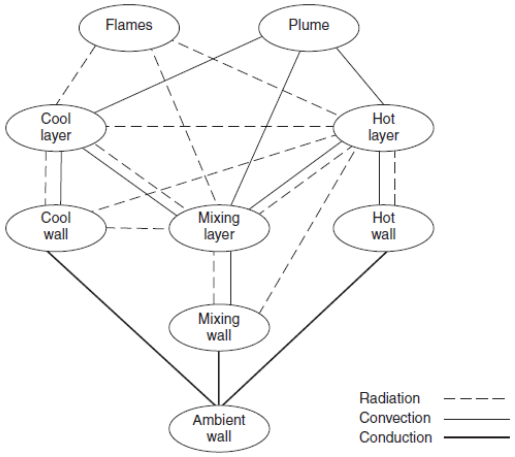

Figure 5.36 Overview of the typical heat-transfer processes in a tunnel fire (Beard and Carvel, 2005).

Another of the main objectives of every fire simulation study, is to determine the most suitable radiation fraction, since the transfer of a considerable portion of heat in fires, is dictated by radiation (c.f. Figure 5.36). Heat from radiation can also be redistributed within the smoke-filled region from the incandescent soot particles. Given the lack of adequate experimental data regarding radiation, the approach of comparative calculations is reasonable for this validation work. Thus, to justify the selection of the most suitable radiative fraction, with respect to the simplified model of radiation used, the numerical errors of each simulation regarding the velocity and temperature profiles are presented in the Figures 5.38, 5.39 and 5.40. As shown, the performance of the simulation case can be greatly improved in key factors, such as temperature and velocity distribution, by using the appropriate radiative factor values. More specifically, the mean temperature error ranges from 47.8% (Case 17) to 49.7% (Case 16) and the WMI, for the velocity profiles, varies from 48% (Case 19) to 54% (Case 20). The value of 0.25 for the radiative fraction (Case 17) seems to provide the best overall prediction for the temperature on both sides of the fire. However, its dominance over the other numerical solutions is slight since the magnitude variation amongst all the computed values is trivial. On the other hand, it is demonstrated that a radiative fraction of 35% (Case 19) offers a considerable enhancement of the velocity error index, while simultaneously providing an acceptable value for the temperature error. Additionally, the latter value constitutes a more reasonable estimation for the radiative heat transfer, since the radiative fraction values for a fuel diameter up to few meters, are in the region of 0.3–0.4 for typical sooty fuels, such as Fuel Oil No.2 (Morgan, 2016; McGrattan, 2020), but tend to decrease with increasing fire size. It is reminded that for Test Case 502 of the Memorial Tunnel's Test Program the nominal size of the fire source is approximately 50 MW. Another reason for decreasing radiative fraction values besides increasing fire size, is that the flames may be optically thicker, depending on the fuel, and the radiation-emitting area (flame area) per unit fire power (kW) will consequently decrease with increasing fire size. At this point, one should consider that, even though Fuel Oil No.2 constitutes a "sooting" fuel, compared to n-heptane for example, there are other aromatic fuels with carbon, hydrogen, etc., that produce far greater amounts of soot (Morgan, 2016). Therefore, the later factor does not significantly affect the solution of the current

case, as comparative calculations have shown. Hence, in the scope of the above factors, a radiative fraction of 35% is a well justified assumption for the physical model simulation.

Figure 5.37 is a postcard that depicts the interior of the Memorial Tunnel, at West Virginia when in operation. It can be seen that multiple features render the internal geometry of the tunnel rather complex, as noted in previous chapters. In the case of a fire, these features act as obstacles that may alter or even block the smoke-air flow. Examples of high influence in tunnel fire simulations are the lightning equipment, the emergency signs and phones as well as necessary technical installations which ensure the proper functioning of the tunnel. The lack of geometrical uniformity has been ascribed via the "roughness" parameter in the FDS code. In this context, a set of cases of different wall roughness values has been developed to properly simulate the implied friction factor from the physical model. The variety of wall roughness values that has been assigned to the simulated case ranges from 0m to 0.9m, providing solutions with distinctive discrepancies, especially regarding the velocity predictions. More specifically, the calculated WMI, regarding the comparison of the velocity numerical predictions and experimental data, varies from 44.5% (Case 25) to 53.7% (Case 23). The wall roughness directly determines how the tangential component of velocity is specified at solid surfaces and hence the observed differences in the WMI value (Figure 5.39), are well justified, considering the order of magnitude of the roughness height. Roughness heights of 0.10m (Case 24) to 0.45m (Case 26) seem to improve the numerical predictions of velocity, when the assumption of 0.25m (Case 25) offers the most fair estimation with a WMI of 44.5%. The smoke temperature errors, at a distance of approximately 13m from both sides of the fire source, predicted by FDS are shown in Figure 5.38. The comparison of the smoke temperature distribution predicted by FDS with the measured values is quite close from case to case. The numerical error varies from 46.7% (Case 23) to 48.1% (Base Case). Besides, the roughness parameter has an indirect effect on the temperature distribution, caused by alterations in the airflow's route, such as the creation of additional eddies or the redirection of the hot smoke near the fire source area. It is quite clear that the zero estimation for the roughness height, along with considerable high roughness values that exceed 0.45m, tend to aggravate the numerical findings, reducing the simulation's accuracy concerning both the velocity and the temperature profiles. Concluding, based on Figure 5.40, where a concise visual summary of the comparison of experimental and numerical results is presented, the value of 0.25m consists a reasonable estimation for the Memorial Tunnels wall roughness height.

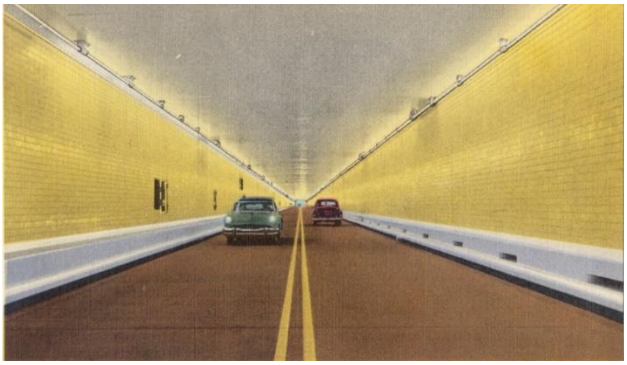

Figure 5.37. Postcard of the interior of the Memorial Tunnel, at West Virginia, when in operation. (https://www.digitalcommonwealth.org/search/commonwealth:cj82kh19b)

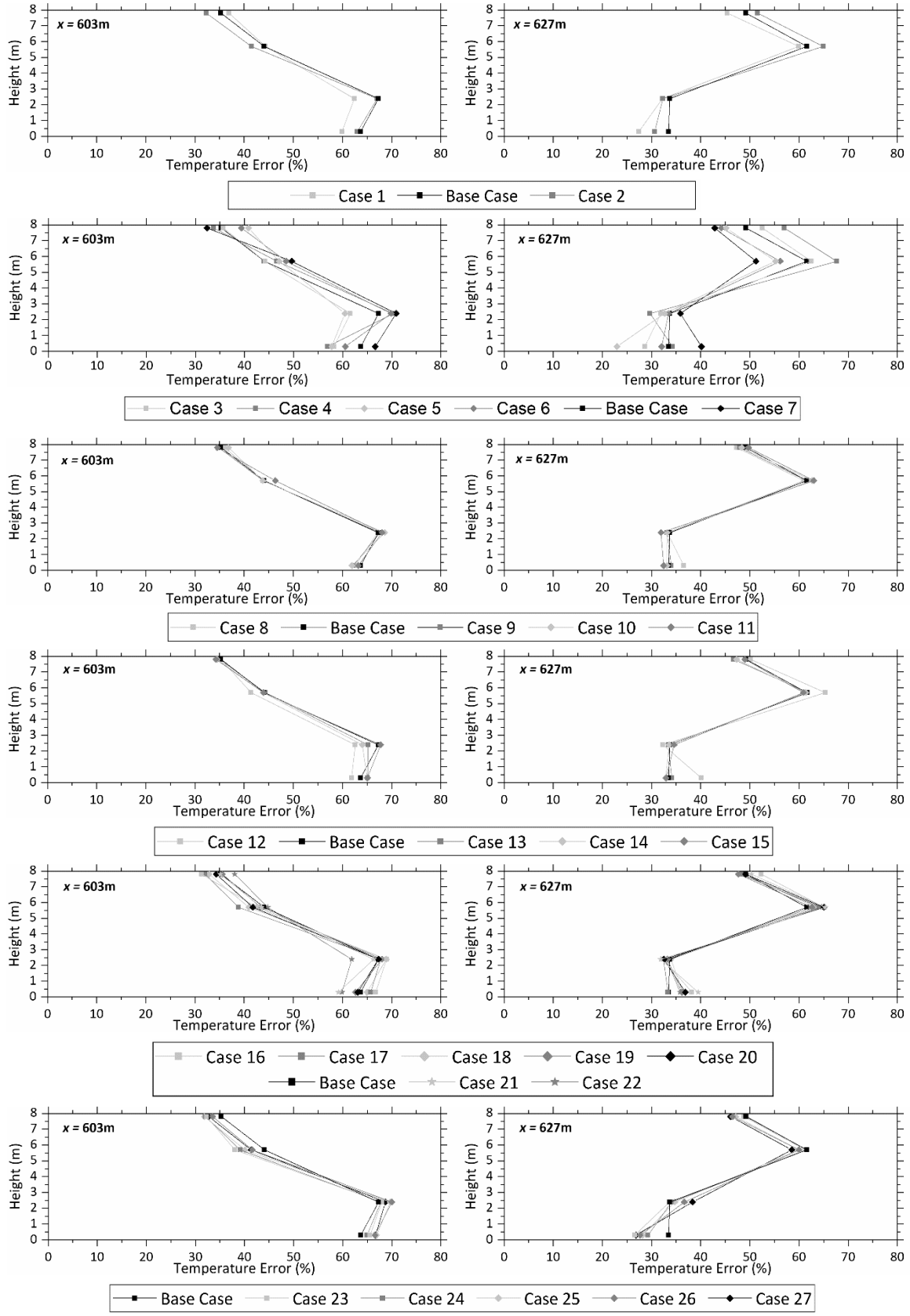

Figure 5.38. Overview of the influence of the turbulent model, grid size, CO yield, soot yield, radiative fraction and the tunnel's wall roughness on the numerical errors of temperature, estimated on both sides of the fire (left: Loop 304, right: Loop 305), during the entire test period.

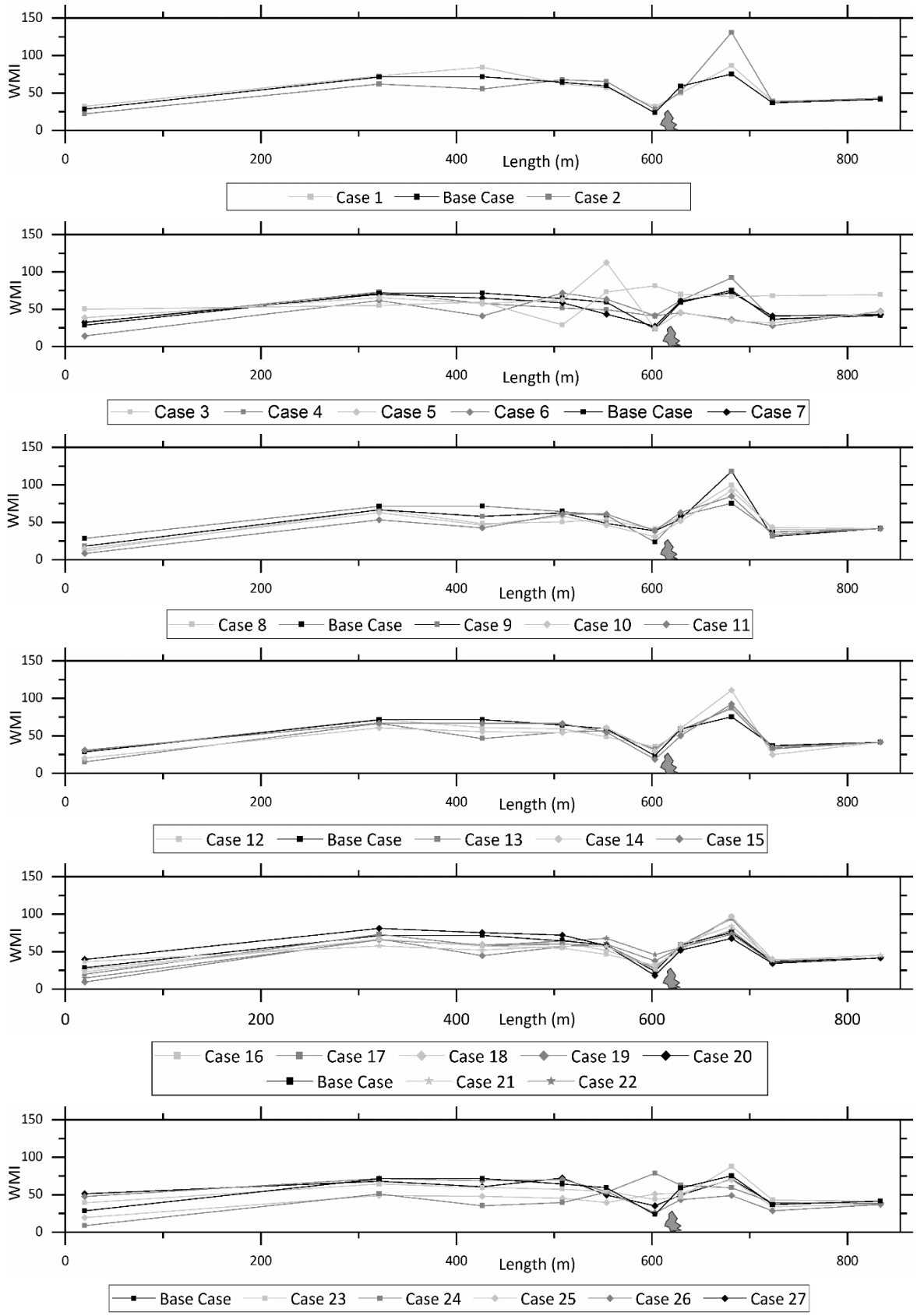

Figure 5.39. Overview of the influence of the turbulent model, grid size, CO yield, soot yield, radiative fraction and the tunnel's wall roughness on the weighted magnitude indexes of velocity. The estimated values regard the velocity profiles throughout the entire tunnel length, 14 minutes after the start of the experiment.

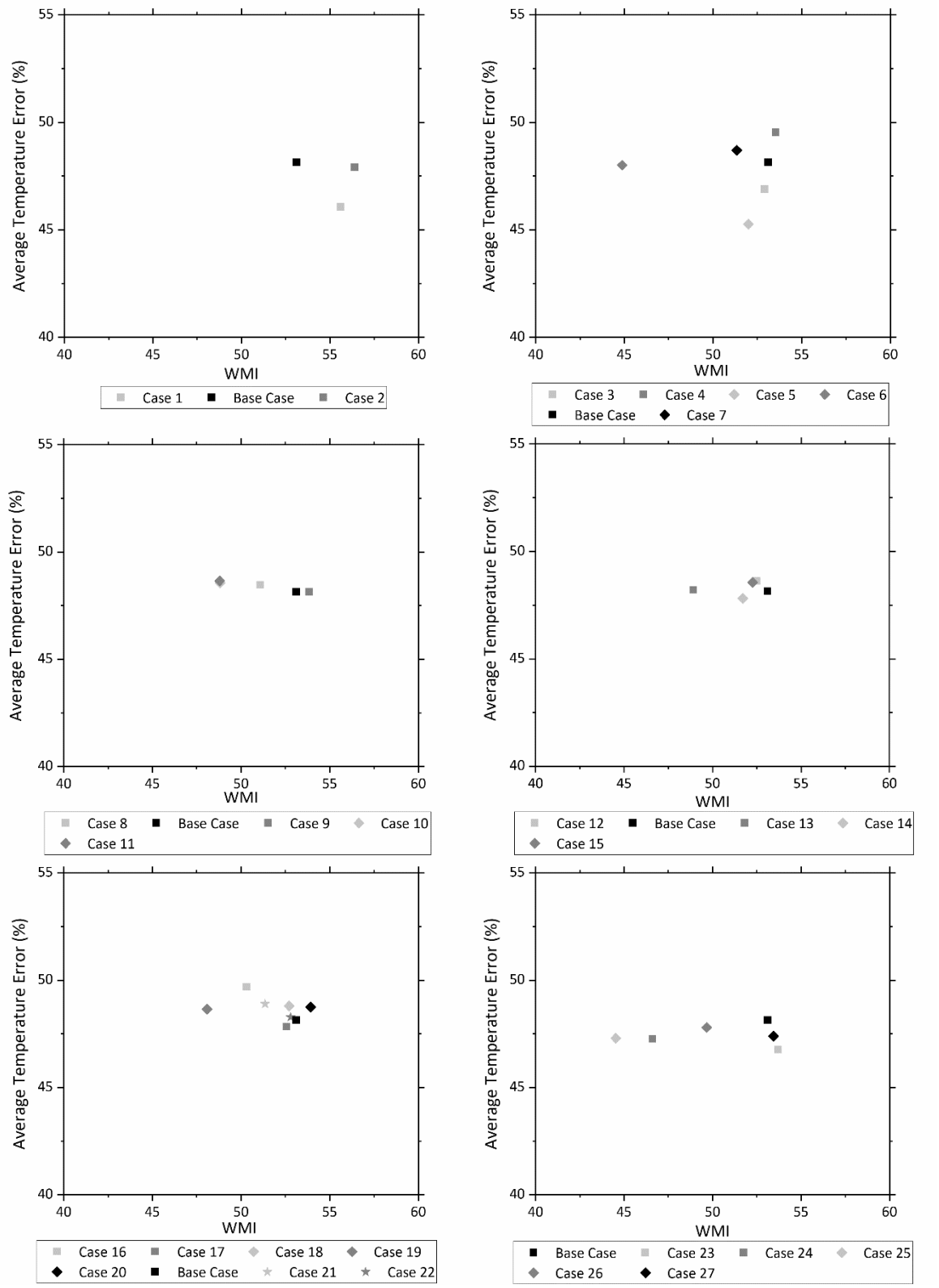

Figure 5.40. Overview of the influence of the turbulent model, grid size, CO yield, soot yield, radiative fraction and the tunnel's wall roughness on the numerical discrepancies in terms of both the temperature (y-axis) and velocity (x-axis) profiles.

5.4.2 Optimum Case Scenario

As far as numerical predictions related to tunnel fires are concerned, their fidelity lies greatly on comparison against the numerical data. For example, at cases where the location of the sensors is relatively close to the fire region, it is highly unlikely that CFD simulations will produce accurate predictions (Xue et al., 1993; Woodburn and Britter, 1996; Wu and Bakar, 2000; Chen and Leong, 2011). The calculated temperatures, for instance near the fire region, can produce significant discrepancies, owning to the fire source simulation approach, namely a volumetric heat source model for example, and the combustion model, which may alter the anticipated outcome from the actual chemistry processes. It is also possible that the turbulent model based on a specific mesh resolution would distort, up to some level the fire driven smoke flow. In general, a numerical inadequacy to the region close to the fire source, may result in quantitatively misleading CFD predictions at regions upstream of the fire source, especially in terms of the velocity profiles. This challenge rises due to the strong interaction between the reversed smoke flow from the fire and the natural ventilation flow. On the contrary, if the location is significantly far away from the fire source, the results obtained are much more easily comparable with the data acquired from the actual experiment. This assumption is also confirmed in the Figures 5.41 and 5.42. However, inaccuracies may arise in the numerical results from the selected simulation mode and mesh resolution, as well, even at tunnel regions far downstream of the fire (c.f. Figure 5.42). In addition to the above factors, inappropriate modeling of the CO and soot yields as well as the amount of radiation emitted can also result in questionable predicted values. With the aim of further reducing the numerical discrepancies and attaining more reliable results, an additional simulation ("optimum case") has been conducted, using the results from the optimum case for each quantity, as determined in subchapter 5.4.1. The recommended values for each factor have been applied to a single FDS input file, with the aspiration of optimizing further the numerical results for Test Case 502. A brief summary of the selected values for each parameter is presented in Table 5.10.

Table 5.10. Review of the key numerical details of the Optimum Case.

Case Name	**Turbulence Model**	**Gride Size (m)**	**CO Yield (kg/kg)**	**Soot Yield (kg/kg)**	**Radiative Fraction**	**Wall Roughness (m)**	**Computational Time**
OPTIMUM	LES	0.25 - 0.50	0.032	0.062	0.35	0.25	8d: 13h: 57min

Even if it is reasonable for one to think that the combination of all the above parameters in one case would yield the optimum results, this objective in practice is not always numerically achievable. One of the main challenges related to CFD simulations is the fact that there is no universal guideline that guarantees that a specific combination of assumptions is the most suitable for the simulation of a particular application, such as the tunnel fire modeled here. With consideration to that, in the analysis that follows, the numerical results acquired from the Optimum Case Scenario are compared against the results from the chosen case of each parameter, that agreed better with the respective experimental data. Temperature distributions are illustrated in Figure 5.41 on both sides of the fire, whereas Figure 5.43 highlights the numerical errors generated by the FDS on the respective numerical predictions. Figure 5.42 demonstrates the velocity profiles throughout the entire tunnel length and in Figure 5.44 the calculated WMI values offer a sharp distinction over the accuracy of the test cases' results. In total, the Pareto front, shown in Figure 5.45, summarizes the information obtained from this numerical analysis and demonstrates the dominance of the case with the most accurate numerical findings.

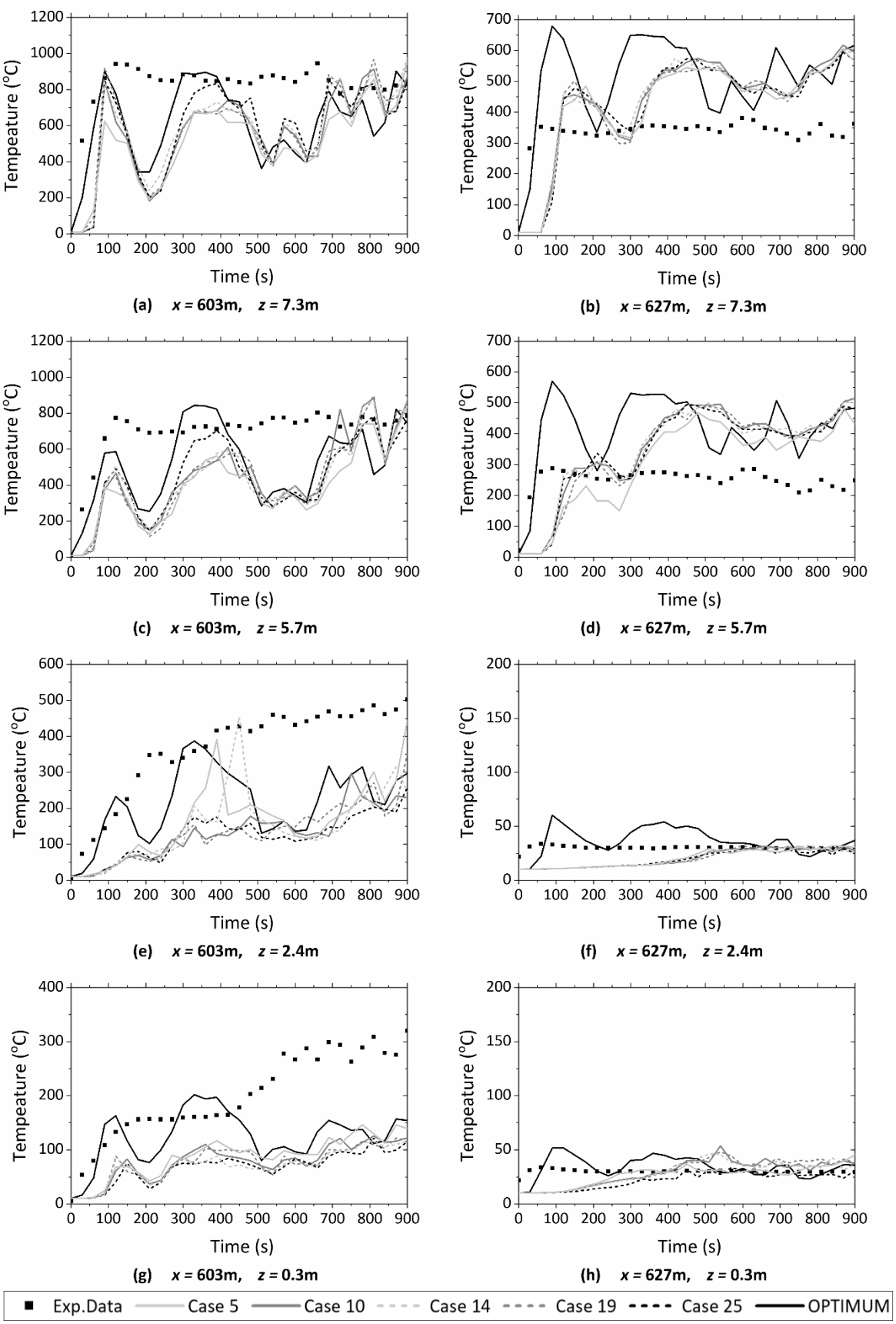

Figure 5.41. The effect of Optimum Case's numerical parameters on the temperature, at different cross-sectional heights of the tunnel, at Loop 305 (left) and 304 (right), during the entire test period.

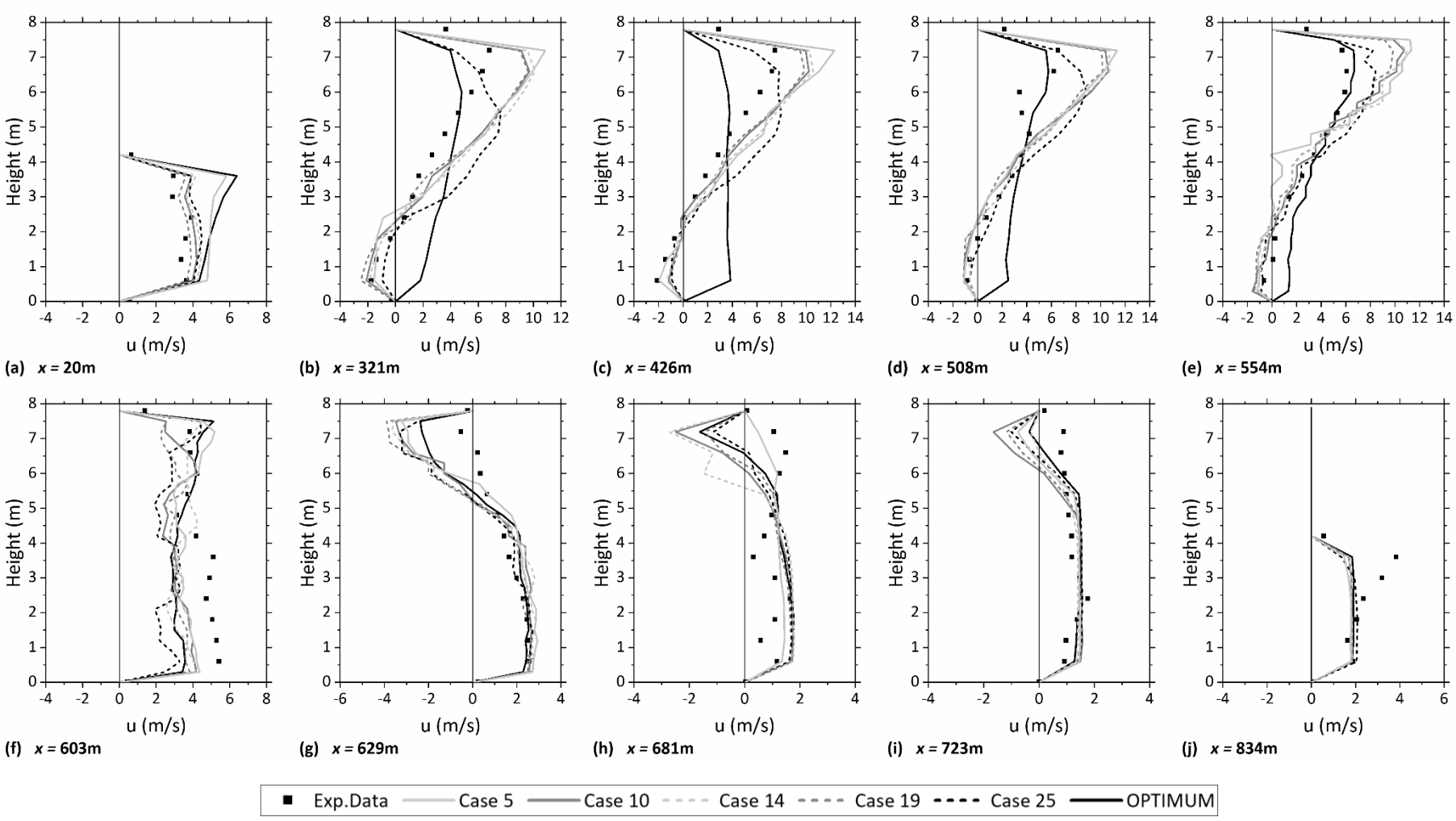

Figure 5.42. The effect of Optimum Case's numerical parameters on the velocity profiles throughout the entire tunnel length, after 14 minutes since the start of the experiment.

The dominance of the Optimum Case scenario is apparent almost in every Figure. With a closer inspection of the temperature distributions, Figure 5.41 indicates that FDS predicted for the Optimum Case much higher temperatures, than the actual ones, at the upstream side of the fire region, towards the south end. However, this over-estimation emerges mainly during the time period right after the developing phase of the fire, and it is only located at the upper section of the tunnel cross section, where the thick layer of smoke exists. Since this phenomenon progressively reaches steady state conditions, the discrepancies at the temperature, are gradually diminished, producing even more reliable results than the other cases after 8 minutes of elapsed experimental time. On the other hand, at the downstream side of the fire source, in the direction towards the north tunnel portal, numerical predictions of temperature for the optimum case are far more accurate than any other case's. This significant decline in the temperature error, against the reference data from the experiment, is clearly shown in Figure 5.43 as well as in the Pareto Front depicted in Figure 5.45. The estimated temperatures do not only improve qualitatively, but in most cases, they reach the exact order of magnitude of the experimentally measured temperatures at all the cross-sectional heights, downstream from the fire.

At the same time, the Optimum Case provides the most accurate results compared to the vast majority of the other test cases, regarding the velocity predictions, especially near the fire region (c.f. Figures 5.42 and 5.44). Near the middle of the tunnel's length, FDS predictions imply that a uniform smoke layer is traveling towards the north end. However, experimental results oppose to that assessment, since in the respective experimental velocity profiles a narrow layer of fresh air, near the tunnel floor seems to move upward, to the fire's direction, forming a distinctive two-layered stratified flow-field. With this single exception, velocity predictions near the fire are remarkably consistent with the experimental data. In particular, they predict correctly the mild backlayering effect of the smoke flow, which is one of the main pursued objectives in this validation study. Therefore, although the WMI for the velocity predictions does not have the lowest possible value, the profiles of the longitudinal component of the velocity indicate that the optimum case scenario in the region of high interest, near the fire source, provides the best numerical results.

As illustrated in Figure 5.45, the main aim of this investigation is achieved. The computational approach of applying the "optimum" values, produced from the parametric study has delivered satisfactory results, in the terms of both quantitative and qualitative criteria of optimization. The inaccuracies in the temperature distribution have been significantly rectified, leading to a particularly diminished numerical error. Perhaps further scope of optimization may be desired in the predicted conditions regarding the velocity. However, even with the current assumptions, the overall velocity discrepancies among the numerical and experimental data are distinctively low. According to the previous parametric study on the FDS simulation mode, in fact, VLES tends to deliver better predictions than LES, in general, regarding the velocity, Figure 5.40. Hence, this may be a sufficient justification for the fact that the velocity predictions of the Optimum Case have not been optimized to a further point, as temperature computations successfully did. Furthermore, it is quite likely that the accuracy of the Optimum CFD simulation findings has been additionally enhanced, up to some level, by the absence of the TIME_SHRINK_FACTOR in the input file case. This conforms to the view that the fidelity of the CFD model depends heavily on the literal development of the actual experimental conditions. Concluding, FDS is a feasible choice for this study, as it is sufficiently describing phenomena of fire-related buoyancy-induced flows and therefore the current validation study has laid a fair foundation for upcoming numerical studies of tunnel fires with natural ventilation conditions.

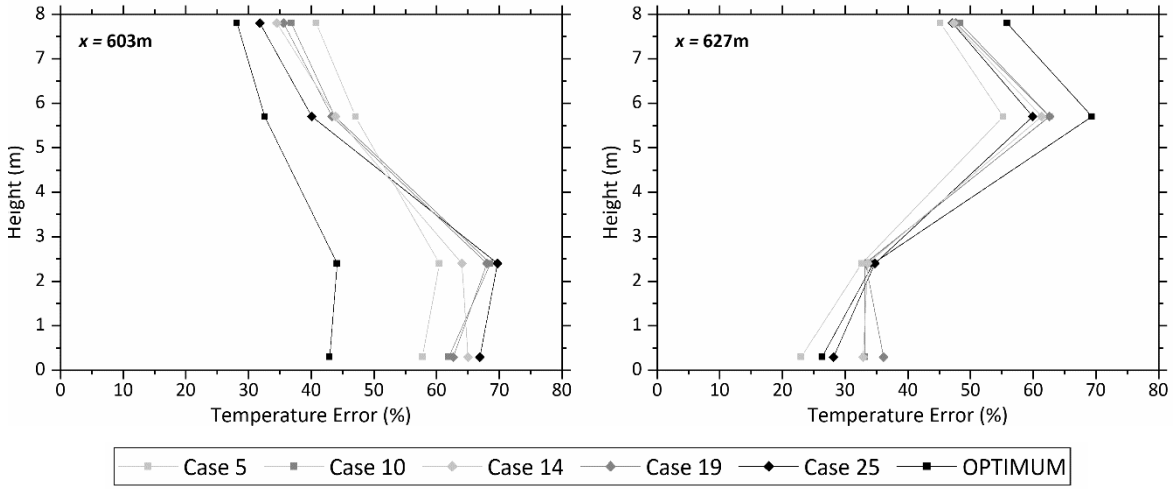

Figure 5.43. Overview of the numerical errors of temperature, estimated on both sides of the fire (left: Loop 304, right: Loop 305), of the optimum values of each parameter.

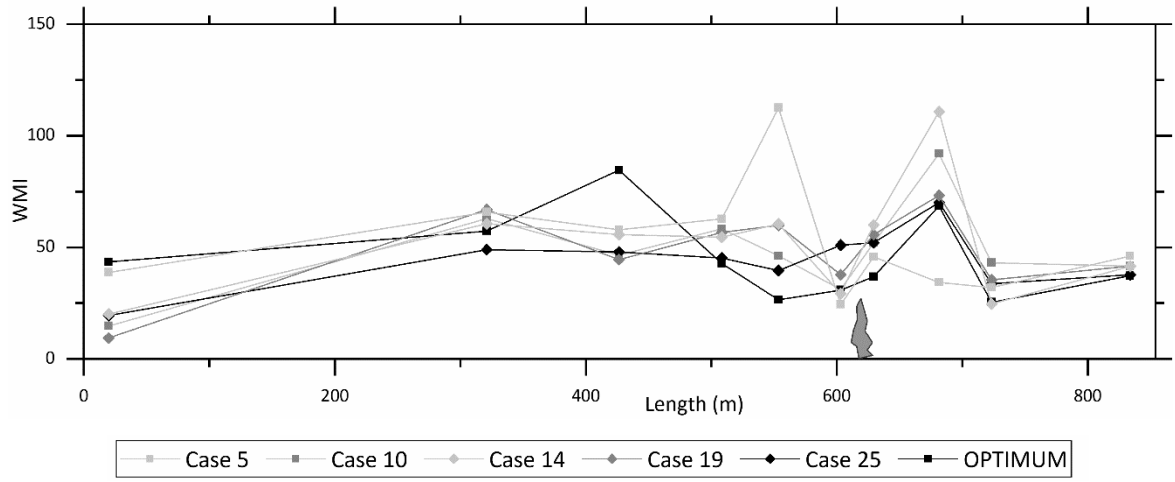

Figure 5.44. Overview of the weighted magnitude indexes of velocity, on the influence of the optimum values of each parameter. The estimated values regard the velocity profiles throughout the entire tunnel length, 14 minutes after the start of the experiment.

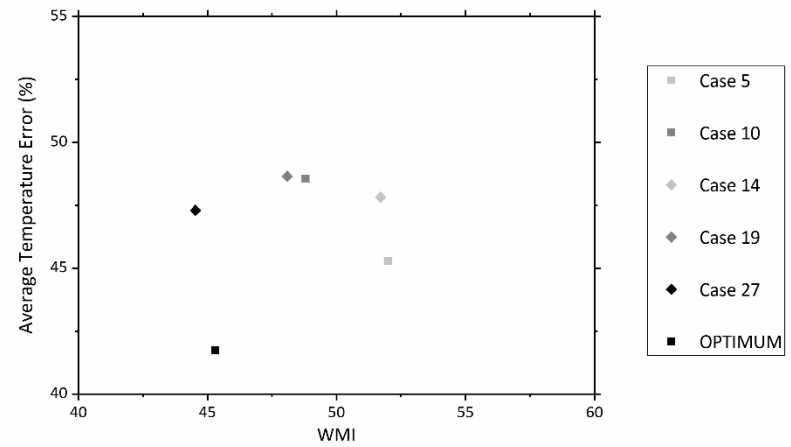

Figure 5.45. Overview of the numerical discrepancies in terms of both the temperature and velocity profiles, on the influence of the optimum values of each parameter.

5.5 Characteristics of the Developing Flow-Field

Smokeview is a post-processing software aimed at visualizing numerical predictions produced by fire models such as the Fire Dynamics Simulator (FDS). This software tool performs visualizations by displaying data related to fire driven fluid flows, but it is not constrained only in this kind of simulations. It also visualizes phenomena associated with evacuation processes, a capability that can be quite handy especially in tunnel fire simulations, where the number of large-scale evacuation tests is limited. However, a post-processing step in both fire and evacuation tunnel simulations is the evaluation of the developing flow field. The numerical results which are composed of both dynamic and static data may either be depicted via the Smokeview graphic environment by animating particle flows (with indicating location and values of tracer particles), 2D contour slices (within the domain and on solid surfaces), vector plots and 3D iso surfaces. Animated 2D shaded color contour plots are usually employed to generate graphic content for gas phase information, such as temperature distribution or density. 2D contour slices also constitute a useful tool in data visualization, especially in terms of the velocity records where colored vectors can be utilized to show flow direction, speed and value. Concluding, Smokeview forms a valid tool for the visualization of the characteristics of a developing flow field, as demonstrated also in Figures 5.46 to 5.49. More specifically, Figure 5.46 depicts the developing flame envelope of the 50 MW fire. In the current approach, the fire is prescribed as a volumetric heat source, which substantially changes the structure of the fire source and hot combustion gases. The individual snapshots demonstrate the intensive turbulent characteristics of diffusion flames induced in a tunnel fire. The heat released is spatially distributed and coupled to the flow field, as shown in Figure 5.48. Additionally, in Figures 5.47 and 5.48, several 2D contour slices, along the y-axis, are presented indicating the gas velocity and the temperature distributions inside the tunnel. The direction and length of the induced vectors reveal the flow's direction and speed. In fact, the vector colors specify the actual value of the predicted velocity, as demonstrated in the legend of Figure 5.47. The propagation of the smoke flow has been also captured in Figure 5.49, where snapshots of the traveling group of soot particles are depicted. These features, in total, depict broadly the flows characteristics at several points in time, during the entire test period. In that manner, anyone acquainted with the current work, can acquire a comprehensive visual perception of the fire related phenomena created under the natural ventilation condition of the Memorial Tunnel Test Case 502.

A brief, but comprehensive, demonstration of the actual characteristics of the Optimum Case flow field, is attained in the following session, assisted by the Smokeview visualized figures. In particular, the fire that develops in the Memorial Tunnel structure, Figure 5.46, seems to interact strongly with the underlying ventilation airflow. In that way, complicated air flow patterns and turbulence-related phenomena, like swirling eddies, Figure 5.47, are introduced in the developing flow, especially at the vicinity of the fire source. The heat produced from the fire warms up the surrounding air, and then progressively both the fire and the hot layer of smoke contribute in the convectional and radiative heat transfer to the entire tunnel's length. In the case of Memorial Tunnel, which is characterized by a 3.2% longitudinal inclination, buoyancy forces are evidently established along the tunnel length. These forces are assisted further by the strong bulk airflow, Figure 5.6, entering the tunnel at the portal with the lowest altitude and, therefore, dominate the movement of the air and smoke flow inside the tunnel. This has consequently led to drastic changes in the fire and ventilation flow patterns in the entire tunnel. As shown in Figure 5.46, the governing airflow conditions are so strong that the fire does not vertically reach the tunnel's ceiling, but it is carried away, towards the airflow direction to the north portal. This phenomenon, regarding the flame's drifting, is also illustrated by the features of the temperature distribution and soot propagation, on the symmetrical Y axis, in Figures 5.48 and 5.49, respectively. However, the resulting longitudinal flow velocity has been proven not high enough to prevent entirely the

reverse flow of hot gases under the ceiling. It is illustrated that at a short distance from the point where the fire plume nearly reaches the tunnel ceiling, the smoke jet is divided in two separate longitudinal flows at both sides of the fire. As the fire further develops, these layers are becoming thicker and less uniform since they tend to descend towards the tunnel's floor. The distance from the fire where the smoke flow impinges to the ceiling and splits is highly associated to the fire size, ventilation conditions and the tunnel's geometry and inclination, as well. For the current airflow's velocity, a relatively good stratification exists, along with the backlayering upstream of the fire, as illustrated in Figure 5.49. In practice, the back-layering effect is clearly displayed on both the velocity and temperature 2D contour slices, Figures 5.47 and 5.48. Yet the most striking testament of this phenomenon is given in Figure 5.49, where the soot distribution inside the tunnel is shown. However, over time the smoke stratification at the downstream region from the fire source becomes worse. This observation is well justified because the uniformity of the smoke flow towards the downstream side and the stratification are difficult to maintain even at a short distance downstream, at such high velocities, Figure 5.47. In order to prevent any type of back-layering, the longitudinal velocity inside the tunnel had to be even higher, exceeding the critical value. The backlayering effect, in general, constitutes one of the main challenges in tunnels with natural ventilation. This is due to the fact that when no forced ventilation is applied not only the tunnel geometry and inclination, the resulting fire size and the location of the fire source rule the flow of hot combustion products in the tunnel, but also external winds and atmospheric conditions outside the portals may have a robust impact on the ventilation conditions.

5.5.1 Flame envelope

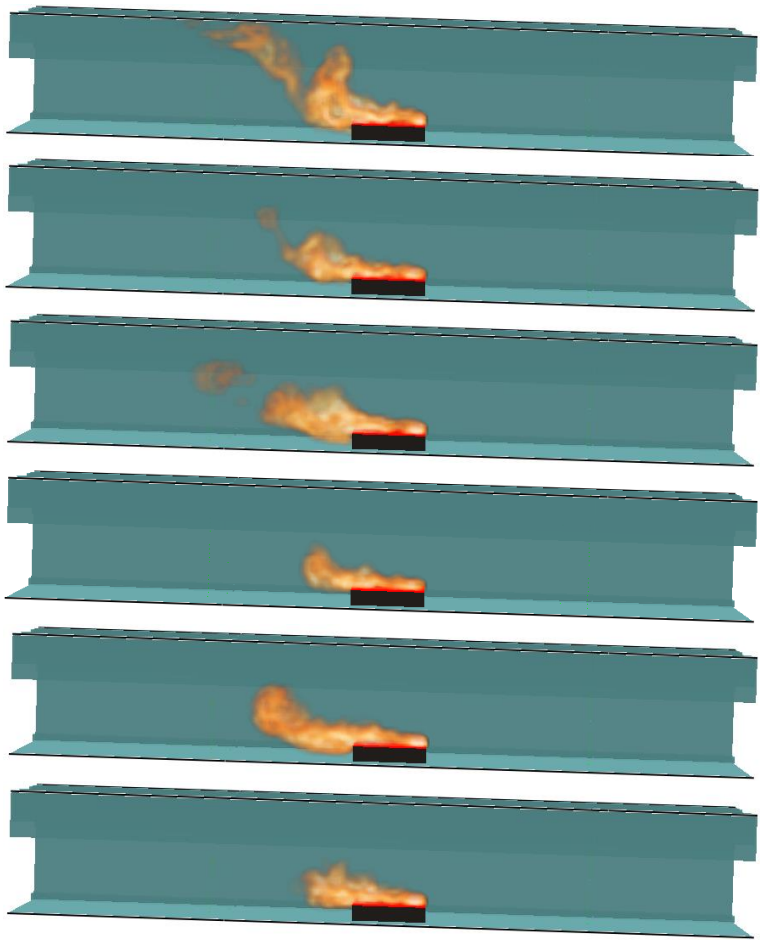

Figure 5.46 Overview of 2D contour slices of flame envelope, at 90s, 240s, 390s, 540s, 690s, 840s. In the figures only a part of the tunnel is depicted, at a distance of 590m to 640m from the north portal.

5.5.2 Gas velocity

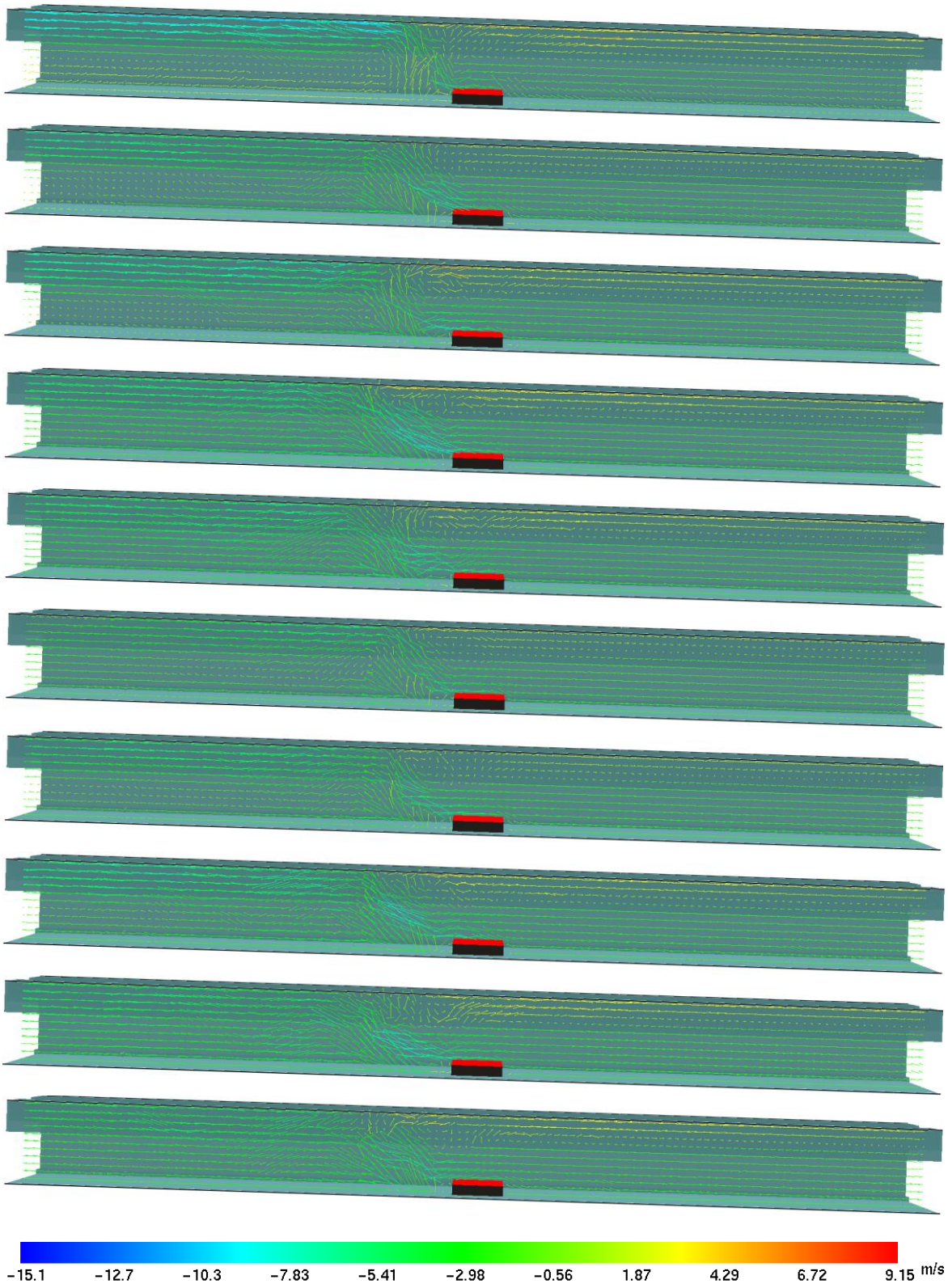

Figure 5.47. Overview of 2D contour slices of Gas Velocity, at 90s,180s, 270s, 360s, 450s, 540s, 630s, 720s, 810s, 900s. In the figures only a part of the tunnel is depicted, at a distance of 300m to 700m from the north portal

5.5.3 Gas temperature

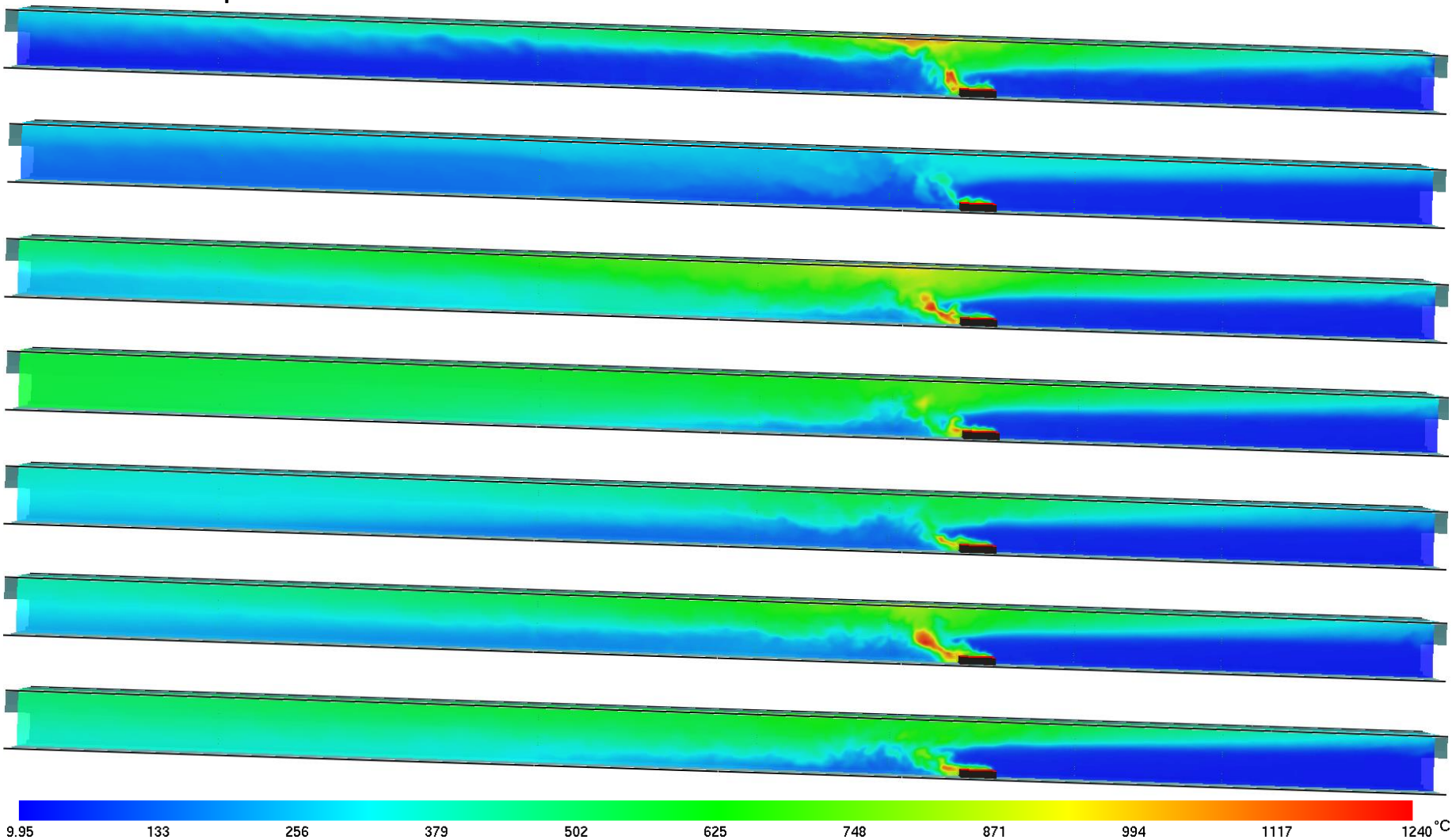

Figure 5.48 Overview of 2D contour slices of Gas Temperature, at 90s, 330s, 450s, 570s, 690s and 810s. In the figures only a part of the tunnel is depicted, at a distance of 480m to 680m from the north portal.

5.5.4 Smoke

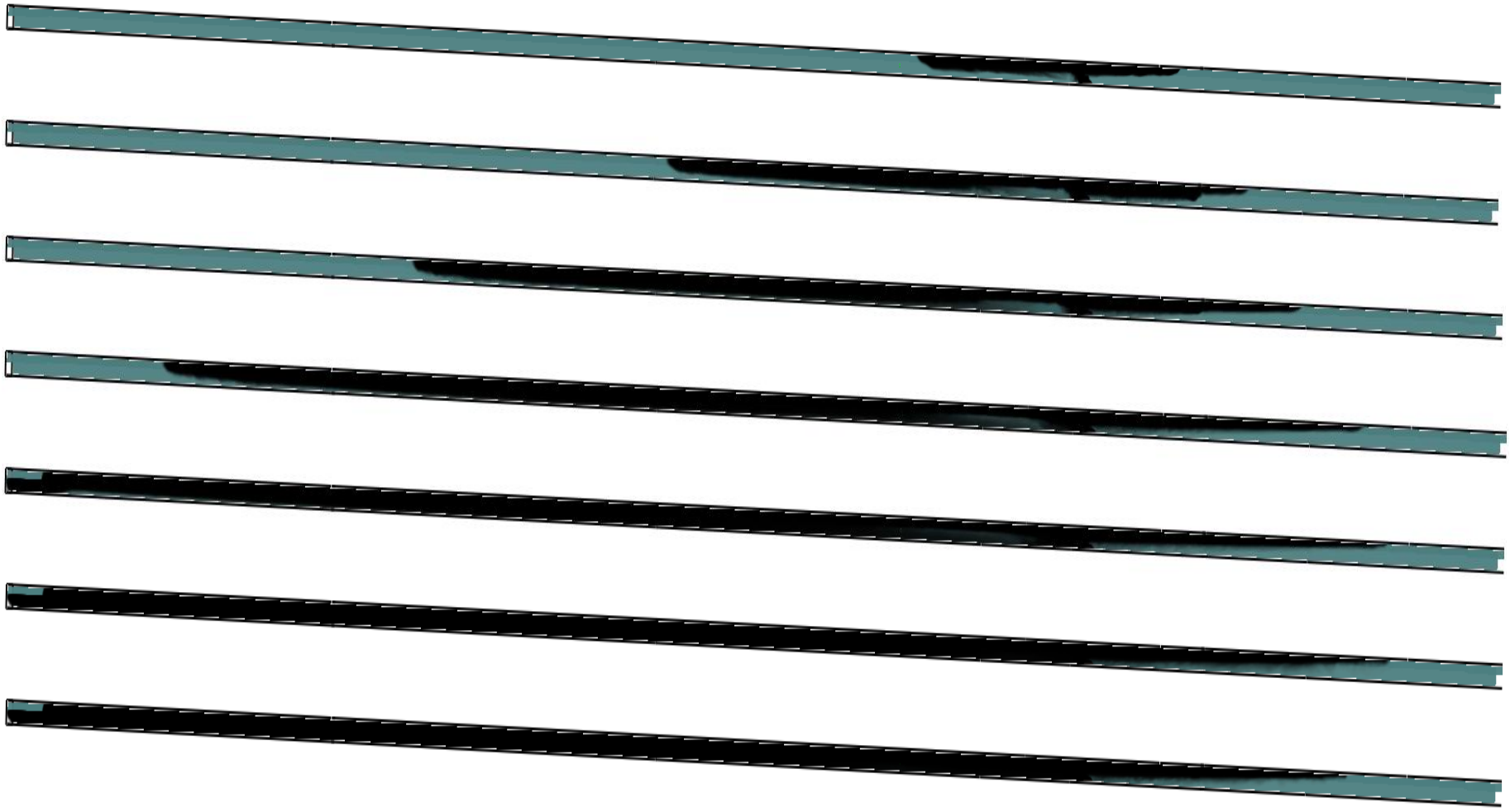

Figure 5.49 Overview of smoke distribution, at 60s, 90s, 120s, 150s, 180s, 600s, 900s, throughout the entire tunnel length.

6. ROAD TUNNEL FIRE SIMULATIONS

6.1 Memorial Tunnel- Validation Test Case 615b

In Unit 5, a validation study of the FDS code, has been conducted based on the experimental findings of the Memorial Tunnel Fire Ventilation Test Program (MTFVTP). Out of the amount of 98 tests, Test 502 has been selected for the main validation case. In that process, various numerical parameters have been investigated and the most precise and reliable results, derived from the adjustment of the main modelling details, have been gathered to orchestrate the optimized numerical case of Test 502. The employment of Test Case 502 out of the remaining cases is owned to the elementary nature of the particular experimental scenario. In this fire scenario, a fire of approximately 50MW has been utilized and all the fire related events have been developed under the effect of natural ventilation. In that manner, a primary assessment of the implied numerical parameters regarding the main experimental characteristics, can be conducted and the most valid findings can be subsequently utilized to describe more complicated fire arrangements and ventilation configurations, for further research. Based on the previous approach, a performance of a supplementary validation case has been established to certify further the FDS accuracy regarding a fire scenario where longitudinal ventilation effectively influences the characteristics of the developing flow field from a certain fire.

The implementation of a mechanical ventilation system is necessary in most road tunnels to efficiently control the concentrations of pollutants and hot smoke from the fire, in order to comply with the tenability levels within the tunnel. Various configurations of ventilation systems have been designed to take account for the specificities of each tunnel structural geometry, operational conditions and utilization. Therefore, the appliance of the appropriate ventilation arrangement would result in regulation of the flow field of toxic effluents inside the tunnel and thereby establishing a fire emergency route for evacuation and fire-fighting procedures. In the case of Memorial Tunnel Test Program various alternative ventilation configurations have been utilized, including full and partial transverse ventilation, with the addition of a single point extraction or with oversized exhaust ports, point supply and point exhaust operation of ventilation systems as well as longitudinal ventilation configurations, with Jet fans. The current study is focused on the latter mechanical arrangement, the one of longitudinal ventilation.

The ventilation strategy of a mechanical system with Jet Fans, acquired to create a longitudinal flow within the tunnel, has been evidently proven highly adequate in managing the direction of smoke propagation for fire sizes up to 100 MW, at inclined and not inclined tunnel structures, according to experimental findings. For that cause, the Test Case 615b of the Memorial Tunnel Fire Ventilation Test Program has been chosen to validate the numerical results of the FDS code, when a longitudinal ventilation system is employed. The general description of the Test Case 615b has been included in Unit 5 (5.1.2). In that section various experimental features and details have been provided including the utilized fuel, the fire source location and the measured heat release rate from the fire, Figure 5.8, along with the governing ventilation conditions within the tunnel - provoked by either pressure discrepancies, environmental conditions or the forced ventilation system- and the airflow conditions at the portals. Additionally, the implemented ventilation strategy has been analyzed. It is reminded that the imposed ventilation strategy has been designed with the minimum amount of only 6 Jet Fans in operation for managing the entire flow within the tunnel. The response time of the system was set at 2 minutes. The above-mentioned experimental information has been summarized in Table 5.5. The main objective of this sequence of tests, at which Test 615B is included, was designed to investigate the ability of a longitudinal ventilation system to control smoke and heat propagation, using the minimum number of jet fans.

Prior to the evaluation of the numerical predictions, a brief overview of the experimental findings, from the Test 615b, is imperative. In particular, at the beginning of the fire experiment, during the initial 2 minutes, no group of jet fans has been operating, and the hot smoke produced from the fire has spread rapidly towards both sides of the fire. The activation of the jet fans has interrupted the propagation of smoke at the upstream direction, while downgrading its stratification at the same time. The latter observation could have been avoided if a steady airflow has already existed within the tunnel, prior to the onset of the fire, originated ideally either by the jet fans downstream of the fire or the ones far upstream. It is apparent that the time interval between the fire ignition and the activation of the mechanical ventilation system is essential in all fire scenarios. Memorial tunnel tests, which were performed under strong longitudinal ventilation, advocated that this time period should be minimized as possible, since the toxic effluents produced from the fire tend to be dispersed rapidly in the fire growth phase, especially for fires of large size. As it regards the measured critical velocity, experimental results have shown that the minimum air velocity to prevent the backlayering effect in Memorial Tunnel corresponds to value of 2.95m/s for a 100MW fire. Implementing a longitudinal ventilation system that can produce and sustain a steady air velocity that equals the critical ventilation conditions, evidently results in managing the airflow inside the tunnel utterly, directing the products of combustion and hot smoke to the downstream end of the tunnel, exhausting them to the atmosphere at the south portal. Additionally, one main aftermath of the Memorial Tunnel fire tests is that the designer of the ventilation system, in every tunnel structure, should always account for the occurrence of damage to technical installations, such as Jet Fans, when exposed to high temperatures for a prolonged period of time. Experimental findings suggest that at least the group of jet fans, which locates near the fire site, is in grave danger due to the underlying high temperatures. As is a well-known, the applied ventilation velocity for hindering the adverse flow of smoke, directs the hot products from the fire solely to the downstream side of the tunnel. Therefore, even though the group of jet fans closer to the fire source, is at a distance of 50 metres away, Memorial Tunnel findings indicate that the resistance of its materials has been compromised.

Table 6.1. Review of the key modelling parameters of the Test Case 615b.

Case Name	**Turbulence Model**	**Gride Size (m)**	**CO Yield (kg/kg)**	**Soot Yield (kg/kg)**	**Radiative Fraction**	**Wall Roughness (m)**	**Computational Time**
Test 615b	LES	0.25 - 0.50	0.032	0.062	0.35	0.25	1d: 19h: 31min

The CFD simulation for the Test Case 615b, has been designed based on prior optimum findings of the Test Case 502. In Table 6.1, the main numerical parameters have been summarized, including the simulation mode, mesh resolution, concentrations of emitted fire products, the amount of heat radiated from the fire source and the roughness specified on the tunnel's walls. The main characteristics of the developing flow-field inside the Memorial Tunnel, provoked by the induced fire of nominal size of 100MW, are depicted in Figure 6.1 & 6.2. In particular, information regarding the temperature and velocity time profiles along with the predicted CO concentration upstream and downstream from the fire source, as derived by the FDS code, are provided through those Figures. The longitudinal central positions of the jet fans groups utilized in the current test Case, as well as the operational period of each fan during the test, have been previously demonstrated at Table 5.3 and Table 5.4, respectively. The cross-sectional position of each group is depicted in the schematic diagram in Figure 6.3 and an actual picture of a Jet Fan utilized in the Memorial Tunnel experiment is shown in Figure 6.4. With a view to reduce the computational time required for the simulation case, a TIME_SHRINK_FACTOR in the order of 10, has been applied to the current validation case, as well.

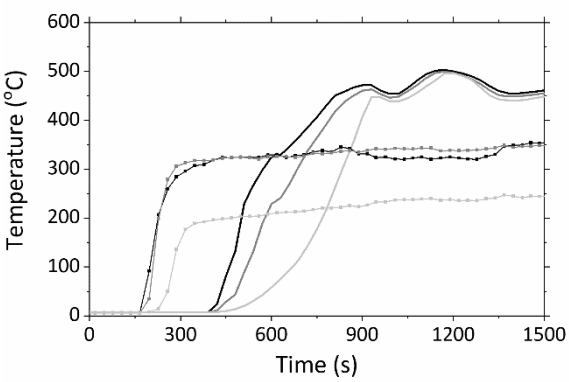

Loop 202 - *x* = 834m

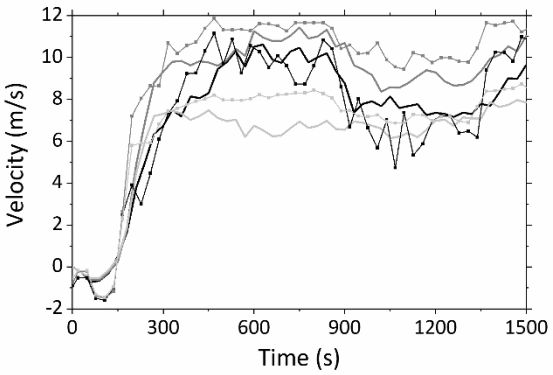

Loop 202 - *x* = 834m

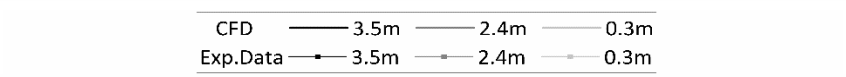

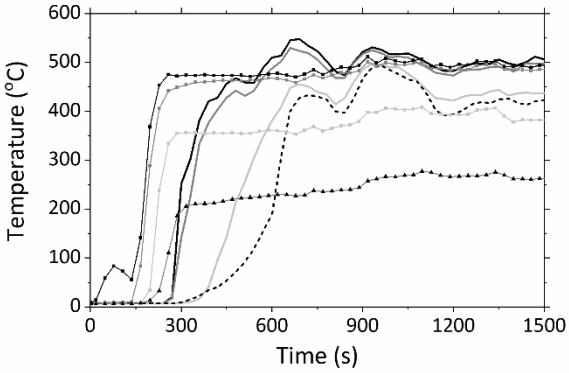

Loop 301 - *x* = 723m

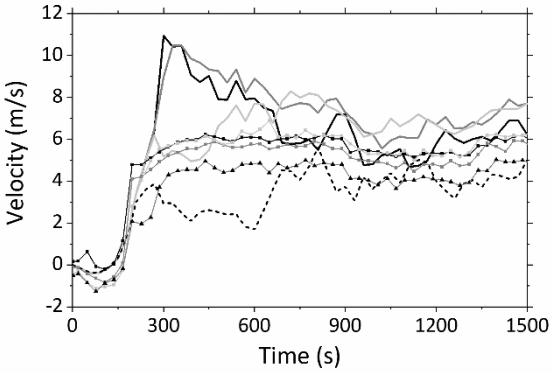

Loop 301 - *x* = 723m

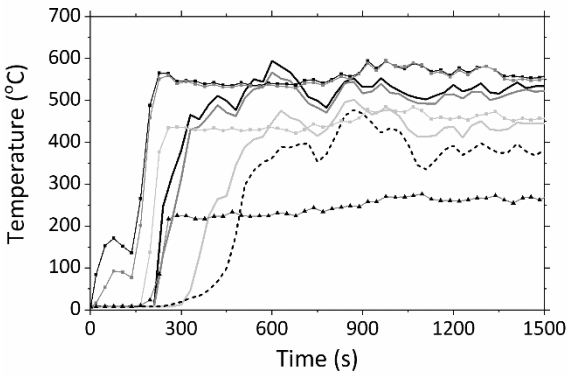

Loop 302 - *x* = 681m

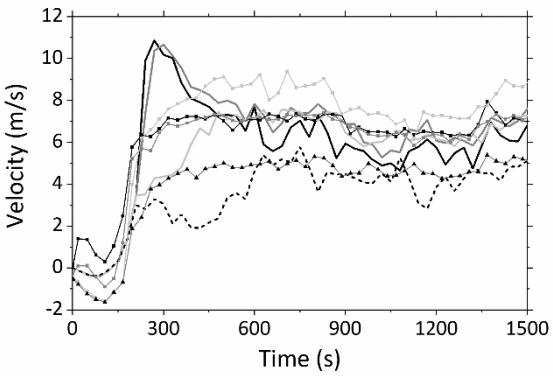

Loop 302 - *x* = 681m

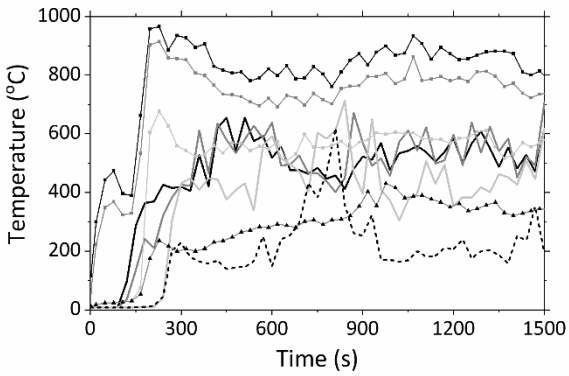

Loop 304 - *x* = 629m

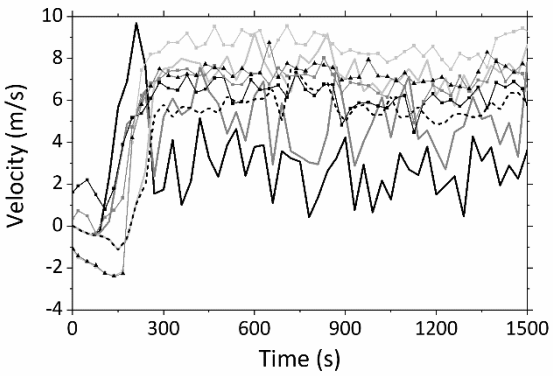

Loop 304 - *x* = 629m

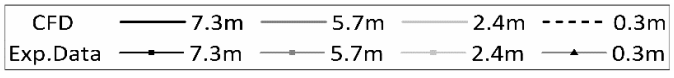

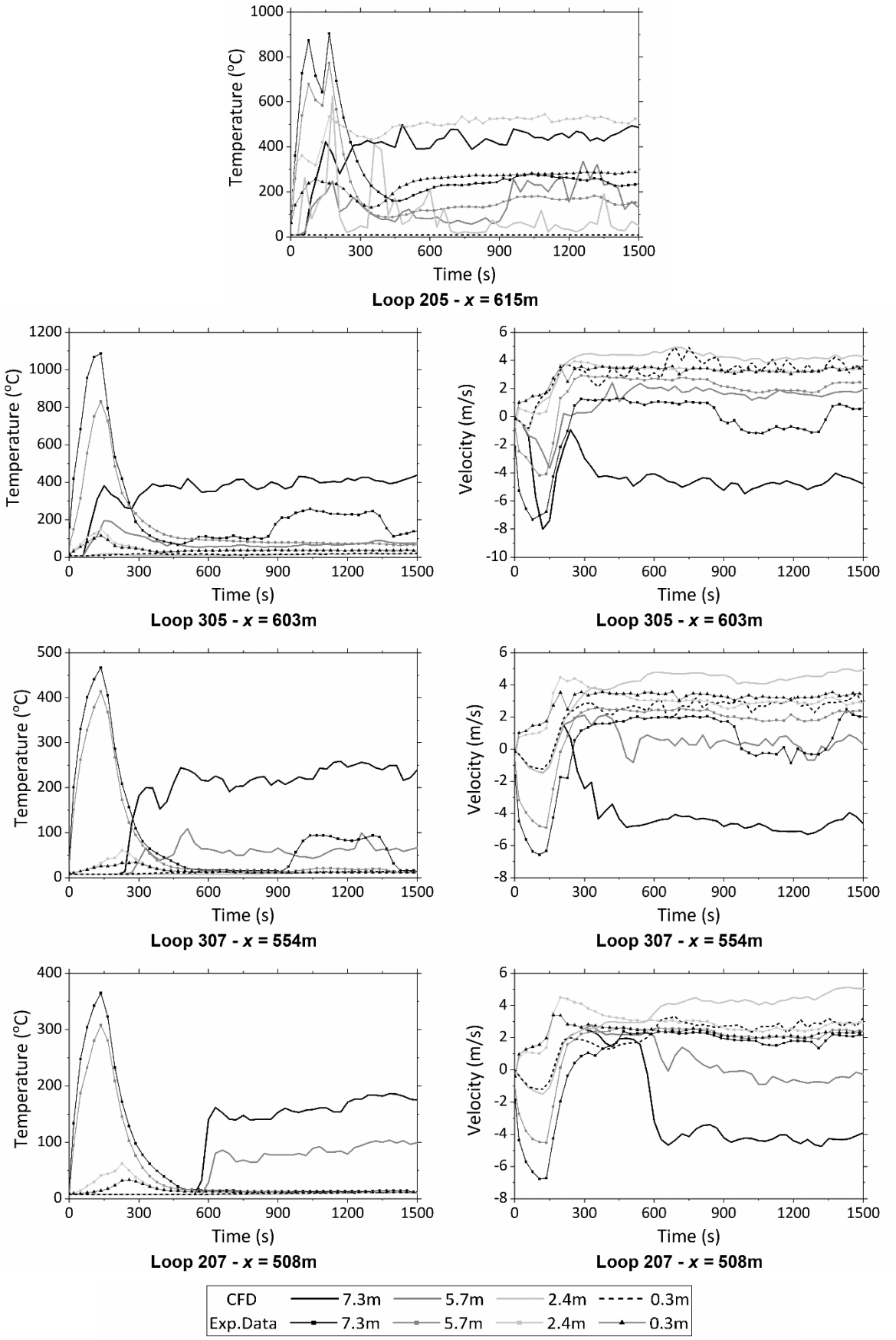

Figure 6.1. Time evolution of the numerically predicted temperature and velocity profiles, at different locations and cross-sectional heights within the tunnel, compared to the respective experimental data.

The experimentally obtained temperature profiles, in Figure 6.1, demonstrate that the fire tends to develop in two distinct phases. As observed, these phases are critically influenced by the dominant ventilation conditions inside the tunnel. Over the first minutes after the onset of the fire, a vigorous rise in the temperature has been measured at the location of the fire source, indicating a period of rapid-fire growth rate. At this point, the jet fan system has not been yet activated, rendering the underlying natural ventilation the leading airflow within the tunnel. In that manner, the initial development of the fire growth is fashioned under the influence of this natural flow, solely. Evaluating further the experimental data of Memorial Tunnel Test Case 615b, the strong relationship between the fire growth and the longitudinal ventilation velocity becomes more apparent. In particular, when the forced airflow from the Jet fans approaches the site of the fire, the measured temperature at 2.4m, right above the fire source evidently increases, which subsequently indicates that the fire growth has increased, too. This observation suggests that ventilation flows near the critical conditions should be avoided in the initial stages of a fire, to hinder the vigorous development of the fire. Nevertheless, the implementation of critical velocity is an indispensable design parameter for fires in many tunnels, so that a smoke-free emergency rout to be created. As it regards the average temperature at the upper cross-sectional area of the tunnel, where the stratified layer of smoke from the fire source is located, it is observed an abrupt degrade to half of its initial value, after the activation of the mechanical ventilation system. The sudden dispersion of the smoke, triggered by the implementation of forced ventilation velocity, is mainly responsible for this dilution in the smoke temperature near the ceiling. Although the computed temperature profiles at the fire location, do not succeed in predicting this sharp increase during the initial stages of fire growth, they seem to comply well overall at all cross- sectional heights resulting in a mean numerical error in the order of 76%.

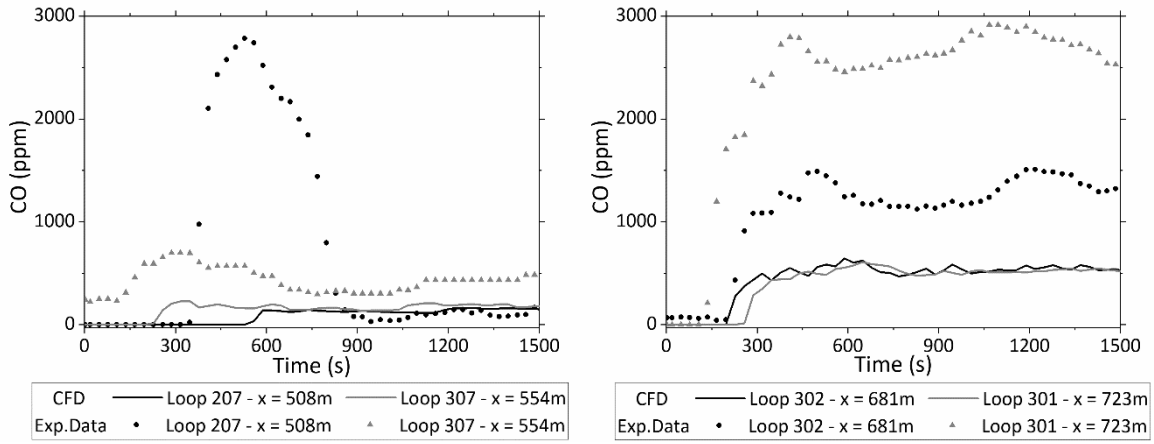

Figure 6.2. The CO concentrations as measured in the actual experiment and predicted by FDS, at 7.1m cross sectional height, upstream and downstream from the fire source.

Numerical findings confirm that during the initial 2 minutes of the simulation, the smoke begins to rapidly propagate under the sole influence of natural ventilation, mainly to the upstream side of the fire, towards the North portal. This smoke tendency is shown in both the temperature and velocity profiles, in Figure 6.1. The ascending grade of the Memorial Tunnel is mainly responsible for the direction of the travelling smoke as the resulting buoyant forces due to pressure differences at the portals, efficiently fashion a strong airflow movement. Even after the activation of the jet fans, the smoke backlayering length continues to increase upstream from the fire source but as the discharge air velocities from the jet fans progressively increase up to their nominal value, the propagation rate decelerates accordingly. In the numerical simulation, the emergency ventilation system is capable of reaching full operational mode, within a maximum of 150 seconds. However, even at full operational conditions the adverse layer of smoke persist on developing towards the

north portal. In fact, when the entire experimental period of 25 minutes has been completed, the thermally driven layer of smoke has efficiently passed by the fifth group of jet fans, which is located at 474m from the North portal, reaching about halfway to the fourth group, at 379m. It is apparent that the back layering phenomenon could not be inhibited entirely by the implied air velocities from the jet fans, in the numerical simulations. Nevertheless, the resulting temperature of the centreline smoke layer has not exceeded 200℃, at a distance of 508 metres away from the North portal. Accordingly, the respective temperature at 426m, has preserved its initial value of about 8℃, which temperature value has prevailed within the tunnel prior to the onset of the fire, until, at approximately 1300 second of elapsed computational time, when a peak temperature of 100℃ has been reached. At the actual experiment, with the contribution of the longitudinal airflow of the jet fans at full operational mode, the backlayering length did not extent further from the Loop 207, at 508m, upgrade of the fire. The discrepancies between experimental and numerical data at these upstream locations, in both temperature and velocities time profiles, have led to exceptional high numerical errors, at measurement positions of 508m to 584m, as depicted in The Figure 6.5.

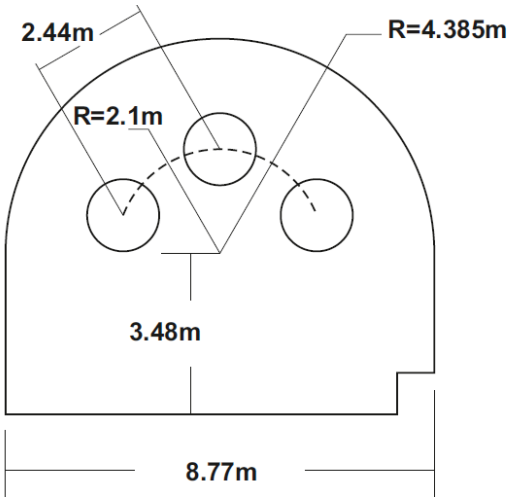

Figure 6.3. The position of each group of Jet Fans in the Memorial Tunnel's cross-sectional area.

As stated, the smoke backlayering length is clearly illustrated by the temperature fields. It is also apparent that a time delay can be traced between the experimental and numerical results, regarding the development of the fire growth and airflow conditions inside the tunnel, as depicted in Figure 6.1. This temporal displacement, illustrated in the results, is efficiently determined at the beginning of the experimental procedures. In the actual experiment, the temperatures upstream from the fire source rise instantly, reaching rapidly excessive values. In the numerical simulations, the fire does not produce a considerable amount of heat for at least 60 seconds. As it regards the developed temperature distribution in the actual experiment, over the first 2 minutes of elapsed experimental time, the mean measured temperature, 15m upstream of the fire source, reaches values of about 1000℃ beneath the ceiling, whereas at distance of 100m on the upstream route, the average temperature is obtained around 400℃, at the time. The respective numerical results do not comply with this sharp and rapid increase in temperature, regardless the existing time delay. It is shown that the fire growth stage is developing in a less abrupt way, attaining lower temperatures at the same time. In fact, the predicted temperature, 15m upstream from the fire source, begins to gradually rise at 60s but as soon as the HRR reaches its nominal value the computed temperatures remain almost constant, to a considerably lower value at each cross-sectional position, respectively. This phenomenon is owned to the fact that the smoke continues to propagate upstream from the fire source, in the numerical simulation, even though a steady

longitudinal ventilation velocity is applied. On the contrary, downstream from the fire source FDS results agree well with the obtained experimental data, regarding the estimated temperature profiles.

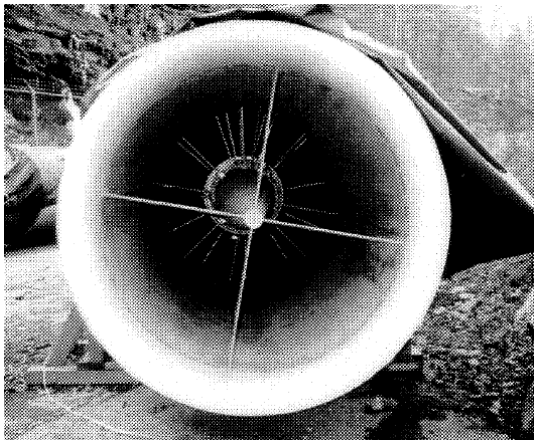

Figure 6.4. View of the Jet Fans utilized in the Memorial Tunnel Ventilation Test Program.

A fundamental difference between experimental and numerical findings, is also spotted at the temperature profiles, at the downstream route from the fire. The temperature distribution at each cross section indicates two distinctive layers of the flow, based on the data obtained from the actual experiment. At the upper section it is identified a uniform layer of hot smoke while at lower heights fresh air consists the dominant component of the flow, as proven by the degraded temperatures at those positions. In the numerical simulations the smoke flow is mainly merged with the fresh air resulting in poorly stratified flow. The above observation regarding the developed flow field at the downstream area is illustrated in a distinctive way at Loop 304. The predicted temperatures by FDS, at cross-sectional heights above 2.4m, vary under the same order of magnitude, ranging from 380℃ to 460℃. On the contrary, in the actual experiment, it is observed that at the upper cross-section, above 5.7m, the temperatures vary between 700℃ to 800℃ whereas at lower cross-sectional heights, for example 2.4m above the floor, the main temperature is measured around 500℃. This differences in the temperature distribution, observed in the numerical simulation, are owned to the decomposition of the stratified smoke layer, as stated, due to the forced ventilation. Accordingly, the same tendency is identified at the rest of the tunnel's length, downstream from the fire.

As it regards the prevailing ventilation velocities within the tunnel in the actual experiment, it is evidently shown that the applied air flow is successfully directing the air and smoke existing throughout the entire cross-sectional area of the tunnel, at the upstream side, towards the south end, in a uniform way. This is clearly illustrated by the fact that the magnitude of the resulting ventilation velocity does not alter significantly as the cross-sectional height increases, throughout the entire tunnel's length. Accordingly, in the numerical results, the smoke back layering flow propagation with time is depicted as well, in velocity figure at Figure 6.1. The developed velocity fields at lower cross-sectional heights, at the upstream side of the fire, are effectively directing the hot smoke towards the North end, as intended. However, the applied ventilation strategy, with the specific volume flow delivered from the Jet Fans, does not prove sufficient enough, at higher heights, allowing the movement of toxic gases, emitted from the fire, to the upstream side, as well. At the downstream side from the fire, the ventilation velocities at all cross-sectional heights are significantly higher than the respective ones upstream. Towards the South portal, downstream from the fire, it is clearly shown that the ventilation velocity rises abruptly after the activation of

the jet fans, in the numerical simulation. However, after approximately 8 minutes of computed simulation time, the ventilation velocity gradually degrades and become steady complying qualitatively with the steady air flow velocities produced from the jet fans. The exception to this observation is traced at Loop 304, 15m downstream the fire source, where the predicted ventilation velocities vary significantly with the cross- sectional height, affected in a major way, by the thermally driven buoyancy forces from the fire.

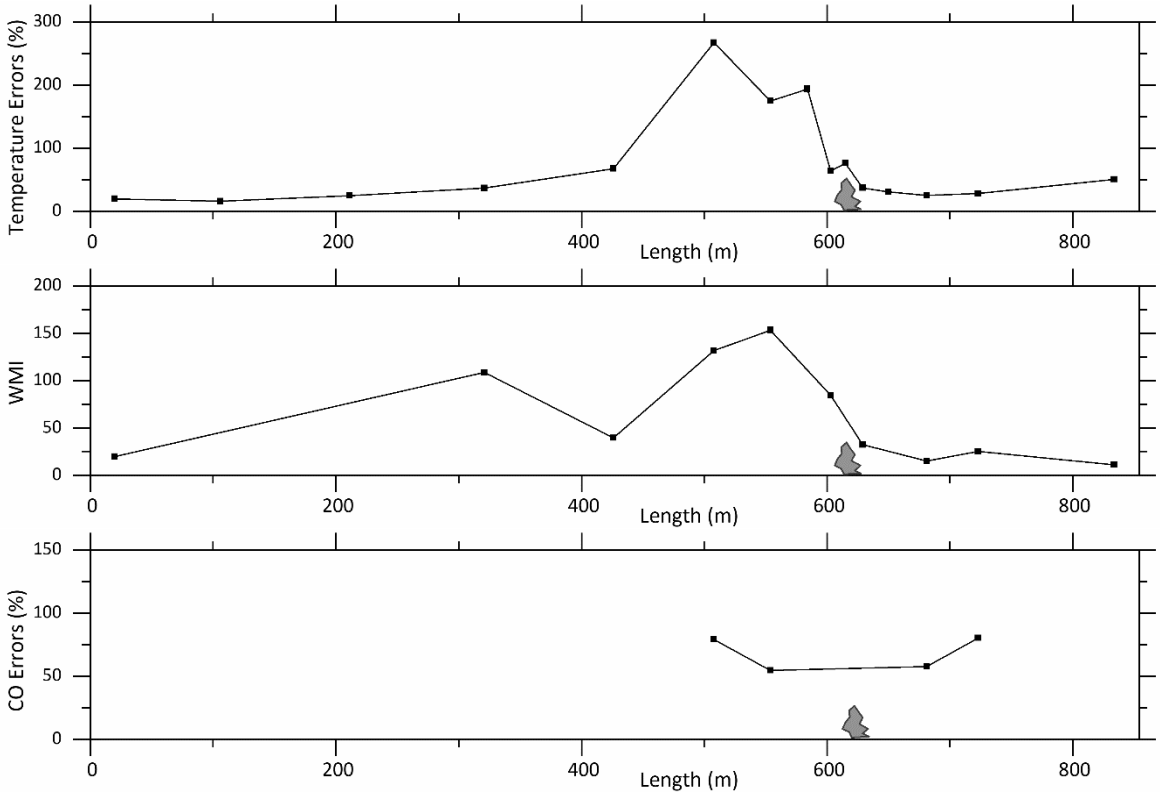

Figure 6.5. Overview of the mean numerical errors of temperature, the weighted magnitude indexes of velocity, and errors of CO concentration, throughout the entire tunnel length, during the entire test period.

FDS greatly underpredicts the CO concentration both upstream and downstream from the fire source, as shown in Figure 6.2. According to experimental data after the activation of jet fans, the CO concentration is progressively diminished at the upstream side from the fire source, over time. A sudden rise is observed at Loop 207, 508m from the North end, right after the activation of jet fans. More specifically, at the time interval between the ventilation flow from the jet fans in operation, reaches that station, and right before it succeeds in hindering entirely the adverse movement of toxic gases, high concentration of CO is gathered at that Loop. Given that the current measurement position, at 508m, is the closer one to the last activated groups of Jet fans, Group 3, it is reasonable that this tendency is solely noticed there. In addition, at the downstream side, the concentrations of CO evidently increase as distance towards the South end decreases. In general, FDS predictions of CO yield, comply quite well with the experimentally derived concentrations upstream from the fire source. However, the numerical model does not succeed in perceiving the steep increment of the CO concentration at Loop 207, that it is illustrated in the experimental process. At the downstream side FDS seriously underpredicts the resulting amount of CO concentration. Those discrepancies are quite justified since the employed fuel for the numerical simulation does not have the exact chemical properties of the Fuel Oil No.2, which is used in the

actual experiment, but the amount of CO produced from the fire is estimated according to the optimum results of validation Test Case 502.

In general, in Figure 6.5, the resulting numerical errors are depicted for the temperature, the velocity within the tunnel and the CO concentration, as well. The comparison among experimental and numerical results is conducted with respect to the actual measurement locations of the experiment, as presented in Table 5.1. It must be noted that the numerical error of temperature and CO production is estimated through the Equation 5.5, whereas the velocity fields errors are provided by the weighted magnitude index of the Equation 5.6. The overall value of numerical error of the temperature distribution and CO concentration within the tunnel, during the whole time period of the experiment, is around 74% and 67.8%, respectively, while the estimated WMI for the velocity profiles is amounted up to 62%. The main characteristics of the developing flow-field inside the Memorial Tunnel that have been predicted by the FDS code, are at the same order of magnitude with the experimental findings. In general, for qualitative assessment of numerical findings, one should also account for the complexity of the investigated modelled case. The challenge in simulating a fire emergency inside a tunnel, lies to the significantly extended computational domain required by the physical model in accordance with the necessity, imposed by the numerical code, of high precision at the region of the fire site to resolve in the most accurate way the fire related phenomena. Therefore, the overall results, produced by FDS, are in good agreement with the respective experimental findings.

An interesting observation constitutes the fact that while in the actual experiment, the backlayering smoke has efficiently began to withdraw at 150seconds of experimental time, the criterium for critical ventilation conditions and backlayering length is not fulfilled, at least in the conventional form. According to the latter, the value of the longitudinal ventilation velocity that it is identified as critical, corresponds to the velocity that hinders entirely the backlayering effect, from the upstream route. The importance of this design parameter lies on the fact that when critical conditions are prevailing a smoke-free emergency route is established at the upstream side of the fire for firefighting and evacuation performances. However, through the temperature and velocity time profiles, in Figure 6.1, along with the CO time yields, in Figure 6.3, it is apparent that a relatively small amount of smoke still succeeds to reach to locations far upstream from the fire, namely to the Loop 307, at 554m, from the North portal. This observation indicates that although the findings from the Memorial Tunnel Fire Ventilation Test Program establish that the backlayering effect has been effectively hinder for 100MW, under the influence of the given ventilation strategy, the emergency route at the upstream side of the fire, is not completely free of smoke. In fact, the measured temperatures of the existing smoke layer near the ceiling reaches values of 200℃, approximately 30m upwards from the fire source, for a prolonged time period of almost 9 minutes. It must be noted that this phenomenon has been observed 14 minutes after the start of the experiment when the prevailing critical longitudinal conditions have already reached steady state. The fact that a portion of smoke has remained in that terrain is well justified, since the distance between the nearest group of Jet Fans in operation to the fire source, is approximately 330m. In that extended length, even the high ventilation velocities produced from the Jet fans, cannot succeed in attaining ventilation conditions that equals the “theoretical” critical near the fire source. Concluding, it is demonstrated that the conservative definition of critical velocity regarding the backlayering length, is not always achievable, in practice, according to experimental findings.

6.2 Establishment of the Model Test Case

6.2.1 Longitudinal Ventilation Systems Implementation - General Directives

The appliance of a longitudinal ventilation system to address a fire emergency inside a tunnel has bilateral functionality. A longitudinal ventilations arrangement is designed either to deliver air at particularly high velocities in order to lead away the hot layer of smoke and toxic products from the fire creating a smoke-free area inside the tunnel or to draw smoke with the aim of accelerating its flow, to reach sooner the extraction location. Both of the above functions can be utilized in a single tunnel fire scenario depending on the location of the existing jet fans. Usually, the fans upstream from the fire are responsible for managing the smoke propagation while the fans at the downstream route, assist in preserving a strong longitudinal airflow through the end of the tunnel. The ventilation system, primarily, must produce sufficient longitudinal air velocity to hinder the backlayering of smoke, at the upstream side. The minimum air velocity necessary to entire prevent the adverse movement of smoke over possible stalled vehicles and entrapped motorists, is identified as the critical velocity, as previously stated. The management of smoke propagation via a longitudinal ventilation configuration, as shown in Figure 6.6, consists the primary objective of this unit and thereby the analysis that follows is focused on the main design parameters of such systems, based on the current legislation directions. The derived results are embedded in the modeling of a new tunnel fire case with the aim of investigating the impact of ventilation velocity on fire and flow characteristics produced by fires of different sizes.

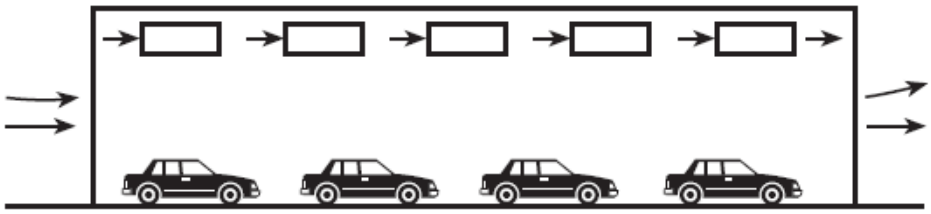

Figure 6.6. Jet fans, owning to the effects of the high-velocity discharge, stimulate a longitudinal airflow throughout the entire length of the road tunnel.

A typical layout of a jet fan, utilized in a road tunnel, is given in Figure 6.7 for reasons of better comprehension of its size and structure. The size of the Jet Fans is an important issue as it concerns the design of the ventilation system. The spare space inside the tunnel for installing such a machine or even groups of them is limited. According to the main ventilation's designs, the fans are usually placed above the vehicle traffic lanes, hanging on the tunnel ceiling or on the side tunnel walls, as depicted in Figure 6.8. A ventilation arrangement involving jet fans mounted within the tunnel consists a paramount mechanical installation in managing the longitudinal flow of the produced fire effluents. More specifically, the jet fans are designed to deliver relatively small air flow volumes at high velocities. The induced momentum is transferred to the entire tunnel length, provoking a steady airflow in the appropriate direction. The unidirectional jet fans, with asymmetrical blades, are designed to provide an optimum performance in one direction (forward), whereas there are also the fully reversible jet fans, equipped with symmetrical blades, which are able to accomplish the same performance in both directions (forward and reverse). In practice, the utility of jet fans is highly elevated when they are able to reverse their direction. The latter technical specification is quite handy in combating a fire emergency inside a tunnel, as it is offering the flexibility of adjustment to the applied ventilation strategy if the fire scenario necessitates so. In Figure 6.9, a primary reasoning is presented, indicating the main design process and considerations before adopting a longitudinal ventilation system in a road tunnel (Maevski, 2016).

Figure 6.7. View of a typical jet fan structure, utilized in road tunnels.

Observing Figure 6.9, it becomes apparent that certain constrains arise on the topic of the implementing a longitudinal ventilation strategy in a tunnel structure. These constrains are either originated by tunnel's geometry, type of operation, utilization or traffic flow. It should be noted that the term of traffic inside a tunnel is identified as demonstrated in Figure 6.10. Although most tunnels would necessitate a ventilation system, capable of creating a longitudinal flow, the resulting flow characteristics inside a tunnel, provoked by longitudinal ventilation arrangements are not suitable for every tunnel. For example, if a fire emergency occurs inside a bidirectional tunnel, the two distinct emergency routes on each side of the fire source, as defined theoretically- the one upstream and the one downstream- cannot exist in practice. Stationary vehicles would exist at both sides on the fire source, and therefore a ventilation system which directs the produced hot smoke from the fire to the one of both sides, would automatically create unbearable conditions for the motorists trapped at that section, jeopardizing their physical integrity. As an aftermath, arrangements that produce longitudinal ventilation are mainly appropriate for tunnels of unidirectional traffic flow. In that manner, when the longitudinal ventilation configuration would manage to control the propagation of heat and smoke at the upstream side of the fire, under the influence of critical conditions, the motorists upstream could evacuate, moving at the smoke free region of the tunnel while the drivers downstream of the fire source could reach the exit portal and escape by continuing to drive. As it regards other types of traffic flow, like tunnel of bidirectional traffic and unidirectional traffic of high congestion densities, a different type of ventilation scheme would support better their requirements. Table 6.2 constitutes general guidelines indicating the necessity of a ventilation and a fire suppression system, at unidirectional and bidirectional tunnels, depending on each tunnel's length and the potential severity of the fire accident (Maevski, 2016). In addition, Table 6.3. demonstrates the directives, presented in the Greek Presidential Decree, No.230 (2007), regarding the ventilation standards in road tunnels.

Figure 6.8. View of two different Jet Fan arrangements, inside modern tunnel structures.

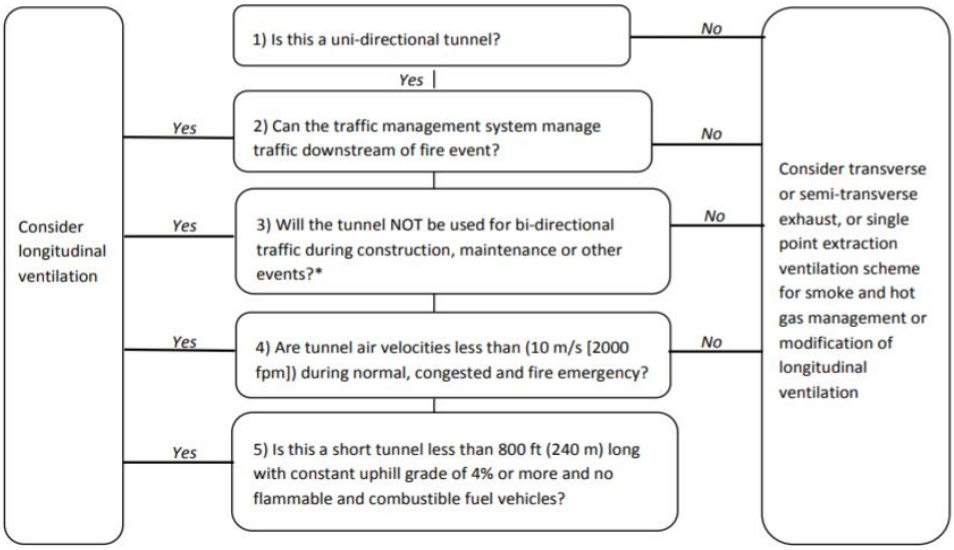

Figure 6.9. Guidelines for assessing the operational suitability of a longitudinal ventilation system inside a road tunnel (Maevski, 2016).

Functionality constrains may arise also with regard to the operational capabilities and mechanical resistance of the involving technical installations of the mechanical ventilation system. The technical specifications of the jet fans signify the maximum temperatures that their material can withstand for a certain time period. Jet fans mounted within a tunnel are subject to elevated temperatures during a fire incident. Jet fans are typically designed to endure temperatures of approximately 250°C for at least one hour. Other, more robust designs necessitate jet fans to withstand temperatures of 400°C for more than two hours and not to be disintegrated during the firefighting procedures. Depending on the size of the fire and its spread, the tunnel's geometry and the distribution or scheme of the ventilation arrangements inside the tunnel, the fans at a certain distance from the fire site are in jeopardy of being damaged. According to the experimental results of Memorial Tunnel (Bechtel /Parsons Brinckerhoff 1995), reference values of the prevailing temperatures at the 7th Group of Jet fans, which was the one closer to the fire at the downstream side, along with the jet fan temperatures bearings are presented at the Table 6.4. In the Table 6.5, the estimated distances at which the jet fans are presumed to be destroyed at a tunnel fire emergency, depending on the fire size, are displayed, as reported by the British Standards (Hall, 2006). Additionally, in cases of excessively large fires, up to 300MW, these installations can be utterly damaged over a distance of up to 300 m on the downstream route of the fire. The likelihood of such fire events should be considered in the design of fire safety analysis inside a tunnel. The design of any ventilation system shall incorporate fan redundancy automatically when the fan is directly imperiled by the fire. The fan damage can be significantly diminished with the installation of a fixed fire suppression system in the tunnel. For that cause in Table 6.2, the presence of Fire Suppression Systems is deemed necessary, for tunnel lengths up to 1000m or up to 300m when both HGV and vehicles with FLC are involved in the traffic flow of the particular tunnel. The failure of the Jet Fans due to the exposure to high temperatures, should be accounted for under all circumstances. In fact, the remaining jet fans, which are capable of operating under the prevailing temperature conditions, ought to introduce into the airflow the designed ventilation velocities, fitting to the fire event, even though the ventilation system cannot operate according to its full potential mode.

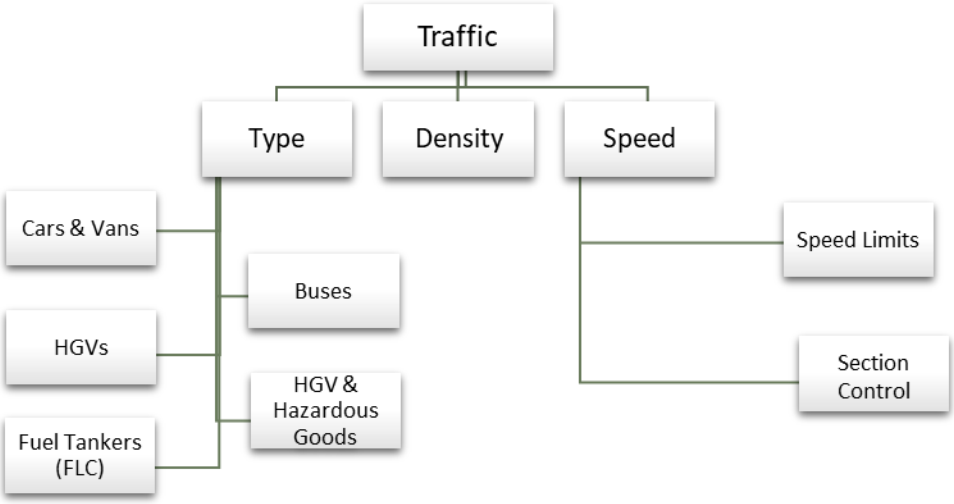

Figure 6.10. The definition of traffic as interpreted in tunnel fire Safety analysis.

The effectiveness of a jet fan system inside the tunnel is also influenced by the spacing of the jet fans in both the longitudinal and the transverse direction. According to the design directives the jet fans shall not be set up too close to one another. The main reason for this instruction lies to the fact that installing the jet fans at a sufficient distance from each other permit the fashion of an approximately uniform and steady airflow profile, without the exhaust air of the first fan affecting directly the flow characteristics at the inlet of the next one. The recommended longitudinal distance between two groups of jet fans, must at least equal to the value of tunnel hydraulic diameter multiplied by the factor of 7 to 10 or sometimes the interval length is specified to extend 100 fan diameters, based on the selected Jet fan (Maevski, 2016). In that manner, the function of the prior jet fan does not disrupt the performance of the following one while a specific longitudinal air velocity still prevails within the tunnel. Additionally, the transverse installation of jet fans to close to each other could highly affect their performance, too. In the view of that the interval distance between two jet fans, belonging to the same "cross-sectional" group, should exceed, from centerline to centerline, the computed length of 2 fan diameters. In this manner they can be identified as a single jet fan of equivalent cross-sectional area for the ventilation design parameter.

Table 6.2. General assessment of the fire safety necessities regarding Ventilation (V) and fire Suppression systems (FS) based on the tunnel length and traffic conditions by Maevski, 2016. The parameters in the brackets refer to optional measures while the rest indicate mandatory appliance.

Tunnel Length	**Unidirectional Traffic Flow**			**Bidirectional Traffic Flow**		
	HGV & FLC	HGV & NO FLC	NO HGV & NO FLC	HGV & FLC	HGV & NO FLC	NO HGV & NO FLC
<90m		-			-	
90-240m	V (FS)	(V)	-	V (FS)	(V)	(V)
240- 305m	V (FS)	(V)	(V)	V ; FS	V (FS)	(V)
305-1000m	V ; FS	V (FS)	(V)	V ; FS	V (FS)	(V)
>1000m	V ; FS	V ; FS	(V)	V ; FS	V ; FS	(V)

A longitudinal ventilation system employing jet fans is highly effective in managing the backlayering effect, as known. However, one important issue arises as it regards the flow condition at both the upstream and the downstream side of the fire. When the jet fans turn on, the high discharge air velocities disrupt the existing thermally stratified smoke layer produced from the fire at both the upstream and the downstream side of the fire. Especially at the upstream side, an important consideration in the selection of a certain volume flow capacity emerges on whether this tactic facilitates the evacuation procedures on terms of stratification of the smoke. As known, the latter phenomenon is directly linked with the tenability conditions inside the tunnel. As is apparent from this observation, the pursued objectives of altering the smoke flow while preserving its stratification negate one another. For that cause, different longitudinal ventilation strategies, with contractionary aims, are utilized in practice, in tunnels worldwide. In most cases, the discharged ventilation velocities from the jet fans are high enough, opting to accelerate the prevailing flow adequately for the backlayering effect to be entirely prevented. However, in that manner, when the ventilation velocity equals the critical one or more importantly when it exceeds by far the critical value, the existing smoke both upstream and downstream of the fire is significantly diluted. It is apparent that a grave risk emerges for people trapped both in the upstream and downstream region from the fire when smoke stratification entirely disappears. Therefore, the distraction of the stratified layer of smoke does not act in favor of the tenability conditions inside the tunnel, and it sought be avoided as far as possible. This is the main cause, alternative longitudinal ventilation strategies have been fashioned, opting to reduce the propagation of smoke instead of eliminating it entirely, with implied flow velocities below the critical values, to preserve the smoke stratification. In addition, operating jet fans close to the fire is often ill-advised as the phenomenon of air recirculation usually exists at the jet fan locations. Thereby, it is recommended to the tunnel's operator not to activate the jet fans near the fire source, at least, at first at the fire growth phase as the recirculation could disrupt stratification and draw smoke and hot fire products in the opposite direction of the one originally intended. IN general, activating the fans which locate furthest away from the fire site will contribute both in accelerating the airflow inside the tunnel, in total, without greatly diminishing the tenability condition due to dilute stratification.

Table 6.3 Directives for the mechanical ventilation's necessity in tunnels, derived from the Greek Legislation, based on the tunnel length and traffic conditions. The indication of "Optional*" signifies that the applied system is optional for unidirectional tunnels but mandatory for bidirectional ones. (ΕΦΗΜΕΡΙΣ ΤΗΣ ΚΥΒΕΡΝΗΣΕΩΣ ΤΗΣ ΕΛΛΗΝΙΚΗΣ ΔΗΜΟΚΡΑΤΙΑΣ)

Tunnel Length	**Traffic Flow <2000 Vehicles**	**Traffic Flow >2000 Vehicles**
	Mechanical Ventilation	
<500m	-	-
500-1000m	Optional	Optional
1000-3000m	Optional	Mandatory
>3000m	Optional	Mandatory
	Special features for (semi)transverse ventilation	
<500m	-	-
500-1000m	Optional*	Optional*
1000-3000m	Optional*	Optional*
>3000m	Optional*	Mandatory

It is well known that the liabilities of every ventilation systems are mainly dictated by the need of maintaining acceptable conditions within the tunnel, in general. In a fire incident, the synchronization between the activation of the fans and the onset of the fire is a matter of key importance. Experimental results indicate that the time interval between the beginning of a fire and fan activation should be diminished, as possible, since produced layer of hot smoke tend to rapidly propagate during the initial 2 minutes. For that cause, the current legislative directives advocate that the emergency ventilation system shall be capable of reaching its full operational mode within a maximum of 180 seconds (Maevski, 2016).

Table 6.4. Maximum air temperatures measured at the 7th Group of Jet Fans, during the Memorial Tunnel Fire Ventilation Test Program.

Fire Size (HRR)	Temperatures at the 7th Jet Fan Group	Motor Bearings	Motor Winding
20MW	204℃	114℃	106℃
50MW	334℃	178℃	138℃
100MW	677℃	Sensor Failed	198℃

Another consideration that addresses the issue of motorist's safety at a tunnel fire event, under the influence of longitudinal ventilation, regards the resulting velocities within the tunnel. It is mentioned significantly that at fire of nominal size of about 30 MW, the existing velocity downstream from its site is augmented by a factor of 2 to 3 compared to the respective velocity at the upstream side (Maevski, 2016). Therefore, this leads to velocities that enhance smoke spreading and scattering, jeopardizing any attempt of self-rescue downstream of the fire location. When strong longitudinal ventilation is added on in a fire event, it may result in exposing motorists to air velocities that are excessively high. Therefore, a significant increase in the imposed ventilation velocity may increase the downstream ventilation at such level, to which the ability of people's walking against this airstream would be unattainable. According to the aftermaths of the effects actual fires, it occurs that motorists under emergency conditions can tolerate ventilation rates at the upper limit of 11m/s. For that cause, the air velocities in total, inside the tunnel are intended to be less than 10m/s, during normal, congested and fire emergency situations, as reported in Figure 6.9, as a precautionary measure. This ventilation philosophy augments the necessity of estimating precisely the critical ventilation conditions, in a fire event and the importance of applying a longitudinal ventilation system only in a unidirectional traffic tunnel.

Table 6.5. Estimated distances at which the jet fans are presumed to be destroyed at a tunnel fire emergency, depending on the fire size (Maevski, 2016).

Fire Size (HRR)	Distance Upstream of the Fire	Distance Downstream of the Fire
5MW	-	-
20MW	10m	40m
50MW	20m	80m
100MW	30m	120m

6.2.2 Description of the Model Test Case

The model tunnel is also a two-lane, 854m long tunnel with unidirectional traffic flow. The width of the tunnel is 9m and the center-line height, 8m. No longitudinal slope has been assigned to the numerical model in order to investigate the main fire and flow characteristics under the sole influence of the induced fire size and ventilation system. It is well known that an inclined tunnel structure would automatically give rise to strong buoyancy forces due to the pressure differences at the portals, and therefore the main flow characteristics within the tunnel would be significantly affected. Attempting to ensure numerical findings of ubiquitous appeal, a model case fire scenario has been created of a particularly simplified nature. In other words, specific parameters which significantly alter from one fire scenario to another, like the existing obstacles near the fire, are deliberately avoided, and for that cause, there is no existing traffic inside the modeled tunnel.

Figure 6.11. Model Tunnel layout. The blue boxes represent each group of Jet Fans.

The ability of tunnels to function properly, providing the requisite degree of safety to its users in a fire event, relies mostly on the effectiveness and reliability of its ventilation system. Therefore, a tunnel longitudinal ventilation system should consist of robust and thermally resilient mechanical fans. The number of fans installed shall meet the specifications or even exceed in total, the minimum number of fans ruled by them. Only in that manner the success of the post-fire safety strategies is guaranteed. In the current case, the longitudinal ventilation is accomplished by the implementation 24 reversible axial flow jet fans, as shown in Figure 6.11. The jet fans mounted within the tunnel, in groups of three, nearly equally spaced along the tunnel length, conforming to the requirements of jet fans longitudinal and transverse spacing. The exact longitudinal position of each group of jet fans is presented in Table 6.6, where the assigned distances are measures from the Left Portal. The design ventilation strategy involving the installed jet fans is derived from the Memorial Tunnel Test Program. The groups have been arranged in a triangular arrangement, as depicted in Figure 6.3. For the sake of completeness, an indication of jet fans technical specification is entailed. Each fan is equipped with a 56kW motor, rated to deliver a maximum volume flow 43 m^3/s at an exit velocity of 34.2 m/s. It should be noted that the fire source location is between the 6th and 7th group of fans, at 615.4m from the left portal. At the following section, the main assessments regarding the numerical model are presented.

Table 6.6. Overview of the longitudinal positions of the jet fans.

Jet Fan Group	Distance from North Portal (m)
Group 1 – [JF1 to JF3]	95
Group 2 – [JF4 to JF6]	190
Group 3 – [JF7 to JF9]	285
Group 4 – [JF10 to JF12]	379
Group 5 – [JF13 to JF15]	474
Group 6 – [JF16 to JF18]	569
Group 7 – [JF19 to JF21]	664
Group 8 – [JF22 to JF24]	758

According to the Jet Fan mechanical endurance to high temperatures, as reported in the sub-Unit 6.2.1 and the estimated distances at which these devices are presumed to be destroyed

at a tunnel fire emergency depending on the fire size, it is selected for the current investigated case that the 7th Group of Jet fans to be out of operation. A preliminary study has been conducted regarded whether or not the 8th group located near the right portal, downstream from the fire source, should operate in the simulations, too. The decision has been made, based on the worst-case scenario, investigated in the current survey. More specifically, the trial simulation regards the development of a 100MW fire, under the influence of critical conditions. In that case, the whole amount of the produced smoke is directed entirely to the downstream side, towards the right portal, provoking the least favorable temperature distribution at this section. Based on the numerical results, the resulting temperatures at the 8th group of Jet Fans are below 400℃. It is reminded that the minimum temperature limit that a robust Jet Fan ought to withstand for at least 2 hours is specified at 400℃. So, the proper functionality of the 8th group downstream from the fire source, is not at risk of been compromised and thereby its utilization is allowed in the simulations. In Figure 6.12, the trial case results are significantly presented at two different snapshots, at which the established longitudinal velocity within the tunnel, after the activation of Jet fans, has been stabilized. The results clearly reveal that the 8th group of Jet Fans is not at risk of thermal damage. It is noted that in the illustrated simulation, the 8th group of Jet Fans, is activated.

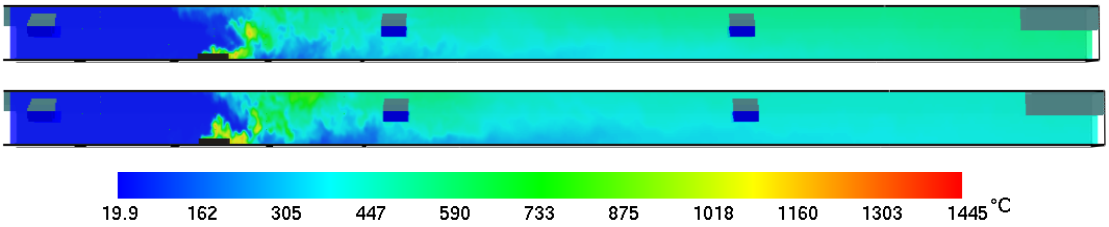

Figure 6.12. Snapshots of temperature distribution from a fire of 100MW, at 800s and 900s. The depicted part of the Tunnel extends from 560m to the 834m (end of the Tunnel).

Based on the former analysis regarding Jet Fans longitudinal spacing, the resulting airflow velocities imposed from the utilized jet fans, are presented in Figure 6.13. Figure 6.13 illustrates the developed flow in terms of velocity between two groups of jet fans, as established in a non-fire scenario. The absence of fire has been selected as the main objective of this survey focuses on the resulting airflow from the fans, without involving the thermally induced alteration to the flow, provoked by a fire event. The specified volume flow to the Jet Fans equals the maximum possible flow capacity that the selected fans can deliver which is in the order of 43m^3/s. In all simulations, it is intended that the specified volume capacity of each jet fans does not affect the ventilation field of the following one, in view of a better performance. As derived by the contour slices in Figure 6.13, the produced jet stream of the preceding fan has fully decayed before being drawn into the inlet side of the next fan, for the maximum jet fan volume flow. The latter is applied in all of three fans that consist each group. In that way for volume flow capacities equal or less than 43m^3/s, the induced airflow stream guarantees jet fans yield maximum efficiency to the current ventilation arrangement.

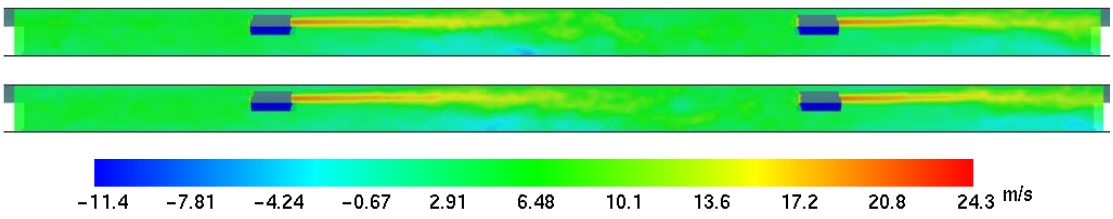

Figure 6.13. Snapshots of Air Velocity distribution, under the influence of 43m^3/s volume flow capacity delivered by each Jet Fan, at 600s and 800s.

When building a numerical case at which a mechanical ventilation configuration is incorporated, one should also account for the delay in activating the system owned to response time of the tunnel's operator. Based on the respective legislation for fire emergencies in tunnel structures, the ventilation system ought to reach the maximum capacity within the first 180s, since the fire broke out. In addition, given Figure 5.8 of the experimental HRR development over time, at Test 615b, it is apparent that the fire reaches its maximum potential size, in an actual fire scenario, 180s at least after the ignition. In that manner, in a numerical simulation, it is reasonable for a mechanical system to be activated from the start when a steady fire of 100MW is induced in the simulation since the beginning. In that manner it is feasible to reduce the required computation time without affecting the circumstances of fire development and ventilation operation, occurring in an actual tunnel fire emergency.

In simulations, the fire source dimensions have been specified as of 7.5m(L) x 6.0m(W) x 1.0m(H). The fire source has been set to the centerline of the tunnel, at distance of 615.4m from the left portal while the utilized fuel is N-Heptane. The main modelling parameters for the modeled tunnel fire scenario, has been designed based on prior optimum findings of the Test Case 502. In Table 6.7 the main numerical parameters have been summarized, including the simulation mode, mesh resolution, concentrations of emitted products, the amount of heat radiated from the fire source and the roughness applied on the tunnel's walls. The only alteration on these key parameters, compared to the optimum ones, is recorded at the simulation mode. The VLES model has been employed instead of the LES, in the aim of reducing the computational time required. As established in Figure 5.40, both the LES and VLES models improve the fidelity of the numerical results, for a mesh resolution of 0.25m grid size, near the fire. The main difference between those models, for the implied mesh, lies on the field of optimization. LES mode evidently enhances the numerical results regarding temperature distribution inside the tunnel whereas the VLES mode significantly improves the predicted ventilation conditions. However, the resulting temperature and velocity distributions within a tunnel, are inextricably linked parameters and therefore, as proven before, the considerable enhancement of one of them, automatically leads to the enhancement of the other, as well, up to a certain level.

Table 6.7. Review of the key modelling parameters of the New Case.

Case Name	**Turbulence Model**	**Gride Size (m)**	**CO Yield (kg/kg)**	**Soot Yield (kg/kg)**	**Radiative Fraction**	**Roughness (m)**
New Case	VLES	0.25 - 0.50	0.032	0.062	0.35	0.25

In the current investigated case, the main pursued objective is to avoid the backlayering effect of smoke at the upstream side of the fire, towards the left portal. This shall be carried out by the implementation of sufficient longitudinal air velocity at the same direction as the speculative traffic flow. The assumed direction of the traffic flow, which will not be presented at the current series of simulations, is selected at random from and the left portal to the right one, to resemble the fire scenario 615b of the Memorial Tunnel Test Program. The current case presents a simplified example of a fire emergency inside an average sized tunnel structure and a potential design of longitudinal ventilation for firefighting strategies.

6.3 Parametric Studies

The specification of the critical ventilation velocity is the main objective of the current sequel of numerical tests. The key details of each simulation of the parametric study, namely the fire size, the Jet Fans volume flow capacity as well as the resulting ventilation velocity right before the fire, are presented in Table 6.8. In addition, the Table 6.8 also entails the evaluation of whether or not the preventing of the backlayering is achieved, under the influence of the respective ventilation and fire conditions. In particular, different values of volume flow have been assigned to the activated Jet Fans in order to avoid the backlayering phenomenon within the tunnel, for fires of varying sizes. Prior to that, a series of test have been conducted without the employment a longitudinal ventilation system, with the aim of assessing the flow conditions within the tunnel under the sole influence of the ongoing fire *(Case I-III)*. Then, with the implementation of the Jet fans, it is intended to determine the sufficient longitudinal airflow, corresponding to the critical ventilation conditions for each fire size. According to the literature review in the sub-Unit 2.2.1, the typical values for critical velocity are in the range of 2.0 to 3.8 m/s, for fire sizes of 20, 50 & 100MW. The need to derive via numerical simulations the exact value of ventilation velocity, sufficient to prevent any upstream movement of smoke along the tunnel, will greatly contribute to increase the confidence in the employment of computational Codes for fire safety analysis inside road tunnels.

Table 6.8. Overview of the parametric study main details.

Case Name	Fire Size HRR (MW)	Jet Fans Airflow Q_{JF} (m^3/s)	Ventilation Velocity Upstream from the Fire Source, at 610m (m/s)	Success in preventing Backlayering? (YES/NO)
Without a Longitudinal Ventilation System				
Case I	20	0	-0.27	NO
Case II	50	0	-0.70	NO
Case III	100	0	-1.15	NO
Jet Fan System in Operation				
Case IV	20	20.35	2.27	NO
Case V	20	22.53	2.62	NO
Case VI	20	23.40	2.74	YES
Case VII	50	25.84	2.69	NO
Case VIII	50	27.69	2.98	NO
Case IX	50	28.33	3.08	YES
Case X	100	27.65	2.43	NO
Case XI	100	29.56	2.77	NO
Case XII	100	31.45	3.08	YES

6.3.1 Heat release rate

One of the objectives of this parametric study is to investigate the developing flow characteristics after the onset of a fire of certain HRR, at an 854m tunnel without a longitudinal ventilation system. Evaluating the magnitude of a fire event, in terms of smoke propagation under natural ventilation, offers fundament knowledge regarding the severity of

the incident while establishing a benchmark for measuring progress at the upcoming simulations with forced ventilation. In the current parametric study, three different fires sizes of 20, 50 and 100MW have been tested, consisting the numerical *Cases I to III.* The corresponding fuel surface area of every fire source is 45m^2, leading to a HRRPUA of 2,222.2, 1,111.1 and 444.4 kW/m^2 for a fire size of 100, 50 and 20MW, respectively. The nominal thermal power assigned to the fire as well as the type of fuel employed, does not alter through this sequence of numerical tests. Figure 6.15 gives at three different times, the tunnel centerline plane contours of the produced smoke, under natural ventilation conditions (OPEN boundary conditions) as produced from heat release rates of 20, 50 and 100MW.

The HRR values assigned to the fire source in the numerical simulation, correspond to the actual fires sizes, as reported in real fire incidents and large-scale experiments. The fire load in a tunnel fire event is mainly determined by the type of the burning vehicle. Therefore, for the design of the modelled fire size (heat release rate), typical values have been utilized with respect to information from various guidelines (PIARC,1999; BD 78/99,1999; NFPA 502, 2011). According to standards for road tunnel the equivalent types of vehicles to the specified HRR values are presented in Figure 6.14 (NFPA 502, 2011).

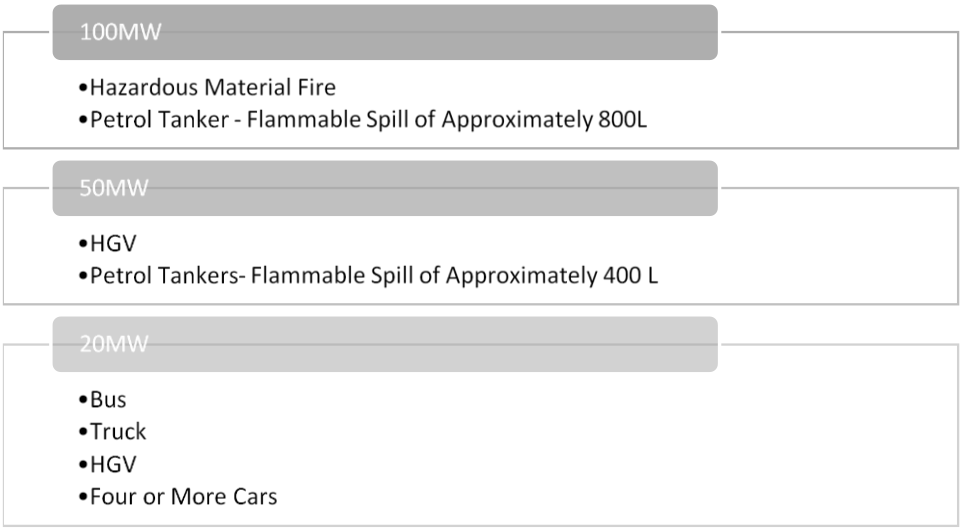

Figure 6.14 Heat Release Rates produced from various types of burning vehicles (NFPA 502, 2011).

6.3.2 Ventilation velocity

The prime concern in a longitudinal system is selecting the ventilation airflow capacity for the critical conditions required. The critical flow conditions are commonly expressed in terms of a specific ventilation velocity, which is generally estimated as the average velocity across the tunnel cross-sectional area. It is a well-known, that thermal effects originated from the fire significantly influence tunnel airflow compared to a non-fire situation. The magnitude of impact is directly linked with the size of the imposed fire. For that cause, in order to create the ventilation conditions which, correspond to a certain value of longitudinal velocity for different fires, different volume flow must be implied to the jet fans. For example, the volume flow, delivered from the jet fans, corresponding to the air velocity of 3.08m/s, for a 100MW fire exceeds its respective value for a fire of 50MW, as depicted in Table 6.8. Alternatively, assuming that the jet fans deliver the same volume flow, a greater number of ventilation devices would be required to generate the same magnitude flow for 100MW fire, compared to the number of fans required for a fire of 50MW. This is an important consideration in the design of any longitudinal ventilation system.

The magnitude of the smoke produced, Figures 6.16 to 6.18, increasing the fire size clearly signifies the importance of the implementation of a longitudinal system. In the view of that, various values of volume flow produced from the fans, have been tested in the current numerical survey for each fire size in order to investigate the numerically derived critical velocity. At the same time the capability of managing the smoke and high temperatures from each fire is evaluated, in general, for the applied arrangement of the Jet Fans ventilation system. According to the conventional definition of critical conditions the corresponding velocity of longitudinal ventilation is regarded as the critical velocity when the back-layering length drops to zero. Nevertheless, in practice, it is unattainable to control the ventilation velocity to make the back-layering length of smoke drop exactly to zero due to the pulsation of the airflow and effect of environmental wind. That fact does not imply that the resulting ventilation velocity is insufficient as long as further propagation of smoke to the upstream direction is precluded. In the current study though, the conservative definition is abided to ensure the optimum tenability conditions at the upstream side of the fire. The numerical results for each fire size and ventilation velocity are given at three different times, via tunnel centerline plane contours of the produced smoke, under the influence of the Jet Fan System.

6.4 Simulation Results

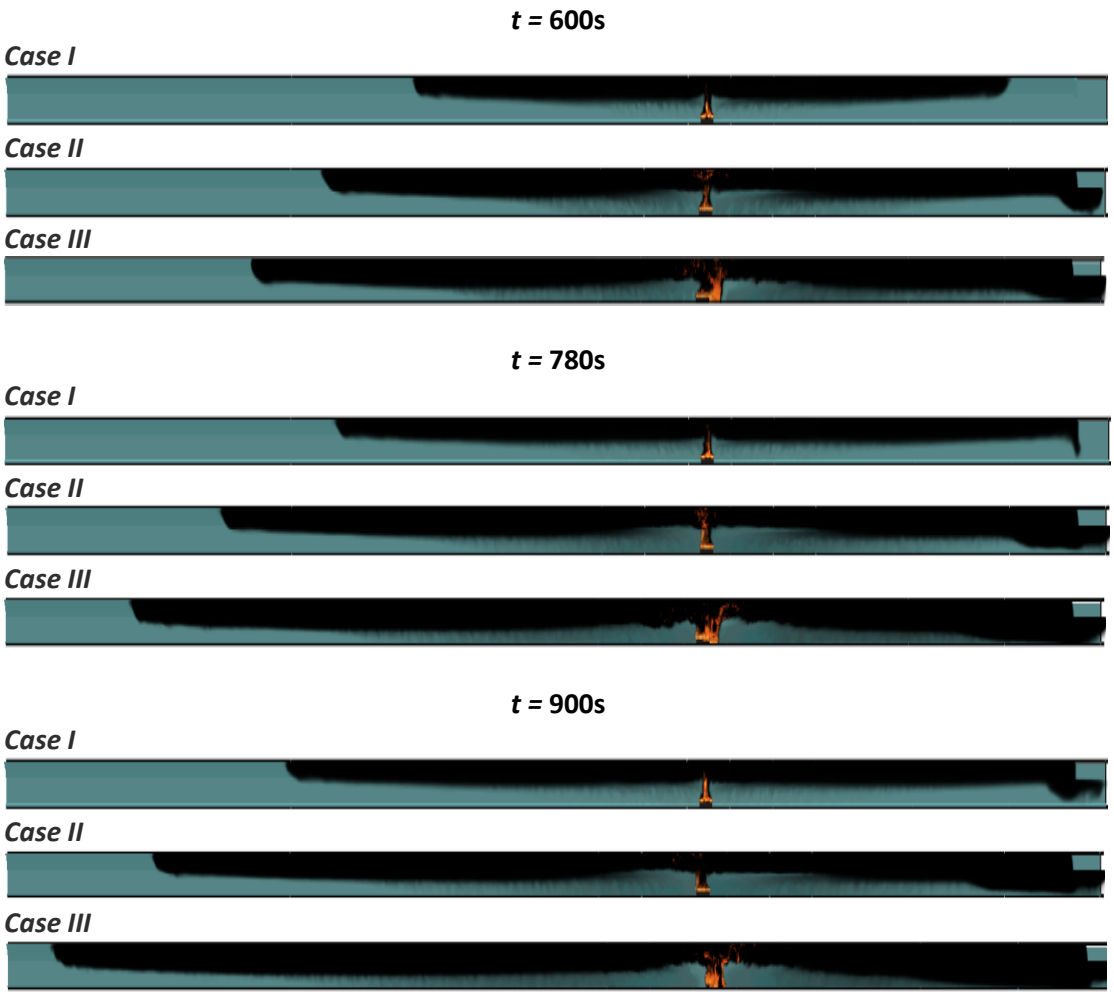

Figure 6.15. Snapshots of smoke propagation from fire of varying sizes in ascending order, along the Y axis, at 600s, 780s, 900s. The depicted part of the Tunnel, extends from 200m to the 834m (end of the Tunnel).

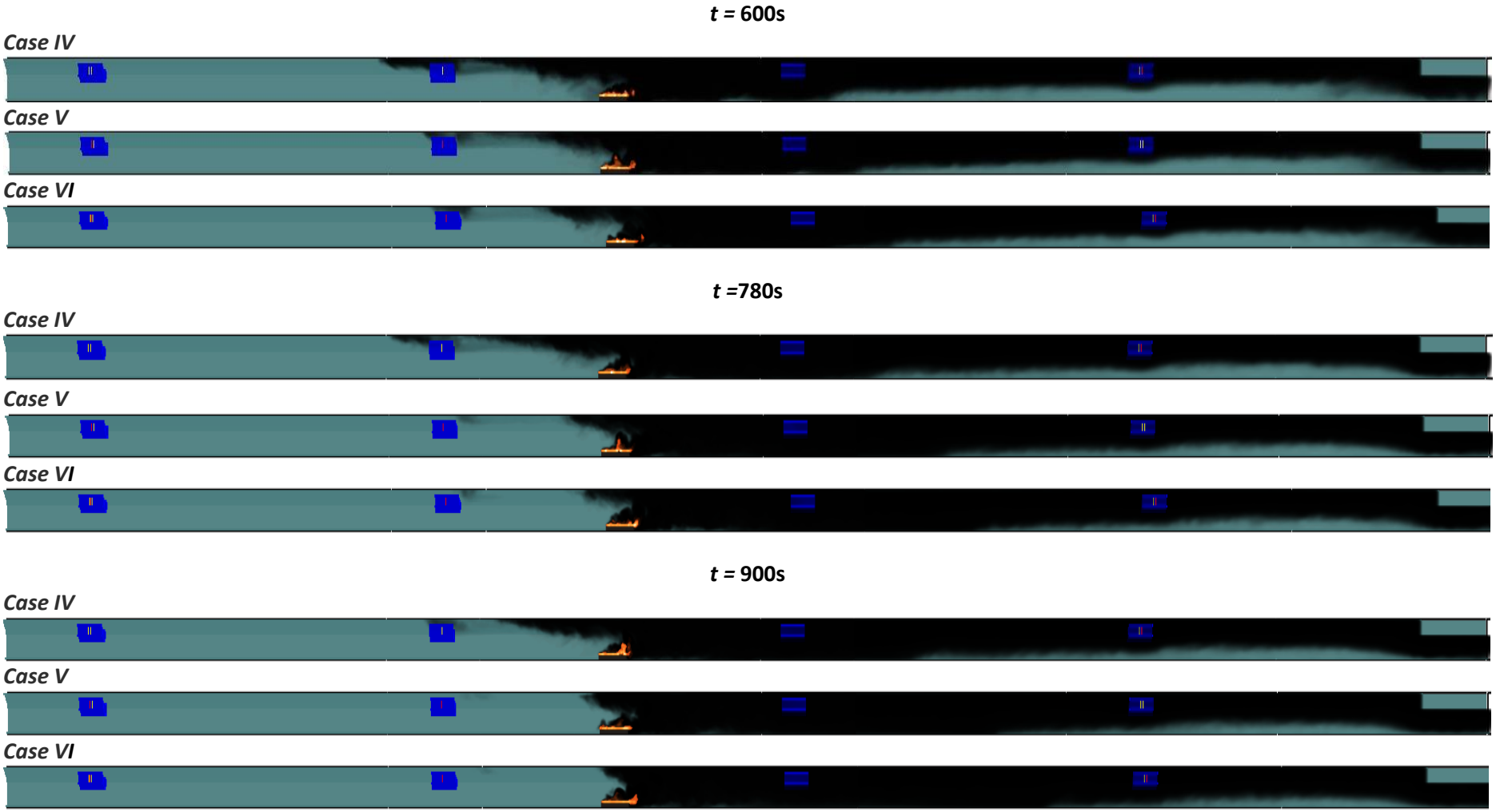

Figure 6.16. Snapshots of smoke propagation from a fire of 20MW, under the influence of varying volume flow capacities, specified at the Jet Fans, at 600s, 780s, 900s (Contour Slice at Y=0 - Tunnel Centerline). The depicted part of the Tunnel extends from 450m to the 834m (end of the Tunnel).

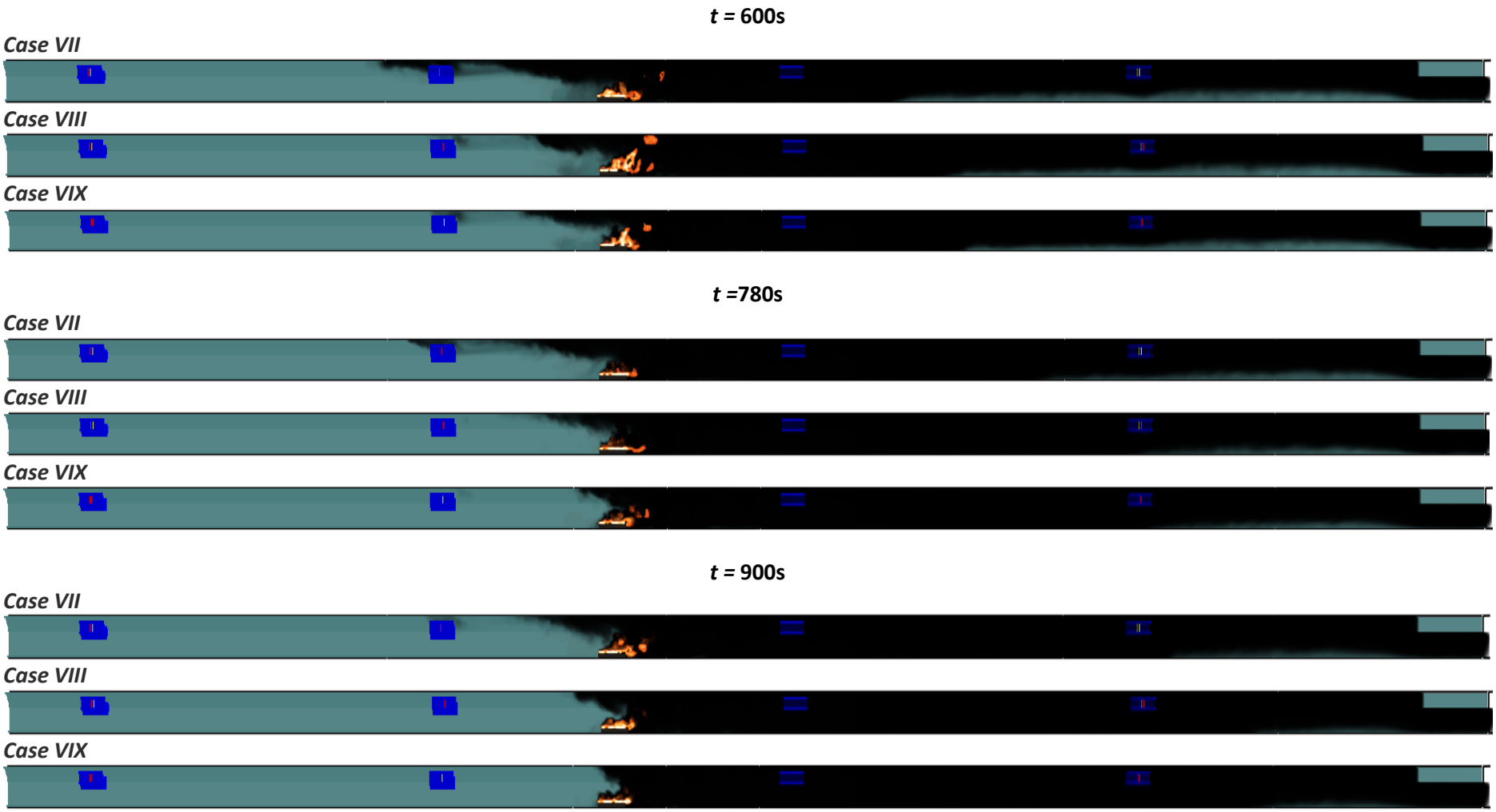

Figure 6.17. Snapshots of smoke propagation from a fire of 50MW, under the influence of varying volume flow capacities, specified at the Jet Fans, at 600s, 780s, 900s (Contour Slice at Y=0 - Tunnel Centerline). The depicted part of the Tunnel extends from 450m to the 834m (end of the Tunnel).

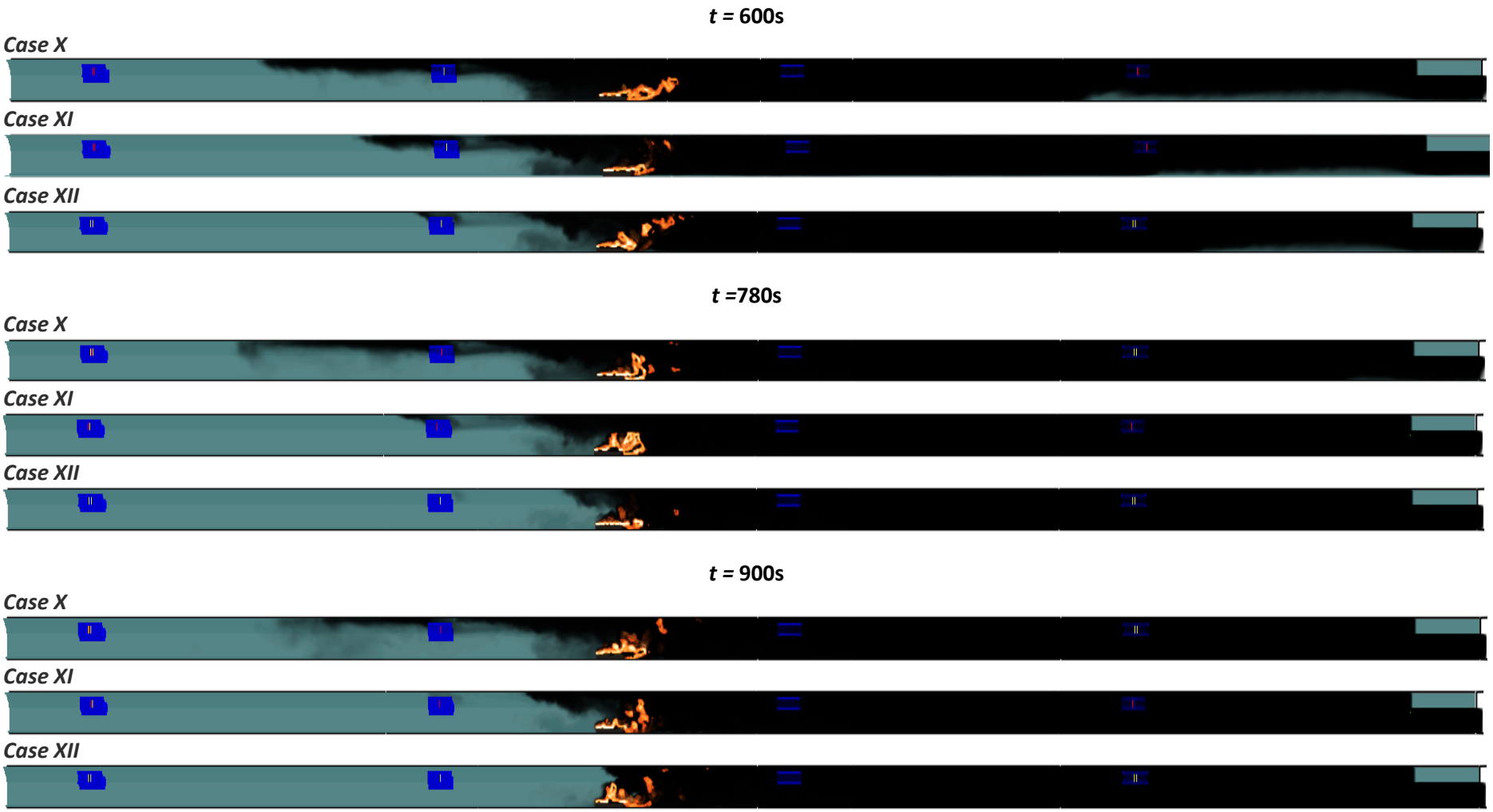

Figure 6.18. Snapshots of smoke propagation from a fire of 100MW, under the influence of varying volume flow capacities, specified at the Jet Fans, at 600s, 780s, 900s (Contour Slice at Y=0 - Tunnel Centerline). The depicted part of the Tunnel extends from 450m to the 834m (end of the Tunnel).

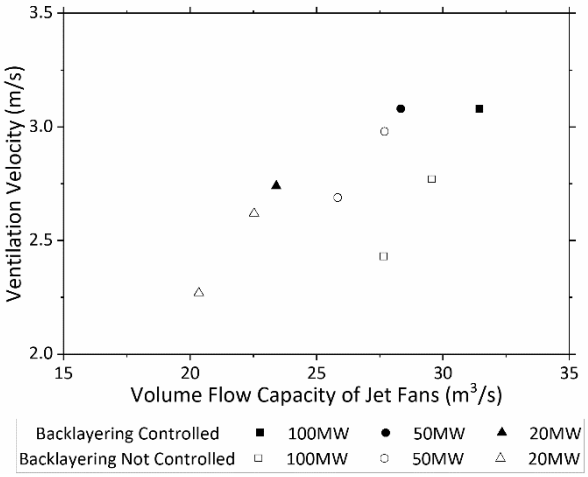

Figure 6.19. Comparison of predicted air flow velocities, depending on the volume flow capacity of the Jet fans.

For reasons of brevity, in Figures 6.16 to 6.28, a denotative number of numerical cases it is presented. Volume flows capacities in the order of 20.3 to 23.4 m^3/s, 25.8 to 28.3 m^3/s and 27.6 to 31.5 m^3/s, are illustrated for fire scenarios of 20, 50 and 100MW, respectively. Figure 6.19 illustrates the comparison of the predicted air velocities, by the FDS, highlining the values of volume flow that have been sufficient enough to create critical conditions and prevent backlayering. In Figure 6.20, a theoretical critical correlation is displayed as established by the guidelines of NFPA 502, 2011, along with the critical ventilation values for each investigated fire size, as derived by the numerical simulations' findings.

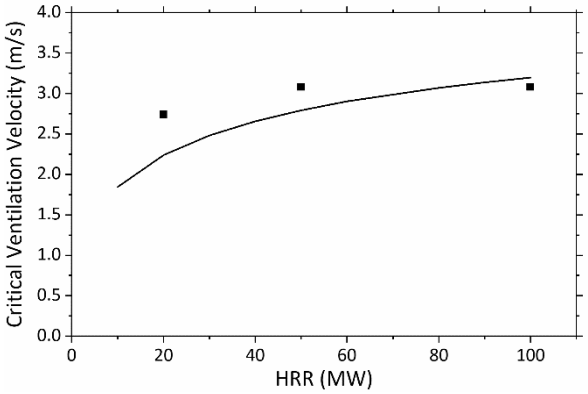

Figure 6.20. Comparison of predicted critical velocity with theoretical correlation (NFPA 502, 2011).

A volume flow capacity of 23.4m^3/s has shown to be capable of managing smoke and heat propagation resulting from heat releases equal to 20MW, creating a critical longitudinal velocity of approximately 2.75m/s. For a fire of 50MW, the required applied airflow to the Jet Fans for establishing critical conditions is 28.33 m^3/s, introducing a longitudinal velocity of 3.08m/s. Additionally for an underlying fire of 100MW, simulation results have shown that the same ventilation velocity with the one of 50MW is adequate of controlling entirely the adverse layer of smoke. This phenomenon complies well with the experimental information that the critical ventilation velocity required to hinder backlayering, remains interchangeable when the HRR exceeds a certain value. However, the required volume quantities specified at the Jet Fan system, significantly differ between these two fire scenarios, of 50 and 100MW, even though they both result in the same longitudinal velocity. As stated before, a larger volume must be delivered from the Jet Fans, for the fire of 100MW compared to the one of 50MW in order to create the same ventilation conditions. Indeed, in *Case XII* the volume flow capacity

equals to 31.45 m^3/s whereas in *Case X* the respective airflow has been in order of 28.33 m^3/s. Hence, even though there is no increase in the critical ventilation velocity beyond 50 MW, as established by the numerical simulations, yet the volume flow from the fans required to generate the resulting velocity, continues to increase with increasing fire size.

Figure 6.21. The distribution of toxic smoke at the cross sectional are of the tunnel, near the fire at 600s for a fire of 20MW and 100MW, respectively. The depicted part of the Tunnel extends from 450m to the 834m (end of the Tunnel).

In addition to highlighting how the concept of critical velocity can be beneficial for the smoke management and the maintenance of tenable conditions during a fire event, Figure 6.15 displays the soot distribution within the tunnel under natural ventilation. The hot layer of smoke at 600, 780 and 900s after the fire's onset, clearly points out the need of the adequately defined ventilation conditions. In particular increasing the fire size, growing distance away from the fire is filled with smoke. The smoke of the fire at the upstream side is extended nearly to 250m away from the fire site for a 20MW fire size and 325m for 50mW fire respectively while for a fire of 100MW, the smoke layer reaches approximately 225m from the north portal. Additionally, imposing a greater HRR, results in increasing the ratio of cross-sectional area filled with smoke to tunnel cross- sectional area, in general. Figure 6.21 clearly illustrates that the smoke-filled cross-sectional area for an 100MW fire significantly extend beyond the one of 20MW. At the later fire two distinctive layers of smoke (upper layer) and fresh air (lower layer) are established near the fire while at the fire with an HRR of 100MW, even the region above the floor is dominated by toxic pollutants.

6.5 Assessment of Empirical Correlations for Critical Velocity

A comparative study has been carried out amongst the current CFD results of the investigated tunnel fire scenario and the theoretical estimations for the critical ventilation velocity from the experimentally derived equations, presented at Unit 2.2.1. Many of those correlations have been excluded owning to the nature of their theoretical approach. For example, some equations for the critical ventilation velocity have been produced for relatively small fires, under 5MW, while their validity for larger fires has not been yet experimentally tested (Hu et al, 2008; Weng et al., 2015). In addition, there are correlations that employ the aspect ratio of a tunnel's cross section, but at those cases the resulting equations are strictly valid for either square or rectangular cross-sectional geometries (Kunsch,2002; Lee and Ryou, 2005). Correlations has been also established particularly to estimate the critical conditions for tunnel fires where there are vehicles or large objects near the fire (Lee and Tsai, 2012; Tang et al., 2013; Jiang et al., 2018b) or at cases where the tunnel structure its distinguished by a particular longitudinal inclination (Yi et al., 2014). In that manner, the previously- mentioned correlations do not collide with the purposes of the current comparative study and thereby they are omitted.

Table 6.9. Comparison of predicted critical velocity by FDS with theoretical correlations of Table 2.2.

Determination of the Critical Ventilation Velocity	Critical Velocity (m/s)			Resulting error of the theoretical correlations compared to the CFD results (%)		
	20MW	50MW	100MW	20MW	50MW	100MW
Thomas, 1968	3.85	4.96	5.84	28.83	37.90	47.26
Hinkley, 1970	2.85	4.02	5.53	3.86	23.38	44.30
Danziger and Kennedy, 1982	2.24	2.80	3.20	-22.32	-10.00	3.75
Oka and Atkinson, 1995	2.95	3.13	3.13	7.12	**1.60**	**1.60**
Kennedy and Parsons, 1996	1.99	2.53	2.95	-37.69	-21.74	-4.41
Wu and Bakar, 2000	2.76	3.65	3.65	**0.72**	15.62	15.62
Li et al., 2010	3.33	3.81	3.81	17.72	19.16	19.16
Li and Ingason, 2017	3.31	3.81	3.81	17.22	19.16	19.16
Tang et al., 2018 b	3.27	3.83	3.83	16.21	19.58	19.58
CFD	**2.74**	**3.08**	**3.08**			

According to actual experimental data, air velocities in the order of 2 to 3.8m/s can effectively hinder the backlayering effect for fires ranging from 20 MW to 100 MW. However, these air velocities are dependent on the HRR, specific tunnel geometry, longitudinal rate grade and presence of obstacle near the fire. Table 6.9 displays the comparison of the numerically obtained critical velocity against previous theoretical equations that have been mentioned in the Unit 2.2.1, for the three different fire sizes. Table 6.9 also entails the underlying error produced from these theoretical equations, in the light of numerical findings. The sign "+" in the theorical correlation's error indicates that theoretical equation tends to overpredict the computed value for the critical velocity whereas the sigh "-" signifies accordingly an under prediction in critical ventilation values. In general, the acquired theoretical data suggest that air velocities in the range of 1.99m/s to 3.85 are sufficient to prevent backlayering for a fire of 20MW, 2.53 to 4.96m/s for a fire of 50MW and 2.95 to 5.84m/s for a fire of 100MW heat release rate. The first induced equations are apparently producing excessive estimations for the examined parameter, considering both the respective experimental data and the remaining theoretical correlations (Thomas, 1968; Hinkley, 1970). However, it must be noted that the recommended equations have been extracted as an aftermath of a preliminary investigation on that topic and it is reasonable that they fail in predicting the order of magnitude for the critical ventilation velocities, especially for large fires. In any way, they may not be the most representative predictions according to recent experimental data, but they have significantly contributed to build the foundation for forthcoming research. Besides Thomas, 1968 equation, the numerical results regarding critical ventilation velocity, evidently, comply well with most findings, acquired by the selected experimental correlations, presented in Table 6.9 (Hinkley, 1970; Danziger and Kennedy, 1982; Oka and Atkinson, 1995; Kennedy and Parsons, 1996; Wu and Bakar, 2000; Li et al., 2010; Li and Ingason, 2017; Tang et al., 2018b). Evaluating the theoretical results, it is apparent that most correlations hold in a great regard the influence of the size of the fire in the resulting critical velocity. In fact, most of them

are expressed by a two-fold equation, divided in terms of HRR (Oka and Atkinson, 1995; Wu and Bakar, 2000; Li et al., 2010; Li and Ingason, 2017; Tang et al., 2018b). In that manner, it is depicted the fact that larger fires, greater than 50MW, result in similar critical conditions based on the reasoning that up to a certain fire size the critical velocity requirement do not alter. A more detailed evaluation of the implemented equations is presented below to display the benefits and constrains of each equation, with respect to the size of the specified fire.

The theoretical relationships between the minimum tunnel air velocity required to prevent backlayering and heat release rare by Thomas, 1968 and Hinkley, 1970 appear to seriously over predict the air velocity requirements for fires above 50MW. This tendency can be justified since in these researches the critical ventilation velocity increases with fire size without accounting for the fact that above a certain HRR value the required longitudinal air velocity to prevent back-layering remains the same. Additionally, the choice of Fr_{cr} = 1 for all sizes of fires is responsible for that difference, as well. However, Hinkley, 1970 results appear to be more realistic that the respective data derived from Thomas, 1968 equation. In fact, for small fires up to 20MW, the resulting errors is exceptionally small, indicating a quite accurate theoretical prediction. The difference between the previous surveys is prompted partly by the selection of the Convective Heat Release Rate, Q_c, instead from the whole HRR value produced from the fire. The rest of the investigated equations and the predicted critical conditions by the FDS code, result in the same order of magnitude in terms of critical velocity for all the ranges of fire sizes. To begin with, comparing the values obtained using CFD and the respective ones obtained by utilizing Danziger and Kennedy's correlation, 1982, clearly reveals that the equation gives quite low critical velocities for both a 20MW and 50MW fires. The selection of Fr_{cr} = 4.5 for all sizes of fires may justify this tendency. On the contrary, for the design of a fire of 100MW in a longitudinal ventilation tunnel with zero inclination, the recommended critical velocity is in good agreement with the numerical one.

Oka and Atkinson, 1995 slightly overpredict the critical velocity for an 20MW fire while the resulting discrepancies between theoretical and numerical predictions are basically neglectable. In addition, this equation almost predicts equal value for critical velocity to the numerically derived one, for fire up to 50MW. The consistency of the respective theorical and numerical values clearly illustrates that parameters such as the type of fuel, the burner size and its position have a great impact on the fashion of critical conditions, for all the imposed fire sizes. It should be mentioned that the current equation tends to provide results of high fidelity for all the range of the investigated HRR due to the fact that it has been specified based on experimental data for fire sizes from 2 to 150MW. Continuing with the next equation, as shown in Table 6.9, the numerical results are higher than the results predicted by Kennedy and Parsons, 1996 equation. This is owned to the fact that the experimental data that provided the foundation for this correlation, are based on the effect of the Convective Heat Release Rate. In should be noted that the sole difference between the formation of equation of Kennedy and Parsons, 1996 and the one of Danziger and Kennedy, 1982 is the utilized quantity related to the HRR value, and thereby lower values regarding the critical ventilation conditions were anticipated from the start.

Moreover, FDS findings are greatly consistent with Wu and Bakar, 2000 predictions, especially for smaller fires (20MW). The fact that the theoretical correlation has been assessed against fires of maximum 50MW, via scaling law, may explain the lack of consistent with the results of larger fires. Proceeding to the next equations, it can be seen that the predicted numerical data correlate reasonably well with the proposed equations by Li et al., 2010; Li and Ingason, 2017; Tang et al., 2018 b. The resulting values from all the above equations, and thereby the computed errors as well, are almost the same for the previous surveys. This is due to the fact

that all of these correlations have been originated and defined based on the same reasoning and for that cause the predicted findings are presented as a group.

In total, the theoretical correlation of Wu and Bakar, 2000 have described in the most consistent way the critical conditions for a 20MW fire, based on the numerical results obtained by FDS, resulting to a theoretical error of approximate 0.72%. Additionally, the prediction model of critical velocity that has fulfilled the requests of the current study, for both 50MW and 100MW fires, is Oka and Atkinson, 1995 correlation with an error of 1.6% at both cases. However, it must be noted, that these values have been derived for ideal conditions inside the tunnel regarding the fire event and the consist an approximate approach. In practice, uncertainties regarding the incident conditions would provoke the need of a more conservative approach and therefore, at cases where the prevention of the adverse layer of toxic effluents is imperative, a slightly higher value of the predicted critical ventilation velocity should always be utilized.

Concluding, it must be noted that, the theoretical correlations provide great insights for critical ventilation velocity and for that they are considered a very handy tool for a preliminary fire safety studies inside road tunnels which necessitate longitudinal ventilation. However, these equations have been produced based on fits to experimental data where both the fit and the underlying experimental data entail a certain level of uncertainty. For that cause, additional research is needed on that topic to ensure reliable results regarding the critical conditions. Accordingly, prior to comparing any CFD results against a theorical correlation, on the current study, it must be considered first the influence of total underlying error to the survey results. For instance, according to experimental findings sometimes the assumed and the actual HRR induced in a fire test case can result in an error in the order of 10% or more. Striking examples of that claim, constitute the fire tests conducted in Runehamar Tunnel in 2005 and in the Memorial Tunnel in 1995. Therefore, based on the previous reasoning, the equations' results which have led to an error under approximately 10%, are considered to be in good agreement with the numerical predictions, in overall terms. The above comparison facilitates the FDS code precision in estimating the main flow field characteristics of a fire emergency inside a tunnel while highlighting the significant benefits from the utilization of longitudinal ventilation arrangements at unidirectional tunnels.

7. SUMMARY CONCLUSIONS

Road tunnels are indispensable pillars of any modern road transportation network. The occurrence of a fire incident, however, is a particularly severe event, and it demands the development of elevated fire safety requirements to guarantee the optimal level of protection to its motorists. Indeed, the propagation of toxic fire products and thermal smoke, within the tunnel, accompanied by the development of excessively high temperature distributions, directly threatens motorists' physical integrity and may even lead to fatalities. Subsequent hazards are also entailed from such incidents, like the partial destruction of the main tunnel structure, serious economic losses and environmental pollution at the near area. A tunnel structure is identified as a very long and narrow space with limited resources of fresh air, due to its confined nature. On that account, long evacuation distances are travelled towards the nearest emergency exit or portal, at cases of fire emergency, undermining evacuation and firefighting attempts. In light of the structure's main characteristics, the magnitude of severeness of a fire incident is highlighted and several objectives have been set with the aim of improving the optimal level of safety. The employment of a ventilation system is both a credible and a reliable strategy, constituting the most paramount approach of combating a fire emergency inside road tunnels. The selection of the appropriate ventilation system, however, is highly associated with the tunnel's length, utilization and traffic flow.

Since the introduction of tunnel structures to the transportation network, numerous fire incidents have actually occurred, leading to injuries, casualties and imposing significant financial burdens. To improve the understanding of such incidents and contribute to elevating the overall safety rate in road tunnels, various sequences of full-scale and reduced-scale experiments have taken place in tunnel structures. While valuable insights have gained by experimental testing, its performance is accompanied by various limits and constrains. Specifically, large-scale experiments have limited applicability as the entire procedure is as expensive as time consuming and logistically complicated to design and execute while reduced scaling models have limited credibility as they generate additional error to the experimental findings due to scaling effects. To remedy this problem, verified and validated CFD codes have been utilized as a handy tool to subscribe to the fundamental fire research in road tunnels. In order to gain a holistic view of tunnel fire emergencies, several large-scale evacuation tests have been performed as well, in road tunnels. Evacuee performance highlights the motorist's interpretation of a fire incident while recording their overall behaviour, offering important information on the design process of ventilation and firefighting systems and strategies. The overall knowledge obtained by means of actual fire incidents, dedicated full-scale and reduced-scale fire testing, evacuation experiments as well as numerical fire simulations, build the foundation of an extensive literature review, fostering the level of knowledge on various key parameters on fire and smoke related phenomena in road tunnel fires.

CFD modeling, in general, offers valuable insights for complex fire scenarios in tunnel structures while cultivating a breeding ground for parametric studies. Fire Dynamics Simulator (FDS), developed by NIST, is a computational fluid dynamics (CFD) model specially designed to resolve fire-driven fluid flows. The model solves numerically a form of the Navier-Stokes equations appropriate for low-speed ($Ma < 0.3$), thermally- driven flows, focused on smoke and heat distribution and propagation from fires. FDS constitutes a paramount computational code, developed to address particularly fire problems but nevertheless, utilizing such a software, always demands particular attention as it entails multiple challenges and

constraints. On that account, a prior calibration of modelling parameters against actual experimental data is imperative before any numerical study. In the current survey, two experimental test cases have been selected for validating the numerical findings, Test Case 502 and Test Case 615b, out of a series of 98 full-scale fire tests of the Memorial Tunnel Fire Ventilation Test Program. The Test Case 502 corresponds to a natural ventilation experiment, with a fire of nominal size of 50MW whereas the Test Case 615b concerns the smoke flow distribution provoked by a fire of approximately 100MW, under the influence of longitudinal ventilation. By this twofold approach, the main simulations parameters have been adequately specified against the elementary fire scenario, Test Case 502, while more elevated knowledge regarding longitudinal ventilation arrangements has been gained from the Test Case 615b. A validation study, in general, augments the level of confidence of the numerical findings which subsequently allows the impact of varying factors outside of the original fire scenario to be further investigated.

Ventilation is essential in most road tunnels to manage the transportation of hot smoke and control the concentrations of toxic fire products to acceptable levels within the tunnel. The type of ventilation system which a tunnel structure necessitates is directly associated to its length, utilization and traffic flow. In long tunnels with unidirectional traffic, where motorists are expected to be located upstream of the fire site, the employment of a longitudinal ventilation system is recommended. The primary objective of this type of ventilation system, is the prevention of the backlayering phenomenon by supplying a sufficient longitudinal air velocity, higher than the critical value for the induced fire size, in the direction of traffic flow. Based on these directives, a CFD modeling is presented in the present thesis, for simulating the effects of longitudinal ventilation in an 854m long, two-lane, unidirectional road tunnel. The modelled tunnel was equipped with a longitudinal ventilation system constituted by eight groups of three axial flow jet fans, equally spaced along the tunnel. Each fan was designed to deliver a volume flow up to $43 m^3/s$. Various legislative directions have been accounted for in the preparation of the investigated ventilation scenario, as certain practical details are fundamental in comprehending the jet fans capabilities and constraints. A fire source of three different fire sizes, is simulated with peak heat release rates of 20, 50 and 100MW. The fire has been placed at 615m away from the left portal of the tunnel. It is a known, that the presence of large obstacles (vehicles) near the fire directly affects the fire development and smoke spread within the tunnel, lowering the requirements of critical velocity, according to previous experimental data, and thereby the presence of traffic is omitted in the present fire survey, with the aim of assessing the longitudinal system effectiveness at the worst case scenario.

Given the above information, a series of large-scale numerical experiments have been conducted, with respect to the geometry of the model tunnel and the configuration of the selected longitudinal ventilation system, in order to estimate the critical ventilation velocity at varying fire sizes. In the light of numerical results, it is found that:

- The larger the fire size, the larger the amount of the produced smoke from the fire. Increasing the fire size, the backlayering length increases as well, whereas the smoke-filled cross-sectional area, provoked by a larger fire significantly outreaches the respective area of a smaller one.
- A longitudinal ventilation system using jet fans, is highly effective in regulating the direction of smoke distribution for the entire range of fire sizes (20, 50 & 100 MW), in 854m long tunnel with zero inclination.

- The implementation of jet fans strongly interacts with the existing flow inside the tunnel. The relative longitudinal and transverse position of each jet fan critically affects the ultimate performance of the whole ventilation system and its full operational capabilities.
- After the activation of the jet fans, the high discharge flow volumes generated by the fans, tend to scatter the well stratified layer of hot smoke that existed upstream of the fire site.
- The backlayering effect decreases with the increasing longitudinal velocities, for ventilation conditions beneath the critical.
- The stratification of the smoke degrades with increasing longitudinal velocities. On that account, for most longitudinal ventilation strategies attempting to create critical ventilation conditions, it is recommended that the imposed longitudinal ventilation velocity does not exceed by far the respective critical one, in order for the stratification of smoke layer to be maintained, both upstream and downstream of the fire site.
- Numerical results are in firm agreement also with the empirical allegation that the critical velocity increases with fire size. They also confirm that the critical ventilation velocity tends to level off above a certain HRR value, becoming independent of the fire size.
- A longitudinal ventilation velocity in the order of 2.75m/s, is capable of dropping the adverse length of toxic smoke to zero, for a medium fire of 20MW. In addition, a critical ventilation velocity in the region of 3.10m/s is predicted for both a 50MW and 100MW fire. However, these air velocities are dependent on the specific tunnel cross section and grade.
- Although the critical ventilation velocity becomes interchangeable for fire sizes above a certain value, that same tendency does not apply to the fans volume flow exhaust rates, which are constantly increasing with increasing fire size. Indeed, a 100MW design fire demands a significantly larger volume flow capacity generated by the jet fans to attain the same critical ventilation velocity with a 50MW fire.
- The functionality of the jet fans located downstream of the fire is directly threatened due to the exposure to high temperatures from the fire. Indeed, the fans of 7^{th} group are subjective to excessive temperatures and were not utilized, as their efficient performance has been compromised for all the investigated fire sizes. However, since the underlying temperature values beneath the ceiling at the location of the 8^{th} group of jet fans, are slightly lower than their thermal endurance, for the worst-case scenario of 100MW, their functionality is not in jeopardy and therefore they can be included in the applied ventilation strategy. The likelihood of mechanical failure of some jet fans, should be anticipated in all fire scenarios, at the design stage, prior to their installation to the tunnel.
- A comparative evaluation of all available theoretical correlations of critical velocity revealed that particular formulas produce calculations that are in firm agreement with the resulting numerical results in the modelled road tunnel, for all the range of fire sizes of 20, 50 and 100MW. In particular, the employment of the equation of Wu and Bakar, 2000, is suitable for medium tunnel fires of approximately 20MW, producing reliable results whereas for larger fires of nominal fire size of 50 or 100MW, the empirical correlation of Oka and Atkinson, 1995 predicts accurately the required critical velocity.

The results of this study are applicable to unidirectional tunnels where a longitudinal ventilation system is employed to combat the hazardous effects of fires in the range of 20 to 100MW nominal heat release rate. However, it should be taken into account that the development of a fire scenario is directly dependent on the tunnel cross section and grade and therefore the numerical findings are strictly valid for the investigated tunnel structure. Concluding, these numerical findings can benefit the critical ventilation assessment and we hope this survey can offer a reference for the fire safety engineering applications of smoke management in unidirectional road tunnels, in the future.

8. Future Research

In fire safety engineering for road tunnel structures, the variety of fire scenarios requiring analysis and evaluation is extremely wide. The selection of the appropriate tunnel fire scenario is a matter of key importance, since the identification and investigation of all possible tunnel fire emergencies are neither feasible in practice nor computationally affordable. However, plenty of potential “alternative scenarios” can be assessed on that topic, extending the level of knowledge in fire events, ventilation configurations and evacuation strategies. The main recommendations for future research regard:

- Longitudinal ventilation system consisting of a different number or arrangement of jet fans.
- Different activation times of the mechanical ventilation system.
- The maximum thermal power released from the fire source and the time profile of the burning fuel.
- The presence of blockage / traffic flow inside the tunnel.
- The assessment of critical ventilation velocity at different tunnel cross-sectional areas.
- The assessment of critical ventilation velocity at a tunnel structure with varying longitudinal inclination.
- The assessment of the backlayering distance, smoke layer thickness, maximum temperature beneath the ceiling, at the investigated fire scenario and the evaluation of the existing empirical correlations on that topics.
- The coupling effect of the longitudinal ventilation system with another ventilation configuration, like centralized mechanical smoke exhaust systems.
- Numerical simulations of evacuation processes, namely “fire drills”, attached to the investigated fire scenarios.

REFERENCES

Bai J., Liao H., Xia Y., (2020) "Study on Fire Accidents in Tunnels", *Materials Science and Engineering 741.*

BD 78/99, *Design manual for roads and bridges, The Highways Agency*, August 1999.

Beard A., Carvel R., *Handbook of Tunnel Fire Safety, Second edition,* ICE Publishing, London, 2005.

Beard A., Carvel R., *Handbook of Tunnel Fire Safety, Second edition*, ICE Publishing, London (2005).

Bechtel/Parsons Brinckerhoff (1995), "Memorial Tunnel Fire Ventilation Test Program", Test Report for Massachusetts Highway Department and Federal Highway Administration.

Binbin W. (2011), "Comparative Research on FLUENT and FDS's Numerical Simulation of Smoke Spread in Subway Platform Fire*", Procedia Engineering* 26, 1065 – 1075.

Blanchard E., Boulet P., Desanghere S., Cesmat E., Meyrand R., Garo J.P., Vantelon J.P. (2012), "Experimental and numerical study of fire in a midscale test tunnel*", Fire Safety Journal* 47, 18–31.

Boer L., Veldhuijzen van Zanten D., "Behaviour on tunnel fire", *Third International Conference on Pedestrian and Evacuation Dynamics*, PED 2005, Vienna, Austria, 2005.

Boer L.C., (2002) "Behaviour of Motorists when Escaping from a Tunnel*"*, *Report TM-02-C34,* TNO Human Factors.

Boer L.C., *Behaviour of drivers during tunnel evacuation*, *(Re)Claiming the Underground Space,* pp 213-217. Tokyo: Balkema (2003).

Boer L.C., Wijngaarden S.V., "Directional Sound Evacuation from Smoke-Filled Tunnels", *First International Symposium*, Prague 2004.

Boer, L.C., "Way finding during emergencies*", TIEMS Conference*, Oslo, 2001.

Borghetti F., Derudi M., Gandini P., Frassoldati A., Tavelli S., *Tunnel Fire Testing and Modeling*, Springer, Milano, Italy 2017

Borghettia F., Frassoldati A., Derudi M., Laic I., Trinchinic C., (2020) "Safety in Road Tunnels: Accident Data Analysis of the Italian Motorway A24 and A25", Chemical Engineering Transactions Vol. 82.

Caliendo C., Ciambelli P., De Guglielmo M.L., Meo M.G., Russo P. (2012), "Numerical simulation of different HGV fire scenarios in curved bi-directional road tunnels and safety evaluation", *Tunnelling and Underground Space Technology* 31, 33–50.

Caliendo C., Ciambelli P., De Guglielmo M.L., Meo M.G., Russo P. (2013), "Simulation of fire scenarios due to different vehicle types with and without traffic in a bi-directional road tunnel", *Tunnelling and Underground Space Technology* 37, 22–36.

Caliendo C., De Gulielmo M.L., (2012), "Accident Rates in Road Tunnels and Social Cost Evaluation", *Procedia - Social and Behavioral Sciences* Volume 53, 166-177.

Chalasani N.R., Greiner M., Suo-Anttila A., "Validation of container analysis fire environment (CAFE) code for Memorial Tunnel Fire Ventilation Test Program", Proceedings of the ASME 2010 Pressure Vessels & Piping Division / K-PVP Conference PVP 2010, Bellevue, Washington, USA, 2010.

Chen F., Leong J.C., (2011) "Smoke flow phenomena and turbulence characteristics of tunnel fires", *Applied Mathematical Modelling 35,* 4554–4566.

Cheong M.K., Cheong W.O., Leong K.W., Lemaire A.D., Noordijk L.M. (2014), "Heat Release Rate of Heavy Goods Vehicle Fire in Tunnels with Fixed Water Based Fire-Fighting System", *Fire Technology*, 50, 249–266.

Cheong M.K., Spearpoint M.J., Fleischmann C.M. (2009), "Calibrating an FDS Simulation of Goods-vehicle Fire Growth in a Tunnel Using the Runehamar Experiment", *Journal of Fire Protection Engineering*, Vol. 19,177-196.

Chung H.C., Seike M., Kawabata N., Hasegawa, Chien S.W., Shen T.S., (2020) "Time gap distribution of bus alighting in tunnel fires", *Fire Safety Journal*, doi: https://doi.org/10.1016/j.firesaf.2020.103152.

Colella F., Rein G., Torero J.L. (2011), "A Novel Multiscale Methodology for Simulating Tunnel Ventilation Flows During Fires", *Fire Technology*, 47, 221–253.

Cuesta A., Abreu O., Balboa A., Alvear D., (2020) "Alone or with others: experiments on evacuation decision making", *Fire Safety Journal*, doi: https://doi.org/10.1016/j.firesaf.2020.103018.

Danziger N.H., Kennedy W.D., "Longitudinal Ventilation Analysis for the Glenwood Canyon Tunnels", *Proceedings of the Fourth International Symposium on the Aerodynamics & Ventilation of Vehicle Tunnels*, York, United Kingdom, 1982.

Ding N., Sun C., (2020) "Experimental study of leader-and-follower behaviours during emergency evacuation", Fire Safety Journal, Vol.117,103189.

Filippidis L., Lawrence P., Galea E.R, “Simulating the interaction of occupants with signage systems”, *Ninth International Symposium on Fire Safety Science,* IAFSS 2008, Karlsruhe, Germany, 2008.
Frantzich H., (2000) “Utrymning av tunnelbanetåg: Experimentell utvårdering av mojligheten att utrymma i spårtunnel” [Evacuation from subway trains: an experimental evaluation of the possibility to evacuate in a rail tunnel], Raddningsverket, Karlstad.
Frantzich, H., Nilsson, D., (2003) “Utrymning genom tat rok: beteende och forflyttning” [Evacuation in dense smoke: behaviour and movement] *Technical Report 3126,* Department of Fire Safety Engineering and Systems Safety, Lund.
Fridolf K., Andrée K., Nilsson D., Frantzich H., (2014) "The impact of smoke on walking speed*", Fire and Materials 38*, pp 744-759.
Fridolf K., Frantzich H., (2015) “Test av vägledande system i en tunnel”, *Technical Report 13580* (DOI: 10.13140/RG.2.2.10757.65762).
Fridolf K., Nilsson D., Frantzich H., (2016) "Evacuation of a Metro Train in an Underground Rail Transportation System: Flow Rate Capacity of Train Exits, Tunnel Walking Speeds and Exit Choice", Fire Technology 52, pp 1481-1518.
Fridolf K., Ronchi E., Nilsson D., Frantzich H., (2013) "Movement speed and exit choice in smoke-filled rail tunnels", *Fire Safety Journal 59*, pp 8-21.
Fridolf K., Ronchi E., Nilsson D., Frantzich H., (2019) "The representation of evacuation movement in smoke-filled underground transportation systems", Tunnelling and Underground Space Technology 90, pp. 28-41.
Glasa J., Valasek L., Weisenpacher P. (2019), “On Impact of Slope on Smoke Spread in Tunnel Fire”, Springer Nature Switzerland AG 2019, APSAC, LNEE 574, pp. 157–162.
Guo X., Zhang Q. (2014), “Analytical solution, experimental data and CFD simulation for longitudinal tunnel fire ventilation”, *Tunnelling and Underground Space Technology* 42, 307–313.
H. Xie, L. Filippidis, E. Galea, D. Blackshields, and P. Lawrence, Experimental study of the effectiveness of emergency signage”, *Fourth International Symposium on Human Behaviour in Fire*, Cambridge, UK, 2009.
Haack, (1998) “Fire Protection in Traffic Tunnels: General Aspects and Results of the EUREKA Project”, T*unnelling and Underground Space Technology,* Vol. 13, No. 4, pp. 377-381
Haerter A., (1994), “Fire Tests in the Ofenegg Tunnel in 1965”, *Swedish National Testing and Research Institute (SP), Fire Technology, Fires In Tunnels, Vol 54,* pp 195- 214.
Hall R.C., (2006) “Ventilation during Road Tunnel Emergencies”, Published Project Report PPR140 3/359, TRL Limited.
Heselden A.J.M, Hinkley P.L. (1970), “Smoke travel in shopping malls experiments in co-operation with Glasgow Fire Brigade -Part 1”, Fire Research Note No.832.
Heselden A.J.M., *Studies of Fire and Smoke Behaviour Relevant to Tunnels,* Building Research Establishment, Glasgow, 1978.
Hinkley P.L., (1970), “The flow of hot gases along an enclosed shopping mall a tentative theory”, *Fire Research Note No. 807*, Fire Research Station.
Hostikka S., *Development of fire simulation models for radiative heat transfer and probabilistic risk assessment*, VTT Publications 683, VTT Technical Research Centre of Finland, Espoo, Finland, 2008.
Hsu W.S., Huang Y.H., Shen T.S., Cheng C.Y., Chen T.Y., (2017) “Analysis of the Hsuehshan Tunnel Fire in Taiwan”, *Tunnelling and Underground Space Technology* 69, pp 108–115.
Hu L.H., Fong N.K., Yang L.Z., Chow W.K., Li Y.Z., Huo R. (2007), “Modeling fire-induced smoke spread and carbon monoxide transportation in a long channel: Fire Dynamics Simulator comparisons with measured data”, *Journal of Hazardous Materials* 140, 293–298.
Hu L.H., Huo R., Chow W.K., (2008) “Studies on buoyancy-driven back-layering flow in tunnel fires”, *Experimental Thermal and Fluid Science 32*, 1468–1483.
Hu L.H., Huo R., Peng W., Chow W.K., Yang R.X. (2006), “On the maximum smoke temperature under the ceiling in tunnel fires”, *Tunnelling and Underground Space Technology* 21, 650-655.
Hu L.H., Huo R., Wang H.B., Li Y.Z., Yang R.X. (2007), “Experimental studies on fire-induced buoyant smoke temperature distribution along tunnel ceiling”, *Building and Environment* 42, 3905–3915.
Hu L.H., Huo R., Wang H.B., Yang R.X. (2007), “Experimental and Numerical Studies on Longitudinal Smoke Temperature Distribution Upstream and Downstream from the Fire in a Road Tunnel”, *Journal of Fire Sciences* Volume 25, 23-43.

Hu L.H., Huo R., Yang R.X., He W.H., Wang H.B., Li Y.Z. (2005), "Full Scale Experiments on Studying Smoke Spread in a Road Tunnel", *Fire Safety Science-Proceedings Of The Eighth International Symposium* pp.1437-1447.
Hu L.H., Peng W., Huo R. (2008), "Critical wind velocity for arresting upwind gas and smoke dispersion induced by near-wall fire in a road tunnel", *Journal of Hazardous Materials* 150, 68–75.
Hu L.H., Tang F., Yang D., Liu S., Huo R. (2010), "Longitudinal distributions of CO concentration and difference with temperature field in a tunnel fire smoke flow", *International Journal of Heat and Mass Transfer* 53, 2844–2855.
Hui Y., Li J., Lixin Y. (2009), "Numerical analysis of tunnel thermal plume control using longitudinal ventilation", *Fire Safety Journal* 44, 1067–1077.
Hurley M.J., *SFPE Handbook of Fire Protection Engineering, Fifth Edition,* Springer (2016).
Hwang C.C., Edwards J.C. (2005), "The critical ventilation velocity in tunnel fires—a computer simulation", *Fire Safety Journal* 40, 213–244.
Ingason H., Li Y.Z., Lönnermark A. (2015), "Runehamar tunnel fire tests", *Fire Safety Journal* 71, 134–149.
Ingason H., Li Y.Z., Lönnermark A., *Tunnel Fire Dynamics*, Springer Science+Business Media, New York, 2015.
Ingason H., Lönnermark A. (2005), "Heat release rates from heavy goods vehicle trailer fires in tunnels", *Fire Safety Journal* 40, 646–668.
Ingason H., Lönnermark A., Li Y.Z. (2012), "Model of ventilation flows during large tunnel fires*", Tunnelling and Underground Space Technology* 30, 64–73.
Ingason H., Lönnermark A., Li Y.Z. (2011), "Runehamar Tunnel Fire Tests", SP Technical Research Institute of Sweden, *Fire Technology*, SP Report 55.
ISO/TC 92/SC 4, (2020) "Design of evacuation experiments", Fire safety Engineering, N.1328
Jain S., Kumar Sh., Kumar Su., Sharma T.P. (2008), "Numerical simulation of fire in a tunnel: Comparative study of CFAST and CFX predictions", *Tunnelling and Underground Space Technology* 23, 160–170.
Ji J., Fan C.G., Zhong W., Shen X.B., Sun J.H. (2012), "Experimental investigation on influence of different transverse fire locations on maximum smoke temperature under the tunnel ceiling", *International Journal of Heat and Mass Transfer 55*, 4817–4826.
Ji J., Tan T., Gao Z., Wan H., Zhu J., Ding L., (2019), "Numerical Investigation on the Influence of Length–Width Ratio of Fire Source on the Smoke Movement and Temperature Distribution in Tunnel Fires", *Fire Technology,* Volume 55, 963–979.
Jiang, X., Zhang, H., Jing, A., (2018b) "Effect of blockage ratio on critical velocity in tunnel model fire tests". *Tunnelling and Underground Space Technology* 82, 584–591.
Jin T., (1976) "Visibility through fire smoke", *Report of Fire Research,* Institute of Japan.
Jin T., (1978) "Visibility through fire smoke", Fire Flammability 9, pp. 135–157.
Jin T., (1997) "Studies on Human Behaviour and Tenability in Fire Smoke", *Fire Safety Science 5,* pp 3-21.
Kang K. (2007), "A smoke model and its application for smoke management in an underground mass transit station", *Fire Safety Journal* 42, 218–231.
Kashef A., Bénichou N. (2008), "Investigation of the Performance of Emergency Ventilation Strategies in the Event of Fires in a Road Tunnel, A Case Study", *Journal of Fire Protection Engineering* Volume 18, 165.
Kashef A., Lougheed G., Crampton G., Liu Z.G., Yoon K., Hadjisophocleous G., Almand K.H. (2009), "Findings of the International Road Tunnel Fire Detection Research Project", *Fire Technology* 45, 221–237.
Kennedy W. D., "Critical velocity: Past, Present and Future", *Seminar of Smoke and Critical Velocity in Tunnels, London*, 1996.
Kim E., Woycheese J.P., Dembsey N.A. (2008), "Fire Dynamics Simulator (Version 4.0) Simulation for Tunnel Fire Scenarios with Forced, Transient, Longitudinal Ventilation Flows", *Fire Technology*, 44, 137–166.
Kinateder M., Pauli P., Müller M., Krieger J., Heimbecher F., Rönnau I., Bergerhausen U., Vollmann G., Vogt P., Mühlberger A., (2013) "Human behaviour in severe tunnel accidents: Effects of information and behavioural training", *Transportation Research Part F17,* pp 20-32
Ko Y.J., Hadjisophocleous G.V. (2013), "Study of smoke backlayering during suppression in tunnels*", Fire Safety Journal* 58, 240–247.

Krausmann E., Mushtaq F., (2005) “Analysis of tunnel-accident data and recommendations for data collection and accident investigation”, SafeT Work package 4*, D4.5 report,* First Deliverable to EU Part II.
Kunsch J.P., (2002) “Simple model for control of fire gases in a ventilated tunnel”, *Fire Safety Journal 37,* 67–81.
Lee C.K., Chaiken R.F., Singer J.M. (1979) “Interaction between duct fires and ventilation flow: an experimental study”, *Combustion Science and Technology 20*, 59–72.
Lee S., Ryou H.S., (2003) “An Experimental Study of the Effect of the Aspect Ratio on the Critical Velocity in Longitudinal Ventilation Tunnel Fires”, *Journal of Fire Science, Volume 23,* Issue 2 119-138.
Lee Y.P, Tsai K.C., (2012) “Effect of vehicular blockage on critical ventilation velocity and tunnel fire behavior in longitudinally ventilated tunnels”, *Fire Safety Journal 53*, 35–42.
Lemaire T., Kenyon Y., (2006), “Large Scale Fire Tests in the Second Benelux Tunnel”, *Fire Technology, 42*, pp 329–350.
Li L., Li S., Wang X., Zhang H. (2012), “Fire-induced flow temperature along tunnels with longitudinal ventilation”, *Tunnelling and Underground Space Technology* 32, 44–51.
Li Y.Z., Ingason H., (2017) “Effect of cross section on critical velocity in longitudinally ventilated tunnel fires” *Fire Safety Journal 91,* 303–311.
Li Y.Z., Lei B., Ingason H. (2011), “The maximum temperature of buoyancy-driven smoke flow beneath the ceiling in tunnel fires”, *Fire Safety Journal* 46, 204–210.
Li Y.Z., Lei B., Ingason H., (2010) “Study of critical velocity and backlayering length in longitudinally ventilated tunnel fires”, *Fire Safety Journal 45*, 361–370.
Lin P., Lo S.M, Li., T. (2014), “Numerical study on the impact of gradient on semi-transverse smoke control system in tunnel”, *Tunnelling and Underground Space Technology* 44, 68–79.
Liu C., Zhong M., Shi C., Zhang P., Tian X. (2017), “Temperature profile of fire-induced smoke in node area of a full-scale mine shaft tunnel under natural ventilation”, *Applied Thermal Engineering* 110, 382–389.
Lönnermark A., Hedekvist P.O., Ingason H. (2008), “Gas temperature measurements using fibre Bragg grating during fire experiments in a tunnel”, *Fire Safety Journal* 43, 119–126.
Lönnermark A., Ingason H. (2005), “Gas temperatures in heavy goods vehicle fires in tunnels”, *Fire Safety Journal* 40, 506–527.
Maevski I., (2016) “Recommended AASHTO Guidelines for Emergency Ventilation Smoke Control in Roadway Tunnels”, *National Cooperative Highway Research Program*, NCHRP Project 20-07, Task 363.
Maevski I.Y, *Design Fires in Road Tunnels*, National Cooperative Highway Research Program, Washington D.C., 2011.
Mancaruso E., Vaglieco B.M, (2013) “An experimental comparison of n-Heptane, RME and diesel fuel on combustion characteristics in a compression ignition engine”, *Fuel Processing Technology 107,* 44–49.
Mawhinney J. R., Trelles J. (2012), “Testing Water Mist Systems Against Large Fires in Tunnels: Integrating Test Data with CFD Simulations”, *Fire Technology*, 48, 565–594.
Mawhinney J. R., Trelles J., “Computational fluid dynamics modelling of water mist systems on large HGV fires in tunnels*”, Journée d’Etude Technique: Brouillard d’Eau – Quoi de Neuf?, at Pôle Européen de Sécurité CNPP* - Vernon, France, 2007.
Mawhinney J. R., Trelles J., “The Use of CFD-FDS Modeling for Establishing Performance Criteria for Water Mist Systems in Very Large Fires in Tunnels”, *Proceedings from the Third International Symposium on Tunnel Safety and Security*, Stockholm, Sweden, 2008.
McGrattan K., Hostikka S., Floyd J., McDermott R., Vanella M., (2020) “Fire Dynamics Simulator Technical Reference Guide Volume 1: Mathematical Model”, *NIST Special Publication 1018-1*, Sixth Edition.
McGrattan K., Hostikka S., Floyd J., McDermott R., Vanella M., (2020) “Fire Dynamics Simulator User’s Guide”, NIST Special Publication 1019 Sixth Edition.
McGrattan K., Hostikka S., Floyd J., McDermott R., Vanella M., (2020a) “Fire Dynamics Simulator User’s Guide”, *NIST Special Publication 1019 Sixth Edition*.
McGrattan K., Hostikka S., Floyd J., McDermott R., Vanella M., (2020b), “Fire Dynamics Simulator Technical Reference Guide Volume 1: Mathematical Model”, *NIST Special Publication 1018-1 Sixth Edition.*
McGrattan K., Hostikka S., Floyd J., McDermott R., Vanella M., *Fire Dynamics Simulator User’s Guide,* NIST Special Publication 1019 Sixth Edition, (2020).

McGrattan K.B., Hamins A. (2001), “Numerical Simulation of the Howard Street Tunnel Fire”, *Fire Technology 42,* pp 273- 281.
Migoya E., Crespo A., Garcia J., Hernandez J. (2008), “A simplified model of fires in road tunnels. Comparison with three-dimensional models and full-scale measurements”, *Tunnelling and Underground Space Technology* 24, 37-52.
Migoya E., García J., Crespo A., Gago C., Rubio A. (2011), “Determination of the heat release rate inside operational road tunnels by comparison with CFD calculations*”, Tunnelling and Underground Space Technology* 26, 211–222.
Morgan JH., *SFPE Handbook of Fire Protection Engineering,* Fifth Edition, Springer, London, (2016).
Munson B. R., Young D. F., Okiishi T.H., *Fundamentals of Fluid Mechanics*, John Wiley and Sons (1990).
NFPA 502, *Standard for Road Tunnels, Bridges, and Other Limited Access Highways*, 2011 Edition.
NFPA 502, *Standard for Road Tunnels, Bridges, and Other Limited Access Highways*, 2011 Edition.
Nilsen A.R., Log T. (2009), “Results from three models compared to full-scale tunnel fires tests”, *Fire Safety Journal* 44, 33–49.
Nilsson D., (2009) “Exit Choice in Fire Emergencies—Influencing Choice of Exit With Flashing Lights”, *Department of Fire Safety Engineering and Systems Safety*, Lund University.
Nilsson D., Frantzich H., Ronchi E., Fridolf K., Walter A.L., Modig H., (2018), "Integrating evacuation research in large infrastructure tunnel projects - Experiences from Stockholm Bypass Project", *Fire Safety Journal 97,* pp. 119-125.
Nilsson D., Johansson A., (2009) “Social influence during the initial phase of a fire evacuation— Analysis of evacuation experiments in a cinema theatre”, *Fire Safety Journal 44,* pp 71-79.
Nilsson D., Johansson M., Frantzich H., (2009) " Evacuation experiment in a road tunnel: A study of human behaviour and technical installations", *Fire Safety Journal 44*, pp 458–468.
Norén A., Winér J., (2003) "Modelling Crowd Evacuation from Road and Train Tunnels - Data and design for faster evacuations", *Department of Fire Safety Engineering, Report 5127*, Lund.
Norén A., Winér J., (2003) “Modelling crown evacuation from road and train tunnels— Data and design for faster evacuations”, Department of Fire Safety Engineering, Report 5127.
OECD Obesity Update 2017: https://www.oecd.org/els/health-systems/Obesity-Update-2017.pdf
Oka Y., Atkinson G.T. (1995), “Control of Smoke Flow in Tunnel Fires”, *Fire Safety Journal* 25, 305-322.
Oka Y., Atkinson T., (1995), “Control of Smoke Flow in Tunnel Fires”, *Fire Safety Journal 25*, pp 305-322.
PIARC, *Fire and smoke control in road tunnel,* Permanent International Association of Road Congress, 1999.
Porzycki J., Schmidt-Polończyk N., Wąs J., (2018) "Pedestrian behaviour during evacuation from road tunnel in smoke condition- Empirical results", Plos One, doi: 10.1371/journal.pone.0201732.
Proulx G. and Sime J., “To Prevent ‘Panic’ in an Underground Emergency: Why Not Tell People the Truth?”, *Third International Symposium on Fire Safety Science*, London, 1991.
Public Works Research Institute, *State of The Road Tunnel Equipment Technology In Japan: Ventilation, Lighting, Safety Equipment*, Japan, 1993
Pucher K., (1994), “Fire Tests in the Zwenberg Tunnel (Austria)”, *Swedish National Testing and Research Institute, Fire Technology, Fire in Tunnels Vol.54*, pp 187-194
Ren R., Zhou H., Hu Z., He S., Wang X., (2019) “Statistical analysis of fire accidents in Chinese highway tunnels 2000–2016”, *Tunnelling and Underground Space Technology 83,* 452–460.
Roh J.S., Yang S.S., Ryou H.S., Yoon M.O., Jeong Y.T. (2008), “An experimental study on the effect of ventilation velocity on burning rate in tunnel fires—heptane pool fire case*”, Building and Environment* 43, 1225–1231.
Ronchi E., Fridolf K., Frantzich H., Nilsson D., Walter L.A., Modig H., (2018) "A tunnel evacuation experiment on movement speed and exit choice in smoke", *Fire Safety Journal 97*, pp 126–136.
Seike M., Kawabata N., Hasegawa M., (2016) "Experiments of evacuation speed in smoke-filled tunnel", *Tunneling and Underground Space Technology 53,* pp 61–67.
Seike M., Kawabata N., Hasegawa M., Lu Y., "Evacuation Speed Distribution by Full-Scale Tunnel Experiments", *8th International Conference ‘Tunnel Safety and Ventilation’*, Graz, 2016.
Sime J., (1984) “Escape behaviour in fires: ‘Panic’ or affiliation?”, *PhD, University of Surrey*, Guilford.
Tang F., He Q., Mei F., Wang Q., Zhang H., (2018b) “Effect of ceiling centralized mechanical smoke exhaust on the critical velocity that inhibits the reverse flow of thermal plume in a longitudinal ventilated tunnel”, *Tunnelling and Underground Space Technology 82*, 191–198.

Tang W., Hu L.H., Chen L.F, (2013) “Effect of blockage-fire distance on buoyancy driven back-layering length and critical velocity in a tunnel: An experimental investigation and global correlations”, *Applied Thermal Engineering 60,* 7-14
Thomas P.H., (1958) “The movement of buoyant fluid against a stream and the venting of underground fires”, *Fire Research Note No. 351*, Fire Research Station.
Thomas P.H., (1968) “The Movement of Smoke in Horizontal Passages Against an Air Flow*”, Fire Research Note No. 723*, Fire Research Station.
Tian X., Zhong M., Shi C., Zhang P., Liu C. (2017), “Full-scale tunnel fire experimental study of fire-induced smoke temperature profiles with methanol-gasoline blends”, *Applied Thermal Engineering* 116, 233–243.
Tomar M.S., Khurana S., “Numerical simulation of road tunnel fires involving heavy goods vehicle with solid fuels”, *Journal of Physics: Conference Series, Volume 1276, International Conference on Recent Advances in Fluid and Thermal Sciences,* Dubai, U.A.E., 2018.
Trelles J., Mawhinney J.R., (2010), “CFD Investigation of Large-Scale Pallet Stack Fires in Tunnels Protected by Water Mist Systems”, *Journal of Fire Protection Engineering*, Vol.20.
United Nations, Department of Economic and Social Affairs, “Population Division World Population Prospects: The 2015 Revision, Volume I: Comprehensive Tables” ST/ESA/SER. A/379. United Nations, New York (2015).
United Nations, Department of Economic and Social Affairs, “Population Division. World Population Prospects: The 2015 Revision, Key Findings and Advance Tables”. ESA/P/WP.241. ST/ESA/SER.A/380. United Nations, New York, (2015).
Vega M.G., Diaz K.M.A., Oro J.M.F., Tajadura R.B., Morros C.S., (2008) “Numerical 3D simulation of a longitudinal Ventilation System: Memorial Tunnel case”, *Tunnelling and Underground Space Technology 23*, pp 539–551.
Vermesi I., Rein G., Colella F., Valkvist M., Jomaas G. (2017), “Reducing the computational requirements for simulating tunnel fires by combining multiscale modelling and multiple processor calculation”, *Tunnelling and Underground Space Technology* 64, 146–153.
Vianello C., Fabiano B., Palazzi E., Maschio G., (2012) “Experimental study on thermal and toxic hazards connected to fire scenarios in road tunnels”, *Journal of Loss Prevention in the Process Industries Volume 25, Issue 4*, 718-729.
Vigne G., Jönsson J., “Experimental Research - Large-Scale Tunnel Fire Tests and the use of CFD modelling to predict Thermal Behaviour”, *Conference: Fire Protection and Life Safety in Buildings and Transportation Systems, International Congress*, Santander, Spain,2009.
Wang F., Wang M., (2016) “A computational study on effects of fire location on smoke movement in a road tunnel”, *Tunnelling and Underground Space Technology 51,* 405–413
Wang H.Y., (2009), “Prediction of soot and carbon monoxide production in a ventilated tunnel fire by using a computer simulation”, *Fire Safety Journal* 44, 394–406.
Wang X., Fleischmann C., Spearpoint M. (2016), “Assessing the influence of fuel geometrical shape on fire dynamics simulator (FDS) predictions for a large-scale heavy goods vehicle tunnel fire experiment”, *Case Studies in Fire Safety* 5, 34–41.
Wang Y., Jiang J., Zhu D. (2009), “Full-scale experiment research and theoretical study for fires in tunnels with roof openings”, *Fire Safety Journal* 44, 339–348.
Weisenbacher P., Halada L., Glasa J., “Computer Simulation of Fire in a Tunnel Using Parallel Version of FDS”, *Seventh Mediterranean Combustion Symposium*, Cagliari (2011).
Weng M.C., Lu X.L., Liu F., Shi X.P., Yu L.X., (2015) “Prediction of backlayering length and critical velocity in metro tunnel fires”, *Tunnelling and Underground Space Technology 47*, 64-72.
Willman C., Scott B., Stone R., Richardson D., 2020 “Quantitative metrics for comparison of in-cylinder velocity fields using particle image velocimetry”, *Experiments in Fluids 61,* Article Number 62.
Woodburn P.J., Britter R.E., (1996), “CFD simulations of a tunnel fire – Part I”, *Fire Safety Journal* 26, 35–62.
Wu Y., Bakar M.Z.A., (2000) “Control of smoke flow in tunnel fires using longitudinal ventilation systems – a study of the critical velocity”, *Fire Safety Journal* 35, 363–390.
Wu Y., Bakar M.Z.A., (2000) “Control of smoke flow in tunnel fires using longitudinal ventilation systems- a study of the critical velocity”, *Fire Safety Journal 35*, 363-390.
Xie H., (2011) “Investigation into the Interaction of People with Signage Systems and its Implementation Within Evacuation Models”, *The University of Greenwich*, Great Britain.

Xu P., Jiang S.P., Xing E.J., Tan J.Q. (2018), "Full-scale immersed tunnel fire experimental research on smoke flow patterns*", Tunnelling and Underground Space Technology* 81, 494-505.
Xue H., Hihara E., Saito T., (1993) "Turbulence model of fire-induced air flow in a ventilated tunnel", *International Journal if Heat and Mass Transfer 36*, 1739–1748.
Yan Z., Guo Q., Zhu H. (2017), "Full-scale experiments on fire characteristics of road tunnel at high altitude*", Tunnelling and Underground Space Technology* 66, 134-146.
Yan Z., Zhu H., Yang Q. (2006), "Large-scaled Fire Testing for Long-sized Road Tunnel", *Tunnelling and Underground Space Technology* 21, 282-287.
Yi L., Xu Q., Xu Z., Wu D., (2014) "An experimental study on critical velocity in sloping tunnel with longitudinal ventilation under fire", *Tunnelling and Underground Space Technology 43*, 198–203.
Zhang N., Tan Z., Jin M. (2015), "Research on the Technology of Disaster Prevention and Rescue in High-altitude Super-long Railway Tunnel*", KSCE Journal of Civil Engineering* 19(3): 756-764.
Zhang X., Lin Y., Shi C., Zhang J., (2021) "Numerical simulation on the maximum temperature and smoke back-layering length in a tilted tunnel under natural ventilation*", Tunnelling and Underground Space Technology 107*, 103661.
Zhong M., Shi C., He L., Shi J., Liu C., Fu T., (2011), "Full-scale experimental research on fire fume refluence of sloped long and large curved tunnel", *SCIENCE CHINA, Technological Sciences Vol.54*, pp 89–94.
Zhong M., Shi C., He L., Shi J., Liu C., Tian X. (2016), "Smoke development in full-scale sloped long and large curved tunnel fires under natural ventilation", *Applied Thermal Engineering* 108, 857–865.
ΕΦΗΜΕΡΙΣ ΤΗΣ ΚΥΒΕΡΝΗΣΕΩΣ ΤΗΣ ΕΛΛΗΝΙΚΗΣ ΔΗΜΟΚΡΑΤΙΑΣ, (2007) "ΠΡΟΕΔΡΙΚΟ ΔΙΑΤΑΓΜΑ ΥΠ' ΑΡΙΘΜ. 230", *ΤΕΥΧΟΣ ΠΡΩΤΟ*, Αρ. Φύλλου 264, 2007.